T cell subsets in the human testis and their potential role in testicular germ cell tumors

Inaugural Dissertation
As part of the binational joint award PhD program of the Justus Liebig University Giessen and the Monash University Melbourne
submitted to the Faculty of Medicine in partial fulfillment of the requirements for the PhD-Degree of the Faculties of Veterinary Medicine and Medicine of the Justus Liebig University Giessen

by
Rashidul Islam
of
(Narayanganj, Bangladesh)

Giessen (2022)

From the

Institute for Veterinary Anatomy, Histology and Embryology

Director / Chairman

Prof. Dr. Dr. Stefan Arnhold

Chair: Prof. Dr. Klaus-Dieter Schlüter

First reviewer and supervisor: Prof. Dr. Daniela Fietz

Second reviewer: Prof. Dr. Sarina Ravens

Vice-Chair and co-supervisor: Prof. Dr. Hans-Christian Schuppe

Date of Doctoral Defense: 31 May 2023

T cell subsets in the human testis and their potential role in testicular germ cell tumors

Rashidul Islam

(Master of Molecular Diagnostics and Biotechnology, Bachelor of Pharmacy)

A thesis submitted for the degree (joint award) of Doctor of Philosophy at the Monash University, Australia and Justus Liebig University Giessen, Germany in December 2022

Department of Molecular and Translational Science,
Faculty of Medicine, Nursing and Health Sciences
&
Centre for Reproductive Health,
Hudson Institute of Medical Research

Under supervision of:

Professor Kate L. Loveland and Professor Mark P Hedger

(Monash University, Australia)

Professor Daniela Fietz and Professor Hans-Christian Schuppe

(Justus Liebig University Giessen, Germany)

Copyright notice

Abstract

As an immune-privileged organ, the normal testis immune environment consists of macrophages, mast cells and few T cells, all having anti-inflammatory effects to protect developing germ cells from autoimmune attack. Recruitment of infiltrating immune cells is commonly observed in human testicular germ cell tumors (TGCT), i.e. seminoma, but the significance for disease progression and prognosis remains unknown. T cells represent the major component of tumor infiltrating lymphocytes (TIL) in TGCT. Potential roles of rarer subtypes, such as regulatory (Treg) and follicular helper T (Tfh) cells, being associated with tumor biology in other cancer entities, have not been investigated in TGCT.

This study provides a detailed analysis of TIL focusing on Treg and Tfh in human testicular specimens characterized by hypospermatogenesis and lymphocytic infiltrates (ly) (n=12), pre-invasive germ cell neoplasia in situ (GCNIS -/+ly) (n=15, each), and seminoma (n=28) compared to normal spermatogenesis (n=10). Using immunohistochemistry (IHC), T cells were confirmed as most abundant TIL, with Treg and Tfh cells most frequently observed in seminomas. TIL from fresh human testicular tissue specimens (seminoma n=12; embryonal carcinoma (≥80%) n=6; mixed TGCT n=6) were analyzed by flow cytometry from different areas of tumor-bearing and contralateral (control) testes. Consistent with IHC, T cells were most abundant in seminomas. Treg and Tfh cells were most frequently detected in tumors, along with helper (CD4+) and cytotoxic (CD8+) T cells.

For further in-depth analyses of T cell subsets and their signatures in human testis samples, data from scRNA-sequencing of normal testis (n=3; pooled data) and TGCT (n=4) was examined. Again, T cells were the most prominent TIL in TGCT. Secondary clustering showed that, in addition to CD8+ cytotoxic, proliferating (activated), CCR7+ (newly recruited), and other CD4+ T cells, Treg and Tfh were present with variable frequencies. Downstream analysis suggested several possible modes of TIL regulation: Treg cell recruitment in TGCT might be regulated by the interaction of NANOG with CXCR4; Treg functionality might be regulated by a cooperation between BATF and CCL5. In addition, the interaction between BCL6 and NANOG might control Tfh cell recruitment in TGCT, and the cooperation between CXCR3 and ICOS is likely

to be important for their functionality. These *in silico* analytical findings are a fertile field for further experimental investigations.

In summary, despite high inter-individual variation and sample heterogeneity, all study approaches showed a similar composition of immune cells in the human testis, with an overall increase of immune cells in TGCT compared to other pathological conditions and normal controls. In addition, it became clear that the predominance of resident macrophages in normal testes is shifted in favor of T cells as the main component of TIL in TGCT.

Furthermore, the number of Treg and Tfh was significantly increased in TGCT compared to other pathological conditions and normal testis, possibly providing a tumor growth advantage. This study has described the complexity of TIL in TGCT and provides first indications that rarer T cell subtypes and their signaling molecules are likely to be of functional importance in the TGCT immune environment.

Declaration

This thesis contains no material which has been accepted for the award of any other degree or diploma at any university or equivalent institution and that, to the best of my knowledge and belief, this thesis contains no material previously published or written by another person, except where due reference is made in the text of the thesis.

Signature:

Print Name: **Rashidul Islam**

Date: **20 December 2022**

Publications during enrolment

Conference proceedings (presenter underlined)

Islam R, Heyer J, Figura M, Dittmar F, Pilatz A, Hartmann K, Pleuger C, Fijak, M, Kliesch S, Wagenlehner F, Hedger M, Loveland B, Loveland K, Fietz D, Schuppe H-Ch. Immune cell infiltration of testicular germ cell tumors – the possible role of T cell subsets. **12th European Congress of Andrology, 19-21 October 2022, Barcelona, Spain.** Poster presentation.

Islam R, Heyer J, Figura M, Indumathy S, Nathaniel B, Hartmann K, Pleuger C, Fijak M, Kliesch S, Dittmar F, Wagenlehner F, Hedger M, Loveland B, Loveland K, Guo J, Schuppe H-Ch, Fietz D. *Tumor infiltrating T lymphocytes in human testis cancer – identification and functional analysis*. **15th GGL Annual Conference, 14-15 September 2022, Giessen, Germany**. Poster presentation.

Islam R, Heyer J, Figura M, Indumathy S, Nathaniel B, Hartmann K, Pleuger C, Fijak M, Kliesch S, Dittmar F, Wagenlehner F, Hedger M, Loveland B, Loveland K, Guo J, Schuppe H-Ch, Fietz D. *Tumor infiltrating T lymphocytes in human testis cancer – identification and functional analysis*. **34th Annual Meeting of the German Society for Andrology, 8-10 September 2022, Giessen, Germany**. Poster presentation (with best poster award)

Figura M, Heyer J, **Islam R**, Hartmann K, Kliesch S, Pilatz A, Dittmar F, Wagenlehner F, Hedger M, Loveland B, Loveland K, Schuppe H-Ch, Fietz D. *Immune characteristics of testicular germ cell tumors – a clinical approach*. **34th Annual Meeting of the German Society for Andrology, 8-10 September 2022, Giessen, Germany**. Oral presentation (with best talk award).

Islam R, Heyer J, Indumathy S, Hartmann K, Pleuger C, Fijak M, Kliesch S, Dittmar F, Wagenlehner F, Herold S, Heiner M, Hedger M, Loveland B, Loveland K, Schuppe, H-Ch, Fietz D. *Tumor infiltrating T lymphocytes in human testis cancer – identification and functional analysis*. **14th GGL Annual Conference, 29-30 September 2021 (online), Giessen, Germany**. Oral presentation.

Islam R, Heyer J, Indumathy S, Hartmann K, Pleuger C, Fijak M, Kliesch S, Dittmar F, Wagenlehner F, Herold S, Heiner M, Hedger M, Loveland B, Loveland K, Schuppe H-Ch, Fietz D. *Tumor infiltrating T lymphocytes in human testis cancer – identification and functional analysis*. **21st European Testis Workshop (ETW), May 30th - June 3rd, 2021 (online), Spain**. Oral presentation.

Islam R, Heyer J, Indumathy S, Hartmann K, Pleuger C, Fijak M, Kliesch S, Dittmar F, Wagenlehner F, Herold S, Heiner M, Hedger M, Loveland B, Loveland K, Schuppe H-Ch, Fietz D. *Tumor infiltrating T lymphocytes in human testis cancer – identification and functional analysis*. **12th International, 11th European and 32nd German Congress of Andrology, 5–9 December 2020 (online), Münster, Germany**. Oral presentation.

Heyer J, **Islam, R,** Dittmar F, Pilatz A, Hartmann K, Kliesch S, Wagenlehner F, Hedger M, Loveland B, Loveland K, Fietz D, Schuppe H-Ch. *Immunopathology of testicular germ cell tumors- a clinical approach*. **12th International, 11th European and 32nd German Congress of Andrology, 5–9 December 2020 (online), Münster, Germany**. Poster presentation.

Islam, R, Heyer J, Indumathy S, Hartmann K, Pleuger C, Fijak M, Kliesch S, Dittmar F, Wagenlehner F, Herold S, Heiner M, Hedger M, Loveland B, Loveland K, Schuppe, H-Ch, Fietz D. *Tumor infiltrating T lymphocytes in human testis cancer – identification and functional analysis*. **13th GGL Annual Conference, 29-30 September 2020 (online), Giessen, Germany**. Oral presentation.

Islam R, Borderies J, Hartmann K, Kliesch S, Loveland B, Wagenlehner F, Pilatz A, Hedger M, Loveland K, Fijak M, Pleuger C, Bergmann M, Schuppe, H-Ch, Fietz D. *Tumor infiltrating T lymphocytes in human testis cancer – identification and functional analysis.* **53rd Annual Conference Physiology and Pathology of Reproduction, at the same time 45th Veterinary-Human Medical Community Conference, 26-28 February 2020, Rostock-Warnemünde, Germany.** Poster presentation (with best poster award).

Acknowledgements

First and foremost, I am grateful to my supervisory panel, Professor Daniela Fietz, Professor Hans-Christian Schuppe, Professor Kate Loveland, Professor Mark Hedger, Professor Bruce Loveland and the DFG IRTG 1871/P2 for giving me such a great opportunity to undertake the binational PhD degree program.

Words cannot express my gratitude to my German supervisors Professor Daniela Fietz and Professor Hans-Christian Schuppe for their guidance, encouragement and suggestions throughout my PhD journey. I have been fortunate enough to have such a great professional working environment and supervisors who cared about my work with genuine appreciation and allowed me to discuss my thoughts whenever I wanted. They have been super friendly and supportive, whether it was about research or personal life. Specially, the way they supported me in the last couple of months of my graduate study period, when I probably had the hardest time writing my PhD dissertation and dealing with my family issues, will be greatly appreciated.

This endeavor would not have been possible without my Monash supervisor Professor Kate Loveland, who has also been very supportive throughout this journey. Without her tremendous care and support I would not have been able to travel to Australia during the strict Covid restriction. She made every effort to collaborate globally to achieve the best outcome of the project. I would also like to extend my sincere thanks to Professor Bruce Loveland and Professor Mark Hedger for their constructive suggestions throughout this journey.

I am extremely grateful to Professor Hans-Christian Schuppe, Professor Adrian Pilatz, Professor Florian Wagenlehner, Dr. Florian Dittmar, Mrs. Kerstin Wilhelm, and Mrs. Tania Bloch from the Department of Urology, Pediatric Urology and Andrology at Giessen University Hospital, and Professor Sabine Kliesch from the Department of Clinical Andrology, Center for Reproductive Medicine and Andrology at the University of Münster, Germany for providing human samples for this study. I would like to extend my sincere thanks to Dr. Jingtao Guo for giving me the access into scRNA-seq datasets, and Dr. Christian Pleuger, Dr. Monika Fijak and Professor Andreas Meinhardt for allowing me to use the flow cytometry facility.

I would like to express my sincere gratitude to Professor Daniela Fietz for providing all the laboratory facilities I needed for this study. I am also thankful to the research

assistants, Alexandra Hax and Sigrid Kettner, for their kind assistance in the laboratory. Special thanks go to our medical doctoral thesis students Jannis Heyer and Miriam Figura. It was a really nice time together in the lab. Many thanks should also go to Dr. Monika Kressin, Dr. Katja Hartmann, Shashika Kothalawala, Seyed Mohsen Aberoumandi, Benedict Nathaniel and Lachlan Cauchi for their guidance and kind support throughout my journey. I would like to mention the contributions of Samira Hosseini and Sneha Biniwale who made my life way easier when I was planning to go Monash University, Australia for completing part of my thesis there.

I would also like to express my sincere appreciation to Ms. Pia Jürgens, Ms. Rose Kiarie and Ms. Tracey Purchas for their admirative supports throughout my time in Germany and Australia.

I would like to express my sincere gratitude to Dr. Bidhan Dhar, who is currently working as a Research Scientist at the Broad Institute of MIT and Harvard, whom I first met at the University of Camerino, Italy during my pursuing master's thesis. Dr. Dhar has been the first person ever guided me in my quest for a PhD position. His caring guidance, inspiration and proper directions led me finding my PhD position successfully. He has been super helpful reaching my career goals.

I am also grateful to my friends Mostafizur Rahman, Amran Hossain, Zulfikat Azam, Abdullah Al Maruf, Atiqul Islam, Ramjan Ali, Khairul Islam, Shanjid Shiplu and many others for sharing happiness and frustration throughout this journey.

Last but not least, I could not thank enough to my family. I am grateful to my parents for their enormous effort, support and love. Everything I have and everything I am, I owe it all to you. Without you I might not be the person I am today. Many thanks again for always believing in me and never giving up on me. To my sisters, million thanks for always being there for me. I really appreciate your constant encouragement and support. To my lovely wife Nafisa Anjum, I am so blessed of having you. Thank you for your love, care, support and every little effort you make for me is simply amazing. A very special thank you for bearing the pain and giving me the greatest blessing of my life sweet little Princess Sehrish Islam. To my little Angle Sehrish Islam, you are more than we ever expected and better than we ever imagined. I never thought I could love so much, until the day I felt your touch. You inspire me every day to grow and be better and please continue to do so.

List of Abbreviations

$A_{2A}R$	A2A receptor
AFP	Alpha fetoprotein
AhR	Aryl hydrocarbon receptor
APCs	Antigen-presenting cells
APECED	autoimmune polyendocrinopathy-candidiasis-ectodermal dystrophy
APTES	3-aminopropyltriethoxysilane
ATLL	Adult T-cell leukemia/lymphoma
ATP	adenosine triphosphate
BG	Interstitial fibrosis
BSA	Bovine serum albumin
BTB	Blood-testis barrier
BV	Blood vessels
CCND2	Cyclin D2
CRC	CXCL12-producing reticular cells
DC	Dendritic cell
DGEs	Differential gene expressions
DV	Tubular diverticle
EAO	Experimentally induced autoimmune orchitis
EC	Embryonal carcinoma
EDTA	Ethylenediaminetetraacetic acid
FBS	fetal bovine serum
FDC	Follicular DCs
FLS	Follicular-like structures
FSC	Focal Sertoli cell only syndrome
FSH	Follicle stimulating hormone
FunRich	Functional Enrichment analysis tool
Gal-1	Galectin-1
GC	Germinal center
GCNIS	Germ cell neoplasia in situ
GEO	Gene Expression Omnibus
GM-CSF	Granulocyte macrophage colony-stimulating factor
GO	Gene Ontology

GSEA	Gene Set Enrichment Analysis
H_2O_2	Hydrogen peroxide
hCG	β-human chorionic gonadotropin
H&E	Hematoxylin and eosin
HYP	Hypospermatogenesis
IDO	Indoleamine 2,3-dioxygenase
IFN-γ	Interferons-γ
IGF-1	Insulin-like growth factor-1
IHC	immunohistochemical analysis
ITS	Insulin Transferrin Selenium
ITSM	Immunoreceptor tyrosine-based switch motif
KITLG	KIT ligand gene
LC	Leydig cells
LDH	Lactate dehydrogenase
LDH3	Lactate dehydrogenase 3
LY	Lymphocytic infiltrates
LPS	Lipopolysaccharide
Mφ	Macrophages
mAb	Monoclonal antibody
MC	Mast cells
mDCs	Myeloid DCs
MHCII	Major histocompatibility complex class II
MSG	Multinuclear spermatogonia
NF-kB	Nuclear factor-kappa B
NSP	Normal spermatogenesis
PBMC	Peripheral blood mononuclear cells
PCA	Principal-Component-Analysis
pDCs	Plasmacytoid DCs
PKR	Protein kinase R
PPI	protein-protein interaction
P/S	penicillin-streptomycin
PTEN	Phosphatase and tensin homolog
RT	Room temperature

SAP	SLAM-associated protein
SCO	Sertoli cell only
SE	Seminoma
SLAM	Signaling lymphocyte activation molecule
SZA	Arrest of spermatogenesis at the level of primary spermatocytes
TBS	Tris-buffer solution
Tc	cytotoxic T
TCGA	The Cancer Genome Atlas
Tfh	T follicular helper
TGCT	Testicular germ cell tumors
TGF-β	Transforming growth factor-β (TGF-β),
Th	T helper
TIL	Tumor infiltrating lymphocytes
TLR	Toll-like receptor
TME	Tumor microenvironment
Treg	Regulatory T
TS	Tubular shadows
t-SNE	t-distributed stochastic neighbor embedding
UALCAN	The University of ALabama at Birmingham CANcer
VEGF	Vascular endothelial growth factor

Table of contents

1 INTRODUCTION

1.1 Overview of human testicular germ cell tumors (TGCT)

Testicular cancer is the most common solid malignant cancer among young men aged between 14-44 years, and accounts for nearly 1% of newly diagnosed cancers in men worldwide (Cheng et al., 2018, Gurney et al., 2019, Huang et al., 2022, Fietz et al., 2022). The incidence rate of testicular cancer varies widely around the world. For example, the lowest incidence (<1 person per 100,000 males) of testicular cancer has been reported in most Asian and African countries, while in the Scandinavian countries, particularly Norway and Denmark, the incidence rate of testicular cancer is 9.4-9.9 persons per 100,000 males (Znaor et al., 2014, Park et al., 2018). Recent studies demonstrated that the incidence rate of testicular cancer in Germany is 10.2 people per 100,000 men and the overall incidence rate of testicular cancer is continuously increasing worldwide, but the underlying reasons for this increase are not well understood (Michaeli et al., 2021). Nonetheless, advanced research has shown that several environmental and genetic factors are involved in the development of testicular cancer (De Toni et al., 2019). Among the various environmental risk factors, cryptorchidism (a condition/birth defect in which one or both testicles did not descend to the scrotum) is the most commonly associated with testicular cancer and increases the risk of testicular cancer by 5 to 10 times (Ferguson and Agoulnik, 2013, De Toni et al., 2019). Interestingly, a recent study found that cryptorchidism is more common on the right side and a small increase in the incidence in right-sided testicular cancer is observed (Leslie et al., 2022). Notably, family history increases the risk by 6 to 10 times in sons or brothers of the man affected with testicular cancer (Hemminki and Chen, 2006, Del Risco Kollerud et al., 2019). Other environmental factors, including hypospadias (a congenital disorder in which the urethral opening is not located at the glans of the penis), impaired spermatogenesis, low sperm count, prior history of testicular cancer or extragonadal germ cell tumors increase the risk of testicular cancer (Møller and Skakkebaek, 1999, Trabert et al., 2013, Lymperi and Giwercman, 2018, Gaddam and Chesnut, 2022). In addition to the above risk factors, genetic factors contribute to >40% of testicular cancer, which is the third highest rate among all cancers (Mucci et al., 2016, Litchfield et al., 2017). Although no specific genetic alteration for the development of testicular cancer has been precisely identified, the highest correlation appears to be with single nucleotide polymorphisms in the KIT

ligand gene (KITLG), located on chromosome 12, and their amplification is commonly identified in human testicular cancer (Ma et al., 2012, Litchfield et al., 2015, Nicu et al., 2022). It has been also demonstrated that alterations in the KIT-KITLG system are strongly associated with human male infertility and an increased risk of human testicular cancer (Galan et al., 2006, Ferlin et al., 2012). In addition to KIT, CCND2 (Cyclin D2) and K-RAS are also located on chromosome 12 and are involved in the development of testicular tumors (Hacioglu et al., 2017, Ding et al., 2019b). Other genetic abnormalities, for example, polymorphisms in Phosphatase and tensin homolog (PTEN), alterations in P53 also influence the risk of testicular cancer (Andreassen et al., 2013, Romano et al., 2016). Notably, many other genes have been characterized as being associated with an increased risk of testicular cancer, but to date there is no evidence of a single important high-penetrance gene known to cause increased susceptibility to testicular cancer (Baroni et al., 2019, Nicu et al., 2022).

Testicular germ cell tumors (TGCT) account for 90-95% of testicular cancer and are histologically categorized into seminoma and non-seminomatous germ cell tumors (Figure 1.1) (Ghazarian et al., 2015, Siegmund et al., 2022, Velado-Eguskiza et al., 2022). The pathogenesis of TGCT is well established and it is accepted that TGCT have a common precursor named germ cell neoplasia in situ (GCNIS), which is the core regulator of TGCT phenotypes (de Vries et al., 2020, Velado-Eguskiza et al., 2022). Briefly, TGCT arises from gonocytes that are unable to differentiate into spermatogonia, and the pluripotency of gonocytes allows them to develop into very diverse histological tumors (Baroni et al., 2019, de Vries et al., 2020). Under normal conditions, primordial germ cells develop into gonocytes, which are comparable to embryonic stem cells in terms of their gene expression pattern of pluripotency markers (*OCT4, NANOG, PLAP1, KIT, Ki-67*, etc.) and are gradually lost throughout the late gestation to neonatal (~1 year) development and replaced by the expression of differentiation markers (*MAGE4A, TSPY* etc.) (Spiller and Bowles, 2017). Mature spermatogonia then start spermatogenesis after the onset of puberty by undergoing meiosis, ultimately giving rise to elongated spermatids (“testicular sperm”). In GCNIS, germ cells fail to mature into spermatogonia, preserve their pluripotency, and remain quiescent until puberty (Rajpert-De Meyts et al., 2016, Spiller and Bowles, 2017, Cheng et al., 2018, Velado-Eguskiza et al., 2022). Later in life, GCNIS cells can

resume proliferation and gradually replace normal spermatogonia in the affected tubules, developing into seminomas and/or non-seminomas over time. In adults, GCNIS cells are located on the basal membrane, whereas in young children, GCNIS cells can be seen both basally and centrally in the seminiferous tubules (Jørgensen et al., 2015). In addition, GCNIS cell nuclei are hyperchromatic and usually have more than a single prominent nucleolus. In advanced stages, GCNIS diminishes the seminiferous tubules' organization by breaking down the basal membrane, proliferating and infiltrating the surrounding tissues, resulting in full-blown TGCT (Donner et al., 2004, Rajpert-De Meyts et al., 2016, Spiller and Bowles, 2017, Velado-Eguskiza et al., 2022).

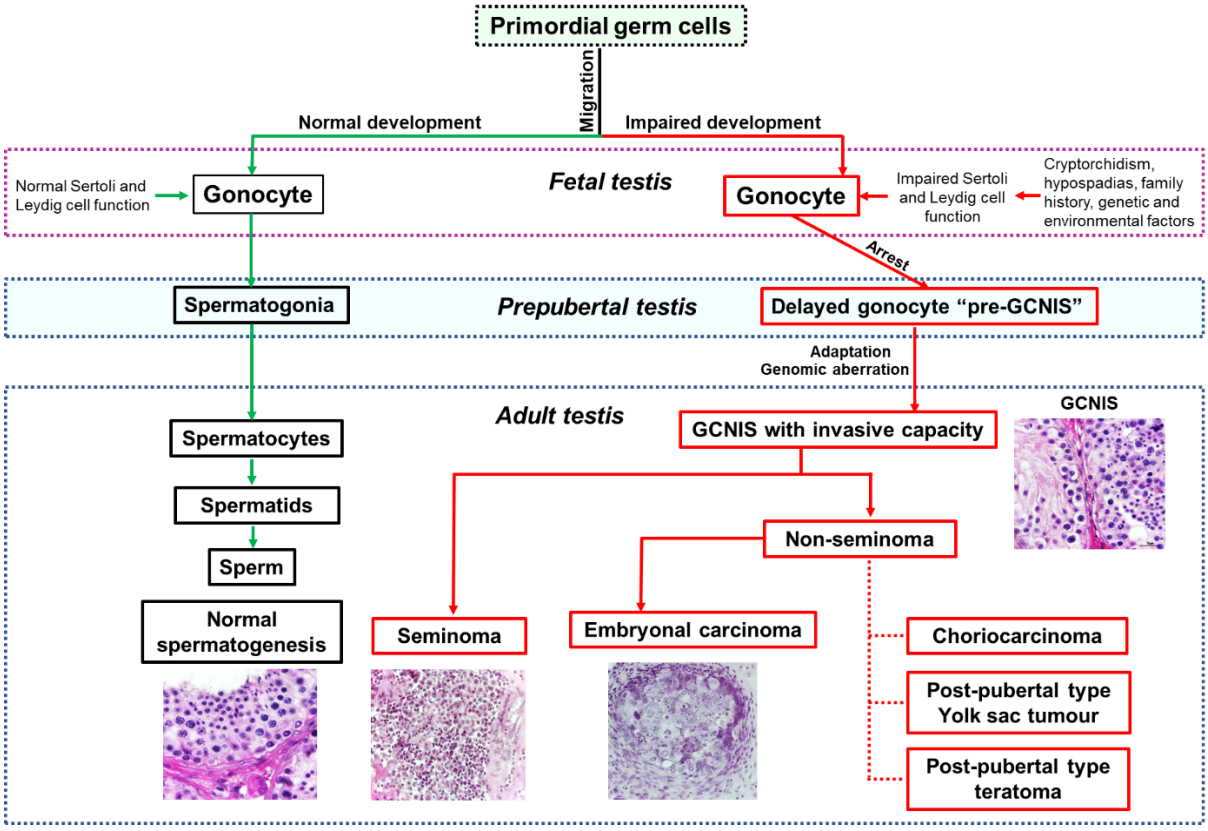

Figure 1.1 Schematic overview of healthy spermatogenesis and pathogenesis of TGCTs and their types. NSP: normal spermatogenesis (NSP); GCNIS: Germ cell neoplasia in situ. Modified from Skakkebaek et al. (Skakkebaek et al., 2016) and Moch et al. (Moch et al., 2022).

TGCT arises from GCNIS and can be differentiated into seminoma and non-seminoma (Figure 1.1). Seminomas account for 60% of the TGCT and are characterized as homogeneous tumors of embryonic germ cells and are blocked at the earliest stage of differentiation, while heterogeneous non-seminomatous tumors consist of embryonal carcinoma, yolk sac tumor, choriocarcinoma and teratoma (Rajpert-De Meyts et al., 2016, Batool et al., 2019, Moch et al., 2022, Berney et al., 2022, Velado-Eguskiza et al., 2022). Each of these TGCT presentations show distinct clinical features and can be differentiated histopathologically by the use of specific immunohistochemical markers. For example, *OCT4 (POU5F1)* and *NANOG* are expressed in both seminoma and embryonic carcinoma, while *PDPN* and *KIT* are solely expressed in seminoma but not in other TGCT. Furthermore, *CD30 (TNFRSF8)* and *SOX2* are exclusively expressed in embryonal carcinoma. Other non-seminomas such as yolk sac tumors can be identified by *GPC3* and alpha fetoprotein *(AFP)*, while choriocarcinomas can be identified by β-human chorionic gonadotropin (hCG) (Rajpert-De Meyts et al., 2015). Although the pathogenesis of TGCT is known, it is still a mystery why and under what circumstances GCNIS develops into a seminoma or non-seminoma. Nonetheless, cumulative studies have shown that there are several risk factors (briefly mentioned above) that can influence the process of development of seminoma and non-seminoma from GCNIS. Importantly, recent studies have shown that immune cells present in testicular pathological and cancerous conditions also contribute to outcomes associated with GCNIS progression, including the invasive development of seminoma and non-seminoma, which is reflected in the disease prognosis (Hvarness et al., 2013, Klein et al., 2016, Siska et al., 2017b).

Diagnosis and treatment of human TGCT

The diagnosis and treatment of TGCT entirely depend on the stages of the disease (Stephenson et al., 2019). First, if an abnormal testicular mass is suspected, physical examination should be performed and must include abdominal and supraclavicular exploration (Laguna et al., 2022). In all patients with suspected neoplasm, ultrasound examination of the scrotum is highly recommended to confirm a testicular tumor. In addition, serum tumor markers, including AFP, hCG and lactate dehydrogenase (LDH) should be drawn and measured before any treatment, and in the meantime, patients should be counseled about the risk of hypogonadism, infertility and sperm banking

(Stephenson et al., 2019, Gilligan et al., 2019). Together with physical examination and scrotal ultrasound, serum tumor marker expression provides maximum sensitivity in diagnosing testicular cancer (Kreydin et al., 2013). Inguinal exploration and radical orchiectomy, should be performed in patients with an unilateral testicular lesion suspected of malignancy and a normal contralateral testis (Stephenson et al., 2019). Testicle-sparing surgery is rarely offered as an alternative to radical inguinal orchiectomy to preserve gonadal function with mandatory counseling on the possible risk of local recurrence, the need for regular monitoring with physical examination and scrotal ultrasound, effects of radiation therapy on sperm and testosterone production etc. (Stephenson et al., 2019). In addition, bifocal tissue biopsies are obtained from contralateral testis. Once the presence of GCNIS is confirmed, testicular radiation has to be discussed with the patient as a treatment option due to the about 50% risk of developing a solid germ cell tumor in the next 5 years. Serum tumor marker controls (AFP, hCG, LDH) are repeated every three months for at least 3 years in the tumor follow-up (Stephenson et al., 2019, Siegmund et al., 2022, Gaddam and Chesnut, 2022). Depending on the confirmed histopathology of the diseased testicle, an individual personalized treatment for testicular cancer is decided (Baird et al., 2018). For example, surveillance without additional therapy is preferred for stage I seminoma without any risk factors. An adjuvant therapy with carboplatin is often recommended in the presence of the risk factors tumor invasion of the rete testis or tumor size > 4 cm, while stage II and III seminomas are treated with cisplatin-based chemotherapy (II+III) or radiotherapy (only II) (Giannatempo et al., 2015, Baird et al., 2018). Importantly, post-orchiectomy patients must undergo a CT scan of the chest and abdomen including nadir serum tumor marker controls (AFP, hCG, LDH) post chemo exposure, to determine whether further high-dose chemotherapy or retroperitoneal lymph node dissection is required or not (Siegmund et al., 2022). In contrast, stage I non-seminoma can be treated with active surveillance or one cycle of cisplatin-based chemotherapy in the presence of risk factor lymphovascular invasion (Baird et al., 2018). Furthermore, cisplatin-based chemotherapy (3 up to 4 cycles) has to be applied to the post-orchiectomy treatment of non-seminoma stages II and III based on the IGCCCG risk classification (good, intermediate, poor prognosis) (Baird et al., 2018). It is important to note that patients must be followed at least for five years after primary treatment of testicular cancer for recurrence (Laguna et al., 2022).

1.2 Immune privilege of the testis

The term “immune privilege” can be defined as a niche in the body where foreign antigens are tolerated without evoking a detrimental immune response. The mammalian testis was first characterized as an immune privileged organ over 2.5 centuries ago when it was observed that rooster testes survived after allotransplantation into hens (Setchell, 1990). Numerous studies later confirmed that the testis is an immune-privileged organ by transplanting histo-incompatible allografts and indeterminate-survival xenografts into the testis (Bobzien et al., 1983, Head et al., 1983). The testis consists of the seminiferous tubules separated by interstitial tissue. Seminiferous epithelium consists of the Sertoli cells and germ cells surrounded by peritubular myoid cells, while the interstitium contains Leydig cells, macrophages, blood vessels, lymphocytes, and fibroblasts (Figure 1.2). Sertoli cells facilitate the development of germ cells through direct contact and by controlling the environmental milieu within the seminiferous tubules (Griswold, 1998, Fietz et al., 2022).

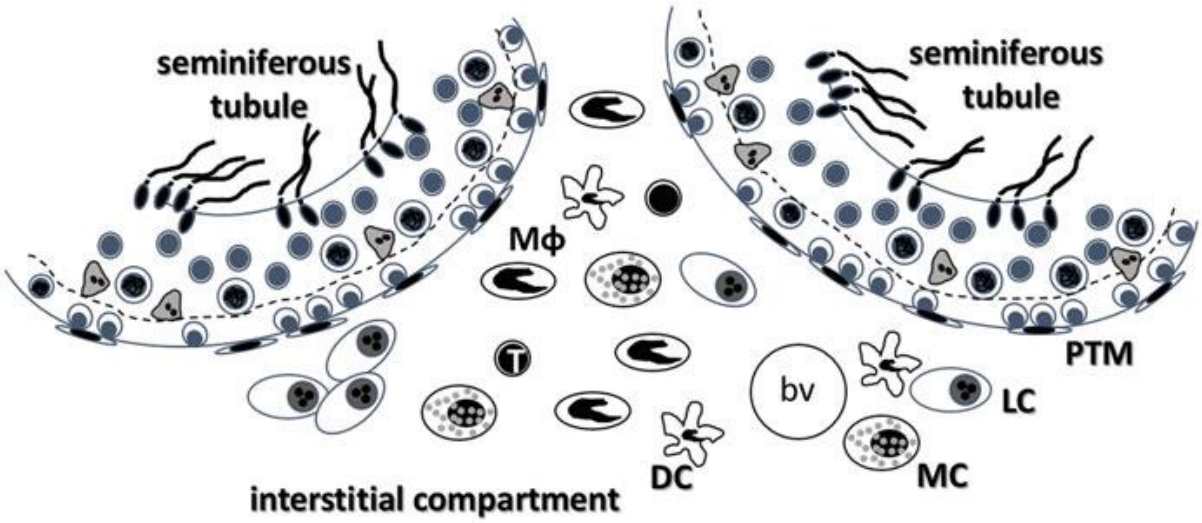

Figure 1.2 Immune cells in the normal adult testis. LC, Leydig cells; bv, blood vessels; Mφ, macrophages; MC, mast cells; DC, dendritic cell; T, T cells. The BTB (blood-testis barrier) is indicated by a dotted line. Adopted from Fietz et al., (Fietz et al., 2022).

During puberty, developing spermatocytes and spermatids express new antigens that were lacking in the establishment of immune self-tolerance, hence they express autoantigens that put them at risk of eliciting a deleterious immune response (Kaur et al., 2021, Fietz et al., 2022). However, due to the immune-privileged environment in the testis, these germ cells do not evoke this response. Conspicuously, most of the testicular cells contribute, at least in part, to the testicular immunsuppressive environment (Washburn et al., 2022). For example, Sertoli cells play the leading role in testicular immune regulation, which was validated by ablation of Sertoli cells, confirming their role in testicular and germ cell development and blood-testis barrier (BTB) formation (Washburn et al., 2022, Fietz et al., 2022). The BTB, also known as Sertoli cell barrier, is one of the tightest BTBs in the mammalian body and prevents molecules, antibodies and immune cells from entering and exiting the seminiferous tubules (O'Donnell et al., 2021, Washburn et al., 2022, Fietz et al., 2022). Sertoli cells produce many different immunomodulatory factors, including galectin-1 (Gal-1), insulin-like growth factor-1 (IGF-1), indoleamine 2,3-dioxygenase (IDO), transforming growth factor-β (TGF-β), activin-A, SERPINA3N, SERPINB9, IL-6, IL1-β, TNF-α, β-defensin, interferons-γ (IFN-γ), protein kinase R (PKR), which inhibit complement-mediated cell lysis, immune cell proliferation and apoptosis to protect germ cells from both infection as well as immune response (Kaur et al., 2021, Washburn et al., 2022, Fietz et al., 2022). Furthermore, Sertoli cells play an important role in the survival of adult Leydig cells and the functions of peritubular cells (Rebourcet et al., 2014, Smith et al., 2015).

Recently, it has been shown that Sertoli cells can survive after being transplanted as an allograft or xenograft to an ectopic site without the use of immunosuppressive drugs (Washburn et al., 2021). Besides, Sertoli cells also prolong the survival of co-grafted allogeneic and xenogeneic tissues (e.g., pancreatic islets), suggesting that these cells can mimic the immune-privileged environment outside the testis (Washburn et al., 2021). In addition to Sertoli cells, Leydig cells and germ cells and their secreted molecules also contribute to the regulation of the testicular immune response. For example, conditioned media containing Leydig cells and germ cells have been shown to inhibit lymphocyte proliferation, cytotoxic T cell (Tc) and NK cell activity and induce regulatory T (Treg) cells (Hurtenbach and Shearer, 1982, Kaur et al., 2013, Fijak et al., 2015, Fietz et al., 2022).

The underlying mechanism of how mammalian testes exhibit immune privileges by preventing unnecessary immune responses against auto-immunogenic germ cells and promoting a preventive response against pathogens and tumorigenesis is well known to date (Kaur et al., 2013, Kaur et al., 2021). Briefly, the successful progression of spermatogenesis is the fundamental role of testicular immune privilege. The tight junctions between adjacent Sertoli cells along with the Sertoli cell body, called the BTB, divides the seminiferous tubules into basal (contains spermatogonia and preleptotene spermatocytes) and adluminal compartments (contains the advanced germ cells). Initially, testicular immune privilege was ascribed to BTB, as it sequesters the majority of autoantigenic germ cells and prevents entry of immune cells and antibodies into the adluminal compartment (Kaur et al., 2013, Kaur et al., 2021). However, it was later observed that autoantigens can be found on preleptotene spermatocytes present outside of the BTB, and development of the BTB after completion of meiosis in non-mammalian vertebrates refutes the role of the BTB because of the testicular immune privilege (Kaur et al., 2013, Kaur et al., 2014, Kaur et al., 2021). Furthermore, it has also been demonstrated despite the continuous degradation and regeneration of BTB between each breeding cycle in seasonal breeders who repeatedly expose the meiotic spermatocytes, no immune response occurs and fertility is fully preserved (Kaur et al., 2021). A recent study discovered that not all antigens such as zonadhesin (ZAN) from meiotic and haploid germ cells are sequestered behind the BTB and are not involved in maintaining tolerance but are protected from an immune response by the BTB, while some other antigens, such as lactate dehydrogenase 3 (LDH3), were detected within the interstitial space outside of the BTB and were implicated in maintaining tolerance (Tung et al., 2017, O'Donnell et al., 2021). Furthermore, it has also been revealed that meiotic germ cell (unsequestered) antigens are exported into residual bodies to induce Treg cell-dependent tolerance, which was confirmed by a negative correlation between Treg and LDH3 antibodies in animal experiments (Tung et al., 2017, O'Donnell et al., 2021).

Importantly, the interstitium of mammalian testis contains regulatory immune cells, including resident macrophages and immature dendritic cells (DCs), which provide an anti-inflammatory environment in the testis, and the testicular interstitial fluid exhibits immunosuppressive activity by inhibiting the activation and/or proliferation of

stimulated peripheral blood lymphocytes (Pöllänen et al., 1988, Pöllänen et al., 1992, Hedger et al., 1998). Testicular interstitial fluid is influenced and regulated by somatic cells (Sertoli cells, Leydig cells and peritubular myoid cells) and tolerogenic macrophages and play a critical role in establishing and maintaining testicular immune privilege (Wang et al., 2017a). For example, treatment of rat monocytes with interstitial fluid resulted in a polarization of granulocyte-macrophage-colony-stimulating-factor-induced M1 macrophages towards regulator M2 macrophages, which secreted a higher level of IL-10 and a lower level of TNF-α after stimulation of lipopolysaccharide and induced significantly higher number of Treg cells when co-culture with T cells (Wang et al., 2017a). Furthermore, the same study also showed that treatment of rat T cells with interstitial fluid led to an increase in Treg cells, suggesting that interstitial fluid is one of the critical regulators for establishing and maintaining testicular immune privilege (Wang et al., 2017a).

Among the different immune cells, macrophages are the leading immune cells in normal testis and play different functional roles. For example, macrophages regulate vascularization of fetal testis and contribute to building the spermatogonia niche in the adult testis (DeFalco et al., 2014, DeFalco et al., 2015). In addition, testicular macrophages are also closely associated with Leydig cell development and steroidogenesis (Hales, 2002). Mechanistically, under normal conditions, testicular macrophages disrupt T cell activation by downregulating genes involved in toll-like receptor (TLR) signaling and upregulating negative regulators of TLR signaling, while under inflammatory conditions, testicular macrophages are able to inhibit nuclear factor-kappa B (NF-kB) activation (Winnall et al., 2011, Bhushan et al., 2015). Furthermore, testicular macrophages stimulate the development of Treg cells while being co-cultured with T cells (Wang et al., 2017a). Taken together, the response of testicular macrophages to inflammatory stimulation is dampened compared to conventional macrophages, suggesting the critical role of macrophages in maintaining testicular immune privilege.

Along with macrophages, DCs play an important role in testicular immune privilege. A very limited number of DCs can be found in normal mammalian testes, while a relatively increased number of DCs are found in inflamed tastes (Fijak et al., 2017). Relevant studies showed that the expression levels of CD80, CD86, and MHC class

II molecules of DCs remains unchanged in rat normal and inflamed testis, while upregulated CCR7 was found in rat inflamed testis (Rival et al., 2007). Furthermore, DCs express IL-10 and IL-12p35 in testes with experimentally induced autoimmune orchitis (EAO) and draining lymph nodes, which significantly stimulates effector T cell proliferation, suggesting a tolerogenic phenotype for DCs with normal testicular functions, leading to a maintained immune privilege (Rival et al., 2007, Guazzone et al., 2011). A recent study found that Gal-1 secreted by murine Sertoli cells is important for the development and maintenance of tolerogenic DCs (Gao et al., 2016). When DCs were co-cultured with allogeneic Sertoli cells, lower levels of MHC II, CCR7, CD11c, CD80, CD83, and CD86, but higher levels of IL-10 and TGF-β were detected (Washburn et al., 2022), and the results remained consistent in xenogeneic co-culture of mouse DCs with neonatal pig Sertoli cells after exposure to a potent inflammatory antigen (lipopolysaccharide), supporting the tolerogenic phenotype of DCs in the testicular immune environment (Washburn et al., 2022).

In contrast, T cells account for about 10-20% of the total immune cells in normal mammalian testes, and an increase in this percentage is positively associated with inflammatory pathologies (Hedger, 2015, Klein et al., 2016, Fijak et al., 2017, Washburn et al., 2022). Different types of T cells, including CD4+ T helper (Th) cell, CD8+ cytotoxic T (Tc) cells, CD4+CD25+FOXP3+ Treg cells have been identified in mammalian testes, however, the interactions and functions of T cells in normal testis are limited (De Rose et al., 2013, Pérez et al., 2013). Nonetheless, relevant studies suggested that various immunosuppressive factors, such as IL-10, TGF-β, activin A produced locally in the testes may promote a decreased testicular T cell response, leading to prolonged tolerance (De Rose et al., 2013, Fijak et al., 2017). In addition, Sertoli cells appear to regulate different T cells, however, the mechanism how Sertoli cells limit T cell expansion is poorly understood to date (Pérez et al., 2013). Sertoli cells can express different granzyme inhibitors, such as SERPINA3N and SERPINB9, which can limit the action of CD8+ Tc cells (Hirst et al., 2001, Horvath et al., 2005, Sipione et al., 2006). Initial study showed that Sertoli cells in the presence of follicle stimulating hormone (FSH) can inhibit the production of IL-2, which is required for T cell proliferation (Selawry et al., 1991). Interestingly, Sertoli cells can also induce Treg from naïve T cells in mammalian testes, which can lead to an alteration in overall T cell populations (Brown et al., 2003, Dal Secco et al., 2008), however the exact

mechanism of how Sertoli cells induce Treg is largely unknown to date. Taken together, testicular immune privilege provides an anti-inflammatory environment involving various cells, including regulatory immune cells, which allows to regulate normal spermatogenesis (NSP) and protect auto-immunogenic germ cells. It is important to note that the immune privilege of the testis can be disrupted by bacterial and viral infections, as well as the development of testicular cancer. However, a knowledge gap still exists regarding the interactions between testis and pathogens and cancer, suggesting that further studies are needed to uncover the underlying mechanisms of how pathogens and cancer use testicular immune privilege to their advantage in order to develop effective therapeutics against them.

1.3 Immune cells in the testis under physiological and pathological conditions

1.3.1 Macrophages

Macrophages are heterogeneous antigen-presenting cells, representing the most abundant immune cells in normal testes, and playing crucial rules in the development of fetal testes and the maintenance of the immune privilege in adult testes (Niemi et al., 1986, Bhushan and Meinhardt, 2017, Wang et al., 2017a, Meinhardt et al., 2022). The heterogeneity of macrophages can be identified based on their anatomical localization, organ-specific function, surface markers, gene expression profile, ontogenesis, and postnatal development (Mossadegh-Keller and Sieweke, 2018). For example, two types of macrophages such as interstitial macrophages characterized by $CD64^{hi}MHC^{lo}$ expression, and peritubular macrophages characterized by $CD64^{lo}MHC^{hi}$ expression, have been identified in the adult mouse testis (DeFalco et al., 2015, Fehervari, 2017, Mossadegh-Keller et al., 2017, Mossadegh-Keller and Sieweke, 2018), and a recent study also suggested that these two macrophage phenotypes may originate from the fetal liver and already exist during fetal life before birth (Lokka et al., 2020). In addition, macrophages can be classified into two functional subtypes: (I) pro-inflammatory M1 macrophages identified by surface markers (such as *CD80, CD86, CD64, CD16, and CD32*), polarized by lipopolysaccharide (LPS) alone or in association with IFN-γ, GM-CSF, and produce pro-inflammatory cytokines such as IL-1β, IL-6, IL-12, IL-23 and TNF-α; (II) anti-inflammatory and immunoregulatory M2 macrophages identified by CD163 and CD206, polarized by IL-4 and IL-13, and produce anti-inflammatory cytokines such as

IL-10 and TGF-β (Shapouri-Moghaddam et al., 2018). In normal testis, resident macrophages are typically M2 macrophages and exhibit normal phagocytic functions (DeFalco et al., 2014). For example, M2 macrophages protect developing germ cells from noxious stimuli, including autoimmune attack against meiotic germ cells through secreting IL-10, TGF-β (Bhushan and Meinhardt, 2017). As mentioned above, macrophages play an essential role in preserving the testicular immune privilege through diverse mechanisms (Wang et al., 2017a, Fijak et al., 2018, Meinhardt et al., 2018). In addition, M2 macrophages interfere with T cell activation, proliferation, and stimulate naïve T cell differentiation into Treg cells (Winnall et al., 2011, Bhushan et al., 2015, Wang et al., 2017a, Bhushan et al., 2020). Importantly, increased numbers of macrophages in the human testis have been observed under pathologic conditions, including TGCT along with their pre-invasive GCNIS (Schütte et al., 1988, Hvarness et al., 2013, Klein et al., 2016).

1.3.2 Dendritic cells

Dendritic cells (DCs) are antigen-presenting cells involved in the initiation and regulation of both innate and adaptive immune responses (Wculek et al., 2020). Based on the expression of different surface markers, DCs can be broadly divided into plasmacytoid DCs (pDCs) and myeloid (classical) DCs (mDCs). In general, DCs can be found in both lymphoid and non-lymphoid tissues, and involved in the activation of T cells (which drive autoimmunity) and the induction of antigen-specific T cell tolerance (pathogen-induced immune responses) depending on various factor (Tarbell and Rahman, 2020). Functional involvement of DCs in the testis is poorly known. Nonetheless, DCs are rarely found in normal testis, exclusively in the interstitial space, and are thought to be involved in maintaining testicular immune privilege (Klein et al., 2016, Bhushan et al., 2020). A significantly increased number of DCs was detected in EAO, suggesting their involvement in the testicular immune response (Rival et al., 2006). Furthermore, Gal-1 secreted by Sertoli cells has been found to be important for the development and maintenance of tolerogenic DCs (De Rose et al., 2013). Unlike other cancers, the putative role of DCs in human testicular cancer is not well characterized. Nevertheless, Klein et al. (Klein et al., 2016) found a higher number of CD11c+ DCs in pre-invasive GCNIS and TGCT (mostly in seminoma) compared to

normal testis suggesting their association with testicular disease development and progression.

1.3.3 Mast cells

Mast cells are tissue-resident immune cells derived from pluripotent bone marrow progenitor cells and are found primarily in mucosal and epithelial tissues throughout the body with heterogeneous phenotypes (Krystel-Whittemore et al., 2016). Functional studies showed that mast cells promote fibrosis by stimulating fibroblast proliferation and collagen synthesis via their proteases, chymase and trypsin (Algermissen et al., 1999, Mechlin and Kogan, 2012). Although, knowledge on the functional involvement of mast cells is limited in the testes, a small number of mast cells are found in the interstitium of normal testes (Hussein et al., 2005), while they are more abundant in the testes of infertile men and those with testicular atrophy (Banek et al., 1999, Yamanaka et al., 2000, Mechlin and Kogan, 2012). Relevant studies have also found that mast cells are critically associated with defective spermatogenesis and that this effect is more pronounced in testicular biopsies with arrested maturation and Sertoli cell only (SCO) phenotypes (Meineke et al., 2000, Hussein et al., 2005, Roaiah et al., 2007). Interestingly, mast cells were found to have a critical impact on the Treg and immune tolerance (Lu et al., 2006, Piconese et al., 2009). In contrast, activated Treg cells may also recruit mast cells via the pleiotropic cytokine IL-9 to facilitate regional immunosuppression (Eller et al., 2011).

Analysis of mast cells in human testes showed that these cells slightly increase in human testicular biopsies showing hypospermatogenesis (HYP) and GCNIS compared to testes presenting normal spermatogenesis, but no mast cells were found in seminoma (Klein et al., 2016), suggesting that mast cells are likely to be involved in maintaining NSP and early stages of disease development and progression, but are not or less involved in TGCT development and progression. However, the functional mechanism by which mast cells are involved in human normal and diseased testes is largely unknown to date. Nonetheless, recent studies have described mast cells as pro-tumor immune cells in human testis (Siska et al., 2017b, Kalavska et al., 2021).

1.3.4 B cells

B cells are one of the most abundant tumor-infiltrating lymphocytes and play an important role in regulating the immune response to different types of cancer (Yuen et al., 2016, Wei et al., 2021). Interestingly, B cells can play a dual role in cancer (Wei et al., 2021). For example, B cells can promote the development and progression of cancer through producing autoantibodies and tumor growth factors (Yuen et al., 2016). In addition, regulatory B cells can suppress the response of CD4+ Th1, NK cells and CD8+ Tc cells via the secretion of IL-10, and also stimulate the conversion of naïve CD4+ Th cells into FOXP3+ Treg cells via the production of TGF-β, and thus promote tumor growth (Olkhanud et al., 2011). In contrast, B cells can also inhibit tumor development and progression by producing tumor-reactive antibodies that promote tumor killing by NK cells, priming CD4+ Th and CD8+ Tc cells, and phagocytose by macrophages (Yuen et al., 2016, Wei et al., 2021). In the testis, no B cells were found in testicular biopsies with NSP and HYP, but increased numbers of B cells were detected in testicular biopsies presenting pre-invasive GCNIS and TGCT accompanied by different regulatory molecules including IL-2, IL-6, IL-1β, TNG-α, TGF-β, IFN-γ, CXCL5, CXCL10, CXCL13, and many more (Willis et al., 2009, Hvarness et al., 2013, Klein et al., 2016), suggesting that B cells are unlikely to be involved in the regulation of NSP but play an important role in the development and progression of TGCT. However, the underlying mechanism how B cells regulate TGCT development and progression remains to be elucidated.

1.3.5 T cells

T cells are specialized lymphocytes that originated from bone marrow progenitors and mature in the thymus to express uniquely rearranging T cell receptors for antigen. Based on the T cell receptor subunits and the expression of core lineage cell surface markers, T cells can be broadly classified into CD8+ Tc cells and CD4+ Th cells. Both Tc and Th cells can be further differentiated into different subtypes, which are mainly characterized by their specific cytokine profiles (Figure 1.3) (Golubovskaya and Wu, 2016, Paul and Ohashi, 2020). Each subtype of CD4+ Th and CD8+ Tc cell is functionally distinct and may have specific roles in normal physiology and in the development and progression of various diseases.

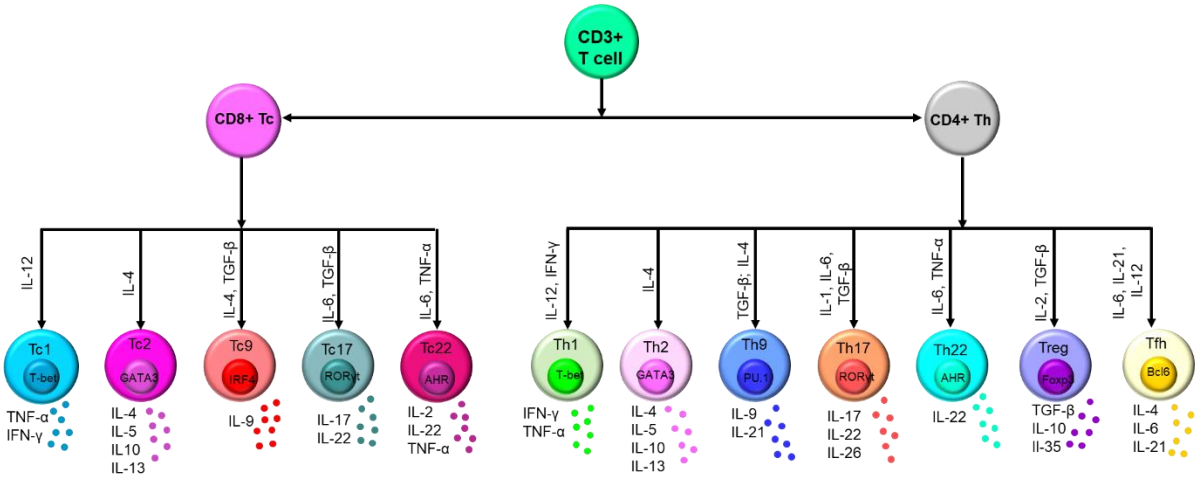

Figure 1.3 T cell subtypes. T cells are forced into different subtypes by the influence of different cytokines (shown on the arrows); In addition, each CD8+ Tc and CD4+ Th subtype is characterized by its specific cytokine production. Only the most important cytokines and regulatory factors are mentioned here.

1.3.5.1 CD4+ Th cells

CD4+ Th cells, along with CD8+ T cells, play a central role in the adaptive immune system and are known for supporting antibody production from B cells, stimulating CD8+ Tc cells and macrophage function (Zhu et al., 2009). CD4+ Th cells are significantly involved in tumor immunity as well as in autoimmunity, asthma, and allergic responses. In the tumor microenvironment (TME), CD4+ Th cells can target tumor cells and eliminate them via different cytolytic mechanisms (Kennedy and Celis, 2008, Melssen and Slingluff Jr, 2017, Borst et al., 2018), while CD4+ Th cells in secondary lymphoid organs increase the magnitude and quality of CD8+ Tc cell and B cell responses (Castellino and Germain, 2006, Borst et al., 2018). CD4+ Th cells can be further differentiated into different subtypes such as Th1, Th2, Th9, Th17, Th22, Treg, and T follicular helper (Tfh) cells, which are also largely characterized by different cytokine profiles and a distinct functional potential (Raphael et al., 2015).

CD4+ Th1 cells

CD4+ Th1 cells are one of the first-defined Th lineages, characterized by their production of IL-2, IL-10, TNF-α, and IFN-γ (Kim and Cantor, 2014). Induction of CD4+ Th1 cells is mediated by antigen-presenting cells (APCs) such as macrophages and DCs, and their secreted cytokines (IL-12 and IFN-γ) (Luckheeram et al., 2012, Annunziato et al., 2014). The differentiation of Th1 cells is regulated by various transcription factors, such as T-bet, STAT1, STAT4, Runx1, Runx3, Eomes and Hlx (Luckheeram et al., 2012, Annunziato et al., 2014). CD4+Th1 cells are thought to be mainly responsible for the immune response against intracellular pathogens and the induction of autoimmune diseases, but a large number of these cells are also detected in the TME associated with various cancers including breast cancer, colon cancer, lung cancer, and others (Tosolini et al., 2011, Mateu-Jimenez et al., 2017, Jia et al., 2021, Lee et al., 2021, Basu et al., 2021). It is believed that CD4+ Th1 cells can directly eliminate tumor cells by releasing cytokines that activate death receptors on the tumor cell surface (Knutson and Disis, 2005). Several studies have been conducted to uncover the functional involvement of Th1 cells in normal testicular function as well as in TGCT. In accordance with others (Disis, 2010, Gong et al., 2020), our research group recently described a significant immune cell infiltration in seminoma compared to normal testis, HYP and GCNIS (Klein et al., 2016). Briefly, cytokine expression profiles revealed increased Th1 cell-driven master cytokines IL-2 and IFN-γ only in pre-invasive GCNIS and seminoma samples, but not in NSP and HYP, suggesting a tumorigenic impact of CD4+ Th1 cells to TGCT (Klein et al., 2016). However, the underlying mechanism of the association of CD4+ Th1 cells with the development and progression of human TGCT needs to be further elucidated to better understand human testis immune surveillance.

CD4+ Th2 cells

CD4+ Th2 cells are characterized by their higher production of the anti-inflammatory cytokines IL-4, IL-5 and IL-13 in conjunction with a lower secretion of IL-9 and IL-10 (Vahedi et al., 2013, Walker and McKenzie, 2018). CD4+ Th2 cells are outstanding for their support to B cells and their critical involvement in host defenses against multicellular parasites, allergies, and atopic diseases (Vahedi et al., 2013, Walker and

McKenzie, 2018). CD4+ Th2 cell differentiation is mainly regulated by IL-4 via GATA3 and STAT6 (Luckheeram et al., 2012, Dobrzanski, 2013). In addition, other transcription factors such as STAT5, STAT3, Gfi-1, c-Maf, and IRF4 are also involved in the differentiation of CD4+Th2 cells (Luckheeram et al., 2012). CD4+ Th2 cells play an ambivalent role in cancer immunity. For example, IL-10 released from CD4+ Th2 cells inhibits antigen processing, DCs presentation, and/or activation of Treg cells, which ultimately suppress the anti-tumor immune response (Ellyard et al., 2007, Chraa et al., 2019). On the other hand, IL-4 secreted by CD4+ Th2 is strongly associated with anti-tumor effects through the recruitment of macrophages and eosinophils (Chraa et al., 2019). Unlike other organs, CD4+ Th2 cells have not been identified in human testis (Duan et al., 2011, Gong et al., 2020), hence the functional involvement of Th2 cells in normal testis and TGCT is largely unknown. Nevertheless, a combination of Th2-secreted cytokines and resident M2 macrophages could be positively associated with physiological circumstances to maintain the testicular immune privilege (Hedger, 2011, Bhushan et al., 2015, Klein et al., 2016). Furthermore, together with the cytokine profiles of CD4+ Th1 cells, our research group showed that either the CD4+ Th2-specific cytokine IL-4 was unaffected, or IL-5, IL-13 and IL-23 were significantly decreased in seminoma compared to testicular biopsies showing NSP and HYP, suggesting their possible superiority in maintaining testicular immune privilege and regulating NSP (Klein et al., 2016, Loveland et al., 2017).

CD4+ Th9 cells

CD4+ Th9 cells are one of the newly discovered CD4+ Th cells, which were originally thought to be a subtype of CD4+ Th2 cells (Luckheeram et al., 2012), but were later established as a distinct subtype of CD4+ Th cells as reflected by their extensive production of the pleiotropic cytokine IL-9 (Veldhoen et al., 2008, Jabeen and Kaplan, 2012). CD4+ Th9 differentiation is largely regulated by the multi-functional cytokine TGF-β in combination with IL-4 (Luckheeram et al., 2012, Dobrzanski, 2013). In addition, the transcription factors IRF4, STAT6 and PU.1 also contribute to CD4+ Th9 differentiation (Jabeen and Kaplan, 2012). CD4+ Th9 cells have been described in different diseases such as parasitic infection, allergic inflammation, transplant tolerance, autoimmune disease, and tumor immunity (Li et al., 2017, Salazar et al., 2020). Although the direct involvement of CD4+ Th9 cells in human malignancies

remains unclear, numerous studies in animal models have shown that IL-9 secreted by CD4+ Th9 cells has higher potency in anti-tumor responses (Lu et al., 2012, Purwar et al., 2012, Li et al., 2017). To the best of our knowledge, no study has previously focused on the identification and characterization of CD4+ Th9 cells in human normal testis or TGCT.

CD4+ Th17 cells

CD4+ Th17 cells are characterized by their higher production of the pro-inflammatory cytokine IL-17 (specifically IL-17A and IL-17F) combined with lower levels of IL-22, pleiotropic cytokine IL-21 and GM-CSF (Stockinger and Omenetti, 2017, Bystrom et al., 2019). The differentiation of CD4+ Th17 cells is regulated by various cytokines and transcription factors such as IL-6, IL-21, IL-23, TGF-β, RORt and STAT3 (Luckheeram et al., 2012, Chraa et al., 2019). In general, CD4+ Th17 cells play a crucial role in fighting extracellular bacteria and fungi as well as in autoimmune diseases (Luckheeram et al., 2012, Chraa et al., 2019). Relevant studies showed that IL-17-producing CD4+ Th17 cells can play a double-edged role in cancer immunity. For example, Th17 cells can promote tumor progression by stimulating angiogenesis and immunosuppressive activities, while they can stimulate anti-tumor immune response by recruiting different immune cells to TME, stimulating CD8+ Tc cells, affecting CD4+Th1 cells phenotype, and altering IFN-γ production (Asadzadeh et al., 2017). Similar to other T cell subsets, the functional role of CD4+ Th17 cells in the testis is still poorly understood. Nevertheless, CD4+Th17 cells have been found in the rat testis with EAO and are believed to be associated with the EAO onset and maintenance of chronic inflammation (Jacobo et al., 2011). In addition, an increased number of CD4+ Th17 cells with high expression of their cytokines (IL-17A, IL-21, IL22), and a reduced level of IFN-γ+ and FOXP3+ cells were observed in testis biopsies from azoospermic men with chronic testicular inflammation, suggesting that cytokines produced by CD4+ Th17 cells can negatively regulate CD4+ Th1 cells (Duan et al., 2011). In contrast, our previous study showed conflicting results at the level of IL-17A mRNA expression in healthy and diseased testes, which may be due to the heterogeneity of human testicular specimens (Klein et al., 2016). Therefore, further investigations should be conducted to uncover the functional involvement of CD4+ Th17 cells in human testis.

CD4+ Th22 cells

CD4+ Th22 cells are known for their higher production of IL-22 with low levels or absence of IL-17 and IFN-γ (Qin et al., 2014). CD4+ Th22 differentiation is strongly regulated by IL-6, RORγt and T-bet, and IL-22 released from CD4+ Th22 plays a crucial role in autoimmune diseases, inflammation as well as various human cancers (Qin et al., 2014, Raphael et al., 2015). However, the contribution of CD4+ Th22 to tumor progression and anti-tumor immunity is still unappreciated. Nonetheless, IL-22 has been detected in human testis and this cytokine has been hypothesized to be mainly released from CD4+ Th17 (Qin et al., 2014). Since both CD4+ Th17 and CD4+ Th22 cells release IL-22, further investigation is needed to clarify whether the increased levels of IL-22 in the human testis (Duan et al., 2011) are due only to CD4+ Th22 cells or to both CD4+ Th17 and CD4+ Th22 cells.

CD4+ Treg cells

Refer to section 1.4.

CD4+ Tfh cells

Refer to section 1.5.

1.3.5.2 CD8+ Tc cells

CD8+ Tc cells are well-known for their ability to kill infected or malignant cells by secreting a high amount of IFN-γ and granzyme B (van der Leun et al., 2020). Initially, CD8+ Tc cells were considered as a uniform population of cells with a common cytotoxic property, but recent studies have identified and characterized different subsets of CD8+ Tc cells such as Tc1, Tc2, Tc9, Tc17, and Tc22 with specific cytokine profiles and distinct cytotoxic properties (Mittrücker et al., 2014, Paul and Ohashi, 2020).

CD8+ Tc1 cells

CD8+ Tc1, also known as typical cytotoxic T cells, are generated in the presence of IL-12, which is mainly produced by APCs such as DCs and macrophages. CD8+ Tc1 cells express high levels of perforin, granzyme B, IFN-α, and TNF-γ along with expression of IL-4, IL-9 and IL-17 (Mittrücker et al., 2014, Paul and Ohashi, 2020). Notably, the high expression of the IL-18 receptor on CD8+ Tc cells helps distinguish them from other CD8+ T cell subtypes (Chan et al., 2001). Several transcription factors such as STAT-4, T-bet and EOMES are critically involved in the regulation of CD8+ Tc1 cell polarization (Pearce et al., 2003, Yang et al., 2007). CD8+ Tc1 cells exhibit exceptional cytotoxicity and can efficiently destroy tumor cells and cells harboring intracellular pathogens (Mittrücker et al., 2014, Paul and Ohashi, 2020). Besides, relevant studies demonstrated that CD8+ Tc1 cells are the most frequently detected CD8+ Tc cells in human tumor infiltrating lymphocytes (TIL) isolated from different cancers including colon cancer, breast cancer, ovarian cancer, lung cancer, and melanoma (Dobrzanski et al., 2000, Sasaki et al., 2006). The presence of CD8+ Tc1 cells is positively associated with disease progression by their secretion of IFN-γ (Fridman et al., 2012, Ayers et al., 2017). In the TME, IFN-γ interacts with activation signals to upregulate MHCI on APCs, thereby enhancing antigen production and activation of naïve T cells (Zaidi and Merlino, 2011). In addition, IFN-γ can reprogram immunosuppressive cells, including Treg cells, and also act directly on tumor cells to upregulate MHCI, thereby increasing susceptibility to CD8+ Tc cell-dependent cytotoxicity (Zaidi and Merlino, 2011, Overacre-Delgoffe et al., 2017). Although CD8+ Tc1 cells are widespread in various cancers, knowledge of their functional role in human testicular cancer is still very limited.

CD8+ Tc2 cells

CD8+ Tc2 cells are known for their high production of IL-4, IL-5, and IL-13 in conjunction with lower production of IFN- γ (Mittrücker et al., 2014, Paul and Ohashi, 2020). Similar to CD8+ Tc1, CD8+ Tc2 cells also express high levels of granzyme B and show a strong cytotoxic property (Kemp and Ronchese, 2001, Mittrücker et al., 2014). IL-4 regulates CD8+ Tc2 cell polarization by activating STAT6 and GATA3 (Pai

et al., 2004). CD8+ Tc2 cells are mostly known for their contribution to allergic responses (Schaller et al., 2005, Hilvering et al., 2018).

Importantly, CD8+ Tc2 cells are also correlated with different human cancers, including cervical cancer, lung cancer, breast cancer, lymphoma, and chronic lymphocytic leukemia (Sheu et al., 2001, Podhorecka et al., 2002, Ito et al., 2005, Anichini et al., 2006, Faghih et al., 2013). However, the clinical relevance and prognostic value of CD8+ Tc2 cells in TME are not yet clear. For example, some evidence suggested that the proportion of CD8+ Tc2 and CD8+ Tc1 cells in the tumor-draining lymph node of breast cancer patients shows no correlation with tumor size (Ehi et al., 2008). In contrast, other studies showed that the CD8+ Tc2:Tc1 ratio in tumor-draining lymph nodes correlates with breast cancer stage rather than tumor size, and it has been also suggested that CD8+ Tc2 cells may be negatively correlated with breast cancer (Faghih et al., 2013). To date, no study has specifically focused on CD8+ Tc2 in human testes, hence its biological importance in normal and diseased testes remains unexplored.

CD8+ Tc9 cells

CD8+ Tc9 cells are one of the recently discovered subsets of CD8+ Tc cells that produce IL-9 and low levels of IFN-γ (Visekruna et al., 2013, Lu et al., 2014). The polarization of CD8+ Tc9 is regulated by STAT6 and IRF4 and mediated IL-4 and TGF-β (Visekruna et al., 2013). Unlike other Tc cells, CD8+ Tc9 cells show poor cytotoxic function due to their limited granzyme B production and longer persistence in vivo (Visekruna et al., 2013, Lu et al., 2014, Wan et al., 2020). It has recently been described that TNF-α promotes CD8+ Tc9 differentiation by activating STAT5 and NF-kB signaling via TNFR2 but not TNFR1 (Yang et al., 2020). CD8+ Tc9 cells detected in different cancer, including breast cancer (Ding et al., 2019a). In addition, it has been revealed that CD8+ Tc9 cells exhibit a stronger anti-tumor effect than other CD8+ Tc cell subtypes due to their high production of IL-6 and TNF-α (Yang et al., 2020, Wan et al., 2020). So far, no evidence of CD8+ Tc9 cells in human testes have not been studied.

CD8+ Tc17 cells

CD8+ Tc17 cells are characterized by high production of IL-17A, IL-17F, and IL-22 together with low expression of IFN- γ (Hinrichs et al., 2009, Liang et al., 2015). Like CD8+ Tc9, CD8+ Tc17 cells express low levels of granzyme B and show weak cytotoxic function (Huber et al., 2009). Differentiation of CD8+ Tc17 cells is regulated by IL-6 and TGF-β, which could be accelerated by IL-1β, IL-21 and/or IL-23 (Liu et al., 2007, Yen et al., 2009). CD8+ Tc17 cells are one of the most extensively studied CD8+ Tc subtypes in various malignancies including cervical cancer, gastric cancer, hepatocellular carcinoma, breast cancer, gallbladder cancer, and bile duct cancer, and appear to play a disease-specific role (Kuang et al., 2010, Zhuang et al., 2012, Faghih et al., 2013, Zhang et al., 2014, Saito et al., 2015, Patil et al., 2016, Chellappa et al., 2017, Corgnac et al., 2020, Zhang et al., 2020). For example, in cervical cancer, high levels of CD8+ Tc17 cells promote expression of CXCR12 in tumor cells via secretion of IL-17, which enhances tumor cell proliferation and migration (Zhang et al., 2020). Notably, the presence of excessive production of IL-17 by CD8+ Tc17 cells in gastric cancer, hepatocellular carcinoma, lung cancer, head and neck cancer, is associated with decreased survival (Zhuang et al., 2012, Wang et al., 2017b, Wang et al., 2017d, Lee et al., 2018). However, the underlying mechanisms how CD8+ Tc17 cells are associated with poor prognosis and overall survival is not clear. Nevertheless, it is believed that IL-17 secreted by CD8+ Tc17 cells can interact with tumor cells and other cells in TME thus stimulating the production of inhibitory and angiogenic factors that facilitate the recruitment of different pro-tumorgenic cells such as neutrophils and CD11b+ myeloid derived suppressor cells (He et al., 2010, Benevides et al., 2015). Although CD8+ Tc17 cells have been analyzed in other cancers, they remain unexplored in human testicular cancer.

CD8+ Tc22 cells

In contrast to CD8+ Tc9 and Tc17, CD8+Tc22 cells show high cytotoxic properties with exceptional anti-tumor activity. However, CD8+ Tc22 cells are still a poorly understood CD8+ Tc subtype due to their high production of the cytokine IL-22 which is usually thought to be produced by CD4+ Th1, Th17 and Th22 cells (Res et al., 2010, Zhang et al., 2013b, Paul and Ohashi, 2020). Along with IL-22 production, CD8+ Tc22 cells also produce small amounts of IL-2 and TNFα (Paul and Ohashi, 2020). The

polarization of CD8+ Tc22 cells is regulated by the combination of IL-6 with TNF-α and the aryl hydrocarbon receptor (AhR) (associated with environmental chemical stimuli with adaptive responses, such as detoxification, cellular homoeostasis or immune responses) (St Paul et al., 2020, Paul and Ohashi, 2020). CD8+ Tc22 cells have been identified in different cancers such as ovarian cancer, gastric cancer, and squamous cell carcinoma (Zhuang et al., 2012, Zhang et al., 2013b, St Paul et al., 2020, Paul and Ohashi, 2020), and it has been suggested that IL-22 producing CD8+ Tc22 cells significantly promote longer relapse-free survival. Yet, the functional role of CD8+ Tc22 cells in human testicular cancer remains to be elucidated.

Although no information is available on the functional involvement of CD8+ Tc cell subtypes in human TGCT, there are numerous studies focusing on the identification and characterization of CD8+ Tc cells (el-Demiry et al., 1987, Bell et al., 1987, Nakanoma et al., 1992, Nouri et al., 1993, Jahnukainen et al., 1995, Bols et al., 2000, Yakirevich et al., 2002, Hadrup et al., 2006, Hvarness et al., 2013, Shami et al., 2020). The biological significance of CD8+ Tc cells in the human testis is still the subject of debate due to conflicting research results. For example, Yakirevich et al. detected “higher activated” CD8+ T cells in seminoma compared to non-seminomas (Yakirevich et al., 2002), whereas Bols et al. suggested that “poorly activated” CD8+ Tc cells are found in GCNIS and seminoma (Bols et al., 2000). Furthermore, it has also been shown that CD8+ Tc cells, in addition to their cytotoxicity, may interact with regulatory effector cells and thereby become a critical regulator of disruption of testicular immune privilege (Hvarness et al., 2013, Barnes and Amir, 2018). Furthermore, consistent with another study (Hvarness et al., 2013), this study also showed that CD8+ Tc cells are one of the most prominent T cells in pre-invasive GCNIS and testicular cancer compared to testis biopsies with normal or impaired spermatogenesis obtained from infertile men. However, further investigations are needed to elucidate the functional importance of CD8+ Tc cell subtypes in testicular biology.

1.4 Regulatory T (Treg) cells

Treg cells are one of the well-studied lineages of CD4+ Th cells, identified in the middle 1990s by analysis of surface expression of CD25 (IL2RA) (Sakaguchi et al., 1995). Subsequently, the transcription factor FOXP3 was identified by the same research

group as a central regulator for the differentiation, stability, and immunosuppressive functions of Treg cells (Hori et al., 2003, Fontenot et al., 2003), and since then these cells have received continuous attention due to their diverse roles in both physiological and pathological conditions (Sakaguchi et al., 2020, Galgani et al., 2021). Treg cells can develop in the periphery (known as pTreg cells) and in the thymus (known as tTreg cells). pTreg cells develop, especially in the gut, from CD4+ conventional T cells in the presence of higher expression of TGF-β, IL-2, and retinoic acid (Coombes et al., 2007, Sun et al., 2007, Cinier et al., 2021), while tTreg cells develop in the thymus via stimulation by self-antigens provided by thymic epithelial cells. After maturation, Treg cells migrate to peripheral tissues to play their role in immunological tolerance with a significantly diverse T cell receptor repertoire (Morikawa and Sakaguchi, 2014). Although NRP1 can distinguish tTreg and pTreg in the mouse, no marker has been identified to distinguish tTreg and pTreg in humans (Yadav et al., 2012, Weiss et al., 2012, Raffin et al., 2020). Therefore, CD25+FOXP3+ Treg cells isolated from human peripheral blood are believed to be a combination of tTreg and pTreg cells. Notably, both tTreg and pTreg cells have similar phenotypic properties and immunosuppressive functions, but differ in stability, epigenetic modification, and expression of specific genes (Cinier et al., 2021).

Treg cells confer immune tolerance via a variety of mechanisms. These cells can target T cells directly or indirectly by modulating APCs through high expression of IL-10, TGF-β, IL-35, CTLA4 (CD152), CD39 (ENTPD1), and CD73 (NT5E) (Onishi et al., 2008, Raffin et al., 2020). For example, CTLA4 (CD152) from Treg cells can bind to CD80/CD86 on APCs, favoring the induction of IDO (Grohmann et al., 2002, Walker and Sansom, 2015). Relevant evidence discovered, that Treg cells mostly migrate to inflammatory sites and suppress different effector lymphocytes including CD4+ Th cells and CD8+ Tc cells (Chaudhry et al., 2009, Koch et al., 2009, Chung et al., 2011, Linterman et al., 2011). In the context of cancer, Treg cells are frequently detected in inflamed tumors harboring large numbers of CD4+ Th cells and CD8+ Tc cells (Spranger et al., 2013, Williams et al., 2017). Importantly, Treg cells can potently suppress anti-tumor immune responses and contribute to the development of an immunosuppressive TME that promotes immune evasion and cancer progression (Li et al., 2020, Cinier et al., 2021). Therefore, it is strongly believed that understanding

of Treg cell homeostasis and functions could provide fundamental insights into the disease pathogenesis and possible therapeutic avenues.

1.4.1 Suppressive mechanisms of Treg cells

Treg cells exhibit their immunosuppressive activities through different mechanisms, including cell contact and secretion of immunosuppressive cytokines and molecules (Togashi et al., 2019, Romano et al., 2019, Cinier et al., 2021). Treg cells highly express CD25 (IL2RA) and therefore bind to and deplete IL-2 from their environments, reducing the availability of this cytokine to effector T cells (Togashi et al., 2019, Romano et al., 2019, Cinier et al., 2021). Treg cells also produce immunosuppressive cytokines such as IL-10, IL-35 and TGF- β can downregulate the activation of antigen-presenting cells and effector T cells (Togashi et al., 2019). In addition, Treg cells also secrete cytotoxic molecules such as granzyme and perforin that can directly destroy effector T cells (Grossman et al., 2004, Togashi et al., 2019). Importantly, Treg cells constitutively express CTLA4 (CD152) that binds to CD80 (B7-1) and CD86 (B7-2) on APCs such as DCs and B cells with a higher affinity than that of CD28 (Tp44) (Figure 1.4), thereby transferring inhibitory signals to APC and reduce their capability to activate effector T cells (Walker and Sansom, 2011, Walker, 2013, Zappasodi et al., 2021). In addition, CTLA4 (CD152) targeting molecules CD80 (B7-1) and CD86 (B7-2) can be transferred to the surface or the cytoplasm of Treg cells from the APCs through trogocytosis, which further inhibit the priming and or activation of effector T cells (Walker and Sansom, 2011, Walker, 2013, Zappasodi et al., 2021). Furthermore, adenosine triphosphate (ATP) released from Treg cells can be converted to adenosine A2A receptor ($A_{2A}R$) by CD39 (ENTPD1) and CD73 (NT5E), providing further immunosuppressive signals to effector T cells and antigen presenting cells (Deaglio et al., 2007, Wilson et al., 2009).

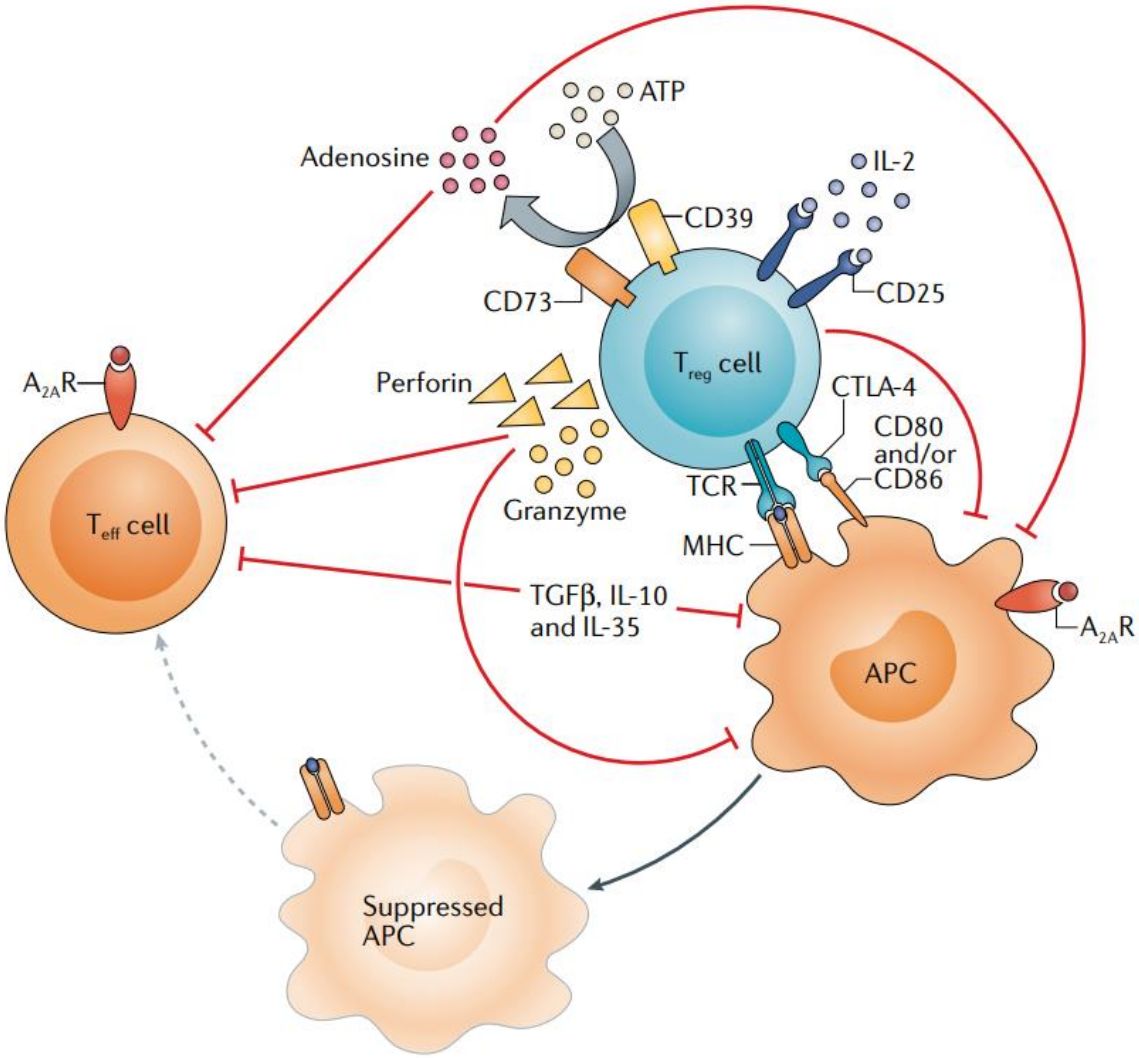

Figure 1.4 Immunosuppressive mechanisms of Treg cells. Treg cells express various functional molecules that bind to APCs and transmit suppressive signals as well as inhibit activation of effector T cells. Treg cells produce different cytokines which can downregulate the activity of both APCs and effector T cells or even Treg cells can kill APCs and effector T cells by secreting granzymes and perforin. Furthermore, excessive amount of ATP can be produced by Treg cells and that can be converted to adenosine and provide immunosuppressive signals to APCs and effector T cells through binding to $A_{2A}R$. Adopted from Togashi et al. (Togashi et al., 2019).

1.4.2 Treg cells in cancer

Immunosuppressive activities of Treg cells in cancers are thought to be one of the main obstacles to achieve an effective anticancer immune response. Treg cells account for 2-5% of CD4+ Th cells in the peripheral blood of persons without cancer, whereas Treg cells heavily (accounting for 10–50% of CD4+ Th cells) infiltrate the

TME and are critically associated with poor prognosis in patients with various cancers, including gastric cancer, ovarian cancer, non-small cell lung cancer, and melanoma (Sakaguchi et al., 2010, Wing and Sakaguchi, 2010, Saito et al., 2016, Togashi and Nishikawa, 2017, Tada et al., 2018, Ohue and Nishikawa, 2019). As previously mentioned, Treg cells are involved in tumor development and progression by inhibiting anti-tumor immunity (Ohue and Nishikawa, 2019, Togashi et al., 2019). Compared to the Treg cells in peripheral blood or normal tissues, Treg cells express high levels of activation markers, such as *CTLA4 (CD152), TIGIT (VSIG9), LAG3 (CD223), TIM3 (HAVCR2), ICOS (CD278), OX40 (TNFRSF4), GITR (TNFRSF18), 4-1BB (TNFRSF9), CD39 (ENTPD1),* etc. in the TME and this particular phenotype supports the notion that Treg cells are activated in the TME and exhibit strong immunosuppressive functions (Sugiyama et al., 2013, De Simone et al., 2016, Togashi and Nishikawa, 2017, Ahmadzadeh et al., 2019). The underlying mechanisms of how Treg cells are highly activated in the TME is poorly understand to date. Nevertheless, it is suggested that proliferating and dying tumor cells may release a massive amount of self-antigens, which are targeted by Treg cells and hence Treg cells are strongly activated in the TME (Nishikawa et al., 2005). In addition, tumor cells can convert immature myeloid DCs into regulatory TGF-β secreting cells that promote the activation and proliferation of Treg cells in animal models (Nishikawa et al., 2005, Ghiringhelli et al., 2005).

1.4.3 Recruitment of Treg in the TME

Recruitment of Treg into the TME is mainly regulated by various chemokine receptors and their cognate ligands, such as CCR4-CCL22/CCL17, CCR10-CCL28, CXCR4-CXCL12, CCR8-CCL18/CCL1, CCR5-CCL5, CCR2-CCL2, CCR6-CCL20 etc., which vary between cancers (Curiel et al., 2004, Gobert et al., 2009, Yan et al., 2011, Zhou et al., 2013, Sugiyama et al., 2013, Xia et al., 2014, Ward et al., 2015, Zhang et al., 2015, Ren et al., 2016, Loyher et al., 2016, Togashi and Nishikawa, 2017, Marshall et al., 2020, Cinier et al., 2021). Briefly, CCR4 is a G-protein-coupled receptor, that is highly expressed by Treg cells as well as by Th2, Th17, and Th22 cells in the periphery (Imai et al., 1999, Iellem et al., 2001, Lim et al., 2008, Duhen et al., 2009, Sugiyama et al., 2013). More than 90% of human Treg cells highly express CCR4 (Gobert et al.,

2009) and migrate toward its major two ligands (CCL17 and CCL22), which are secreted by tumor cells, tumor-associated macrophages and/or DCs that stimulate Treg cell recruitment toward the TME and show immunosuppressive effects in patients with different cancers including breast cancer, ovarian cancer, prostate cancer, gliomas, gastric cancer, cervical carcinoma, colorectal carcinoma, head and neck squamous cell carcinoma, esophageal cancer, etc. (Curiel et al., 2004, Mizukami et al., 2008, Gobert et al., 2009, Ménétrier-Caux et al., 2012, Cao et al., 2014, Zhou et al., 2015, Wiedemann et al., 2016, Fujimura et al., 2018, Wang et al., 2019b, Marshall et al., 2020). Relevant studies showed that tumor cell-derived IL-1α, cancer associated fibroblast-derived IL-1β promotes the production of CCL22 by tumor cells in the TME (Tsujikawa et al., 2013, Wiedemann et al., 2016, Huang et al., 2019b). Furthermore, in cooperation with IRF4, T cell-derived granulocyte macrophage colony-stimulating factor (GM-CSF) induces DC-derived CCL22 as well as macrophage-derived CCL17 production and stimulates recruitment of Treg cells into the TME (Hsu et al., 2018, Piseddu et al., 2020). Treg cells express the chemokine receptor CCR10, which binds its ligand CCL28 produced by tumor cells as well as other cells, and positively regulates the recruitment of Treg cells into the TME (Eksteen et al., 2006, Simonetti et al., 2006, Ren et al., 2016, Martinez-Rodriguez et al., 2017). For example, in chronic inflammation, epithelial cells produce CCL28, which favors recruitment of Treg cells to limit tissue damage (Eksteen et al., 2006). Furthermore, tumor cells in murine ovarian cancer models produce CCL28, which stimulates Treg recruitment into the TME and accelerates tumor growth (Facciabene et al., 2011). It has also been revealed in ovarian cancer and hepatocellular carcinoma, that hypoxia promotes excess production of CCL28 by cancer cells and stimulates the recruitment of Treg cells into the TME and is associated with tumor growth and progression (Facciabene et al., 2011, Ren et al., 2016, Cinier et al., 2021).

CXCR4 is a G-protein coupled receptor expressed by different cells including Treg and is known to regulate cell migration through interaction with its ligand CXCL12 (Mezzapelle et al., 2022). Relevant studies showed that the CXCR4-CXCL12 axis is critically involved in Treg recruitment in the TME. For example, tumor cells in various cancers such as renal cell carcinoma, breast cancer, cervical cancer, ovarian cancer, and malignant pleural mesothelioma secrete excessive amounts of CXCL12, which

binds to CXCR4 on the Treg surface and enhances Treg recruitment to the TME, thereby promoting cancer progression (Righi et al., 2011, Yan et al., 2011, Polimeno et al., 2013, Lecavalier-Barsoum et al., 2018, Mezzapelle et al., 2022).

CCR8 is highly expressed by different cells including Treg cells and plays an important role in regulating Treg recruitment in the TME via CCL18 and CCL1 (Mikhak et al., 2009, Kidani et al., 2022). In the TME, CCL18 is highly expressed by tumor-associated macrophages, neutrophils, B cells, plasma cells, T cells as well as cancer cells, and binds to CCR8 on Treg cells, thereby enhancing the recruitment of Treg cells in the TME and stimulating poor prognosis of various cancers, including breast cancer, colon cancer and glioblastoma (Chen et al., 2011, Ma et al., 2019, Sun et al., 2019, Vila-Caballer et al., 2019). In addition to CCL18, CCL1 is another ligand of CCR8 that has been reported to play a critical role in Treg recruitment and enhances stability and immunosuppressive functions (Barsheshet et al., 2017, Vila-Caballer et al., 2019, Cinier et al., 2021).

CCR5 is a seven-transmembrane G-protein coupled receptor binding with high affinity to CCL5 that favors Treg recruitment as well as tumor progression and metastasis (Aldinucci et al., 2020, Cinier et al., 2021). CCL5 is mainly produced by cancer cells, endothelial cells and cancer-associated fibroblasts that bind with CCR5 on Treg cells and migrate them towards the TME of different cancer such as pancreatic cancer and colorectal cancer, and stimulate potent immunosuppressive function which was confirmed by a loss-of-function study in murine model (Mack et al., 2001, Tan et al., 2009, Ward et al., 2015, Aldinucci et al., 2020).

CCR2, a chemokine receptor highly expressed by both monocytes and Treg cells, can bind to the chemoattractant ligand CCL2 and promotes recruitment of Treg cells into the TME (Loyher et al., 2016). In different tumors, CCL2 can be secreted by tumor cells, microglial cells, and tumor stromal cells that target CCR2 expressed by Treg and enhance Treg recruitment in the TME, thus stimulating tumor progression and immunosuppression with poor prognosis (Qian et al., 2011, Ma et al., 2014, Galluzzi et al., 2015, Loyher et al., 2016, Wang et al., 2016).

CCR6 is predominantly expressed on a variety of immune cells, including Treg cells, Th17 cells, Th22 cells, CD8+ Tc cells, and B cells, and plays a critical role in the specific migration of these cells to sites of inflammation by binding to its ligand CCL20 (Kondo et al., 2007, Annunziato et al., 2007, Yamazaki et al., 2008, Duhen et al., 2009, Lee and Körner, 2019). CCL20 is mainly secreted by tumor-associated macrophages, Th17 cells, B cells, NK cells, DCs, as well as epithelial cells, stromal cells, and cancer cells (Scapini et al., 2001, Yamazaki et al., 2008, Nandi et al., 2014, Zhao et al., 2018, Wang et al., 2019a). However, it has been observed that cancer cells require a supporting environmental factor for CCL20 production (Cremonesi et al., 2018). For example, tumor-associated macrophages favor the production of CCL20 by cancer cells through secreting IL-1β, IL-6 and TNF-α (Liu et al., 2011). In various cancers such as non-small cell lung cancer, colorectal cancer, different cells in TME including tumor cells secrete CCL20 that stimulates Treg cells recruitment and associated with tumor progression (Zhang et al., 2015, Wang et al., 2019a).

Overall, different chemokine receptors and their cognate ligands are critically involved in regulating the recruitment of Treg cells into the TME. Numerous groups have performed loss-of-function and/or gain-of-function studies and confirm the underlying mechanism of how different chemokine receptors and their associated ligands predominantly regulate the recruitment of Treg cells into the microenvironment under different pathological conditions. Further studies also indicated that effective targeting of different chemokines will be beneficial to control Treg cell recruitment in the TME to avoid systemic and/or tissue-specific autoimmune manifestation and promote an antitumor response.

1.4.4 Immunotherapeutic potential of targeting Treg cells in cancer

The presence of high numbers of Treg cells in the TME is associated with poor prognosis, therefore it is believed that inhibition of Treg cell functions or Treg cell depletion could be effective immunotherapies (Togashi et al., 2019, Raffin et al., 2020, Shan et al., 2022, Chen et al., 2022). Several direct or indirect strategies including Treg depletion, immune checkpoint inhibitors, Treg cell modulation etc. have been tested preclinically and/or clinically to control Treg-mediated immunosuppression

(Togashi et al., 2019, Raffin et al., 2020, Shan et al., 2022, Chen et al., 2022). For example, targeting Treg cell-specific molecules such as *CD25 (IL2RA), CTLA4 (CD152), CCR4, ICOS (CD278), OX40 (TNFRSF4), GITR (TNFRSF18)* and functional molecules and signals such as T cell receptor and IL-2R signaling pathways responsible for Treg cells survival and function are considered as direct strategies for eliciting an anti-tumor immune response (Togashi et al., 2019, Raffin et al., 2020, Shan et al., 2022, Chen et al., 2022). Targeting other immunosuppressive cells (e.g., tumor-associated macrophages, myeloid-derived suppressor cells that produce cognate ligands of chemokine receptors and stimulate Treg recruitment) or functional molecules ((e.g., vascular endothelial growth factor (VEGF), TGF-β)) in the TME that are closely associated with Treg survival and/or functions considered as indirect strategies to inhibit of Treg functions (Voron et al., 2014, Gabrilovich, 2017, Mantovani et al., 2017, Metelli et al., 2018, Togashi et al., 2019, Shan et al., 2022, Chen et al., 2022).

Treg cell depletion

Treg cells were originally identified as CD4+CD25+ T cells, and several studies put tremendous efforts to explore the effects of Treg cell depletion via targeting CD25 by antibodies or a recombinant protein composed of IL-2R with the active domain of diphtheria toxin (Dannull et al., 2005, Foss, 2006, Litzinger et al., 2007, Mahnke et al., 2007). First, an anti-CD25 monoclonal antibody (mAb) was administered in mice to deplete Treg, resulting in tumor rejection and tumor growth inhibition (Onizuka et al., 1999, Shimizu et al., 1999). Later, the anti-CD25 mAb daclizumab was tested in breast cancer patients; vaccination with multiple tumor-associated peptides resulted in prolonged stable disease in 60% of patients with a median progression-free survival of 4.8 months (Rech et al., 2012). In contrast, administration of anti-CD25 mAb daclizumab in melanoma patients showed depletion of both Treg cells and effector T cells, but no anti-tumor immune response nor antibody production was observed, and no significant progression-free survival was observed (Jacobs et al., 2010). Indeed, CD25 expression is induced upon activation of effector T cells, therefore CD25-targeted Treg cell depletion might be accompanied by a reduction of effector T cells, suggesting the limitation of the use of anti-CD25 mAb for Treg cell depletion to increase anti-tumor T cell responses (Abbas et al., 2018, Togashi et al., 2019). In

addition, it should be noted that systemic depletion of Treg cells might increase the risk of autoimmune disorders (Kim et al., 2007). Therefore, it is highly recommended to selectively deplete effector Treg cells, which are abundant in the TME, instead of total Treg cells to ensure the safety of Treg-targeted therapies with efficient antitumor effects (Sugiyama et al., 2013).

CTLA4 is constitutively expressed by CD4+FOXP3+ Treg cells which can be upregulated upon activation of effector T cells. Although, initially, it was assumed that anti-tumor activity of anti-CTLA4 mAb mainly depends on the reinvigoration of dysfunctional CTLA4-expressing effector T cells (Ribas, 2012), later preclinical studies showed that the anti-tumor effect of anti-CTLA4 mAb is dependent on the depletion of CTLA4-expressing Treg cells in the TME through antibody-dependent cellular cytotoxicity, thereby increasing CD8+ Tc:Treg cell ratio (Bulliard et al., 2013, Simpson et al., 2013, Selby et al., 2013, Arce Vargas et al., 2018). Furthermore, only in Treg cells, CTLA4 depletion showed increased anti-tumor immunity in mice, suggesting that anti-CTLA4 mAb-mediated anti-tumor effects are mainly due to the successful suppression of Treg cell function and elimination of Treg cells in the TME (Ohue and Nishikawa, 2019, Togashi et al., 2019). However, further investigations are needed to elucidate the functional roles of CTLA-4 in effector T cells and Treg cells in different human cancer settings.

CCR4 expressed in Treg cells binds to its associated ligands CCL17 and CCL22, which are mainly produced by tumor cells and tumor-associated macrophages (Cinier et al., 2021). Depletion of CCR4 leads to a reduction in the frequency of tumor infiltrating Treg cells and increased anti-tumor activity (Cinier et al., 2021). A recent study observed no significant reduction in tumor growth when CT-26 tumor-bearing mice were treated with the CCR4 antagonist CCR4-351 alone, while treatment with the combination of CCR4-351 and anti-CTLA4 mAbs showed a significant anti-tumor effect (Marshall et al., 2020). In addition, a potent small molecule (piperidinyl-azetidines) antagonist of CCR4 was recently developed to inhibit Treg cell recruitment in the TME without affecting Treg cells in healthy tissue (Jackson et al., 2019, Robles et al., 2020). To date, several CCR4 antagonists have been analyzed preclinically and their effects on Treg recruitment and anti-tumor efficacy have been successfully observed. For example, FLX475 is one of the most potent CCR4 antagonists that is in

phase I/II and is being studied to determine its efficacy and antitumor activity both as monotherapy and in combination with pembrolizumab or ipilimumab (Ho et al., 2019, Powderly et al., 2020). Notably, an anti-CCR4 mAb named mogamulizumab was approved for the treatment of T cell leukemia and/or lymphoma (ATLL), and a study showed that mogamulizumab effectively depletes not only ATLL cells but also Treg cells (Sugiyama et al., 2013). In addition, mogamulizumab was tested in patients with lung cancer and oesophageal cancer where it was found to be safe and well-tolerated with no dose-limiting toxicities (Kurose et al., 2015). Also, mogamulizumab is currently tested as an effector Treg cells depletion agent alone and in combination with nivolumab with either anti-PDL1 mAbs durvalumab or tremelimumab or with the anti-4-1BB agonistic mAb utomilumab in patients with advanced-stage solid tumors (Doi et al., 2019). A phase I study of the combination of mogamulizumab with nivolumab showed no dose-limiting toxicities but clinical responses in hepatocellular carcinoma, gastric cancer and pancreatic carcinoma (Doi et al., 2019).

Targeting co-stimulatory and co-inhibitory molecules on Treg cells

Treg cells constitutively express immune co-stimulatory and co-inhibitory molecules, which are also being investigated as targeted for therapies against Treg cells. There are different co-stimulatory molecules such as GITR, 4-1BB, OX40, CD27, ICOS and co-inhibitory molecules such as CTLA4, PD1, TIGIT, LAG3, TIM-3 that regulate the biology of Treg cells (Togashi and Nishikawa, 2017, Togashi et al., 2019, Ohue and Nishikawa, 2019). Briefly, OX40 (TNFRSF4) is a co-stimulatory molecule of the tumor necrosis factor receptor super family expressed by effector T cells as well as Treg cells, which can be considered as a potential candidate for Treg cell depletion (Togashi et al., 2019, Cinier et al., 2021). To date, various OX40 agonists have been clinically investigated alone or in combination with other immunotherapies or stereotactic body radiotherapy in patients with advanced-stage solid tumors, B cell lymphoma, head and neck cancer, metastatic breast cancer etc. (Jensen et al., 2010, Ohue and Nishikawa, 2019). Notably, in a phase-I study, mouse anti-OX40 agonistic mAb showed promising anti-tumor activity but no objective clinical responses were observed in advanced-stage solid tumors such as melanoma or renal cell carcinoma (Curti et al., 2013). Furthermore, human anti-OX40 agonistic mAb monotherapy resulted in stable disease

for more than six months with an increased number of memory T cells in patients previously treated with immunotherapies (Hamid et al., 2016).

GITR (TNFRSF18) is another co-stimulatory molecule that is highly expressed by Treg and weakly expressed by resting CD4+ Th cells and CD8+ Tc cells, represents a potential candidate for Treg depletion (Knee et al., 2016, Mahne et al., 2017). A relevant study showed that agonistic GITR mAb DTA-1 is effective in reducing FOXP3 expression in Treg cells, functional activities and Treg cell numbers in the TME but can stimulate tumor immunity (Knee et al., 2016, Murakami et al., 2021). Furthermore, it has also been discovered that agonistic GITR mAbs can reprogram Treg cells into IFN-γ expressing Th1 cells as well as alleviates the inhibition of anti-tumor response of Treg cells in murine glioblastomas (Amoozgar et al., 2021). Clinical studies have shown that GITR mAb agonists can effectively deplete Treg cells and effector T cells can proliferate into Treg cells, however only limited clinical results have been observed (Zappasodi et al., 2021). Notably, compared to monotherapy, the combination of GITR mAb MK-1248 with the anti-PD-1 mAb pembrolizumab in patients with advanced solid tumors showed more acceptable safety profiles and anti-tumor responses (Buzzatti et al., 2019, Geva et al., 2020). Therefore, despite the ability to deplete Treg cells, it is recommended that GITR mAbs be used in combination with other immunotherapies to achieve the maximum benefit for Treg depletion.

ICOS (CD278) is associated with the production, proliferation, survival and immunosuppressive capacity of Treg cells (Li and Xiong, 2020a). An agonistic anti-ICOS mAb JTX-2011 (vopratelimab) plays a dual role in effector T cell activation and selective Treg cell depletion (Yap et al., 2018, Hanson et al., 2020). In mice, JTX-2011 monotherapy demonstrated potent anti-tumor activity, which was further improved when JTX-2011 was administered in combination with immune checkpoint inhibitors (Hanson et al., 2020). In a phase II study, the disease control rate of agonistic anti-ICOS mAb JTX-2011 monotherapy was 19%, while it increased to 32% when JTX-2011 co-administered with nivolumab in gastric cancer (Burris et al., 2017, Yap et al., 2018). In addition, a new ICOS immunoglobulin G1 antibody (KY1044) was recently developed, which can effectively deplete ICOS+ Treg cells and increase the ratio of effector T cells to Treg cells (Sainson et al., 2020).

Immune checkpoint inhibitors

Although the effects of PD-1 blockade on Treg cells remain controversial, the anti-PD-1 mAb has received considerable attention due to its potent ability to inhibit immune checkpoints and has become a promising therapeutic approach in the treatment of tumors (Wu et al., 2019). PD-1 inhibits excessive activation of effector T cells by suppressing T cell receptor and CD28 signaling and rendering them dysfunctional or exhausted (Yokosuka et al., 2012, Kamphorst et al., 2017, Hui et al., 2017). As Treg cells in the TME show comparable expression of PD-1 to that of effector T cells and are dependent on T cell receptor and CD28 signaling, it is presumed that PD-1 inhibition effectively alters the activation and immunosuppressive function of Treg cells (Zhang et al., 2013a, Weissler and Caton, 2014, Levine et al., 2014, Togashi et al., 2018). A recent study showed, that PD-1-deficient Treg cells possess potent immunosuppressive activity and rescue autoimmune phenotypes (Zhang et al., 2016). In addition, Treg cells highly expressing PD-1 in glioblastoma showed reduced immunosuppressive function (Lowther et al., 2016), while anti-PD-1 mAb nivolumab increases proliferation and immunosuppressive function of Treg cells in the TME in gastric cancer patients with hyper-progressive disease (Togashi et al., 2018). The effect of anti-PD-1 mAb or PD-1 deficiency on Treg cell-mediated immunosuppression was further confirmed in *in vitro* and *in vivo* studies (Togashi et al., 2018, Togashi et al., 2019). In contrast, another study showed that PD-1-inhibited Treg cells have low immunosuppressive activity, suggesting that further analysis is important to elucidate the functional role of PD-1 in Treg cells as well as effector T cells in different types of cancer (Gianchecchi and Fierabracci, 2018). Other checkpoints such as TIGIT, LAG-3 and TIM-3 inhibitors have also been evaluated and most of them are in clinical trials.

1.4.5 Treg cells in the testis

Treg cells have been identified in mammalian testes, including mice (Wheeler et al., 2011), rats (Jacobo et al., 2009) and humans (Duan et al., 2011), and are mainly found in the testis-draining lymph nodes, where they interact with tissue-specific autoantigens and maintain their suppressive function (Garza et al., 2000). Under normal conditions, Treg cells are able to effectively control effector T cells through various immunosuppressive mechanisms and maintain a balance between effector T

cells, by this positively regulating testicular homeostasis. On the other hand, Treg cells are present in pathological states (e.g., testicular chronic inflammation, infection) and increased Treg cell numbers disrupting the balance between Treg and effector T cells, result in impaired spermatogenesis, autoimmune orchitis, and/or azoospermia (Gong et al., 2020).

Briefly, in EAO, Treg cells were increased in testis-draining lymph nodes compared to lymph nodes from the site of immunization with a memory or activated phenotype (Jacobo et al., 2015). It was also shown that Treg cells from testis-draining lymph nodes of normal and EAO rats elicit a strong proliferative response to germ cell-specific antigens and exhibit suppressive effects preventing proliferation of conventional T cells (Jacobo et al., 2015). Compared to normal rats, Treg cells from EAO animals show a more suppressive phenotype, possibly due to their higher expression of TGF-β and testicular inflammatory microenvironment that stimulates Treg cell activation (Jacobo et al., 2015). In humans, defects in testicular Treg cells are involved in the pathogenesis of autoimmune polyendocrinopathy-candidiasis-ectodermal dystrophy (APECED) (Kekäläinen et al., 2007). Furthermore, in vasectomized mice, Treg cells mediated immune tolerance to meiotic germ cell antigens egressing from normal tubules, while depletion led to a meiotic germ cell antigen-specific autoimmune response and bilateral orchitis, suggesting the possible role of Tregs in preventing organ-specific autoimmunity (Wheeler et al., 2011, Tung et al., 2017). Interestingly, functional studies of Treg cells in testes have shown conflicting results. For example, in human azoospermia with chronic inflammation, a reduced number of Treg cells and an increased level of the pro-inflammatory cytokine IL-17 were detected, while in rats, an increased number of Treg cells was detected at the onset of EAO and later gradually decreased during chronic phase (Jacobo et al., 2009, Duan et al., 2011). This discrepancy between humans and rats is most likely due to the use of different antibody panels to identify Treg cells (Gong et al., 2020). In addition, Siska et al. identified Treg in human TGCT (Siska et al., 2017b).

1.5 T follicular helper (Tfh) cells

Tfh cells are specialized cell types of CD4+ Th cells that differentiate into germinal center (GC, is a specialized microstructure that forms in the follicles of secondary

lymphoid tissues where B cells are stimulated by antigens and Th cells to undergo maturation, leading to the generation of memory B cells and plasma cells that produce long-lived, high-affinity antibodies) and play a crucial role in the production of antibodies and memory B cells (Crotty, 2015, Mayberry et al., 2022). These cells have the unique ability to migrate in and out of GC as they complete their differentiation and hence, they can be found in the GC, at the T: B junction, or become extrafollicular Tfh cells (Shulman et al., 2013, Ribeiro et al., 2022). Tfh cells maintain a core transcriptional signature and express specific markers based on their location (Haynes et al., 2007, Kerfoot et al., 2011, Shi et al., 2018, Ribeiro et al., 2022). For example, GC-Tfh cells strongly express *CXCR5, ICOS and PD-1* and weakly express *PSGL-1* and produce CXCL13 (in humans but not in mice) and IL-21, while extrafollicular Tfh cells in the T cell zone strongly express PSGL-1 and downregulate CXCR5 (Chtanova et al., 2004, Haynes et al., 2007, Poholek et al., 2010, Ribeiro et al., 2022). In addition, memory Tfh cells derived from GC-Tfh cells upregulate CCR7 but downregulate BCL6, ICOS, and PD-1 (Chevalier et al., 2011, Lüthje et al., 2012, Weber et al., 2012, Sage et al., 2014, Ribeiro et al., 2022).

1.5.1 Molecular and cellular biology of Tfh

The interaction of naïve CD4+Th cells with APCs (mostly DCs) is the starting point for the differentiation of Tfh cells (Figure 1.5). The fate decision of CD4+ Th cells *in vivo* is determined as early as the second cell division whether they become Tfh cells or non-Tfh cells (Crotty, 2019, Choi and Crotty, 2021a, Mayberry et al., 2022). After differentiation, non-Tfh cells such as Th1, Th2, Th17, Th9 cells leave the lymphoid tissue and migrate to sites of infection or inflammation, while Tfh cells remain in the lymph nodes and spleen because of their purpose to support B cells (DiToro et al., 2018, Crotty, 2019). Both antigen presenting DCs and B cells are required for normal Tfh cell differentiation (Crotty, 2014, Crotty, 2019). For example, DCs are required for early differentiation of Tfh cells, while B cells are required for later events and full maturation of GC-Tfh (Crotty, 2014, Crotty, 2019, Mayberry et al., 2022). Although both DCs and B cells provide similar signals, only DCs are capable of priming CD4+ Th cells, but not B cells (Hong et al., 2018, Crotty, 2019). Nonetheless, B cells excessively produce various cytokines, including IL-6, which may facilitate differentiation of Tfh cells (Karnowski et al., 2012). Activated B cells strongly express

MHC class II and co-stimulatory molecules such as CD80 and CD86, which make B cells more potent APCs for Tfh cells (Crotty, 2019). In addition, activated B cells can migrate to the marginal zone of T cell-B cell junction to increase their likelihood of interacting with Tfh cells (Crotty, 2019).

As previously mentioned, DCs are capable of priming CD4+ Th cells, and upon priming by DCs, CD4+ Th cells received Tfh cell-induction signals that upregulate BCL6, which is a master transcription factor for Tfh differentiation, proliferation and function (Hollister et al., 2013, Crotty, 2019, Choi and Crotty, 2021a). BCL6 can regulate differentiation and function of Tfh cells through several aspects, however, most available data indicate that BCL6 is an obligate repressor of gene expression (Hatzi et al., 2013, Hatzi et al., 2015, Béguelin et al., 2016). Briefly, BCL6 expression levels can be upregulated by activating CD28 and downregulating cytokines that activate STAT1 or STAT3 or both (Weber et al., 2015, Vinuesa et al., 2016). BCL6 can repress BLIMP1 (PRDM1), which is a negative regulator of Tfh cells differentiation (Johnston et al., 2009, Choi et al., 2020, Choi and Crotty, 2021a). In addition, BCL6 downregulates various genes such as *CCR7, CCR6, EB12, S1PR1 and PSGL1* by binding to their promoters and enhancers, thereby inhibiting the exit from secondary lymphoid organs and stimulates the migration of Tfh cells to the marginal zone of T cell-B cell junction or central part the follicle or both (Suan et al., 2015, Hatzi et al., 2015, Vinuesa et al., 2016, Choi and Crotty, 2021a). Supplementary analysis also revealed that BCL6 can repress promoters and enhancers of other genes, cytokines, receptors involved in the differentiation of other CD4+Th cells (i.e., IFNGR1, TBX21, STAT4, IL-12R, IL-23R for CD4+Th1 cells, IL-4R, GATA3 for CD4+Th2 cells, RORA, IL-17A, IL-17F, IL-23R, TGF-βR for CD4+Th17) (Kusam et al., 2003, Nurieva et al., 2009, Yu et al., 2009, Hatzi et al., 2015, Vinuesa et al., 2016, Choi et al., 2020, Choi and Crotty, 2021a). Furthermore, BCL6 can repress T cell receptor signaling via AKT, IL-7R and several microRNAs associated with Tfh cell biology (Hatzi et al., 2015, Choi et al., 2020, Choi and Crotty, 2021a). Importantly, overexpression of BCL6 upregulates various Tfh cell effector molecules such as PD-1, CXCR4, CXCR5 and SAP (Hatzi et al., 2015, Crotty, 2019, Choi et al., 2020, Choi and Crotty, 2021a). In addition to BCL6, other transcription factors are also involved in the differentiation of Tfh cells. For example, c-MAF induced by ICOS signaling induces IL-21, which positively regulates the differentiation of Tfh cells as well as Th1 and Th17 cells (Bauquet et al., 2009).

BATF, another transcription factor, induces transcription of BCL6 and c-MAF, which are required for GC-Tfh cells (Betz et al., 2010). Likewise, SATA1 and SATA3 induce IL-21 and IL-6, favoring Tfh cell differentiation by regulating BCL6 expression (Nurieva et al., 2009, Vinuesa et al., 2016). There are other transcription factors like IRF4 (Bollig et al., 2012), ASCL2 (Liu et al., 2014), TCF-1 (Xu et al., 2015, Choi et al., 2015), EGR2 (Ogbe et al., 2015) etc. that have been also characterized as a critical regulator of Tfh cell differentiation. In contrast, quite a few transcription factors such as FOXO1, FOXP1, BLIMP1, and KLF2 repress Tfh cell differentiation. For example, FOXO1 regulates the differentiation of Tfh cells through negative regulation of BCL6 (Stone et al., 2015), while FOXP1 suppresses the expression of ICOS and IL-21 upon activation of the T cell receptor and thus negatively regulates the differentiation of Tfh cells (Wang et al., 2014).

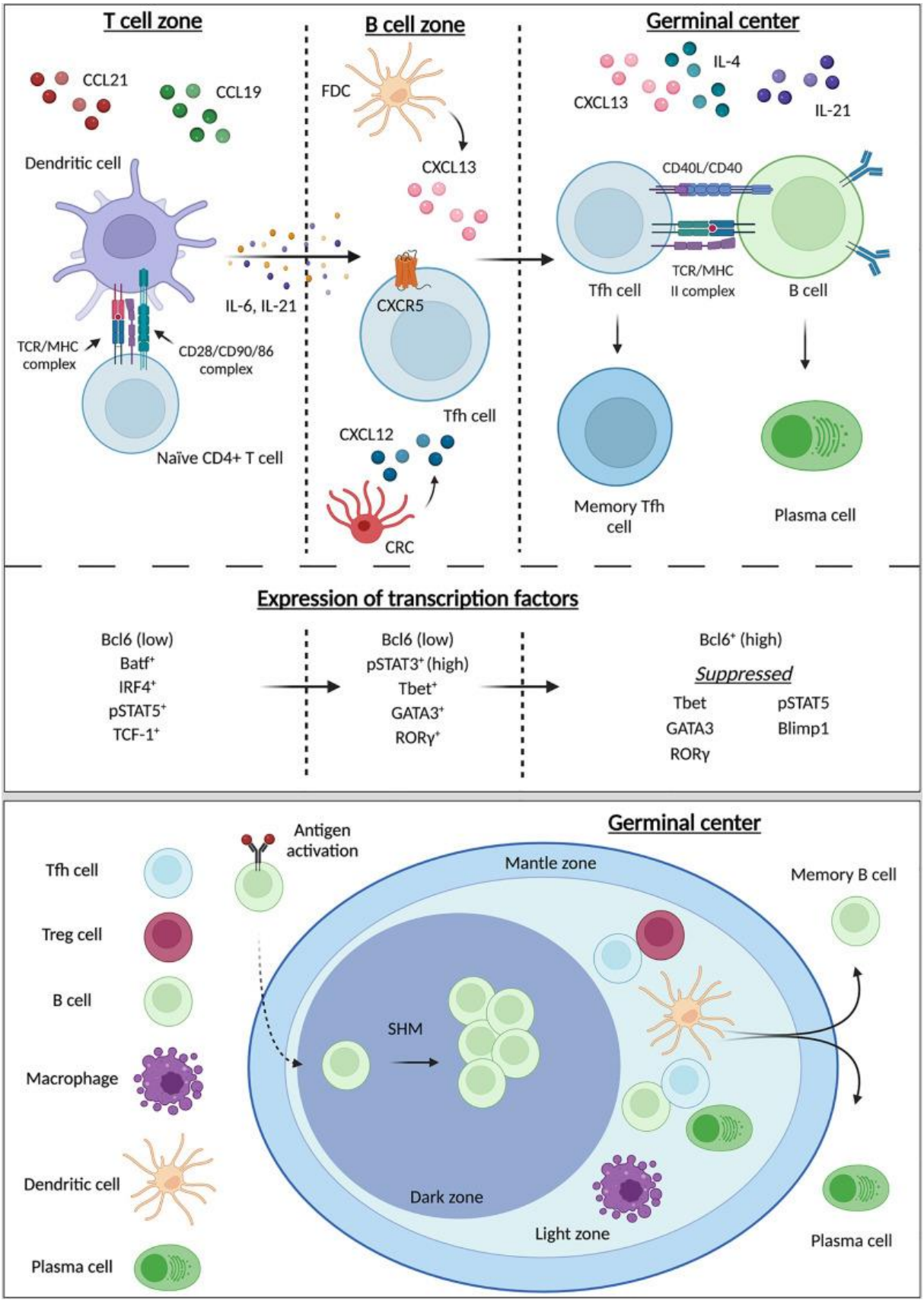

Figure 1.5 See next page for caption.

Figure 1.5 Differentiation and maturation of Tfh cells. Tfh cell differentiation begins in the T cell zone through interaction between DCs and naïve CD4+ T cells, and final maturation occurs within the GC. IL-6 and IL-21 produced by interaction between DCs and naïve CD4+ T cells upregulate CXCR5 on the pre-Tfh cells and stimulate CXCL13 production by follicular DCs (FDC) and CXCL12 by CXCL12-producing reticular cells (CRC) in the B cell zone. CXCR5-CXCL13 binding stimulates recruitment of immature Tfh cells to the B-cell zone, and both CXCR5 and ICOS signaling support Tfh cell migration into the GC. Finally, Tfh cells interact with B cells in the GC and produce plasma cells for antibodies production. The entire process is crucially regulated by the expression of various transcription factors. The GC consisted with different zones with special properties. For example, T cell homing and interaction between T cells and B cells mostly occurs in the light zone, while B cells differentiated into plasma cells and long-lived memory B cells within the dark zone. Adopted from Mayberry et al. (Mayberry et al., 2022).

BLIMP1, induced by STAT5 and IL-2 signaling, can antagonize the function of BCL6, thereby inhibiting the differentiation of Tfh cells and promoting the formation of other effector T cells (Johnston et al., 2009, Johnston et al., 2012). Also, KLF2 promotes the expression of various genes such as Blimp1, TBX21, and GATA3 that negatively regulate Tfh cell differentiation (Lee et al., 2015, Weber et al., 2015). In addition to transcription factors, different co-stimulatory molecules play important roles in the differentiation and maintenance of Tfh cells. During Tfh cell differentiation, both positive costimulatory molecules like CD28, ICOS, SAP and negative costimulatory molecules like CTLA4 (CD152), PD1, BTLA cooperate with T cell receptor signals to regulate activation, proliferation, differentiation, migration, survival, and effector functions (Ramiscal and Vinuesa, 2013, Jogdand et al., 2016, Vinuesa et al., 2016, Qin et al., 2018). Markedly, disruption of the balance between positive and negative co-stimulatory signaling leads to increased Tfh cell and consequently Tfh-derived autoimmunity (Gong et al., 2016, Qin et al., 2018). CD28 binds to its ligands CD80 or CD86 and regulates T cell-dependent B cell responses (Qin et al., 2018). However, various studies have shown a controversial finding that loss of CD28 or CD28 blockade may or may not be associated with a reduction in the number of Tfh cells, suggesting that in some situations the requirement for CD28 for maintenance of Tfh cells can be replaced by other functional molecules such as ICOS (Linterman et al., 2014, Weber et al., 2015). Nevertheless, CD28 signaling can regulate the expression of PD-1, ICOS, OX40, CXCR5 and BCL6 in the early stage of Tfh cell differentiation and maintain Tfh cell survival (Linterman et al., 2014, Weber et al., 2015).

ICOS is one of the most functional co-stimulatory molecules critically associated with Tfh cell differentiation and GC formation (Jogdand et al., 2016, Wali et al., 2016). Generally, ICOS signaling is essential for T cells help to B cells (Vinuesa et al., 2016). In contrast to CD28, which is mainly involved in the early stages of Tfh cell differentiation, Tfh cell specific ICOS plays an important role in maintaining the phenotype of already differentiated Tfh cells (Weber et al., 2015). Relevant studies showed that the absence or disruption of ICOS results in fewer Tfh cells and smaller GC in both mice and patients (Nurieva et al., 2008, Weber et al., 2015). The co-stimulatory function of ICOS is exerted through PI3K signaling, and ICOS-PI3K signaling via AKT promotes differentiation of Tfh cells (So and Fruman, 2012, Weber et al., 2015). Furthermore, activation of the PI3K-AKT pathway phosphorylates FOXO1, which remains in the cytoplasm and becomes functionally inactive (Weber et al., 2015). Notably, inactive FOXO1 abolishes its repression of BCL6 expression and its activation of KLF2 expression, thereby promoting the formation of Tfh cells (Kerdiles et al., 2009, Stone et al., 2015, Weber et al., 2015). Moreover, ICOS also plays a role in Tfh maintenance. For example, the interaction between ICOS:ICOSL promotes calcium flux in Tfh cells and shift the localization of Tfh cells and B cells to the outer edge of the GC (Liu et al., 2015), while suppression of ICOS-mediated KLF2 helps to keep Tfh cells in the GC and prevent them from translocating to the T zones (Weber et al., 2015, Lee et al., 2015). GC-Tfh cells express SAP ((SLAM (signaling lymphocyte activation molecule)-associated protein)), which plays an important role in the formation of GC, long-lived plasma cells, and memory B cells (Crotty et al., 2003, Yusuf et al., 2010, Cannons et al., 2011). Notably, SAP is not required for early stages of Tfh cell differentiation but is obligatory for sustained T:B cell interactions and full polarization to GC-Tfh cells through binding to immunoreceptor tyrosine-based switch motif (ITSM) and and competition with the tyrosine phosphate SHP-1 for the Ly108-ITSM binding (Latour et al., 2003, Cannons et al., 2010). PD-1 (PDCD1) is a member of the CD28 superfamily that is highly expressed by exhausted T cells, Treg, Tfh, as well as B cells, NK cells, and myeloid cells and plays a critical role in formation, proliferation, and function these cells (Qin et al., 2018). Regarding Tfh cells, PD-1 is highly expressed in Tfh cells from old mice compared to Tfh cells from young mice, and PD-1 blocked from old mice can restore the function of Tfh cells, suggesting a cellular intrinsic role of PD-1 in Tfh cells (Lages et al., 2010, Sage et al., 2015). However, it should be noted that PD-1 expressed by DCs can inhibit the differentiation

of Tfh cells (Badell et al., 2018). In contrast to other CD4+ Th cells, neither a specific cytokine is obligatory for the differentiation of Tfh cells, nor a single cytokine alone capable for Tfh cell differentiation, but the cumulative presence of various cytokines facilitates the differentiation of Tfh cells. Generally, IL-6, IL12, TGF-β positively regulate the differentiation of Tfh cells (Yan et al., 2017, DiToro et al., 2018, Crotty, 2019), while IL-2 is the most potent inhibitor of Tfh cell differentiation (Ballesteros-Tato et al., 2012, DiToro et al., 2018). Although the surface protein marker phenotype, gene expression profile, and BCL6 expression of mouse and human GC-Tfh cells are similar, the cytokines involved in Tfh cell differentiation appear to differ substantially between these two species (Crotty, 2019).

In humans, different cytokines such as IL-12, IL-23, and TGF-β support Tfh cell differentiation (Schmitt et al., 2014, Vinuesa et al., 2016). Human naïve CD4+ Th cells can be activated in the presence of IL-12 and IL-23 and strongly express Tfh cell-specific markers including *CXCR5, ICOS, and BCL6* (Schmitt et al., 2009, Ma et al., 2009). Furthermore, the multifunctional cytokine TGF-β in conjunction with IL-12 and IL-23 activates STAT3 and STAT4 and induces Tfh cells (Schmitt et al., 2014). Moreover, human plasmablast-derived IL-6 also appears to increase circulating Tfh cells (Chavele et al., 2015). In contrast to humans, IL-6 and IL-21 play central role in the differentiation of Tfh cells in mice (Vinuesa et al., 2016). A previous study showed that IFN can stimulate IL-6 production by DCs, thereby increasing Tfh cell differentiation (Cucak et al., 2009). In addition, IL-6 can initiate BCL6 expression, which is the core regulator of Tfh cell differentiation and maintenance with the help of other factors (Eto et al., 2011, Vinuesa et al., 2016, Crotty, 2019). Loss-of-function studies of IL-6 or its receptor in mice showed reduced or delayed formation of Tfh cells due to impaired signaling by STAT1 and STAT3 (Nurieva et al., 2008, Karnowski et al., 2012, Choi et al., 2013). In contrast, the functional role of IL-21 in the formation of Tfh cells was examined *in vivo* and showed that IL-21-deficient mice had a lower number of Tfh cells and IL-21R-deficient T cells that were intrinsically impaired in Tfh cell formation, suggesting that there is an autocrine regulation of Tfh cells (Vogelzang et al., 2008, Nurieva et al., 2008). Furthermore, collective blocking of IL-6, IL-7 and IL-21 following viral infection showed complete inhibition of Tfh cell differentiation (Nurieva et al., 2008). In addition to cytokines positively associated with Tfh cell differentiation, elevated levels of the pleiotropic cytokine IL-2 inhibit Tfh cell

differentiation (Ballesteros-Tato et al., 2012, León et al., 2014, DiToro et al., 2018). Mechanistically, IL-2-dependent activation of STAT5 enhances BLIMP1 expression and displaces STAT3 from binding to the BCL6 locus, thereby inhibiting Tfh cell differentiation (Johnston et al., 2009, Johnston et al., 2012, Nurieva et al., 2012, Oestreich et al., 2012). Furthermore, inhibition of signaling by IL-10R was also shown to increase Tfh cell number, suggesting that IL-10 negatively regulates Tfh cell formation (Cai et al., 2012).

1.5.2 How do Tfh cells interact with B cells?

GC B cells, plasma cells, and Tfh cells are interdependent, which is considered to be one central aspect to the regulation of humoral immunity (Crotty, 2019). Tfh cells can migrate to the T:B junction during their early differentiation and interact with antigen-specific B cells (Crotty, 2019). Relevant evidence showed that most B cells die within 24 hours of antigen recognition and their response cannot further progress without the support of helper T cells, including Tfh cells (Akkaya et al., 2018, Crotty, 2019). Tfh cells provide IL-21 and CD154 (CD40L) signaling required for B cell proliferation and differentiation toward both GC as well as extrafollicular fates (Lee et al., 2011). At the GC T cell-B cells junction, B cells compete for support from Tfh cells, and their competitive success depends on their abundance and antigen affinity (Schwickert et al., 2011, Abbott et al., 2018, Yeh et al., 2018). B cell maturation and antibody affinity maturation occur in GC consisting of light zones containing GC-Tfh cells, follicular DCs and GC-B cells (Figure 1.5) (Crotty, 2019, Mayberry et al., 2022). In addition to follicular DCs that provide antigens to the GC-B cells (Heesters et al., 2013, Heesters et al., 2016). GC-Tfh cells also help GC-B cells with higher expression of peptide–MHCII (major histocompatibility complex class II (MHCII)) (Gitlin et al., 2014, Ersching et al., 2017). Notably, the portion of GC-B cells that do not receive support from the GC-Tfh cells die, while the GC-B cells supported by the GC-Tfh cells migrate to the dark zone and undergo rounds of division and division-linked somatic hypermutation (Gitlin et al., 2014, Ersching et al., 2017). Furthermore, in addition to CD154 (CD40L), B cells cooperatively express IL-21 and IL-4 to obtain maximum support from GC-Tfh cells (Weinstein et al., 2016). In contrast, it has also been shown that GC-Tfh can often kill GC-B cells directly via FasL-Fas, however, only a small amount of FasL expressed

by GC-Tfh cells and its role in GC selection yet to be proven (Bentebibel et al., 2011, Butt et al., 2015).

As mentioned more generally above, there are some differences between mouse and human Tfh cells. For example, human GC-Tfh cells, but not mice Tfh cells, secrete dopamine that enhances rapid ICOSL surface expression by human GC-B cells and creates a feedforward help loop between interacting Tfh cells and B cells in the GC (Papa et al., 2017). In addition, some human GC-Tfh cells express IL-10, which is a known factor for B cell differentiation, but mouse IL10-expressing Tfh cells are believed to support B cells, but their biology is not clear yet (Bryant et al., 2007, Xin et al., 2018). In addition to the selection of high-affinity GC-B cells, GC-Tfh cells decisively regulate the differentiation of GC-B cells into memory B cells, and plasma cells thus develop long-term humoral immunity (Crotty, 2019). For example, differentiating plasma cells with ki67 expression, also known as plasma blast, induced by IL-21 from GC-Tfh cells (Zhang et al., 2018). Further studies also showed that GC-Tfh-secreted IL-21 that required to induce BLIMP1 expression in early plasma cells expressing high IRF4 and low BCL6 to complete their cell fate (Kräutler et al., 2017, Ise et al., 2018).

1.5.3 Tfh cells in cancer

Compared to other diseases, Tfh cells show the most surprising association with cancer. Accumulating evidence revealed that Tfh cells are positively correlated with long-term survival of various human cancers such as breast cancer, colon cancer, pancreatic ductal adenocarcinoma, etc. (Bindea et al., 2013, Gu-Trantien et al., 2013, Gu-Trantien et al., 2017, Lin et al., 2021). Tfh cells have been identified in breast cancer as residents of peri-tumoral tertiary lymphoid structures and are associated with CXCL13 expression (Gu-Trantien et al., 2013). CXCL13 is a B cell chemoattractant that primarily regulates the immune protective functions of Tfh cells (Vinuesa et al., 2016). Interestingly, in colorectal cancer, CXCL13 has been found in both T cells and tumor cells, and loss of CXCL13 leads to reduced numbers of B cells and Tfh cells (Bindea et al., 2013). It is known that GC-Tfh cells in human lymphoid organs are a potent CXCL13 producer and also co-express PD-1, CXCR5, ICOS, BCL6, and CD200 (Kim et al., 2004, Rasheed et al., 2006, Yu and Vinuesa, 2010,

Wang et al., 2011, Kroenke et al., 2012, Havenar-Daughton et al., 2016, Gu-Trantien et al., 2017). However, in human breast cancer, CXCL13+CD4+ T cells with several characteristics of GC-Tfh cells were CXCR5 negative (Gu-Trantien et al., 2013, Buisseret et al., 2017). Furthermore, CXCR5-CXCL13+CD4+ T cells were also observed in melanoma tumors and rheumatoid synovitis but were not considered as Tfh cells due to the absence of CXCR5 (Manzo et al., 2008, Kobayashi et al., 2013, Li et al., 2019).

The existing evidence shows that Tfh cells can develop or support tertiary lymphoid structures to recruit CD8+ Tc cells, NK cells, and macrophages involved in the anti-tumor immune response (Vinuesa et al., 2016). In addition, it is also hypothesized that Tfh cells support anti-tumor antibody responses from B cells, although little data is available for this hypothesis, hence further studies are needed to uncover the antigen specificity of the B cell co-localized with Tfh cells in tumors (Vinuesa et al., 2016, Garaud et al., 2018). It is important to mention, that Tfh cells are not only positively associated with the long-term survival of patients with various types of cancer, but they can also be negatively associated with the survival of cancer (Shalapour et al., 2017). For example, in contrast to breast cancer and colon cancer, where Tfh cells were positively associated with survival, Tfh cells are negatively associated in hepatocellular carcinoma, with a prominent role of IgA+ plasmablasts, suggesting the complexity of Tfh cell biology in cancer (Shalapour et al., 2017). Although Tfh cells have been characterized under various physiological and pathological conditions, no study on Tfh cells in human testis has been performed to our knowledge. Therefore, this study attempted for the first time to uncover the functional involvement of Tfh cells in normal testes and in the development and progression of human testicular cancer.

1.6 Project rationale and objectives

To answer a long-awaited unsolved question of whether the infiltrating immune cells reflect an anti-tumor response (immune surveillance) or whether they are positively associated with an inflammatory and/or autoimmune response in human TGCT, a broad-spectrum analysis of the infiltration density and distribution of different immune cells such as T cells, B cells, macrophages, and DCs was performed by immunohistochemical analysis (IHC) in retrospective human testicular specimens from diseased testis including HYP with lymphocytic infiltrates (HYP+ly), GCNIS with and without lymphocytic infiltrates (GCNIS ± ly) and seminoma compared to the healthy NSP without lymphocytic infiltration. In addition, this study intensely focused on the analysis of T cells, including their main subtypes CD4+Th cells and CD8+Tc cells, in human TGCT. As described in the Introduction, both Th and Tc cells can be further differentiated into distinct subtypes with specific roles in disease development and progression. Among the different subtypes of CD4+Th cells, Treg and Tfh cells have drawn our attention because these two cell types have been extensively studied and characterized as critical regulators of the development and progression of various types of cancer (Togashi et al., 2019, Baumjohann and Brossart, 2021), yet their involvement in the development and progression of human TGCT remains to be elucidated. Therefore, we aimed to identify and characterize Treg and Tfh cells in human TGCT compared to non-cancerous ("normal") testis by IHC. Although the semi-quantitative analysis of infiltrating immune cells by IHC can primarily provide an indication of the relationship between the composition of infiltrating immune cells and disease states, it is not yet sufficient to achieve a clinical impact (Paijens et al., 2021). Therefore, high-throughput flow cytometry (employing two panels of antibodies) was used to analyze and quantify different infiltrating immune cells using prospective fresh human testicular samples (containing heterogeneous cells) from the different areas of the tumor-bearing (tumor central: Tumor; Tumor-Adjacent: Tumor-Adj; Tumor-Distant: Tumor-Dis) and contralateral "normal" testis (Contralateral 1; Contralateral 2) to support our detailed phenotypic analysis of different infiltrating immune cells in human normal testis and TGCT samples by IHC as well as to understand the complexity of infiltrating immune cells. By this, we aimed to translate the immune cell composition into a prognostic tool in human TGCT as well as to improve personalized immune therapy.

In addition, scRNA-seq of normal testes (n=3; pooled data) and TGCT (n=4) were performed for further in-depth analysis of the immune cells, including T cell subsets and their signatures in human testicular samples. Finally, an *ex vivo* approach - hanging drop culture of human testicular tissue was preliminary used to analyze tumor infiltrating immune cells, and we do believe that this approach would help to elucidate the underlying mechanism of the involvement of infiltrating immune cells in the onset and progression of TGCT, which is limited by the lack of experimental animal models, with the ultimate goal of understanding the functional details of "immune editing" during TGCT initiation and progression.

2 MATERIAL AND METHODS

2.1 Patients

To perform comprehensive phenotypic characterization of the infiltrating immune cells by IHC analysis, a retrospective patient cohort was utilized. Testicular specimens were collected from men who underwent testicular biopsies during andrological evaluation for infertility (Bergmann and Kliesch, 2010, Teixeira et al., 2019, Fietz and Kliesch, 2022), during a vasectomy reversal, or during testicular cancer surgery at the Department of Urology, Pediatric Urology and Andrology at Giessen University Hospital and at the Department of Clinical Andrology, Center for Reproductive Medicine and Andrology at the University of Münster, Germany.

For flow cytometric analysis, patient samples were used from the prospective Giessen TGCT cohort. From this cohort, fresh testicular tissue samples were obtained from patients undergoing testicular cancer surgery (n=25, 23-56 years, median age 34 years) for analysis of immune cell infiltrates by flow cytometry (Table 2.1). A histopathological assessment of excised tissue (rapid sectioning) was performed at the Institute of Pathology, at Giessen University Hospital to confirm the existence of a testicular tumor during surgery**.** In case tumor diagnosis was confirmed, fresh tissues were collected from different areas of the tumor-bearing (Tumor, Tumor-Adj, Tumor-Dis) and contralateral (Contralateral 1 and Contralateral 2) testes (Figure 2.1 and Table 2.1). Tissue fractions were collected directly into RPMI medium and into hanging drop culture medium DMEM F12 (Cat. No.: 21331020, Gibco) + 10% fetal bovine serum (FBS, Cat. No.10500064, Gibco) + 1% penicillin-streptomycin (P/S, Cat. No.15140122, Gibco) + 1X -Insulin Transferrin Selenium (ITS -G, Cat. No: 41400045, Gibco) on ice for flow cytometric analysis and hanging drop culture, respectively (resp.). At the same time, tissues from the same localization were also collected separately and one piece of tissue was snap frozen for RNA extraction and other pieces of tissue were immediately fixed by immersion in Bouin's solution overnight and embedded in paraffin for histological evaluation and IHC analysis**.** Due to the strict ethical restrictions, it was not possible to obtain fresh testis tissue to use for flow cytometry from healthy donors or infertile, azoospermic patients. As an "internal" control, we alternatively collected tissue from the contralateral (not-affected) testis of TGCT patients along with the tumor-bearing testis.

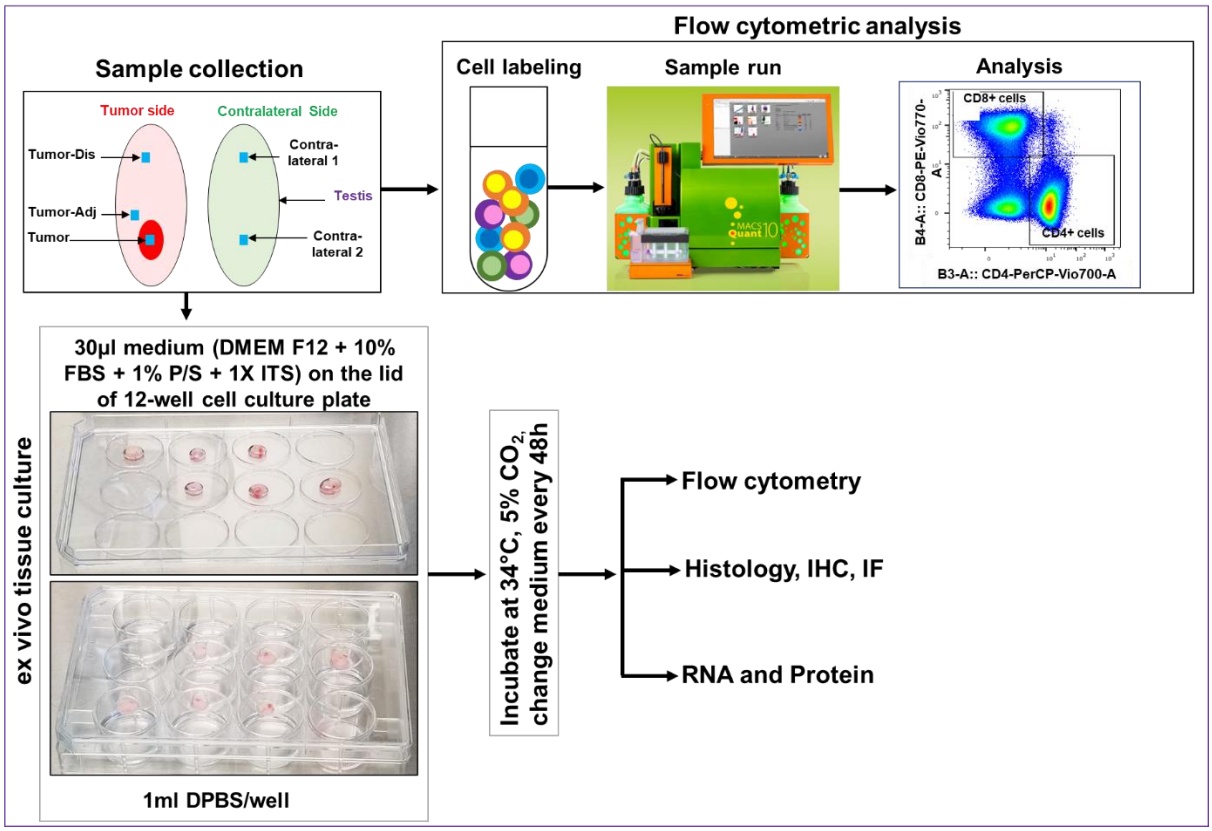

Figure 2.1 Schematic representation of the sampling sites during the surgery of TGCT. (Tumor: center of the tumor; Tumor-Adj: adjacent to the tumor; Tumor-Dis: distant from the tumor; Contralateral 1: upper pole of the contralateral testis, Contralateral 2: lower pole of the contralateral testis), and workflow of the flowcytometric analysis and hanging drop culture.

Typically, it is very rare to develop TGCT in both testes at the same time, and the contralateral testis mostly contains NSP and/or HYP (Table 2.1), which was further considered as a relative control for comparison with tumor-bearing testis. All patients gave their written consent to the use of their tissue samples for research purposes (approved by the ethics committee of the Medical Faculty of the Justus Liebig University Giessen; Ref. No. 26/11; 156/16). For scRNA-seq, human testicular tumor biopsy samples were obtained through the University of Utah Andrology laboratory consented for research (IRB approved protocol #00075836).

Table 2.1 List of patients with their age and different sampling sites as well as their histological assessment. SE: seminoma; Ly: lymphocytic infiltrates; HYP: hypospermatogenesis; GCNIS: germ cell neoplasia in situ; FSC: focal Sertoli cell only syndrome; TS: tubular shadows; BG: interstitial fibrosis; SZA: arrest of spermatogenesis at the level of primary spermatocytes; NSP: normal spermatogenesis; SCO: Sertoli cell only syndrome; FLS: follicular-like structures; EC: embryonal carcinoma; DV: tubular diverticle; Tu: tumor; MSG: multinuclear spermatogonia.

Internal patient number	Age (years)	Tumor and Contralateral side (1= left; 2= right)	Tissue sample location	Tissue weight	Histological assessment (in-house) of each section	Overall clinical histopathological assessment (Primary tumor histology %), notes
HoCa-51	43	1	Tumor	-	SE	100% SE
HoCa-55	35	2	Tumor	-	SE, Ly, HYP, GCNIS	100% SE
			Tumor-Dis	-	HYP, GCNIS, FSC, TS	
HoCa-56	34	2	Tumor	-	SE, BG, Ly, ts, FSC	100% SE
			Tumor-Adj	-	HYP, GCNIS, FSC	
			Tumor-Dis	-	SZA, GCNIS, FSC, Ly	
HoCa-59	27	1	Tumor	129.9 mg	SE+LY	100% SE
			Tumor-Adj	101.4 mg	GCNIS, Ly	
			Tumor-Dis	32.9 mg	GCNIS, Ly, SZA	
HocA-68	37	2	Tumor	114.79 mg	SE, ly	100% SE
			Tumor-Adj	35.79 mg	GCNIS+ Ly	
			Tumor-Dis (sorting)	122.9 mg	HYP+LY	
		1	Contralateral 1 (sorting)	3.3 mg	NSP/HYP	
			Contralateral 2 (sorting)	5.59 mg	NSP/HYP	
HocA-69	45	1	Tumor	40.1 mg	GCNIS, FSC, TS, Ly	100% SE
			Tumor-Adj	9.3 mg	HYP, TS	
			Tumor-Dis	76.7 mg	HYP	
		2	Contralateral 1	20.8 mg	NSP/HYP	
			Contralateral 2	40.12 mg	NSP/HYP	
HoCa-73	54	2	Tumor	1190 mg	SE, Ly	100% SE
			Tumor-Adj	55 mg	SE, TS	
			Tumor-Dis	6.3 mg	FSC, TS, SE	
		1	Contralateral 1	4.9 mg	HYP	
			Contralateral 2	26 mg	HYP	
HoCa-76	36	2	Tumor	29 mg	SCO, TS, Ly	100% SE
			Tumor-Adj	24 mg		
			Tumor-Dis	25 mg		
		1	Contralateral 1	6.5 mg	SCO, TS, Ly	
			Contralateral 2	6.5 mg		
HoCa-78	43	2	Tumor	1827 mg	SE+FLS, Ly	100% SE
		1	Contralateral 1	11.5 mg	HYP	
			Contralateral 2	11.6 mg	HYP	

Table 2.1 continue

Internal patient number	Age (years)	Tumor and Contralateral side (1= left; 2= right)	Tissue sample location	Tissue weight	Histological assessment (in-house) of each section	Overall clinical histopathological assessment (Primary tumor histology %), notes
HoCa-82	56	2	Tumor	516 mg	SE	100% SE
			Tumor-Adj	22.5 mg	TS	
			Tumor-Dis	21.2 mg	TS, FSC	
		1	Contralateral 2	26 mg	HYP	
HoCa-83	39	2	Tumor-Dis	9.8 mg	FSC, TS	100% SE right testis, however, only inflammatory infiltrates but no more tumor in the orchiectomy specimen
			Tumor-Dis	9.3 mg	SCO, TS	
HoCa-84	52	1	Tumor	102 mg	SE/EC, Ly, HYP	100% SE
			Tumor-Adj	36.7 mg	HYP+Ly	
			Tumor-Dis	8 mg	HYP	
		2	Contralateral 1	10.7 mg	HYP	
			Contralateral 2	6.5 mg	DV, HYP	
HoCa-90	32	1	Tumor	3.4 mg	GCNIS, FSC, TS, FLS, Ly	100% SE
			Tumor-Adj	6.3 mg	TS, BG	
HoCa-61	45	2	Tumor	238.6 mg	EC, Ly, SE	80% EC + 20% Post-pubertal Teratoma
			Tumor-Adj	60.4 mg	HYP, SZA	
			Tumor-Dis	71.1 mg	HYP	
HoCa-60	34	2	Tumor	125.7 mg	EC, Ly	95% EC+ 5% Post-pubertal Teratoma
HocA-70	26	2	Tumor	543.2 mg	TS, Tu, EC	99% EC+ 1% SE
			Tumor-Adj	156 g	HYP, GCNIS	
			Tumor-Dis	40.9 mg	HYP	
		1	Contralateral 1	13 mg	HYP, TS	
			Contralateral 2	4 mg	HYP	
HocA-71	25	2	Tumor	147.9 mg	EC, Ly	85% EC+15% Yolk sac
			Tumor-Adj	61 mg	GCNIS	
			Tumor-Dis	35 mg	HYP, SZA	
		1	Contralateral 1	3.9 mg	HYP	
			Contralateral 2	2.9 mg	HYP	
HoCa-79	28	1	Tumor	76 mg	EC, Ly	95% EC+ 5% yolk sac
			Tumor-Adj	64 mg	GCNIS, Ly	
			Tumor-Dis	34 mg	GCNIS, Ly, TS	
		2	Contralateral 1	11 mg	HYP	
			Contralateral 2	14 mg	HYP	
HoCa-80	29	2	Tumor	835 mg	EC, Ly	100% EC
			Tumor-Adj	42.6 mg	GCNIS, SCO, SZA	
		1	Contralateral 1	3 mg	HYP	
			Contralateral 2	15 mg	HYP	
HoCa-64	30	1	Tumor	82.6 mg	EC, LY, TS, FSC	30% EC+70% Post-pubertal Teratoma
			Tumor-Adj	15.6 mg	GCNIS, Ly, TS	
			Tumor-Dis	32.1 g	GCNIS, Ly, TS	
HocA-66	33	2	Tumor	26.4 mg	FSC, Ly	50% SE+ 50%EC (Hematoma + scarring)
			Tumor-Adj	37.5 mg	GCNIS, TS	
			Tumor-Dis	18 mg	GCNIS, Ly	

Table 2.1 continue

Internal patient number	Age (years)	Tumor and Contralateral side (1= left; 2= right)	Tissue sample location	Tissue weight	Histological assessment (in-house) of each section	Overall clinical histopathological assessment (Primary tumor histology %), notes
HocA-67	49	2	Tumor (sorting)	577 mg	SE	70% SE + 30%EC
HocA-72	23	1	Tumor	84.8 mg	FSC, Ly	70% EC+30%SE
			Tumor-Adj	16.2 mg	GCNIS, FSC, TS	
			Tumor-Dis	16.5 mg	GCNIS, TS	
		2	Contralateral 1	12 mg	HYP, BG, SZA, MSG	
			Contralateral 2	1.5 mg	HYP, BG, SZA, MSG	
HoCa-74	26	2	Tumor	118.8 mg	SCO, TU (EC?)	30% post peritubular teratoma+ 20% EC+ Yolk sac tumor. 15%+ small amount of choriocarcinoma (plus GCNIS)
			Tumor-Adj	80.5 mg	HYP, GCNIS, SCO	
			Tumor-Dis	46.9 mg	GCNIS	
		1	Contralateral 1	12.3 mg	NSP/HYP	
			Contralateral 2	49.2 mg	NSP/HYP	
HoCa-86	26	2	Tumor	91.5 mg	GCNIS+Lly	70% SE+ 30% EC
			Tumor-Adj	59.2 mg	GCNIS, HYP	
			Tumor-Dis	23.7 mg	HYP	
		1	Contralateral 1	3.6 mg	HYP	
			Contralateral 2	16.5 mg	HYP	
HoCa-91	24	1	Tumor	39.2 mg	EC, Ly	EC in rapid cut, but in the further processing by Patho primarily GCNIS, percentage breakdown unfortunately not possible.
			Tumor-Adj	49.8 mg	GCNIS, HYP, SZA	
			Tumor-Dis	68.8 mg	HYP	
		2	Contralateral 1	13.5 mg	HYP	
			Contralateral 2	5.9 mg	HYP	
HoCa-93	38	2	Tumor	32.3 mg	tumor? TS, Ly	Not defined yet
			Tumor-Dis	22.2 mg	HYP, SZA	
		1	Contralateral 2	1.1 mg	HYP	

2.2 Human testicular biopsies: Histological evaluation

To perform histological and IHC of human testicular tissues, specimens were immediately fixed by overnight immersion in Bouin's solution and embedded in paraffin. Then, 5 µm thick sections were prepared and stained with hematoxylin and eosin (H&E) for histological evaluation. The overall histopathological assessment was combined with a score count analysis of spermatogenesis. To describe the frequency of tubules containing elongated spermatids, a score count range of 0 to 10 was set, with "0" representing the complete absence of elongated spermatids and "10" representing the presence of elongated spermatids in each tubular cross-section (Bergmann and Kliesch, 2010, Teixeira et al., 2019, Fietz and Kliesch, 2022). At the

same time, a pathological assessment was performed to identify various conditions such as GCNIS and seminoma specimens. For the phenotypic characterization of infiltrating immune cells by IHC analysis, a total of five sample groups were used. The number of samples in each group varied between different antibodies used; these are listed in Table 2.2.

Table 2.2 Number of samples in each group to analyze different immune cells with different antibodies.

Antibody	Number of samples (n) in each group				
	NSP	HYP+ly	GCNIS	GCNIS+ly	Seminoma
CD3	10	15	15	16	28
CD20cy	10	14	14	16	28
CD68	10	14	15	15	27
CD11c	10	12	15	15	28
CD4	10	12	14	15	26
CD8	10	11	14	15	26
CD25	10	11	14	12	24
FOXP3	10	12	14	15	26
CXCR5	10	11	14	16	24
BCL6	10	12	14	16	27

For the samples used for flow cytometric analysis, the histopathological composition of the primary tumors was assessed at the Department of Pathology at Giessen University Hospital and the patients were broadly categorized into three groups: (I) classical seminoma (100% pure seminoma), (II) embryonal carcinoma (≥80%) and (III) mixed tumors (Figure 2.2). In addition, a histological analysis of the individual tissue sections from the different localizations was performed in order to obtain an overview of the clinical heterogeneity of the samples (Table 2.3 and Supplementary Table 1).

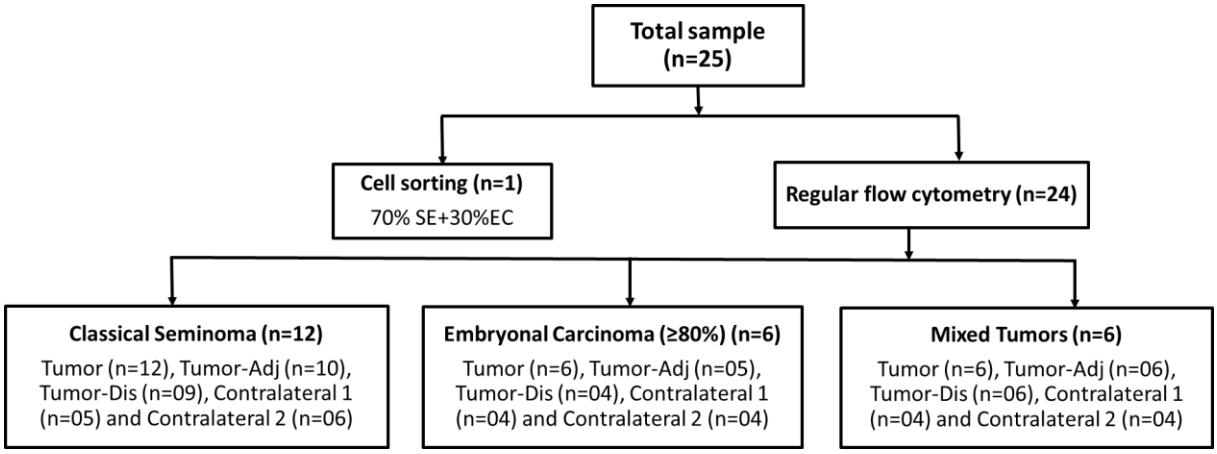

Figure 2.2 Total number of samples from the different locations of different TGCT.

Table 2.3 Histopathological heterogeneity of the samples (most frequent in bold).

Homogeneous Pathology	Heterogeneous pathology					
SE (n=6)	SE+ GCNIS+ HYP+ly (n=1)	SE+FSC+ BG+TS+ly (n=1)	SE+TS (n=1)	SE+FSC+T S (n=1)	SE+FLS+ly (n=1)	SE+EC+HYP+l y (n=1)
EC (n=5)	EC+SE+l y (n=1)	EC+FSC+ TS+ly (n=1)	EC+TS (n=1)	SCO+EC (n=1)	SCO+TS+ly (n=2)	
GCNIS (n=2)	GCNIS+l y (n=5)	GCNIS+TS (n=2)	GCNIS+HYP (n=2)	GCNIS+TS+ ly (n=3)	GCNIS+HY P+SZA (n=1)	GCNIS+FSC+T S+ly+FLS (n=1)
	GCNIS+ FSC+TS +ly (n=2)	GCNIS+H YP+FSC (n=1)	GCNIS+FSC+ SZA+SGA+ly (n=1)	GCNIS+SZ A+ly (n=1)	GCNIS+SC O+SZA (n=1)	GCNIS+HYP+F SC+TS (n=1)
NSP/HYP (n=30)	HYP+SZ A (n=3)	HYP+ly (n=2)	HYP+TS (n=2)	HYP+BG+S ZA+MSG (n=2)	HYP+GCNI S+SCO (n=1)	HYP+DV (n=1)
TS (n=1)	TS+FSC (n=2)	SCO+TS (n=1)	TS+LY (n=1)	ESC+ly (n=2)	TS+BG (n=1)	

2.3 Immunohistochemical (IHC) analysis

Bouin's-fixed paraffin embedded tissues were cut into 5 µm thick sections and two sections per slide were mounted on 3-aminopropyltriethoxysilane (APTES)-coated slides (HistoBond®+ adhesive microscope slides, Cat. 0810401, Paul Marienfeld GmbH & Co. KG). The slides were allowed to dry at 37°C for two days and IHC was performed according to standard laboratory protocols. Briefly, slides with 5µm thick tissue sections were placed in a glass staining tray, deparaffined in xylol for 2 x 10 minutes (min), and rehydrated in reduced concentrated ethanol (100%, 96%, 80%,

70%) for 5 min at each concentration and then washed in double distilled water (ddH2O) for 2x5 min. Next, heat-mediated antigen retrieval was performed in Tris-EDTA buffer (pH 9) for 20 min (first 5 min at 770 W and then 15 min at 460 W) in a microwave oven and then returned to room temperature (RT) for 15 min to cool the slides. The slides were washed once with wash buffer ((Tris-buffer solution (TBS, pH 7.4) + 0.1% Triton-X-100)) for 3 min and then incubated in 3% hydrogen peroxide (H_2O_2, Roth, Karlsruhe, Germany, Cat. 9681.1) in wash buffer for 15 min at RT on the shaker plate to inhibit endogenous peroxidase activity. Thereafter, the sections were washed in wash buffer for 3 x 3 min and then incubated with 1.5% bovine serum albumin (BSA, Roth, Karlsruhe, Germany, Cat. 8076.2) in wash buffer at RT for 30 min in order to block unspecific binding sites. Primary antibodies (Table 2.4) were diluted in 1.5% BSA and applied to the tissue sections (1.5% BSA solution was used instead of primary antibodies in negative controls) and incubated overnight at 4° C in a humidified chamber.

Table 2.4 List of antibodies used for IHC and their working conditions.

Primary antibody	**Specificty**	**Supplier and Catalogue no**	**Dilution**	**Staining**
Polyclonal rabbit anti-human CD3	Pan T cells	DAKO, A0452	1:100	AEC
Monoclonal mouse anti-human CD20cy	B cells	DAKO, M0755	1:100	AEC
Monoclonal mouse anti-human CD68	Macrophages	DAKO, M0876	1:100	NovaRED
Monoclonal mouse anti-human CD11c	DCs	Novocastra, NCL-L-CD11c-563	1:100	NovaRED
Monoclonal rabbit anti-human CD4	Th cells	Abcam, ab133616	1:100	AEC
Monoclonal mouse anti-human CD8a	Tc cells	eBioscience, Product: 14-0008-82	1:250	AEC
Polyclonal rabbit anti-human IL2RA (CD25)	Treg	Sigma, HPA054622	1:500	AEC
Monoclonal mouse anti-human FOXP3	Treg	eBioscience, Product: 14-4777-80	1:100	AEC
Polyclonal rabbit anti-human CXCR5	Tfh	Sigma, HPA042432	1:2000	AEC
Monoclonal mouse anti-human BCL6	Tfh	DAKO, M7211	1:50	AEC
Secondary antibody				
Biotinylated goat anti-rabbit		DAKO, E0432	1:100	
Biotinylated goat anti-mouse		DAKO, E0433	1:100	

The next day, the sections were washed in wash buffer for 3 x 3 min and incubated with appropriate biotinylated secondary antibodies (Table 2.4) at RT for 1 hour. Next, the sections were washed for 3 x 3 min and incubated with VECTASTAIN Elite ABC kit, Peroxidase (standard) (Cat. PK-6100, Vector Laboratories, USA) according to the manufacturer's instructions for 45 min at RT, followed by ABC solutions were removed by washing three times for 3 min in wash buffer. Finally, immunostaining was visualized using ImmPACT AEC Substrate Kit, Peroxidase (Cat. SK-4205, Vector Laboratories, USA) for maximally 25 min or Vector NovaRED Peroxidase Substrate (Cat. SK-4800, Vector Laboratories, USA) for a maximum of 10 min. After achieving sufficient staining, AEC or NovaRED solutions were removed by washing three times in ddH2O for 3 min and counterstained (only for the antibodies expected in the cytoplasm) with Mayer's hematoxylin (Cat. 1092492500, Sigma-Aldrich, Germany) for a very short time (5-10 sec) and immediately washed with ddH2O for 5 min. Sections stained with NovaRED were then dehydrated in increased concentration of ethanol (70%, 80%, 96%, 100% for 3 min at each concentration) and in xylol (2 x 5 min). Finally, the sections were mounted with Kaiser's glycerol gelatine (phenol-free, Cat. 2848.2, Roth, Karlsruhe, Germany) or Eukitt® quick-hardening mounting medium (Cat. 04-0004, R. Langenbrinck GmbH, Germany). All antibodies were optimized on human tonsil tissue as a positive control. For IHC image analysis, slides were transferred to Monash University, Australia and scanned with the Aperio ScanScope AT Turbo at Monash Histology Platform. Finally, Images were analyzed using the Aperio ImageScope (V12.4.3.5008) software.

2.4 Semi-quantitative IHC scoring of testicular immune cell infiltration

To describe the degree of immune cell infiltration, a semi-quantitative scoring system consisting of five different scores (absent = 0, single cell = 1, scattered = 2, sparse = 3, dense = 4) was developed by Klein et al. (Klein et al., 2016) and optimized for the present study. Evaluation was performed by four independent investigators. Along with the infiltration density, spatial distribution (including focal, multifocal, disseminated) of the immune cell infiltration (Figure 2.3) were also performed for all samples by two independent examiners. However, when necessary, slides with unclear classification were further examined by a 3rd and 4th examiner. Finally, an average score was used

to generate the plots and perform statistical analysis (Ordinary One-way ANOVA including a post-hoc test named Tukey's Honest Significant Difference Test) by GraphPad Prism 9.3.1.

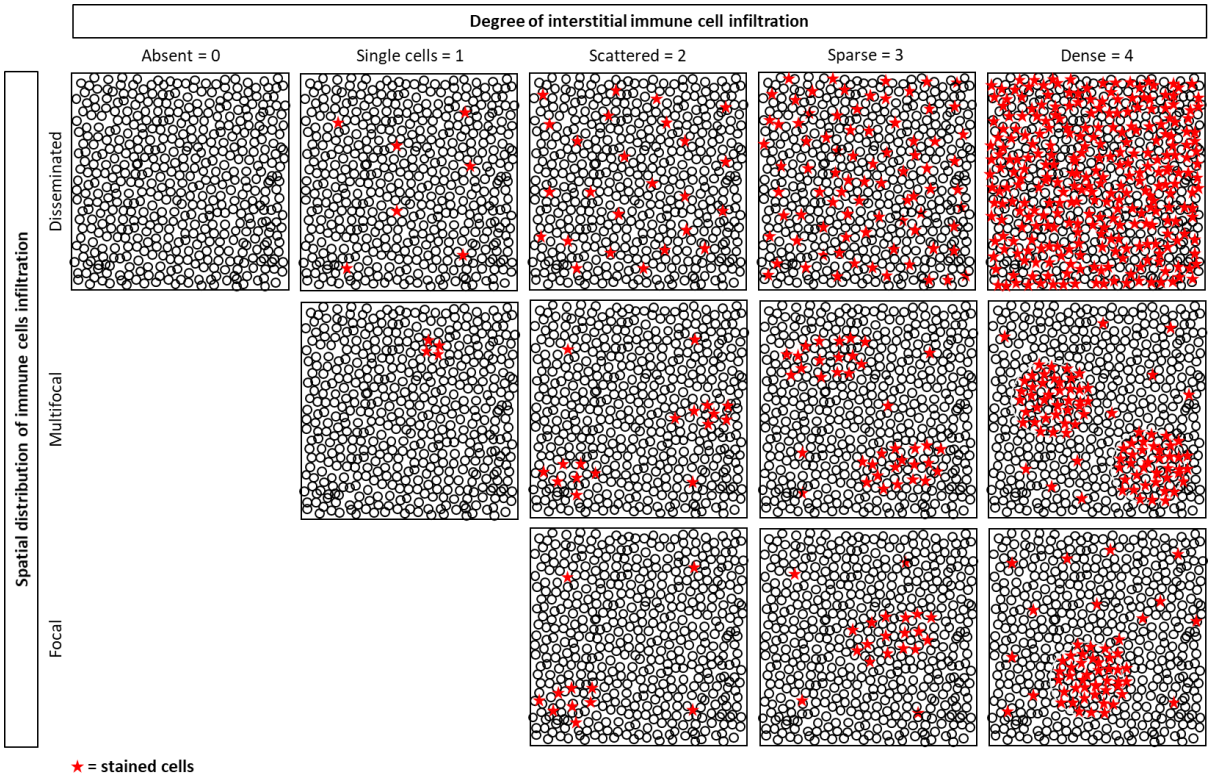

Figure 2.3 Schematic presentation of the semi-quantitative scoring system used to describe the degree and distribution of immune cell infiltration.

2.5 Flow cytometric analysis of infiltrating immune cells in human testis samples

Fresh human testicular tissue sections were collected directly from the operation theater in RPMI medium on ice and immediately proceeded with sample preparation and perform flow cytometric analysis. If it was not possible to perform the experiments on the same day, the specimens were stored in MACS® Tissue Storage Solution (Miltenyi Biotec, Cat. 130-100-008) for a maximum of 48 hours (h) at 4°C. The tissue storage solution allows for an optimized storage of fresh tissue samples for at least 48 h without any background effects such as cell activation or apoptosis induction and

ensure that a maximum number of viable cells are retained for flow cytometric analysis.

First of all, the samples were weighed (Table 2.1), and then mechanical and enzymatic dissociations were performed according to the internal laboratory protocol. Briefly, tissues were transferred to 300 µl PBS in a 2 ml Eppendorf vial, minced with scissors for 4-5 min (until fully chopped into smaller pieces), and then 700 µl collagenase D (2 mg / ml) (Sigma-Aldrich, Cat. 11088858001) was added to get final working concentration of collagenase D of 1.5 mg/ml. The tissue suspensions were then incubated at 37° C for 45 min in a shaking heater at 800 rpm. The suspensions were then mixed well with a syringe needle and filtered into a new 50 ml tube using a 100 µM cell strainer (Greiner Bio-One GmbH, Cat. 542000). Next, the supernatant was transferred to 15ml centrifuge tubes and PBS added to make a final volume of 15 ml. The tubes were then centrifuged at 1300 rpm for 10 min at 4°C and the supernatant, left-over tissue fragments, sediments etc. were transferred to a new 15 ml tube and stored at -150° C for later analysis (controlling for the fate of TGCT cells, germ cells, and non-immune testicular somatic cells). Cell pellets were resuspended in 1 ml RBC lysis buffer (QIAGEN, Cat.158902) and incubated for 3 min at RT, and 14 ml PBS were added to make a final volume of 15 ml. The tubes were then centrifuged at 1300 rpm for 10 min at 4°C. The supernatant was discarded, and the cell pellets were resuspended in 200 µl PBS and finally the cell suspensions were transferred to a 1.5 ml Eppendorf vial. For the detection and discrimination of dead cells, 1µl (recommended for up to 10^7 cells/100 µ) Viobility™ 405/520 Fixable Dye (Miltenyi Biotec, Cat. 130-109-814) was added to the cell suspension and incubated for 15 min at RT in the dark. Then, 1 ml MACs Quant buffer (2mM EDTA+0.05% BSA in PBS) was added and the cell suspension was divided into two 1.5 ml Eppendorf vials for the two panels and additional MACs Quant buffer was added to make a final volume of 1ml and centrifuged at 1300 rpm for 10 min at 4°C. Next, the supernatant was discarded, and the cell pellets were resuspended in 70 µl PBS. Thereafter, the antibodies directed to the cell surface (Table 2.5) were added accordingly, and then additional PBS was added to make a final volume of 100 µl. At the same time, the isotype control of each antibody was included in the experiments. Generally, it is recommended to keep the isotype control in each experiment, which was not possible

in our study due to the small size of tissue samples. Nevertheless, if the tissue size was large and the number of viable cells high enough, isotype control was included in the experiment. This ensures that the observed staining is due to specific antibody binding to the target rather than an artifact.

Table 2.5 List of the antibodies with their conjugated dye used for Flow cytometric analysis and their working conditions. All the antibodies were purchased from the Miltenyi Biotec (except FOXP3, from Biolegend). Intercellular targeted antibodies are marked with purple color.

Channel	PANEL 1		Channel	PANEL 2	
V1	CD3-VioBlue, Cat. 130-114-710	1:50 (2µl)	**V1**	CD3-VioBlue, Cat. 130-114-519	1:50 (2 µl)
V2	Viobility™ 405/520 Fixable Dye, Cat. 130-109-814	1µl	**V2**	Viobility™ 405/520 Fixable Dye, Cat. 130-109-814	1µl
B1	CD45-VioBright 515, Cat. 130-110-640	1:50 (2 µl)	**B1**	CD25-VioBright 515, Cat. 130-113-287	1:50(2 µl)
B2	CD20cy-PE, Cat. 130-108-313	1:11(10 µl)	**B2**	BCL6-PE, Cat. 130-118-346	1:50(2 µl)
B3	CD4-PerCP-Vio700, Cat. 130-113-790	1:50 (2 µl)	**B3**	CD4-PerCP-Vio700, Cat. 130-113-228	1:50(2 µl)
B4	CD8-PE-Vio770, Cat. 130-110-818	1:50 (2 µl)	**B4**	CD185 (CXCR5)-PE-Vio770, Cat. 130-117-508	1:50(2 µl)
R1	Alexa Fluor® 647 anti-human FOXP3 Antibody, Cat: 320114, Biolegend	1:50(2 µl)	**R1**	Alexa Fluor® 647 anti-human FOXP3 Antibody, Cat: 320114, Biolegend	1:50(2 µl)
R2	CD68-APC-Vio770, Cat. 130-114-463	1:50 (2 µl)	**R2**	CD45-APC-Vio770, Cat. 130-110-635	1:50(2µl)

The cell suspension was then mixed by pipetting or brief vortexing and incubated at 4° C for 15 min in the dark. To wash the cells, 1 ml of MACs Quant buffer was added and centrifuged at 1300 rpm for 10 min at 4°C. Supernatants were then discarded and cell pellets were resuspended accordingly with FOXP3 staining buffers (Miltenyi Biotec, Cat. 130-093-142) and incubated for 30 min at 4°C in the dark. The cell suspension was then centrifuged at 1300 rpm for 10 min at 4°C and the supernatant discarded. Next, the cell pellets were resuspended with 1 ml 1X permeabilization buffer and centrifuged at 1300 rpm for 10 min at 4°C and the supernatant discarded. Again, the cell pellets were resuspended with 50 µl of 1X permeabilization buffer and

to increase the specificity of the Foxp3 antibody, the cell pellets were incubated with 20 µl (recommended for up to 10^7 cells) of FcR blocking reagent (Miltenyi Biotec, Cat. 130-059-901) for 10 min at 4°C in the dark. Subsequently, the intracellular targeted antibodies (Table 2.5) were added accordingly and additional 1X permeabilization buffer was added to make a final volume of 100 µl. Then, it was incubated for 30 min at 4°C in the dark and 1ml 1X permeabilization buffer was added for washing. Finally, the cell suspensions were centrifuged at 1300 rpm for 10 min at 4°C. The supernatant was discarded, and cell pellets were resuspended with 100-200 µl MACs Quant buffer and run the sample in MACSQuant® Analyzer 10 Flow Cytometer.

2.6 Composition of the flow cytometry panels

A flow cytometry panel consisted of multiple fluorochrome-conjugated antibodies, and each of the fluorochromes had broad emission spectra that may overlap with the spectra of other fluorochromes. Therefore, it is obligatory to detect overlaps and correct fluorescence spillover for proper analysis. In this study, the MACS comp Bead Kit, anti-REA (Miltenyi Biotec, Cat. 130-104-693) was used to compensate the fluorescence spillover from fluorochrome-conjugated REAfamily antibodies, while Ultracomp eBeads™ Compensations-Beads (Catalog number: 01-2222-42, Invitrogen) was only used for FOXP3 (Alexa Fluor® 647 anti-mouse FOXP3 Antibody) according to the manufacturer's protocol. Each bead drop contained two populations - a positive population that captures the antibody, and a negative population that does not react with the antibody. Briefly, 100 µl of the MACSQuant running buffer was added to each sample tube (label a tube for each fluorochrome used in the experiment), and the appropriate amount of antibodies were added to the appropriate sample tube. Then, one drop (equivalent to 50 µl) of the MACS Comp Beads – anti-REA and one full drop of the MACS Comp Beads – blank to each tube of REAfinity antibody, while one drop of UltraComp eBeads was added for FOXP3 and mixed well and incubated for 5-10 min (15-30 min for UltraComp eBeads) in the dark room at RT. Next, 1ml of the MACSQuant running buffer was added to dilute each sample and then proceed to calibrate the MACSQuant instrument.

2.7 PBMC isolation from buffy coat

After compensation, the flow cytometry panels composed of different antibodies were tested on peripheral blood mononuclear cells (PBMC) isolated from the buffy coat collected from the Center for Transfusion Medicine and Hemotherapy, University Hospital Giessen and Marburg, Giessen, Germany. Briefly, 15 ml of buffy coat was filled into a 50 ml tube. PBS was then added to make a final volume of 50 ml and mixed well by pipetting or shaking. Then, 35 ml of diluted buffy coat was transferred to a new 50 ml tube and 15 ml of Ficoll® Paque Plus (Cytiva, Cat. 17-1440-03) was added and centrifuged for 30 min at RT at 15000 rpm (without break) and the plasma was discarded. After that, the PBMC containing layer was collected into a new 50 ml tube and PBS was added to make up to 50 ml and centrifuged again at 1700 rpm (without break) at 4°C for 10 min. Next, the supernatant was discarded and the white layer, which is the PBMC, was transferred into a new 50 ml tube and the tube filled with PBS. The suspension was then centrifuged at 1700 rpm (without break) at 4°C for 10 min and the supernatant was discarded. The procedure was repeated twice. Finally, the PBMC were collected, resuspended in 15-20 ml PBS, and counted. Flow cytometric analysis was performed according to the protocol above.

2.8 Flow cytometric data analysis

A specific strategy was followed to identify different immune cells from the total analyzed events in panel 1 (general immune cells) (Figure 2.4). From the total analyzed events, single cells were selected by SSC-H vs SSC-A gating to remove doubles and other aggregated particles. Live and dead cells were separated by viability dye which binds to the dead cells. Next, further gating was performed to detect CD3+ T cells, CD4+ Th cells, CD68+ macrophages, and CD20cy+ B cells in total live cells. For panel 2 (T cells), doubles and other aggregated particles were also removed from the total analyzed events and then dead and live cells were separated by viability dye. Next, further gating was performed to identify CD25+FOXP3+ Treg and CXCR5+BCL6+ Tfh cells (Figure 2.5). Data was analyzed with FlowJo™ v10.8.1 and graphs were generated with GraphPad Prism 9.3.1 software.

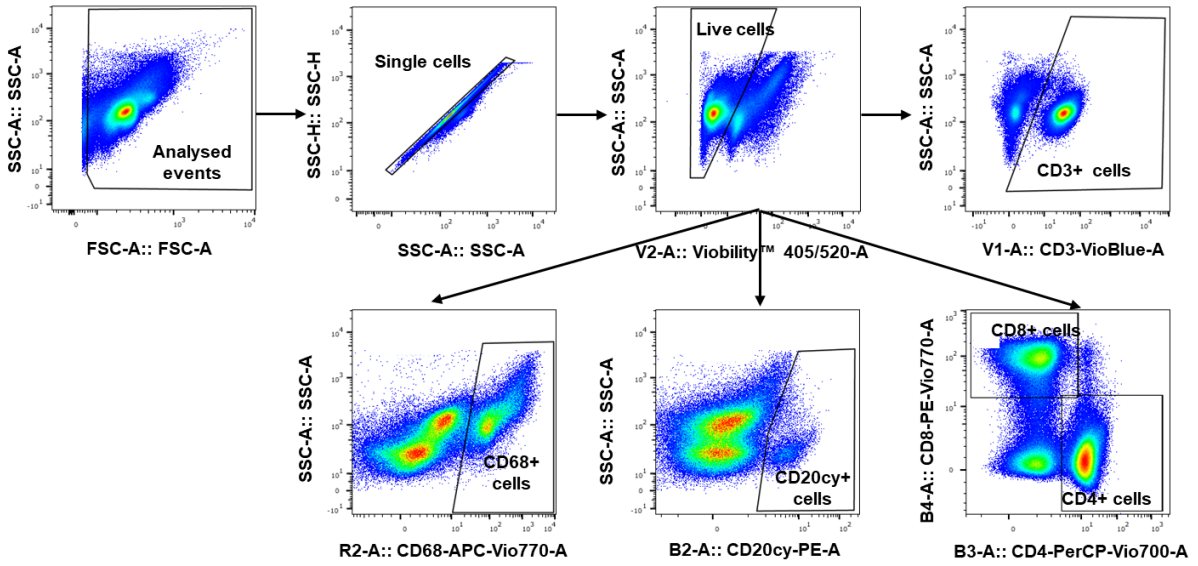

Figure 2.4 Flowcytometric analysis and corresponding gating strategies to analyze different infiltrating testicular immune cells using antibody panel-1 (CD45, CD20cy, CD68, CD3, CD4, CD8).

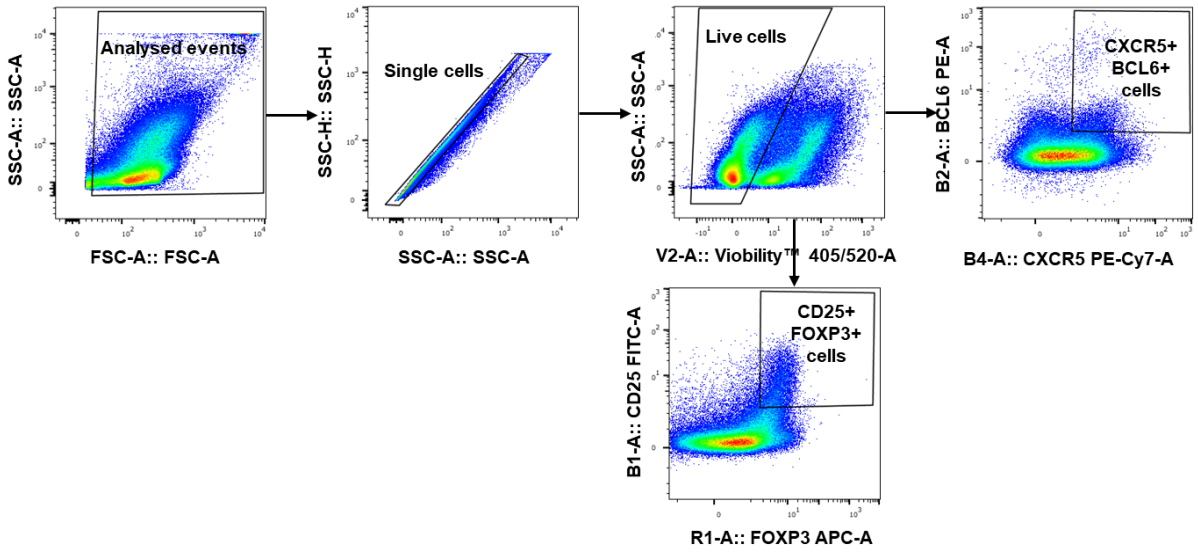

Figure 2.5 Flowcytometric analysis and respective gating strategy to analyze CD25+FOXP3+ Treg and CXCR5+BCL6+ Tfh cells using antibody Panel-2 (CD45, CD3, CD4, CD25, FOXP3, CXCR5, BCL6).

2.9 Sample preparation for scRNA-seq

Human testicular tissues were stored in cold PBS and transported from operating room to the laboratory on ice. Tissues were digested following the standard two step enzymatic isolation protocol as described in (Guo et al., 2018). Briefly, testicular tissues were digested with collagenase type IV (Sigma Aldrich, Cat. C5138–500MG) for 5 min at 37 °C with gentle agitation (250 rpm), then shaken vigorously and incubated for another 3 min. The tubules were sedimented by centrifugation at 200× g for 5 min and washed with HBSS before digestion with 4.5 mL 0.25% trypsin/ethylenediaminetetraacetic acid (EDTA; Invitrogen, Cat. 25300054) and 4 kU DNase I (Sigma Aldrich, Cat. D4527–500ku). The suspension was triturated vigorously three to five times and incubated at 37 °C for 5 min. The process was repeated in 5 min increments for up to 15 min total. The digestion was stopped by adding 10% FBS (Gibco, Cat. 10082147). Single testicular cells were obtained by filtering through strainers with mesh size 70 µm (Fisher Scientific, Cat. 08–771–2) and 40 µm (Fisher Scientific, Cat, 08–771–1). The cells were pelleted by centrifugation at 600× g for 15 min and washed twice with 1× PBS. Cell viability was measured using acridine orange/propidium iodide (AO/PI) and approximately 80% viable cells were found in all samples. Cell number was measured using a hemocytometer. Cells were re-suspended in 1× PBS + 0.4% BSA (Thermo Fisher Scientific, Cat, AM2616) and the single cell suspension was then loaded into 10x Chromium Controller using the Chromium Single Cell 3′ v3.1 reagents.

2.10 scRNA-seq library construction and sequencing

Chromium Next GEM Single Cell 3' v3.1: Dual Index Libraries Kit was used for the library preparation. The sequencing libraries were prepared following the manufacturer's instructions, using 13 cycles of cDNA amplification, followed by an imput of ~100 ng of cDNA for library amplification using 12 cycles. The resulting libraries were then sequenced on a 2 X 100 cycle paired end run on an Illumina HiSeq 2500 or Novaseq 6000 instruments.

2.11 Publicly available normal control data

scRNA-seq of human normal testicular tissue samples dataset were acquired from the Gene Expression Omnibus (GEO) database under accession code GEO: GSE120508 (Guo et al., 2018) and analyzed together with our own dataset. Both publicly available datasets from normal testis and newly generated scRNA-seq data sets from TGCT sample were prepared in the same way. In addition, data integration was performed during the analysis to remove batch effects across different samples.

2.12 scRNA-seq data analysis

10X data matrix of normal testes (n=3; pooled data) and TGCT (n=4) were imported into the Seurat V4.0 R package (https://satijalab.org/seurat/) to perform analytical quality control, data normalization, dimensional reduction, data visualization etc. First, Seurat object was created for each dataset and then merged them into a single object. Then the following criteria were applied on merged datasets containing 4 TGCT and 3 normal testes: nCount_RNA (total number of molecules detected within a cell) >1000, nFeature_RNA (number of genes detected in each cell) between 200 and 8000, percent.mt (mitochondrial gene percentage) < 5 to remove low-quality cells and possible cell multiplets (Supplementary Figure 1). After filtration and normalization, a total number of 10,153 cells were left for the following analysis (Supplementary Table 2). Then, data integration was performed to remove batch effects across different samples. The filtered matrix was normalized in the Seurat v.4 with default parameters and top 2000 variable gene were then identified using the “vst” method in Seurat FindVariableFeatures function. Variable “nCount_RNA “and “percent.mt” were regressed out in the scaling step and Principal-Component-Analysis (PCA) was performed using the top 2000 variable genes. Then t-distributed stochastic neighbor embedding (t-SNE) was performed on the top 30 principal components for visualizing the cells. In the meantime, clustering was performed on the PCA-reduced data with resolution 3 to obtain a better result. A total of 46 clusters were generated in the primary analysis (Supplementary Figure 2A) and then the contribution of each sample to each cluster was calculated (Supplementary Figure 2B and C). Subsequently, the clusters were identified/annotated based on the expression of well-established cell-specific marker genes throughout the 46 primary clusters (Supplementary Figure 3

and Supplementary Figure 4) and the same cells found in different clusters were merged for better visualization with their origin.

As of our core interest, secondary clustering of T cells was performed with resolution 2 to obtain finest outcome and then each cluster was identified based on the expression of well-established T cell subtypes-specific marker genes throughout the 17 secondary clusters (Supplementary Figure 5A and Supplementary Figure 6). Correspondingly, the same cell type in the secondary clusters of T cells were merged for better visualization with their origin (Supplementary Figure 5B).

2.13 Differential gene expression analysis

Differential gene expressions (DGEs) analysis was performed using the FindMarkers function based on the non-parametric Wilcoxon rank sum test and at same time the adjusted p-values were calculated based on the Bonferroni correction. Using these parameters, multiple comparisons of DGEs were performed, including T cells vs rest of the cells, individual TGCT sample vs. donors (Supplementary Figure 7), only T cells of individual TGCT sample vs. donors (Supplementary Figure 8) and only Treg cells of individual TGCT sample vs. donors (Supplementary Figure 9).

2.14 Gene Set Enrichment Analysis (GSEA)

A computational approach named Gene Set Enrichment Analysis (GSEA) in various contexts was performed by multiple web tools such as WebGestalt (WEB-based Gene SeT AnaLysis Toolkit) (Liao et al., 2019) and Enrichr (Xie et al., 2021). to determine whether an *a priori* defined set of genes shows statistically significant, concordant differences between two biological states (e.g., phenotypes). GSEA-Gene Ontology (GO) analysis was performed using functional databases such as biological process (to represent a specific objective that the organism is genetically programmed to achieve), molecular function (to analyze the possible function that can be carried out by the action of a single macromolecular machine, usually via direct physical interactions with other molecular entities), cellular component (to determine the location that relative to cellular compartments and structures, and occupied by a

macromolecular machine when it carries out a molecular function) in the WebGestalt and Enrichr. To translate the list of genes that are differentially expressed across the given phenotypes into meaningful biological phenomena, GSEA-pathway analysis was performed using different functional databases such as BioPlanet (Huang et al., 2019a), WikiPathways (Slenter et al., 2017), KEGG (Kanehisa et al., 2017), Panther (Mi and Thomas, 2009) in the WebGestalt and Enrichr.

2.15 Additional bioinformatics analysis and data visualization

Volcano plots of DGEs were created by EnhancedVolcano function in the Seurat V4.0 R package (Blighe et al., 2019), FunRich (Functional Enrichment analysis tool) was used to create Venn diagrams to illustrate the logical relationship between multiple sets of differentially expressed genes (Pathan et al., 2015, Fonseka et al., 2021). A web-based versatile matrix visualization and analysis software, named Morpheus software (https://software.broadinstitute.org/morpheus/) was used to create heatmaps. Besides, protein-protein interaction (PPI) network functional enrichment analysis of selected proteins was generated by STRING (https://string-db.org/) online platform (Szklarczyk et al., 2021). In addition to that, an interactive web resource UALCAN (The University of ALabama at Birmingham CANcer) for analyzing cancer OMICS data (Chandrashekar et al., 2022) was used to cross validate the selected genes expression in publicly available TCGA (The Cancer Genome Atlas)-testis germ cell tumors (seminoma n=63 and non-seminoma n=70) data. Finally, co-expression analysis of selected gene performed by cBioPortal using TCGA-Testicular Germ Cell Cancer (Source data from GDAC Firehose) dataset (n=156 samples) (Gao et al., 2013).

2.16 Hanging drop culture

Hanging drop culture medium consisted of DMEM F12 + 10% FBS + 1% P/S+ 1X ITS -G was used to culture human testicular tissue. The sample was immediately collected in cell culture media and transported to the laboratory (within 2 hours after surgical removal). First, 1ml DPBS (Cat. No: 14190-094, Gibco) was added to the each well of the 12-well plate to prevent dehydration and 30 µl medium was taken on the lid of a 12-well plates. Meanwhile, the specimens were cut into ~1 mm3 pieces and then a

single piece of tissue was placed into each droplet of hanging drop culture medium in the lid and then the lid was carefully inverted to keep the drops intact with the tissue suspended. Tissues were cultured at 34°C in 5% CO2 for 3-7 days with medium changes every 48 hours. Finally, sample were collected for Flow cytometry, H&E, IHC, and RNA extraction.

3 RESULTS

3.1 Investigation of immune cells infiltrates in human testicular cancer and controls by IHC

3.1.1 Analysis of immune cells in human normal testis

Deep IHC analysis of a panel of human testicular tissue samples showed that CD68+ macrophages were most abundant resident immune cells in human testicular tissues with NSP compared to other analyzed immune cells in this study (Figure 3.1D, Supplementary Figure 10C). Along with that, CD3+ pan T cells (Figure 3.1B, Supplementary Figure 10A), CD4+Th cells (Figure 3.1F, Supplementary Figure 10E), and CD8+ Tc cells (Figure 3.1G, Supplementary Figure 10F) were also detected with low infiltration density compared to the other analyzed sample, while CD11c+ DCs (Figure 3.1E, Supplementary Figure 10D), CD25+ Treg cells (Figure 3.1H, Supplementary Figure 10G), FOXP3+ Treg (Figure 3.1I, Supplementary Figure 10H) were found rarely, but no CD20cy+ B cells (Figure 3.1C, Supplementary Figure 10B), CXCR5+ Tfh (Figure 3.1J, Supplementary Figure 10I) and BCL6+ Tfh cells (Figure 3.1K, Supplementary Figure 10J) were detected in human normal testis presenting NSP. However, germ cells are often stained as an unspecific staining.

Briefly, macrophages were detected in all NSP samples with a median infiltration density score of 2.5 and were fully distributed throughout the interstitium as resident immune cells (Figure 3.2C, Supplementary Table 3). In the further course of writing, the median infiltration density score is referred to as “median score”. Similarly, T cells were also found disseminated at relatively low densities throughout the interstitium in 80% of cases with a median score of 1.5. In very rare cases (10% of cases) T cells were focally found (score 2.5) or absent in NSP (Figure 3.2A, Supplementary Table 3).

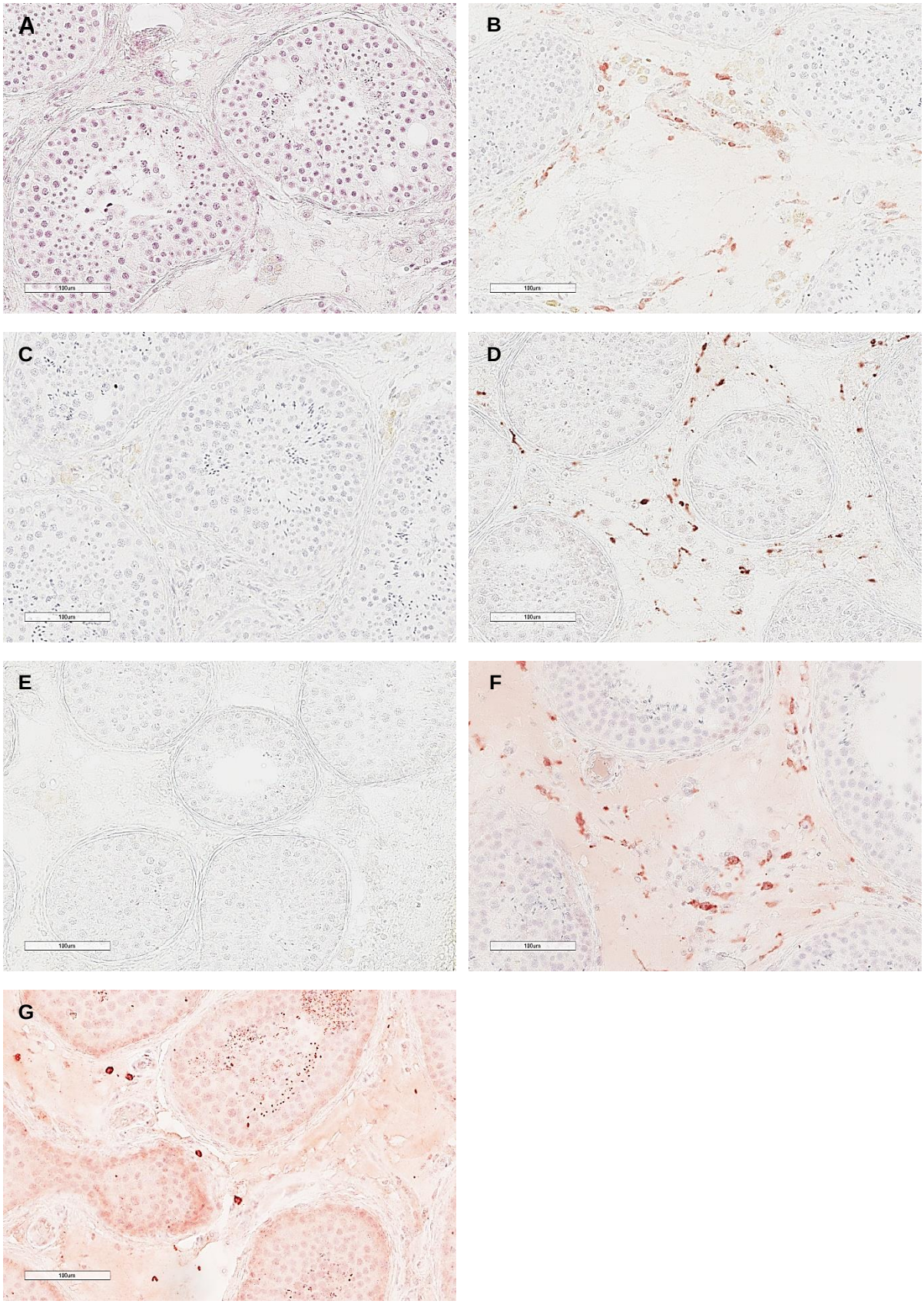

Figure 3.1 See next page for caption

Figure 3.1 Cont.

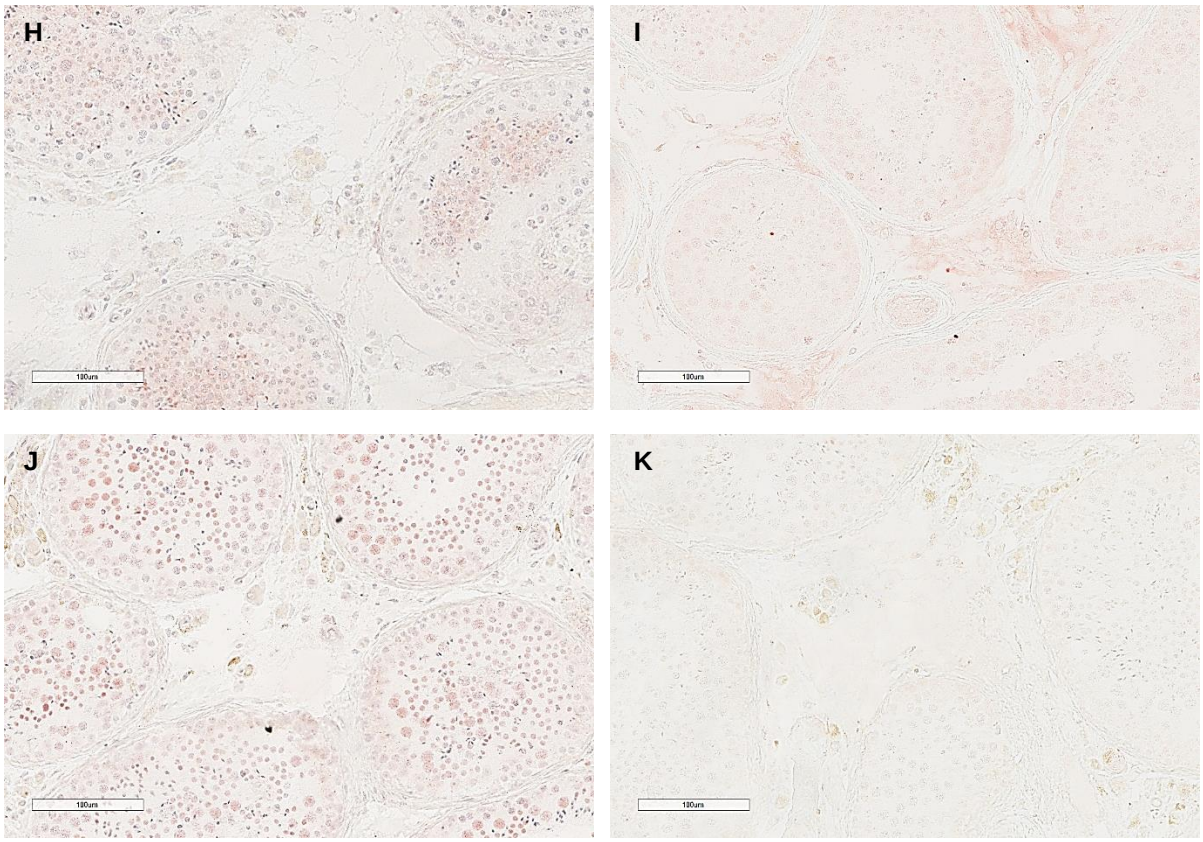

Figure 3.1 Analysis of infiltrating immune cells in human testis with NSP. H&E staining (A), CD3+ Pan T cells (B), CD20cy+ B cells (C), CD68+ macrophages (D), CD11c+ DC (E), CD4+ Th cells (F), CD8+ Tc cells (G), CD25+ Treg cells (H), FOXP3+ Treg (I), CXCR5+ Tfh (J) and BCL6+ Tfh (K). Macrophages represent the relatively major components of infiltrating immune cells in healthy testis. White bar indicates 100µm.

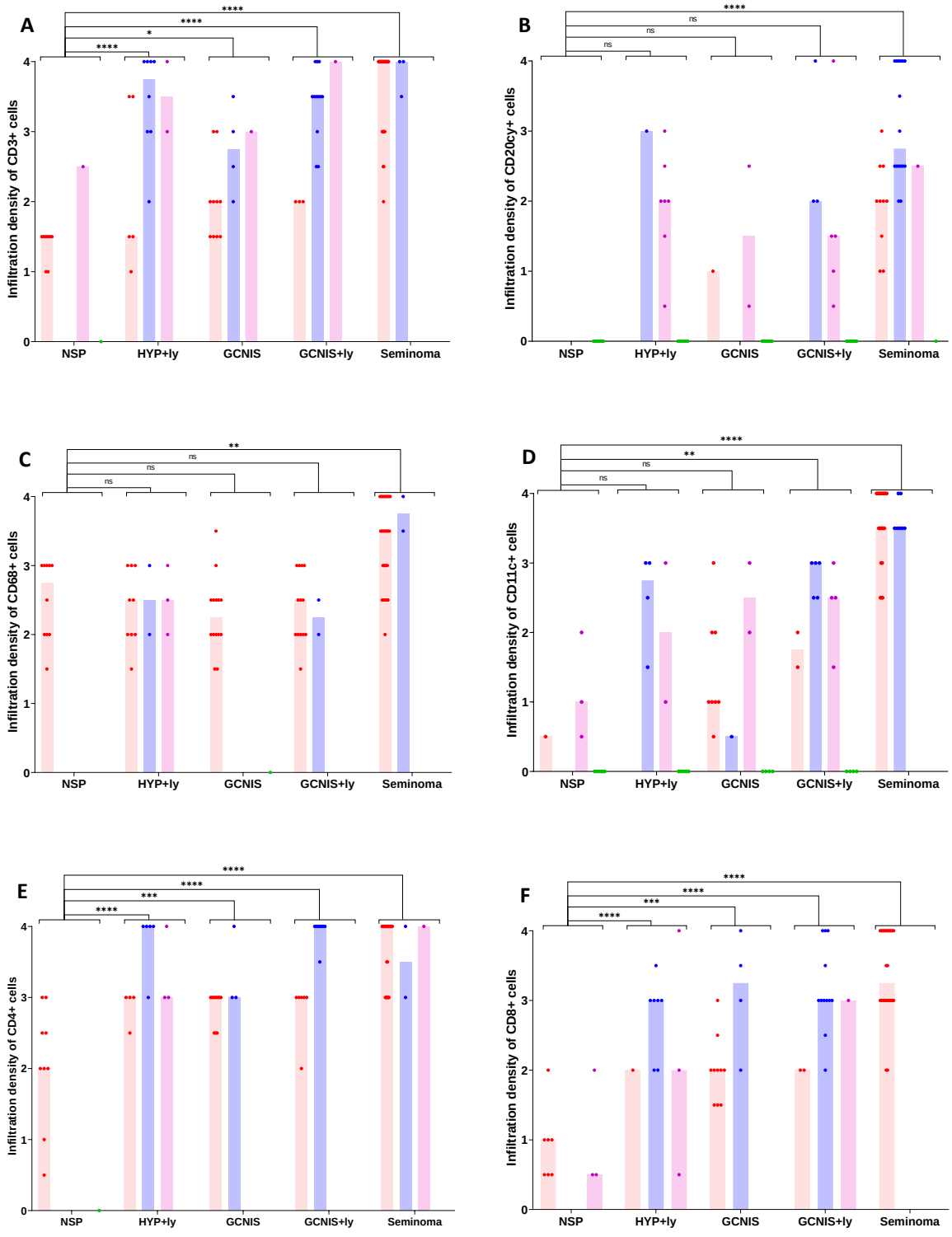

Figure 3.2 See next page for caption

Figure 3.2 Cont.

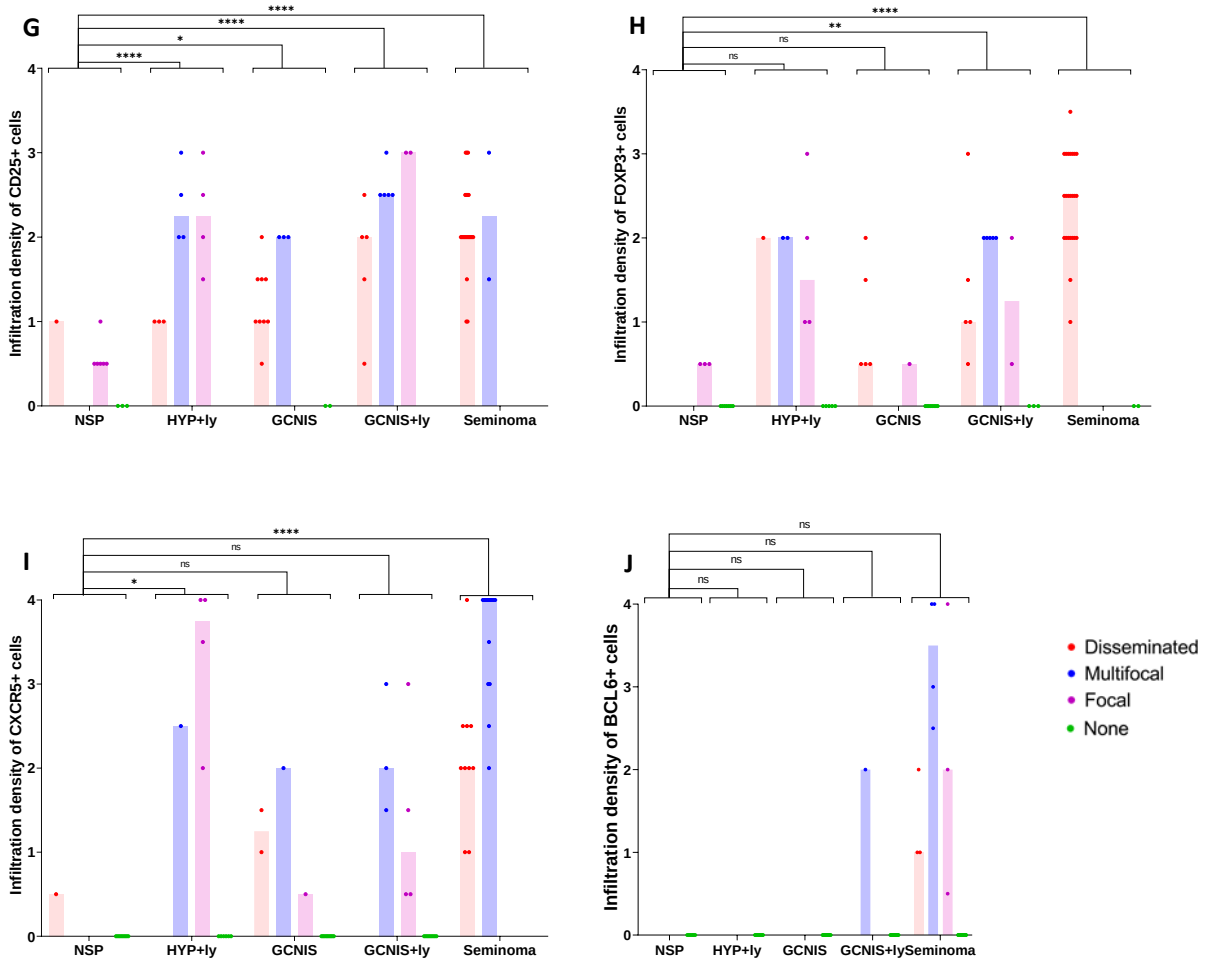

Figure 3.2 Semi-quantitative scores of different infiltration density and distribution of immune cells observed in IHC on various testicular morphologies. Each point represents the individual samples in each category and the top of the bar represents the median infiltration density in each distribution category. Infiltration density 0=absent, 1=single cells, 2=scatter, 3=sparse, 4=dense. The distribution of the infiltrating immune cells describes with individual colors, e.g., red= disseminated, blue = multifocal, purple= focal and green= none/absent. Significance tested by ordinary one-way ANOVA including Tukey's Honest Significant Difference Test [(Not significant (ns)= p-value ≥ 0.05), (Significant, *= p-value 0.01 to 0.05, **= p-value = 0.001 to 0.01, ***= p-value 0.0001 to 0.001, ****= p-value <0.0001)].

In addition, the main subtypes of T cells, CD4+ Th cells and CD8+ Tc cells were also found disseminated throughout the interstitium in 90% and 70% of the NSP samples, with a median score of 2 and 1, resp. (Figure 3.2E-F, Supplementary Table 3). It was also observed that CD8+ Tc cells were rarely found focally in 30% of NSP samples

(median socre of 0.5) and CD4+ Th cells were often not found in NSP (Figure 2. 7E-F, Supplementary Table 3). CD11c+ DCs were not found in 60% of the NSP samples, but in 30% of the cases DCs were focally found with a median score of 1 and in the remaining 10% of cases DCs were extremely low in number (score 0.5) were distributed over the interstitium (Figure 3.2D, Supplementary Table 3). Interestingly, no CD20cy+ B cells were found at all in human testicular NSP (Figure 3.2B, Supplementary Table 3).

Importantly, Treg specific marker CD25+ cells were focally found in 60% of the NSP samples with a median score of 0.5 and in 10% of cases they were found disseminated across the interstitium (Figure 3.2G, Supplementary Table 3). In 30% of NSP samples, no CD25+ cells were found (Supplementary Table 3). Treg-specific FOXP3+ cells were not observed in 70% of the NSP samples, while they were focally detected in 30% of the NSP samples with a median score of 0.5 (Figure 3.2H, Supplementary Table 3). Tfh-specific marker CXCR5+ cells were not observed in 90% of the NSP samples but were found disseminated only in 10% of NSP samples with extremely low numbers (score 0.5) (Figure 3.2I, Supplementary Table 3). Furthermore, other Tfh-specific marker BCL6+ cells were completely absent in NSP samples (Figure 3.2J, Supplementary Table 3).

3.1.2 Analysis of infiltrating immune cells in human testis with HYP+ly

An abundance of different infiltrating immune cells has been identified in human testicular tissue presenting with HYP+ly. Pan T cells and their major subtypes CD4+ Th and CD8+ Tc cells represent the main components of the infiltrating immune cells in HYP+ly (Figure 3.3 B, F, G and Supplementary Figure 10A, E-F). Followed by macrophages representing the second most common immune cell type in HYP+ly samples (Figure 3.3D, Supplementary Figure 10C). In contrast, B cells (Figure 3.4C, Supplementary Figure 9B), DCs (Figure 3.3E, Supplementary Figure 10D), CD25+ Treg cells (Figure 3.3H, Supplementary Figure 10G), and FOXP3+ Treg (Figure 3.3I, Supplementary Figure 10H) were rarely observed in HYP+ly. Although CXCR5+ Tfh cells (Figure 3.3J, Supplementary Figure 10I) were detected in single samples, no BCL6+ cells (Figure 3.3K, Supplementary Figure 10J) were found in human testis with HYP+ly.

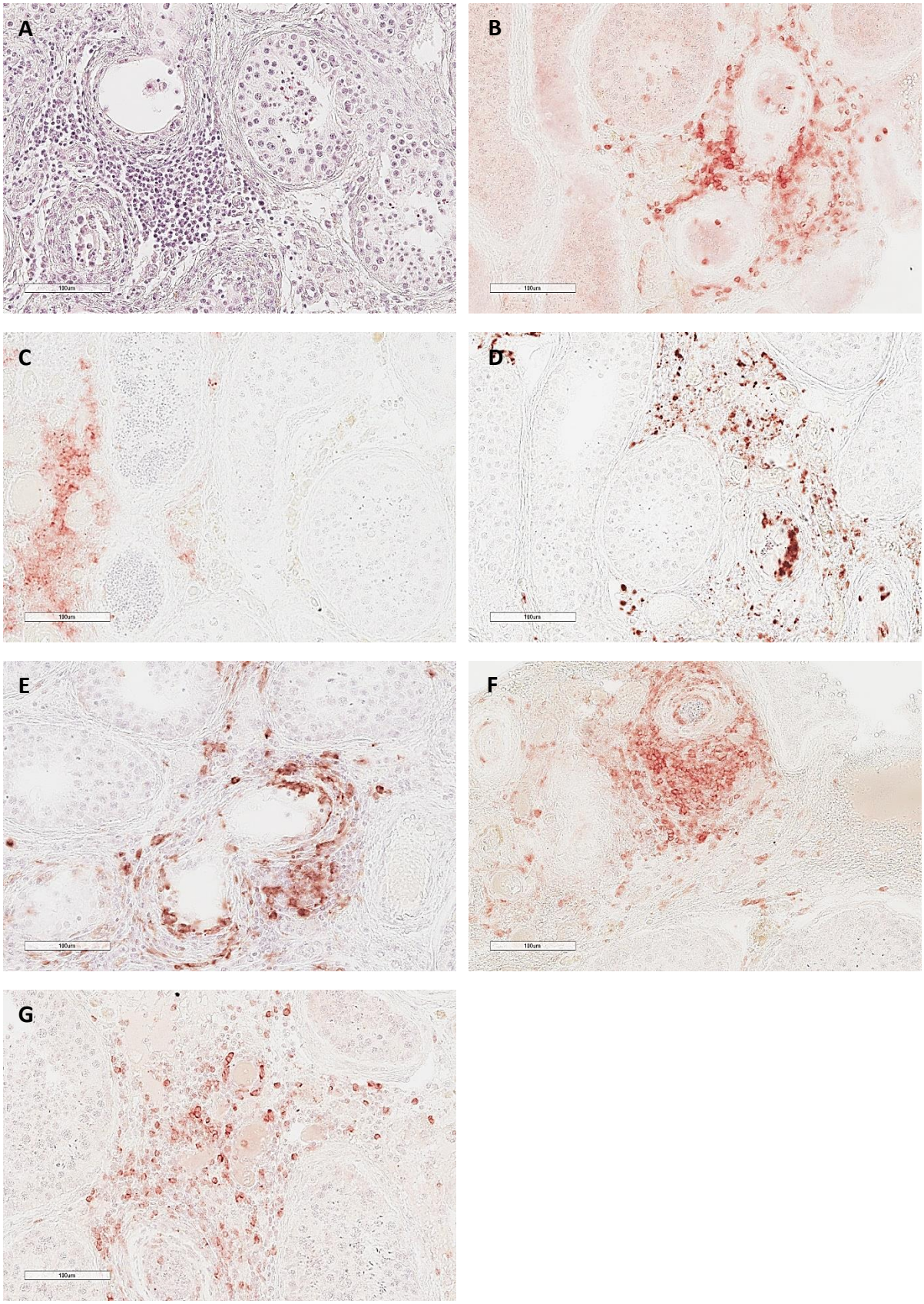

Figure 3.3 See next page for caption

Figure 3.3 Cont.

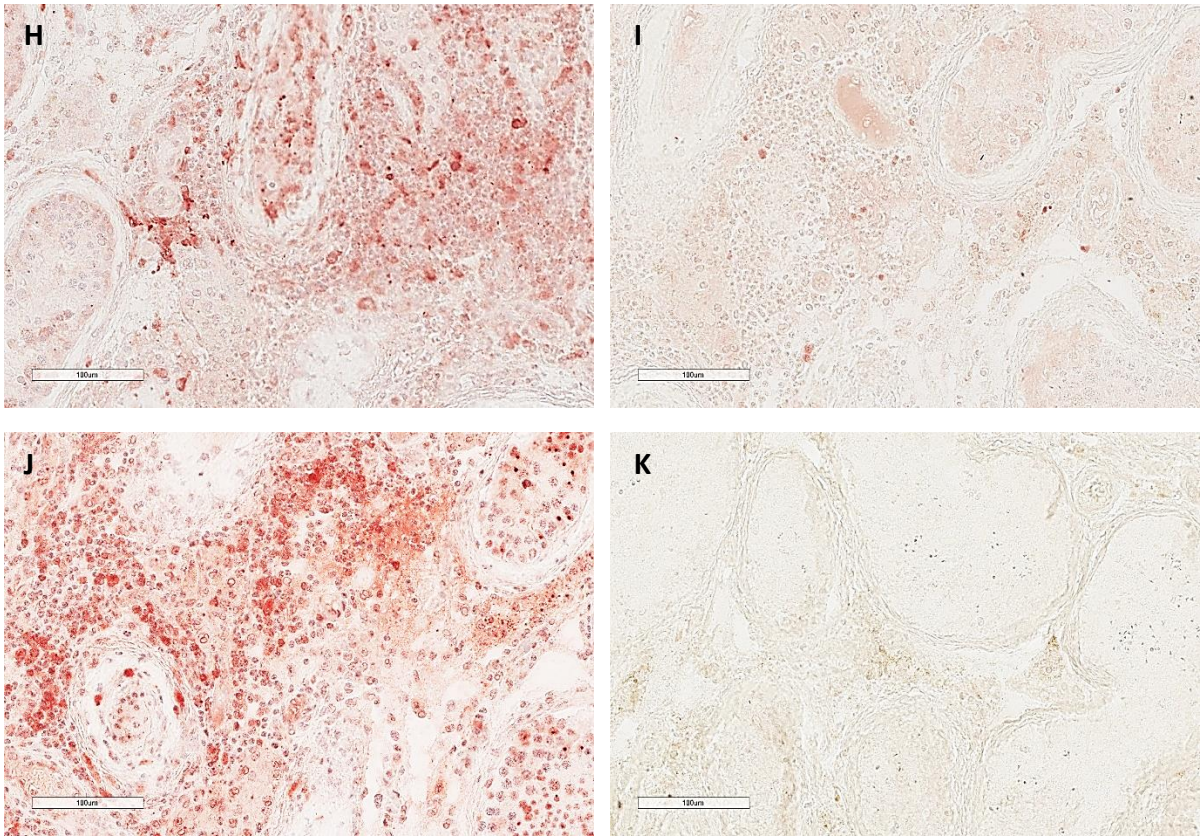

Figure 3.3 Analysis of infiltrating immune cells in HYP+ly. H&E staining (A), CD3+ Pan T cells (B), CD20cy+ B cells (C), CD68+ macrophages (D), CD11c+ DC (E), CD4+ Th cells (F), CD8+ Tc cells (G), CD25+ Treg cells (H), FOXP3+ treg (I), CXCR5+ Tfh (J) and BCL6+ Tfh (K). T cells represent the major components of the infiltrating immune cells in HYP+ly. White bar indicates 100µm.

Briefly, compared to the NSP, pan T cell prevalence was significantly higher (p-value <0.0001) in HYP+ly with a diverse infiltration density and distribution pattern across the samples (Figure 3.2A, Supplementary Table 4). For example, T cells were found in multifocal areas over the interstitium in 53.33% of cases with a median score of 3.75 (Figure 3.2A, Supplementary Table 4). Besides, T cells were disseminated in 33.33 % of HYP+ly samples with relatively low infiltration density (median score of 1.5), and also focally found in 13.33 % of cases with relatively higher infiltration density (median score of 3.5) (Figure 3.2A, Supplementary Table 4). Like pan T cells, Th and Tc cells were also highly abundant (p-value <0.0001) in human testicular tissue with HYP+ly compared to NSP. In most cases (41.67% and 63.64%, resp.), both Th and Tc cells were found in multifocal areas across the interstitium with a median score of 4 and 3,

resp. (Figure 3.2E-F, Supplementary Table 4). Th cells were disseminated in 33.33% of cases with a median score of 3, while Tc cells were dispersed in only 9.09% of the samples (score 2) (Figure 3.2E-F, Supplementary Table 4). In addition, Th cells were focally found in 25% of cases with a median score of 3, while Tc cells were found focally in 27.27% of cases with a median score of 2 (Figure 3.2E-F, Supplementary Table 4). In terms of infiltration density, there is no difference between the abundance of Th and Tc cells in human testicular tissue presenting HYP+ly (Supplementary Figure 10 E-F).

Macrophages, the second most frequent immune cells in HYP+ly, were not statistically significant different in number and distribution compared to NSP. However, in 64.29% of the HYP+ly samples, macrophages were mainly found disseminated throughout the interstitium with a median score of 2.5 (Figure 3.2C, Supplementary Table 4). In addition, macrophages were also found focally and multifocally with a median score of 2.5 in 21.43% and 14.29% of testis with HYP+ly, resp. (Figure 3.2C, Supplementary Table 4). Overall, the increase in macrophages density is relatively small in HYP+ly compared to NSP.

Compared to the normal testis (no B cells detectable), B cells were found focally over the interstitium in 50% of the HYP+ly samples with a median score of 2 (Figure 3.2B, Supplementary Table 4). In addition, B cells were found in multifocal areas with a score of 3 in 7.14% of the cases (Figure 3.2B, Supplementary Table 4). It was also observed that B cells were absent in almost half (42.86%) of the HYP+ly samples. Similar to the normal testis presenting NSP, DCs were not found in 50% of the testicular samples with HYP+ly (Figure 3.2D, Supplementary Table 4). Nevertheless, DCs were multifocally present in 33.33% of samples with a median score of 2.5 and were also detected focally in 16.67% of samples with a median score of 2 (Figure 3.2D and Supplementary Table 4). Their overall presence in HYP+ly was not significantly different from NSP.

Importantly, Treg specific marker CD25+ cells were significantly more frequent in HYP+ly compared to the NSP. Briefly, CD25+ cells found focally and multifocally in 36.36% of the samples with a median score of 2.25 (Figure 3.2G, Supplementary Table 4). In addition, CD25+ cells were found disseminated over the interstitium in

27.27% of cases with a median score of 1 (Figure 3.2G, Supplementary Table 4). While other Treg specific marker FOXP3+ cells frequency in HYP+ly not different from NSP, but they were found focally (median score of 1.75) in 33.33% of human testicular tissue with HYP+ly (Figure 3.2H, Supplementary Table 4). In addition, FOXP3+ cells were also found multifocally and distributed across the interstitium with a median score of 2 in 16.16% and 8.33% of cases, resp. (Figure 3.2H, Supplementary Table 4). It was also observed that FOXP3+ cells were absent in 41.67% of the HYP+ly samples.

Tfh-specific marker CXCR5+ cells were significantly more frequent in HYP+ly samples compared to the NSP. However, CXCR5+ cells were not found in more than half (54.56%) of the HYP+ly samples. Nevertheless, CXCR5+ were detected in focal area with a median score of 3.5 and in multifocal areas with a median score of 2.5 in 36.36% and 9.09% of the HYP+ly samples, resp. (Figure 3.2I, Supplementary Table 4). Beware, CXCR5 is not only expressed by Tfh but also by mature circulating B cells (Naka et al., 2002). Other Tfh-specific marker BCL6+ cells were not found at all in the HYP+LY samples (Figure 3.2J and Supplementary Table 4).

3.1.3 Analysis of infiltrating immune cells in human testis presenting GCNIS with and without lymphocytic infiltrates (GCNIS±ly)

The infiltration density of different immune cells varies greatly between the pre-invasive precursor form of seminoma called GCNIS with and without immune cell infiltrates. T cells represent the leading immune cell type in both (Figure 3.4B, Figure 3.5B, Supplementary Figure 10A). In addition, it was also observed that CD4+ Th and CD8+ Tc cells were found in both sample groups with the highest density in GNCIS+ly samples (Figure 3.4F-G, Figure 3.5F-G, Supplementary Figure 10E-F). Macrophages represent the second most abundant immune cells in both samples and were detected more frequently in GCNIS+ly than in GCNIS (without infiltrates) samples (Figure 3.4D, Figure 3.5D, Supplementary Figure 10C). B cells were often found in GCNIS+ly while they were hardly detected in the GCNIS (Figure 3.4C, Figure 3.5C, Supplementary Figure 10B). DCs were often found in GCNIS (without infiltrates) but highly detectable in GCNIS+ly (Figure 3.5E, Supplementary Figure 10D).

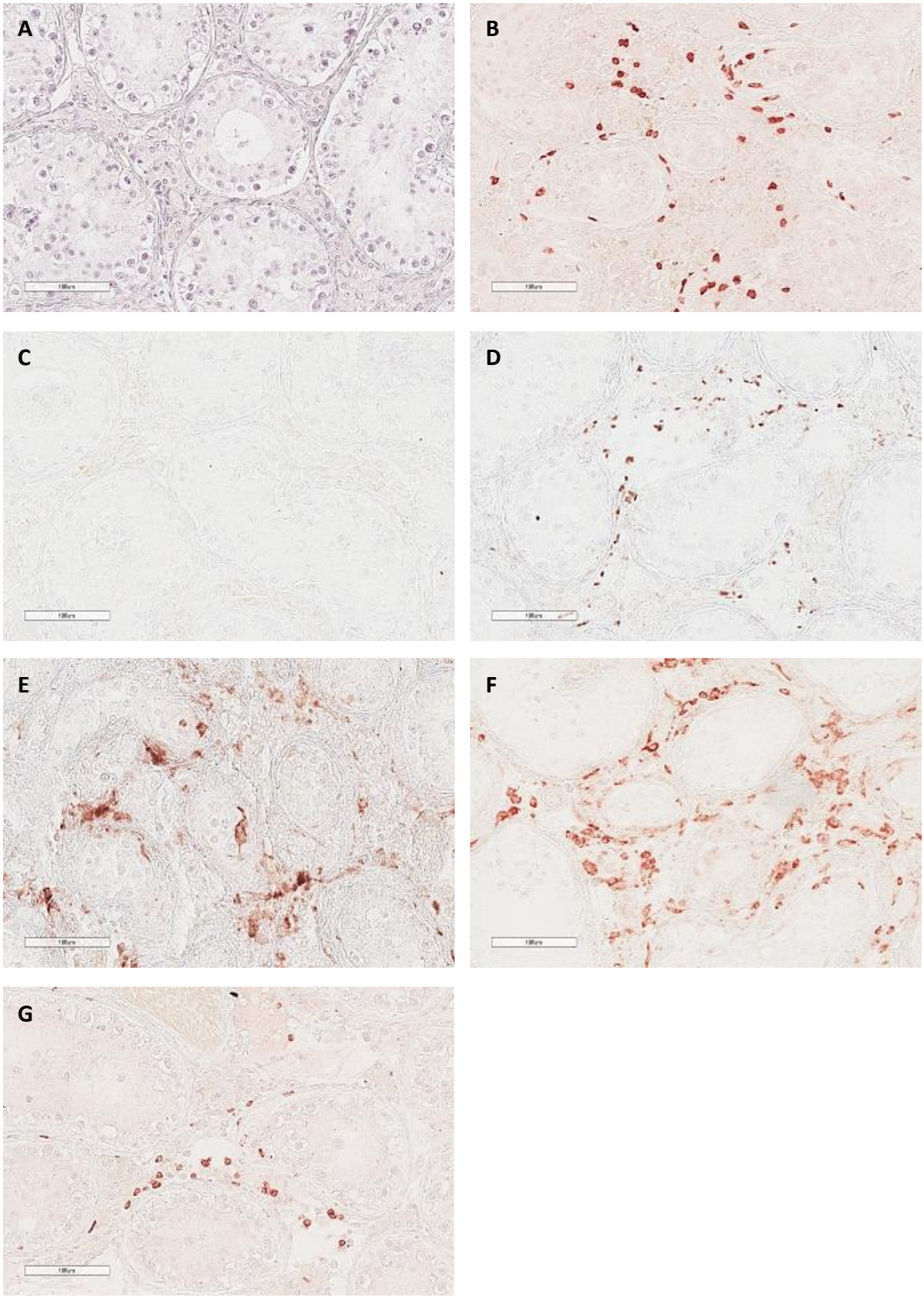

Figure 3.4 See next page for caption

Figure 3.4 Cont.

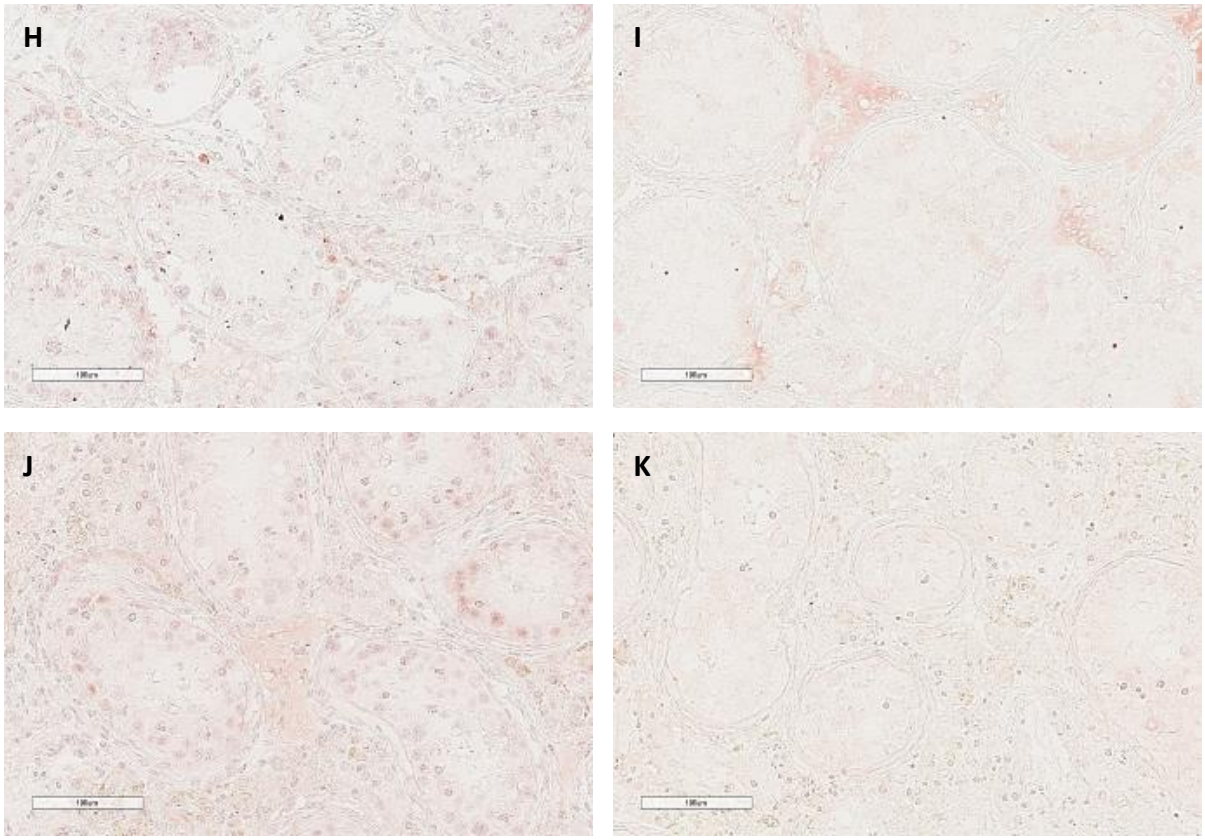

Figure 3.4 Analysis of infiltrating immune cells in GCNIS. H&E staining (A), CD3+ Pan T cells (B), CD20cy+ B cells (C), CD68+ macrophages (D), CD11c+ DC (E), CD4+ Th cells (F), CD8+ Tc cells (G), CD25+ Treg cells (H), FOXP3+ treg (I), CXCR5+ Tfh (J) and BCL6+ Tfh (K). T cells represent the major components of the infiltrating immune cells in GCNIS. White bar indicates 100µm.

Treg specific marker CD25+ cells were observed in both GCNIS (without infiltrates) and GCNIS+ly (Figure 3.4H, Figure 3.5H, E Supplementary Figure 10G), but FOXP3+ Tregs were mainly found in GCNIS+ly samples (Figure 3.4I, Figure 3.5I, Supplementary Figure 10H). Tfh cell marker CXCR5+ cells were rarely found in GCNIS and GNCIS+ly samples (Figure 3.4J, Figure 3.5J, Supplementary Figure 10I), whereas the other Tfh marker BCL6+ was not detected in any samples of these two groups (Figure 3.4K, Figure 3.5K, Supplementary Figure 10J).

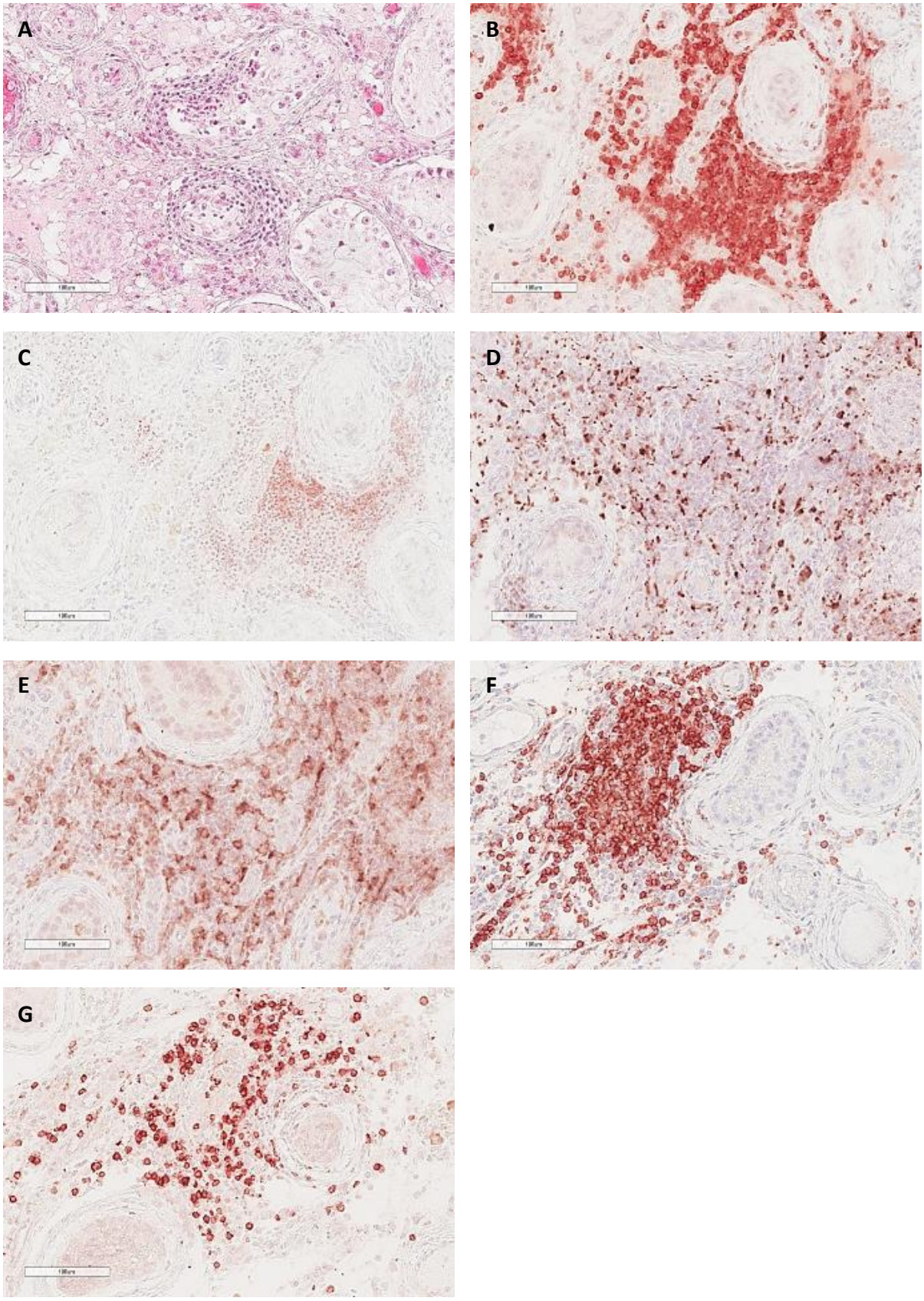

Figure 3.5 See next page for caption

Figure 3.5 Cont.

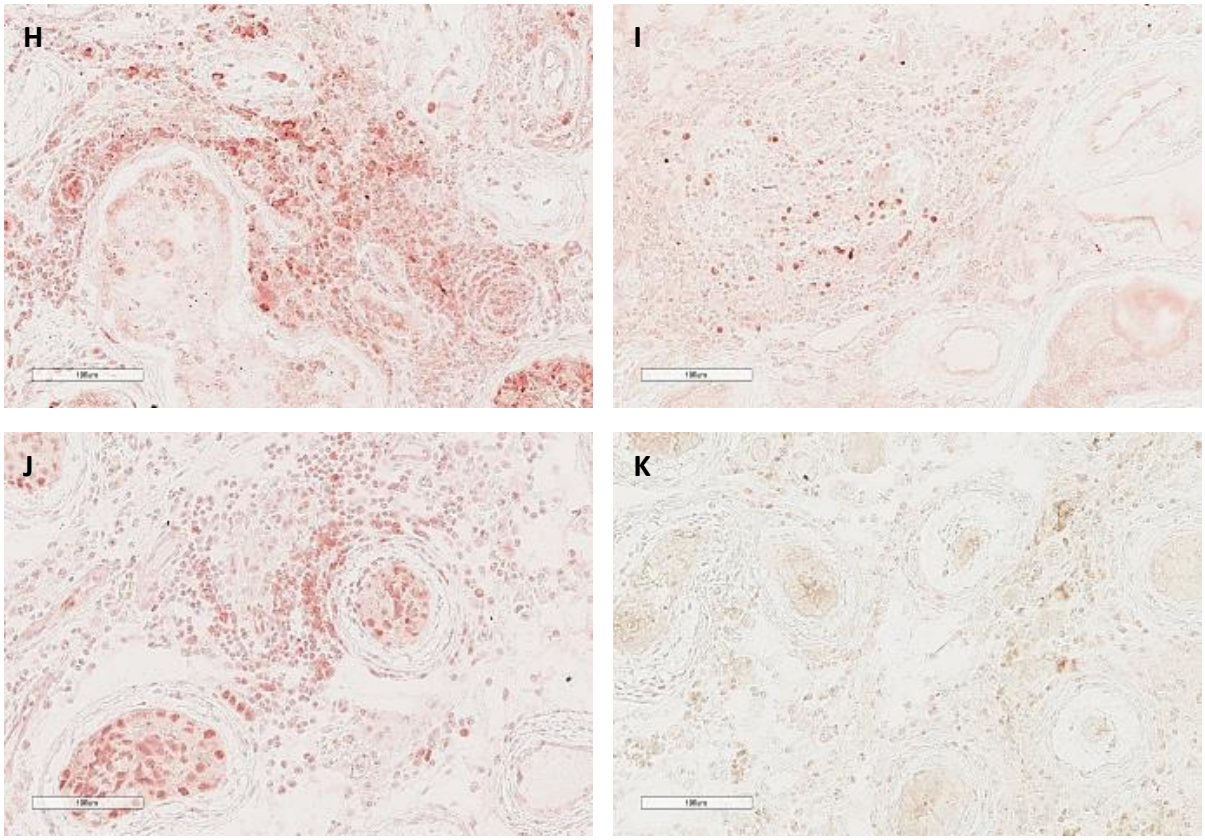

Figure 3.5 Analysis of infiltrating immune cells in GCNIS+ly. H&E staining (A), CD3+ Pan T cells (B), CD20cy+ B cells (C), CD68+ macrophages (D), CD11c+ DC (E), CD4+ Th cells (F), CD8+ Tc cells (G), CD25+ Treg cells (H), FOXP3+ treg (I), CXCR5+ Tfh (J) and BCL6+ Tfh (K). T cells represent the major components of infiltrating immune cells in GCNIS+ly. Magnifications x20. White bar indicates 100µm.

Briefly, T cells were significantly more frequent in both GCNIS (without infiltrates) and GCNIS+ly compared to the NSP. In the majority (66.67%) of GCNIS samples, pan T cells were found disseminated throughout the interstitium with a median score of 2 (Figure 3.2A, Supplementary Table 5). In addition, T cells were also found multifocally (median score of 2.75) in 26.67% and focally with relatively high scores in 6.67% of GCNIS samples (Figure 3.2A, Supplementary Table 5). While in GCNIS+ly samples, T cells were mostly found (in 75% of cases) in a multifocal fashion with a median score of 3.5 and in 18.75% of cases T cells were distributed over the interstitium with a median score of 2 (Figure 3.2A, Supplementary Table 6). In 6.25% of GCNIS+ly samples, T cells were detected focally, with high infiltration density (score 4) (Figure 3.2A, Supplementary Table 6). The main subtypes of T cells, Th and Tc cells were

significantly more frequent in both GCNIS (without infiltrates) and GCNIS+ly compared to normal testicular tissue. Both Th and Tc cells were observed in GCNIS (without infiltrates) and GCNIS+ly with different infiltration densities and distribution patterns. For example, Th cells were sparsely disseminated throughout the interstitium in 78.57% of cases (with a median score of 3) and were multifocally found in 21.43% of GCNIS samples (with a median score of 3) (Figure 3.2E, Supplementary Table 5). On the other hand, Th cells were multifocally present in 60% of GCNIS+ly samples and disseminated in 40% of GCNIS+ly samples with a median score of 4 and 3, resp. (Figure 3.2E, Supplementary Table.6). Tc were relatively low abundant compared to Th cells in both GCNIS and GCNIS+ly samples. Briefly, in 71.43% of GCNIS samples and in 13.33% of GCNIS+ly samples, Tc cells were found disseminated across the interstitium, with a median score of 2 in both sample groups (Figure 3.2F, Supplementary Table 5 and 6). In 80% of the GCNIS+ly and 28.57% of the GCNIS samples, Tc cells were found multifocally with a median score of 3 and 3.25, resp. (Figure 3.2F, Supplementary Table 5 and.6. In addition, Tc were only found focally (in 6.67% of cases) with a score of 3 in GCNIS+ly (Figure 3.2F, Supplementary Table 6). Overall, Th cells were relatively more abundant than Tc cells in both GCNIS (without infiltrates) and GCNIS+ly samples (Supplementary Figure 10E-F).

B cells were not detectable in 78.57% of the GCNIS and in 50% of the GCNIS+ly samples (Figure 3.2B, Supplementary Table 5 and 6). In GCNIS+ly samples with positive staining, B cells were often found focally (in 31.25% of cases) and multifocally (in 18.75% of cases) with relatively low infiltration density (median score of 1.5 and 2, resp.) (Figure 3.2B, Supplementary Table 6), While in GCNIS, B cells were only found focally (14.29% of cases) or in disseminated over the interstitium (7.14% of cases) with a median score of 1.5 and 1, resp. (Figure 3.2B, Supplementary Table 5). In both GCNIS (93.33% of cases) and GCNIS+ly (86.67% of cases) samples, macrophages were mainly distributed throughout the interstitium with median score of 2.25 and 2.5 resp. (Figure 3.2C, Supplementary Table 5 and 6). In addition, macrophages were also found multifocally in 13.33% of the GCNIS+ly samples with a median score of 2.25 (Figure 3.2C, Supplementary Table 6).

Antigen presenting DCs were significantly (p-value = 0.0044) more abundantly present in GCNIS+ly samples compared to NSP. DCs were differentially distributed in GCNIS

and GCNIS+ly samples. For example, DCs with low infiltration density (median score of 1) were found disseminated in 53.33% of the GCNIS samples (Figure 3.2D, Supplementary Table 5), while DCs were disseminated in only 13.33% of the GCNIS+ly samples with a median score of 1.75 (Figure 3.2D, Supplementary Table 6). In addition, DCs were found in multifocally in 33.33% of GCNIS+ly and in 6.67% of GCNIS with a median score of 3 (Figure 3.2D, Supplementary Table 5 and 6) and focally in 26.67% of GCNIS+ly samples and 13.33% of GCNIS samples with a median score 2.5 (Figure 3.2D, Supplementary Table 5 and 6). It should also be noted that no DCs were observed at all in 26.67% of these two samples groups (Figure 3.2D, Supplementary Table 5 and 6).

Treg cells were significantly more frequent in GCNIS+ly samples but not in GCNIS compared to NSP. Briefly, Treg-specific marker CD25+ cells were found disseminated throughout the interstitium in 64.29% of GCNIS (without infiltrates) and 41.67% of GCNIS+ly samples with a median score of 1 and 2, resp. (Figure 3.2G, Supplementary Table 5 and 6). In addition, CD25+ cells were also found multifocally in 21.43% of GCNIS (without infiltrates) and in 41.67% of GCNIS+ly samples with a median score of 2 and 2.5, resp. (Figure 3.2G, Supplementary Table 5 and.6). Furthermore, CD25+ cells were also focally found in 16.67% of the GCNIS+ly samples with relatively high infiltration density (median score of 3) (Figure 3.2G, Supplementary Table 6). It was also observed that no CD25+ cells were found in 14.29% of the GCNIS (without infiltrates) samples (Figure 3.2G, Supplementary Table 5). Another Treg marker FOXP3+ cells were found disseminated in 35.71% of GCNIS (without infiltrates) and 33.33% of GCNIS+ly samples with a median score of 0.5 and 1, resp. (Figure 3.2H, Supplementary Table 5 and 6). FOXP3+ cells were also found multifocally in 33.33 of the GCNIS+ly samples with a median score of 2 (Figure 3.2H, Supplementary Table 6). FOXP3+ cells were found focally in 7.14% of GCNIS and in 13.33% of GCNIS+ly samples with a median score of 0.5 and 1.25, resp. (Figure 3.2H, Supplementary Table 5 and 6). Moreover, no FOXP3+ cells were found in more than half (57.14%) of GCNIS (without infiltrates) and in 20% of GCNIS+ly samples (Figure 3.2H, Supplementary Table 5 and 6). Nevertheless, a putative abundance of Treg cells were mostly found in GCNIS+ly samples.

Tfh cells were not found in either GCNIS (without infiltrates) or GCNIS+ly samples. Briefly, Tfh-specific marker CXCR5+ cells were not found in 71.43% of GCNIS and 56.25% of GCNIS+ly samples (Figure 3.2I, Supplementary Table 5 and 6). In 25% of the GCNIS+ly and 7.14% of the GCNIS (without infiltrates) samples, CXCR5+ cells were only found focally with a median score of 1 and 0.5, resp. (Figure 3.2I, Supplementary Table 5 and F6). Whereas in 18.75% of the GCNIS+ly and in 7.14% of the GCNIS (without infiltrates) samples, CXCR5+ cells were also solely found multifocally with a median score of 2 (Figure 3.2I, Supplementary Table 5 and 6). Moreover, CXCR5+ cells were scarcely distributed over the interstitium in 14.29% of the GCNIS (without infiltrates) samples with a median score of 1.25 (Figure 3.2I, Supplementary Table 5). Other Tfh marker BCL6+ cells were absent in 100% of GCNIS (without infiltrates) and 93.75% of GCNIS+ly samples (Figure 3.2J, Supplementary Table 5 and 6). However, BCL6+ cells were very rarely found in 6.25% of the GCNIS+ly samples with an infiltration density score of 2 (Figure 3.2I, Supplementary Table 6). Overall, it was observed that Tfh cells were not found in GCNIS (without infiltrates) and extremely rarely in GCNIS+ly conditions.

3.1.4 Analysis of infiltrating immune cells in human testis with seminoma

T cells were most prominent in seminomas with the highest infiltration density. All other investigated immune cells were also abundant in seminomas compared to the other sample groups (Figure 3.6A-K, Supplementary figure 10A-J). Most importantly, BCL6+ Tfh cells were found in seminomas while absent in other sample groups (Figure 3.6K, Supplementary figure 10J). Remarkably, all infiltrating immune cells (except Tfh) were significantly more frequent in seminoma compared to the NSP samples. In addition, a statistical analysis of the presence of infiltrating immune cells was performed not only against NSP but also against HYP+ly, GCNIS±ly samples (Supplementary table 7).

T cells were significantly more frequent in seminomas compared to the testicular tissues with NSP. In 89.29% of the cases, T cells were found disseminated throughout the interstitium with the maximum intensity (median score of 4) (Figure 3.2A, Supplementary table 7). In rare cases (10.71% of samples), T cells were detected multifocally with a median score of 4 (Figure 3.2A, Supplementary table 7).

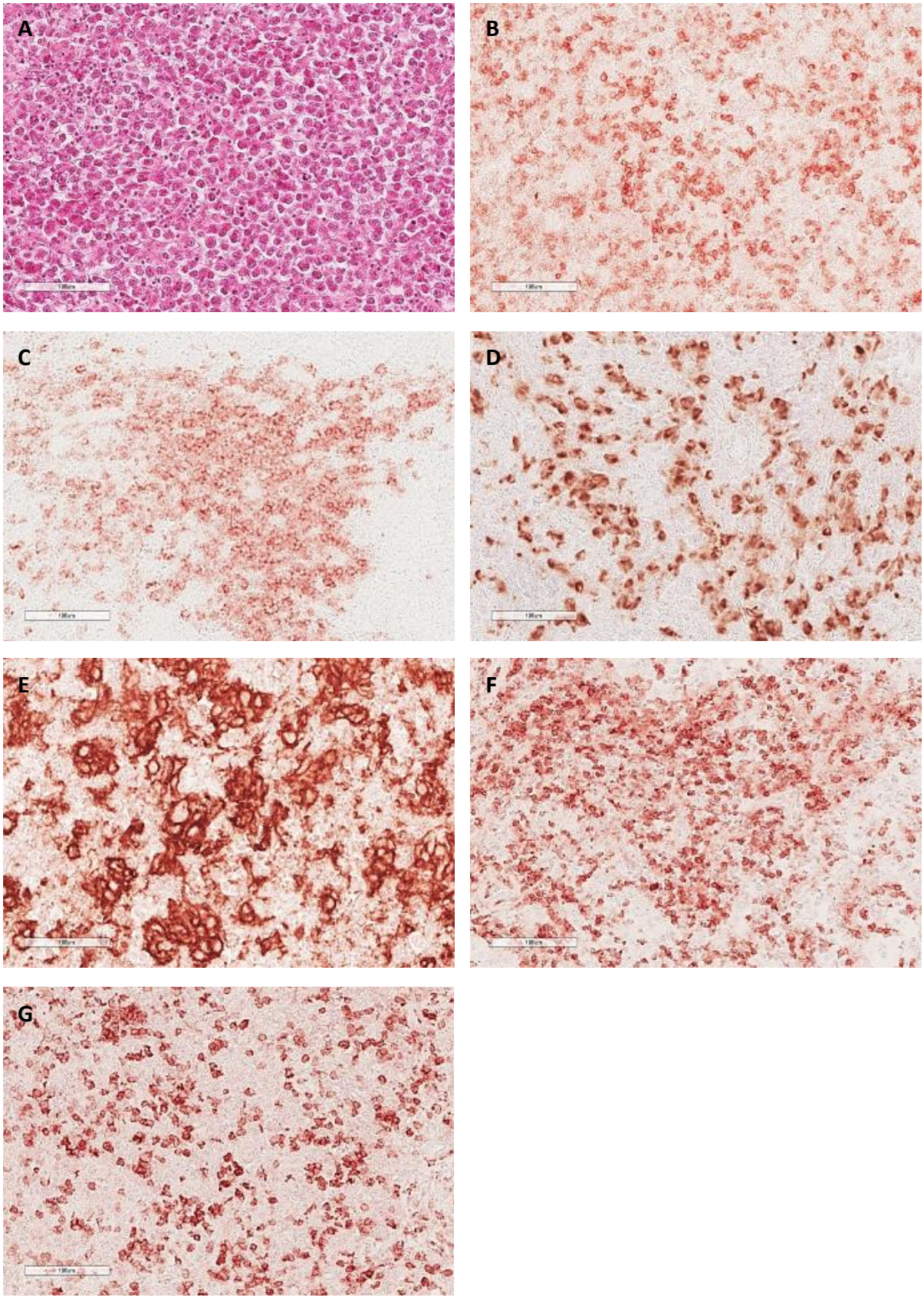

Figure 3.6 See next page for caption

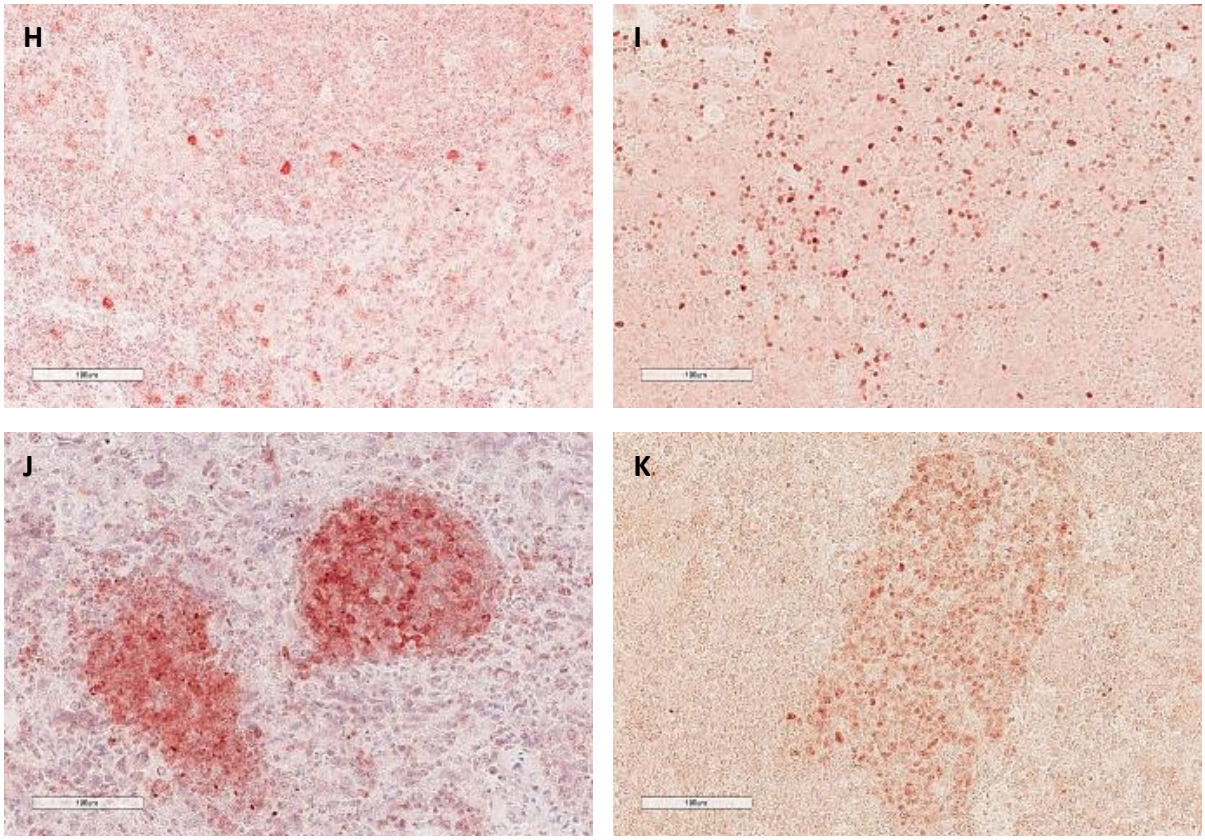

Figure 3.6 Analysis of infiltrating immune cells in Seminoma. H&E staining (A), CD3+ Pan T cells (B), CD20cy+ B cells (C), CD68+ macrophages (D), CD11c+ DC (E), CD4+ Th cells (F), CD8+ Tc cells (G), CD25+ Treg cells (H), FOXP3+ treg (I), CXCR5+ Tfh (J) and BCL6+ Tfh (K). T cells represent the major components of infiltrating immune cells in GCNIS+ly. White bar indicates 100µm.

Further analysis showed that Th cells are relatively more prevalent in seminomas than Tc cells. However, both cells were significantly more frequent in seminomas compared to the healthy testis (Supplementary figure 10E-F). The infiltration density and distribution of both cells varied across the seminoma samples. For example, Th cells showed a disseminated distribution in 88.46% of the cases, whereas Tc cells were disseminated in 100% of the samples with a median score of 4 and 3.25, resp. (Figure 3.2E-F, Supplementary table 7). In addition, Th cells were also found focally and multifocally in 7.69% and 3.84% of the samples, with a score of 4 and 3.5, resp. (Figure 3.2E, Supplementary table 7).

The highest number of B cells was found in seminoma compared to all other sample groups. Compared to NSP, B cells were significantly more frequent in seminomas with

distinct infiltration density and distribution (Figure 3.2B, Supplementary figure 10B). For example, B cells were relatively abundant (57.14% of cases) in multifocal areas with a median score of 2.75 (Figure 3.2B, Supplementary table 7), whereas in 35.71% of cases B cells showed a disseminated distribution with a median score of 2 (Fig. 2.7B, Supplementary table 7). In addition, some seminoma samples showed only focal B cell infiltration (score 2.5) or no B cells at all in 3.57% of samples (Fig. 2.7B, Supplementary table 7).

As with other infiltrating immune cells, the highest density of DCs was significantly more frequent in seminomas compared to normal testis with NSP (Figure 3.2D, Supplementary table 7). For example, in 75% of the seminoma samples, DCs were found distributed throughout the interstitium with a median score of 3.5 and in the remaining 25% of the samples, DCs were also found in multifocal areas with a median score of 3.5 (Figure 3.2D, Supplementary table 7).

Importantly, a high density of Treg cells was found in seminomas, which significantly differed from NSP (Figure 3.2G-H, Supplementary table 7). The infiltration density and distribution of Treg cells varied across the human testicular tissue samples with seminoma. For example, CD25+ Treg cells were predominantly (in 91.67% of cases) found disseminated throughout the interstitium with a median score of 2 (Figure 3.2G, Supplementary table 7). In addition, CD25+ cells were also found multifocally in 8.33% of seminomas with a median score 2.25 (Figure 3.2G, Supplementary table 7). FOXP3+ cells were mainly found disseminated throughout the interstitium with a median score of 2.5 in 92.30% of cases (Figure 3.2H, Supplementary table 7). In addition, it was also observed that FOXP3+ cells were absent in 7.69% of seminomas (Figure 3.2H, Supplementary table 7).

Most importantly, Tfh cells were not detectable in the other human testicular samples within this study, but only in seminomas. For example, in 58.33% of seminomas, Tfh-specific marker CXCR5+ cells were mostly found in multifocal areas with a high infiltration density (median score of 4) (Figure 3.2I, Supplementary table 7). In addition, CXCR5+ cells were also distributed across the interstitium in 41% of cases with a relatively low median score of 2 (Figure 3.2I, Supplementary table 7). Other Tfh cell marker BCL6+ cells were found in multifocal areas in 14.81% of cases, or focally and

disseminated in the interstitium in 11.11% of cases with median scores of 3.5, 2, and 1, resp. (Figure 3.2J, Supplementary table 7). In almost half (45.90% of cases) of the seminomas BCL6+ cells were not found (Figure 3.2J, Supplementary table 7). It should be noted that BCL6+ cells were only found in seminomas tissue containing follicle-like structures (FLS).

3.2 Analysis of immune cell infiltrates in fresh human testicular specimens from tumor-bearing and contralateral testes using flow cytometry

3.2.1 Analysis of the immune cell composition in TGCT and unaffected human testicular tissue

Despite the extensive phenotypic heterogeneity of the tissue samples (Table 2.3 and Supplementary Table 1), consistent with the IHC findings described in section 3.1, comprehensive flow cytometric analysis of infiltrating immune cells using antibody panel-1 (Table 2.5) in fresh human testicular tissues specimens from the both tumor-bearing and contralateral testis of TGCT patients showed that the highest frequency of T cells (18.96-88.52% of total live cells with a median of 71.49%) was present in Tumor sites of seminoma compared to other localizations in seminoma, embryonal carcinoma (≥80%), mixed TGCT, or specimens from contralateral, tumor-free testes (Figure 3.7A and Table 3.1). In addition, the highest percentages of CD4+ Th cells and CD8+ Tc cells (17.03-60.69% and 0.56-43.98% of total live cells with a median of 42.6055 and 25.425%, resp.), were also detected in Tumor sites of seminoma, compared to Tumor-Adjacent or Tumor-Distant localizations in seminoma, embryonal carcinoma (≥80%), mixed TGCT, or the contralateral sides (Figure 3.7B-C and Table 3.1). Interestingly, CD68+ macrophages represent the second most abundant infiltrating immune cells in human TGCT and were more frequently found in Tumor sites of embryonal carcinoma (≥80%) compared to other TGCT (Figure 3.7D). In addition, it was also observed that CD68+ macrophages represent the most abundant type of immune cells in contralateral testes. Compared to the T cells and macrophages, a relatively small number of CD20cy+ B cells was found in all localizations of all samples (Figure 3.7E); however, the highest number of B cells were found in Tumor sites of seminoma.

Table 3.1 Percentage of infiltrating immune cells in human testicular tissue using Panel 1 antibodies.

Internal patient number	Histology	Tissue/sample location (s)	Total number of single live cells	% Single total live cells	% Of cells in total single live cells					
					CD20cy+ cells	CD68+ cells	CD4+CD68 + cells	CD3+ cells	CD4+ cells	CD8+ cells
Hoca-51	100% seminoma	Tumor	388688	85.02	6.04	1.37	0.64	86.26	49.01	30.12
Hoca-55		Tumor	40238	61.79	3.5	1.16	0.96	84.35	37.17	40.76
		Tumor-Dis	11024	53.26	1.36	6.55	0.62	10.26	5.63	4.67
Hoca-56		Tumor	197834	86.66	1.6	3.06	2.57	82.44	53.61	27.58
		Tumor-Adj	31843	53.56	0.99	3.93	3.31	25.07	16.40	13.31
		Tumor-Dis	11024	53.26	18.1	3.55	0.62	10.26	5.63	4.67
Hoca-59		Tumor	149037	94.84	6.11	1.01	0.05	88.52	60.69	20.44
		Tumor-Adj	25007	65.43	3.63	5.9	2.90	78.54	67.21	12.46
		Tumor-Dis	1988	73.25	1.02	3.65	0.20	38.48	26.51	5.18
HoCa-68		Tumor	25481	6.16	7.52	12.60	4.86	52.88	35.91	26.64
		Tumor-Adj	110997	84.59	2.45	7.74	0.87	10.55	6.74	4.58
HoCa-69		Tumor	5918	86.88	0.69	1.65	0.32	30.48	26.75	7.65
		Tumor-Adj	7006	82.54	0.87	3.81	0.37	9.39	1.36	0.10
		Tumor-Dis	21096	68.64	0.41	28.10	0.05	0.72	0.45	0.03
		Contralateral 1	19074	84.05	1.15	5.31	2.54	3.28	5.48	0.03
		Contralateral 2	15092	80.77	0.74	2.33	5.69	2.01	12.08	0.06
HoCa-73		Tumor	923897	74.77	1.39	2.65	2.16	85.65	49.85	28.51
		Tumor-Adj	17723	76.24	3.96	2.95	1.27	71.62	41.24	41.69
		Tumor-Dis	2442	73.40	0.70	3.48	0.20	12.49	5.45	3.60
		Contralateral 1	3008	78.87	0.93	12.10	1.96	11.60	9.74	4.82
		Contralateral 2	46410	94.88	0.14	5.5	1.75	1.80	3.24	0.59
HoCa-76		Tumor	538	41.04	2.35	5.28	4.46	18.96	23.23	0.56
		Tumor-Adj	1517	8.23	1.43	0.31	0.20	12.13	3.89	0.26
		Tumor-Dis	1495	39.26	1.54	2.21	0.80	8.16	6.22	0.94
		Contralateral 1	3303	77.70	2.94	3.30	6.63	30.28	13.84	1.24
		Contralateral 2	2364	72.49	1.48	2.71	2.07	23.22	8.67	1.67
HoCa-78		Tumor	242720	58.63	1.1	15	7.91	72.09	53.85	25.13
		Contralateral 1	9961	90.90	0.57	8.65	4.34	1.97	9.21	0.10
		Contralateral 2	11100	91.51	0.38	4.42	6.23	1.00	13.06	0.22

Table 3.1 continue

Internal patient number	Histology	Tissue/sample location (s)	Total number of single live cells	% Single total live cells	% Of cells in total single live cells					
					CD20cy+ cells	CD68+ cells	CD4+CD68+ cells	CD3+ cells	CD4+ cells	CD8+ cells
HoCa-82	100% seminoma	Tumor	53196	26.78	9.64	3.2	2.09	70.89	48.04	25.72
		Tumor-Adj	294	34.51	2.60	0.97	0.00	6.12	4.42	1.02
		Tumor-Dis	1592	57.33	2.26	3.71	0.13	28.96	0.69	0.63
		Contral ateral 2	25265	89.05	0.075	8.82	0.60	0.71	1.35	0.31
HoCa-83		Tumor-Adj	1423	65.88	0.53	5.65	0.77	8.22	4.71	5.06
		Tumor-Dis	2187	69.78	1.1	4.48	0.27	6.26	1.92	3.66
HoCa-84		Tumor	25205	79.94	11.90	6.3	1.98	21.18	17.03	4.66
		Tumor-Adj	25521	92.12	0.19	4.59	0.05	0.49	1.48	0.22
		Tumor-Dis	2920	78.54	0.31	23.3	0.07	2.36	0.79	0.14
		Contral ateral 1	7286	82.39	0.37	4.75	1.51	3.03	2.42	0.15
		Contral ateral 2	3489	78.19	1.2	3.55	5.16	5.79	5.19	0.09
HoCa-90		Tumor	1291	51.11	2.30	3.61	3.49	30.36	32.67	6.97
		Tumor-Adj	1737	58.84	6.01	5.72	1.73	28.27	22.34	9.44
Hoca-61	80% EC + 20% Post-pubertal Teratoma	Tumor	252399	67.60	0.91	7.17	0.48	77.32	35.90	43.98
		Tumor-Adj	95159	92.63	1.76	6.66	0.19	11.64	5.61	0.00
		Tumor-Dis	117875	86.93	1.31	3.91	0.02	15.96	8.77	6.67
Hoca-60	95% EC, 5% Post-pubertal Teratoma	Tumor	6493	81.66	2.34	17.7	10.55	50.05	36.25	18.20
Hoca-70	99%EC+ 1%SE	Tumor	147292	34.79	3.63	24.8	6.21	37.49	45.13	14.63
		Tumor-Adj	30791	70.91	0.24	5.96	4.90	3.83	11.28	18.16
		Tumor-Dis	69599	92.73	0.042	3.57	0.02	0.23	0.74	27.89
		Contral ateral 1	4626	77.41	0.26	1.69	2.96	1.28	3.29	1.80
		Contral ateral 2	1780	65.71	1.4	1.54	6.18	4.21	18.60	56.29
Hoca-71	85% EC+15% Yolk sac	Tumor	16607	1.02	1.32	34.4	7.23	11.47	28.31	3.71
		Tumor-Adj	273187	56.01	0.38	0.14	0.02	0.40	4.08	0.13
		Tumor-Dis	49462	89.02	0.17	7.30	0.22	0.57	1.49	0.24
		Contral ateral 1	4673	85.68	1.52	21.6	0.90	3.85	4.22	0.11
		Contral ateral 2	6149	83.76	0.72	7.61	2.52	1.22	4.90	0.28
Hoca-79	95% EC+5% yolk sac	Tumor	52175	64.05	1.21	11.7	5.45	52.87	34.53	23.68
		Tumor-Adj	7886	59.30	1.01	12.80	1.38	14.96	5.82	4.77
		Tumor-Dis	3761	58.20	0.80	9.15	1.65	7.50	5.50	2.47

Table 3.1 continue

Internal patient number	Histology	Tissue/sample location (s)	Total number of single live cells	% Single total live cells	% Of cells in total single live cells					
					CD20cy+ cells	CD68+ cells	CD4+CD68+ cells	CD3+ cells	CD4+ cells	CD8+ cells
Hoca-79	95% EC+5% yolk sac	Contral ateral 1	5241	73.41	0.61	11.80	3.53	3.24	6.09	0.04
		Contral ateral 2	6253	83.01	1.63	17.10	6.22	5.95	10.27	0.06
Hoca-80	100% EC	Tumor	116945	69.07	3.2	12.2	14.98	61.51	38.68	33.68
		Tumor-Adj	2210	48.41	0.35	5.89	3.57	5.29	13.80	1.18
		Contral ateral 1	2362	67.10	0.72	22.30	1.35	1.14	2.46	0.21
		Contral ateral 2	13006	81.39	0.81	5.22	3.44	0.98	3.90	0.07
Hoca-64	Mixed TGCT (30% EC+70% Post-pubertal Teratoma)	Tumor	8327	89.39	37.3	1.31	0.90	42.22	28.09	12.09
		Tumor-Adj	1297	77.43	2.94	1.33	0.23	11.64	2.78	0.93
		Tumor-Dis	2796	86.94	1.47	2.04	0.54	12.09	6.62	4.61
Hoca-66	Mixed TGCT (50% SE+ 50%EC) Hematoma + scarring	Tumor	3431	39.02	0.74	22.9	2.39	6.35	29.32	0.00
		Tumor-Adj	9478	49.15	2.94	9.02	5.44	36.58	37.90	7.82
		Tumor-Dis	5679	81.64	0.88	2.71	2.47	9.40	13.14	2.39
Hoca-72	Mixed TGCT (70% EC+30% SE)	Tumor	3114	55.37	0.78	42.10	15.51	30.60	31.95	12.27
		Tumor-Adj	1093	68.01	0.88	2.83	2.38	9.88	14.27	2.65
		Tumor-Dis	1349	71.22	0.89	10.30	0.67	3.63	8.60	1.48
		Contral ateral 1	23000	93.49	0.45	21.8	2.70	0.62	4.06	0.11
		Contral ateral 2	1157	64.96	0.86	6.66	1.38	4.15	3.37	0.00
Hoca-74	Mixed TGCT (30% post pub. teratoma, 20% EC, Yolk sac tu. 15%, + small amount of choriocarcinoma (plus GCNIS)	Tumor	48751	70.66	1.39	8.25	1.34	55.25	41.42	19.74
		Tumor-Adj	5213	25.83	1.72	5.17	2.63	31.33	19.91	13.24
		Tumor-Dis	3818	48.74	2.54	7.02	3.77	25.77	22.24	11.29
		Contral ateral 1	12313	84.05	0.41	6.62	1.37	1.84	2.67	0.12
		Contral ateral 2	81665	98.15	3.15	4.97	2.14	3.08	14.53	0.20
Hoca-86	70% SE + 30% EC	Tumor	3510	72.99	0.77	27.9	10.11	39.15	42.93	16.13
		Tumor-Adj	94652	76.35	0.45	6.85	5.19	2.58	7.47	1.07
		Tumor-Dis	28063	91.60	1.61	14.20	0.64	0.52	0.81	0.13
		Contral ateral 1	2527	80.43	0.79	8.90	3.72	1.82	5.70	0.04
		Contral ateral 2	10326	82.31	2.29	40.5	7.70	0.33	2.88	0.08

Table 3.1 continue										
Internal patient number	Histology	Tissue/sample location (s)	Total number of single live cells	% Single total live cells	% Of cells in total single live cells					
					CD20cy+ cells	CD68+ cells	CD4+CD68+ cells	CD3+ cells	CD4+ cells	CD8+ cells
Hoca-91	Mixed TGCT (% Breakdown unfortunately not possible)	Tumor	1031	55.67	9.03	5.92	2.91	30.46	21.14	11.83
		Tumor-Adj	1859	59.70	0.11	7.02	0.59	1.72	14.42	0.11
		Tumor-Dis	6052	84.96	1.21	8.76	0.68	0.25	2.33	0.00
		Contralateral 1	5803	84.25	1.52	5.08	7.24	1.90	11.10	0.16
		Contralateral 2	6615	93.62	0.91	3.98	9.42	2.90	21.44	0.05

Briefly, immune cells composition and infiltration were distinct across the different tissue sites of TGCT. For example, the highest percentage of CD3+ T cells (18.96-88.52 % of total live cells, with a median of 71.49%) was found in the Tumor sites of seminoma compared to the other localizations of seminoma and other tumor samples (Figure 3.7A and Table 3.1). The highest number of T cells in the Tumor sites compared to Tumor-Adj (0.49-78.54%, median 11.34%), Tumor-Dis (0.72-38.48%, median 10.26%) and the contralateral sides (1.97-11.60%, median 3.24%) and 0.71-23.22%, median 1.905% in contralateral 1 and contralateral 2, resp.) of the seminoma was highly significant (Supplementary Table 9). The number of CD3+ T cells (11.47-77.32%, median 51.36%) in Tumor sites of embryonal carcinoma (>80%) was also significantly higher than the other localizations including the contralateral sites (Tumor-Adj 0.40-14.96%, median 5.29%, Tumor-Dis 1.72-36.58%, median 10.76%, contralateral 1 1.38-3.85%, median 2.31%, and contralateral 2 0.98-5.95%, median 2.71%) (Figure 3.7A, Table 3.1 and Supplementary Table 9). A relatively low number of CD3+T cells (6.35- 55.25 %, median of 34.88%) were detected in mixed tumors but they were no significant differences in localizations (Tumor-Adj 0.23-15.96%, median 4.035 %, Tumor-Dis 0.25-25.77%, median 6.515 %, contralateral 1 0.62-1.90%, median 1.83, contralateral 2 0.33-4.15%), possibly be due to extensive histological heterogeneity of the tissues (Figure 3.7A, Table 3.1 and Supplementary Table 9). Taken together, it is clearly shown that the abundance of T cells is greatly reduced from the Tumor site to the Tumor-Adj and Tumor-Dis sites of all TGCT.

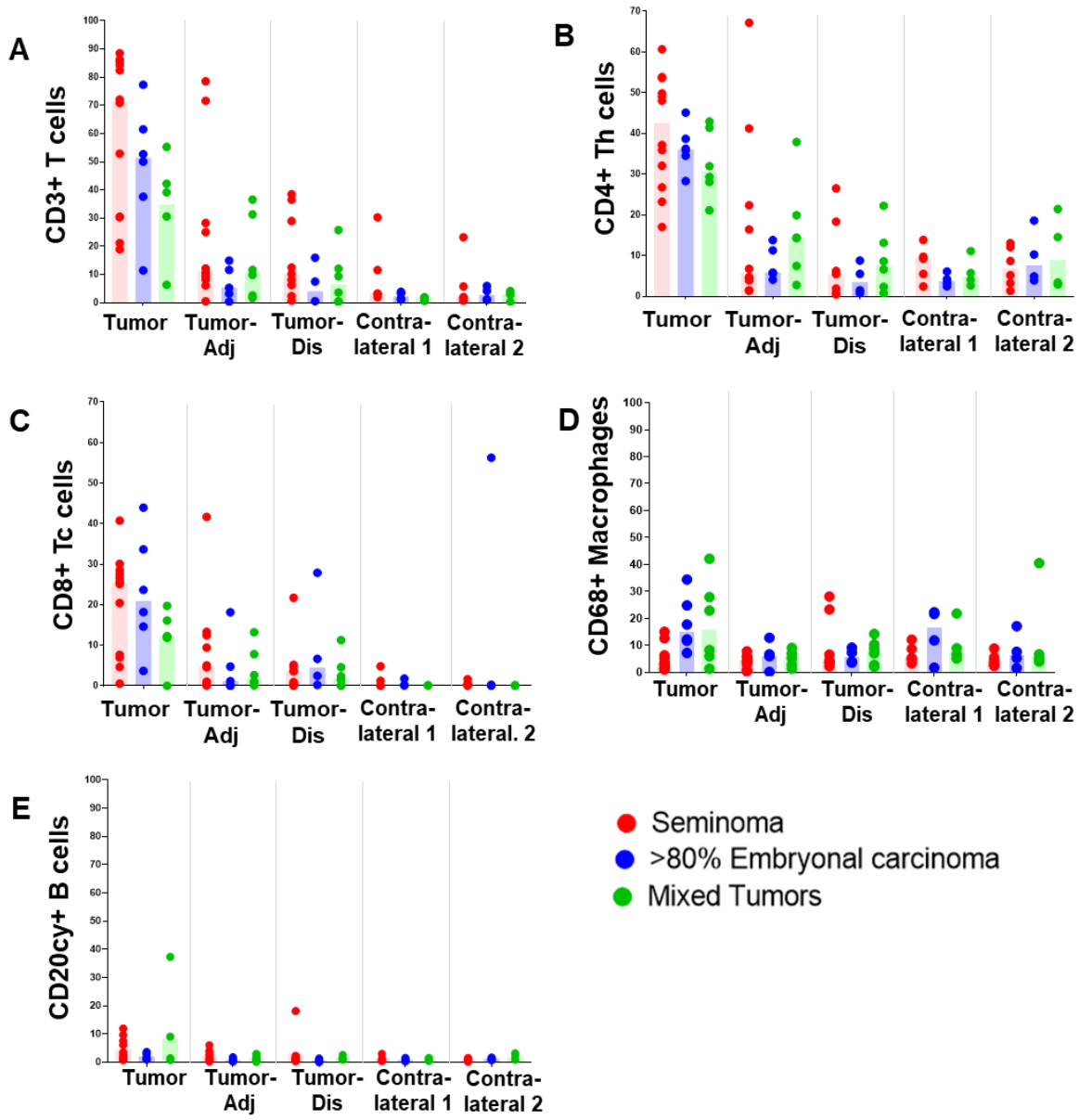

Figure 3.7 Flow cytometric analysis of human testicular immune cells. A-E: Overview of the measured individual values of different immune cells (CD3+ T cells, CD4+Th cells, CD8+ Tc cells, CD68+ macrophages, CD20cy+ B cells) in tumor-bearing and contralateral testes from n=24 patients [seminoma: Tumor n=12; Tumor-Adj n=10; Tumor-Dis n=9; Contralateral 1 n= 5; Contralateral 2 n= 6; embryonal carcinoma: Tumor n=6; Tumor-Adj n=5; Tumor-Dis n=4; Contralateral 1 n=4; Contralateral 2 n=4; mixed TGCT: Tumor n=6; Tumor-Adj n=6; Tumor-Dis n= 6; Contralateral 1 n=4; Contralateral 2 n= 4].

In addition to CD3+T cells, further analysis showed that CD4+ Th cells were also abundantly found in Tumor sites of seminoma compared to the other localizations of classical seminoma and other TGCT. The highest percentage of CD4+Th cells (17.03-60.69% of total live cells with a median of 42.605%) was significantly more frequent in

Tumor sites of seminoma compared to the other localizations (Tumor-Adj 1.36-67.21%, median 5.725%, Tumor-Dis 0.45-26.51%, median 5.45%, contralateral 1 2.42-13.84%, median 9.21, contralateral 2 1.35-13.06%, median 6.93%) of seminoma and other TGCT (Figure 3.7B, Table 3.1 and Supplementary Table 10). In embryonal carcinoma (≥80%), higher numbers of CD4+Th cells (28.31-45.13%, median 36.075%) were found in Tumor sites compared to other localizations (Tumor-Adj 4.08-13.80%, median 5.82%, Tumor-Dis 0.74-8.77%, median 3.495%, contralateral 1 2.46-6.09%, median 3.755%, contralateral 2 3.90-18.60%, median 7.585%) (Figure 3.7B, Table 3.1 and Supplementary Table 10). In addition, a relatively low number of CD4+Th cells (21.14-42.93%, median 30.635%) was found in Tumor sites of mixed TGCT compared to their other localizations (Tumor-Adj 2.78-37.90%, median 14.345%, Tumor-Dis 0.81-22.24%, median 7.61%, contralateral 1 2.67-11.10%, median 4.88% and contralateral 2 3.37-21.44%, median 8.95%) (Figure 3.7B, Table 3.1 and Supplementary Table 10).

Compared to the CD3+ T cells and CD4+Th cells, relatively low numbers of CD8+Tc cells were detected in the different localization of sample. Similar to total CD3+ T cells and CD4+ Th, CD8+ Tc cells were also abundantly found in Tumor sites of seminoma compared to the other localizations of seminoma and other TGCT. The highest percentage of CD8+Tc cells (0.56-40.76% of total live cells with a median of 25.425%) was found (statistically not significant) in the Tumor sites of seminoma compared to the other localizations (Tumor-Adj 0.10-41.69%, median 4.82%, Tumor-Dis 0.03-21.73%, median 3.60%, contralateral 1 0.03-4.82%, median 0.15%), contralateral 2 0.06-1.65%, median 0.265%) of seminoma and other TGCT samples (Figure 3.7C, Table 3.1 and Supplementary Table 11). The number of CD8+ Tc cells (3.71-43.98%%, median 20.64%) in Tumor sites of embryonal carcinoma (>80%) was higher than the other localizations (Tumor-Adj 0.00-18.16%, median 1.18%, Tumor-Dis 0.24-27.89%, median 4.57%, contralateral 1 0.04-1.80%, median 0.16%, contralateral 2 0.06-56.19%, median 0.175% of total live cells), but not statistically significant (Figure 3.7C, Table 3.1 and Supplementary Table 11). In contrast to seminoma and embryonal carcinoma (>80%), relatively low numbers of CD8+Tc cells (0.00-19.74% of total live cells with a median of 12.18%) were detected in mixed tumors, but there was no significant difference compared to other localizations (Tumor-Adj 0.11-13.24%, median 1.86%, Tumor-Dis 0.00-11.29%, median 1.935%, contralateral 1 0.04-0.16%,

median 0.115%, contralateral 2 0.00-0.20%, median 0.065%) (Figure 3.7C, Table 3.1 and Supplementary Table 11).

CD68+ macrophages represent the second most frequently detected infiltrating immune cells in the different localizations of tumor-bearing and contralateral testis of TGCT. The highest percentage of CD68+ macrophages was found in the different localization of embryonal carcinoma (≥80%) and mixed TGCT compared to seminoma (Figure 3.7D and Table 3.1). However, CD68+ macrophages across the different localizations of TGCT samples was not statistically significant (Supplementary Table 12). Nevertheless, 7.17-34.4% (median 14.95%) and 1.31-42.10% (median 15.58%) of total live cells were CD68+ macrophages detected in Tumor sites of embryonal carcinoma (≥80%) and mixed tumors, resp. (Figure 3.7D and Table 3.1), while only 1.01-12.60% (median 3.13%) of total live cells were CD68+ macrophages in Tumor sites of seminoma (Figure 3.7D and Table 3.1). Besides, CD68+ macrophages accounted for 0.14-12.80% (median 5.96%) of total live cells in Tumor-Adj sites of embryonal carcinoma (≥80%), 1.33-9.02% (median 6.01%) of total live cells in Tumor-Adj sites of mixed tumors, and 0.31-7.74% (median 4.26) of total live cells in Tumor-Adj sites of seminoma (Figure 3.7D and Table 3.1). Whereas in Tumor-Dis sites of embryonal carcinoma (≥80%), mixed tumors and seminoma, CD68+ macrophages accounted for 3.57-9.15% (median 3.91%), 2.04-14.2% (median 7.89%) and 2.21-28.1% (median 3.71%) of total live cells, resp. (Figure 3.7D and Table 3.1). In addition to tumor-bearing testis, CD68+ macrophages represent the highest infiltrating immune cell type found in contralateral sites (representing mostly NSP and/or HYP) of all TGCT (Figure 3.7D and Table 3.1). For example, the median percentage of CD68+ macrophages were 16.7% (1.69-22.3%) and 6.415% (1.54-17.10%) of total live cells, resp., found in contralateral 1 and contralateral 2 site of embryonal carcinoma (≥80%) (Figure 3.7D and Table 3.1). While in contralateral 1 and contralateral 2 site of mixed tumors, CD68+ macrophages accounted for a median percentage of 7.76% (5.08-21.8%) and 5.815% (3.98-40.5%) of total live cells, resp. (Figure 3.7D and Table 3.1). In addition, a relatively low amount of CD68+ macrophages with a median percentage of 5.31% (3.30-12.1%) and 3.985% (2.33-8.82%) of the total live cells were found in the contralateral 1 and contralateral 2 site of seminoma, resp. (Figure 3.7D and Table 3.1). Taking together, among the various infiltrating immune cells, macrophages represent the leading immune cells in the contralateral sites of all TGCT. On the other

hand, macrophages were identified as a second highest infiltrating immune cell type in the different localizations of tumor-bearing testis of TGCT patients, also indicating their functional involvement in different TGCT development and progression.

Compared to T cells and macrophages, only a small percentage of CD20cy+ B cells were found in the different locations of TGCT, though CD20cy+ B cell numbers were not significantly different across the sample localizations (Figure 3.7E, Table 3.1 and Supplementary Table 13). For example, the median percentage of CD20cy+ B cells was 4.51% (0.69-11.9%), 2.27% (0.019-6.01%), 2.98% (0.31-18.1%), 1.192% (0.37-2.94%), and 0.67% (0.07-1.48%) of total live cells found in Tumor, Tumor-Adj, Tumor-Dis, contralateral 1 and contralateral 2 sites of seminoma, resp. (Figure 3.7E, Table 3.1). While CD20cy+ B cells accounted for a median percentage of 2.10% (0.91-3.63%), 0.748% (0.24-1.76%), 0.58% (0.042-1.32%), 0.77% (0.26-1.52%), and 1.14(0.72-1.63) of total live cells found in Tumor, Tumor-Adj, Tumor-Dis, contralateral 1 and contralateral 2 sites of embryonal carcinoma (≥80%), resp. (Figure 3.7E, Table 3.1). In addition, the median percentage of CD20cy+ B cells was 8.335% (0.74-37.3%), 1.50% (0.11-2.95%), 1.43% (0.88-2.54%), 0.79% (0.45-1.52%), and 1.80% (0.86-3.15%) of total live cells found in Tumor, Tumor-Adj, Tumor-Dis, contralateral 1 and contralateral 2 sites of mixed tumors, resp. (Figure 3.7E, Table 3.1). Taken together, CD20cy+ B cells were mostly found in the tumor-bearing testis rather than in contralateral testis.

3.2.2 Analysis of CD25+FOXP3+ Treg and CXCR5+BCL6+ Tfh cells in human testicular tissues

Comprehensive flow cytometric analysis showed that both CD25+FOXP3+ Treg and CXCR5+BCL6+ Tfh cells are present in the different localizations of both the tumor-bearing and contralateral testis of TGCT patients.

Table 3.2 Percentage of CD25+FOXP3+ Treg and CXCR5+BCL6+ Tfh cells in human testicular tissue using Panel 2 antibodies.

Internal patient number	Histology	Tissue/sample localization(s)	Total number of single live cells	% Single total live cells	% Of CD25+FOXP3+ in total single live cells	% Of CD185+BCL6+ in total single live cells
Hoca-68	100% Seminoma	Tumor	66680	6.44	1.10	0.05
		Tumor-Adj	109761	85.86	0.11	0.04
Hoca-69		Tumor	16893	95.30	1.52	0.30
		Tumor-Adj	13829	92.32	0.42	0.06
		Tumor-Dis	15601	69.33	2.01	0.10
		Contralateral 1	21902	88.48	0.16	0.12
		Contralateral 2	23697	83.58	0.31	0.08
Hoca-73		Tumor	1120864	84.96	1.05	0.44
		Tumor-Adj	15459	77.45	0.68	0.12
		Tumor-Dis	2612	83.34	0.11	0.23
		Contralateral 1	3324	80.14	0.69	0.75
		Contralateral 2	20783	86.74	0.02	0.11
Hoca-76		Tumor	2013	73.09	0.10	0.30
		Tumor-Adj	7552	30.30	0.37	0.09
		Tumor-Dis	3991	67.87	0.58	0.63
		Contralateral 1	3138	81.63	0.83	0.10
		Contralateral 2	3307	79.78	0.39	0.18
Hoca-78		Tu	254958	61.24	0.33	2.40
		Contra.1	7718	90.39	0.13	0.27
		Contra.2	9530	85.20	0.02	0.12
Hoca-82		Tumor	51506	23.75	2.89	0.74
		Tumor-Adj	1069	57.60	0.30	0.20
		Tumor-Dis	1863	63.98	0.32	0.16
		Contralateral 2	25542	86.69	0.16	0.00
Hoca-84		Tumor	289193	86.63	1.53	0.21
		Tumor-Adj	66522	89.26	0.20	0.30
		Tumor-Dis	5421	78.24	0.26	0.52
		Contralateral 1	6390	84.66	0.00	0.00
		Contralateral 2	2521	75.46	0.12	0.24
Hoca-90		Tumor	4579	66.35	2.51	0.23
		Tumor-Adj	2820	71.37	1.10	0.04
Hoca-70	99%EC+ 1%SE	Tumor	382857	44.03	1.45	0.25
		Tumor-Adj	61599	66.71	0.03	0.01
		Tumor-Dis	37156	85.62	0.28	0.01
		Contralateral 1	4944	79.07	0.14	0.22
		Contralateral 2	3071	83.68	0.26	0.13
Hoca-71	85% EC+15% Yolk sac	Tumor	468516	31.79	0.02	0.08
		Tumor-Adj	376549	58.59	0.02	0.12
		Tumor-Dis	398298	61.26	0.32	0.18
		Contralateral 1	3889	82.73	0.69	0.05
		Contralateral 2	3489	79.08	0.23	0.06
Hoca-79	95% EC+5% yolk sac	Tumor	74296	65.04	0.83	0.37
		Tumor-Adj	11788	52.15	0.13	0.12
		Tumor-Dis	7642	68.11	0.05	0.30
		Contralateral 1	7121	77.35	0.08	0.56
		Contralateral 2	4908	68.83	0.12	0.69

Table 3.2 continue						
Internal patient number	**Histology**	**Tissue/sample localization(s)**	**Total number of single live cells**	**% Single total live cells**	**% Of CD25+FOXP3+ in total single live cells**	**% Of CD185+BCL6+ in total single live cells**
Hoca-80	100% EC	Tumor	122161	63.16	0.39	0.12
		Tumor-Adj	4882	58.43	0.53	0.31
		Contralateral 1	4051	81.81	0.17	0.05
		Contralateral 2	19327	81.62	0.55	0.02
Hoca-64	Mixed TGCT (30% EC+70% Post-pubertal Teratoma)	Tumor-Adj	4672	89.50	0.88	0.06
		Tumor-Dis	4862	83.00	1.15	0.02
Hoca-66	Mixed TGCT (50% SE+ 50%EC) Hematoma + scarring	Tumor	13541	87.12	0.12	0.16
		Tumor-Adj	20093	50.58	0.06	0.17
		Tumor-Dis	13216	92.28	0.42	0.14
Hoca-72	Mixed TGCT (70% EC+30% SE)	Tumor	9293	56.96	0.14	0.14
		Tumor-Adj	1392	72.31	1.15	0.29
		Tumor-Dis	1040	59.56	0.77	0.19
		Contralateral 1	23156	89.02	0.28	0.02
		Contralateral 2	1379	76.65	0.07	0.29
Hoca-74	Mixed TGCT (30% post pub. teratoma, 20% EC, Yolk sac tu. 15%, + small amount of choriocarcinoma (+ GCNIS)	Tumor	71851	73.41	0.66	0.63
		Tumor-Adj	8595	40.18	0.52	0.08
		Tumor-Dis	3445	55.72	0.52	0.49
		Contralateral 1	10778	85.01	0.47	0.07
		Contralateral 2	36073	75.68	0.22	0.00
Hoca-86	70% SE + 30% EC	Tumor	2275	67.77	0.38	0.26
		Tumor-Adj	79009	74..96	0.37	0.06
		Tumor-Dis	15648	86.59	0.10	0.16
		Contralateral 1	2770	77.81	0.04	0.04
		Contralateral 2	2335	72.38	0.00	0.00
Hoca-91	Mixed TGCT (% Breakdown unfortunately not possible)	Tumor	3803	46.33	1.03	0.37
		Tumor-Adj	4551	63.83	0.44	0.04
		Tumor-Dis	4771	67.98	0.38	0.13
		Contralateral 1	4741	68.42	0.93	0.02
		Contralateral 2	5056	65.42	0.04	0.00

Among the different tissue sites of different patient specimens, the highest percentage of Treg and Tfh cells were found in the Tumor sites of seminoma compared to the other localizations of seminoma, embryonal carcinoma (≥80%), and mixed tumors (Figure 3.8A-B and Table 3.2). For example, Treg and Tfh cells accounted for 0.10-2.89% (median 1.31%) and 0.05-2.40% (median 0.30%) of the total live cells found in Tumor sites of patients with pure seminoma, resp. (Figure 3.8A-B and Table 3.2).

Statistical analysis showed that the number of Treg cells found in the Tumor sites of seminoma was significantly higher compared to the other localization in tumor-bearing (Tumor-Adj and Tumor-Dis) and contralateral testis (contralateral 1 and contralateral 2) of seminoma (Supplementary Table 14 and Supplementary Table 15). However, the significant Tfh cells in Tumor sites of seminoma was not significant compared to the other localizations of seminoma (Supplementary Table 14 and Supplementary Table 15). In addition, Treg and Tfh cells accounted for 0.02-1.45% (median 0.61%) and 0.08-0.37% (median 0.185%) of the total live cells respectively found in Tumor sites of embryonal carcinoma (≥80%), and 0.12-1.03% (median 0.38%) and 0.14-0.63% (median 0.26%) of the total live cells found in Tumor sites of mixed tumors, resp. (Figure 3.8 and Table 3.2).

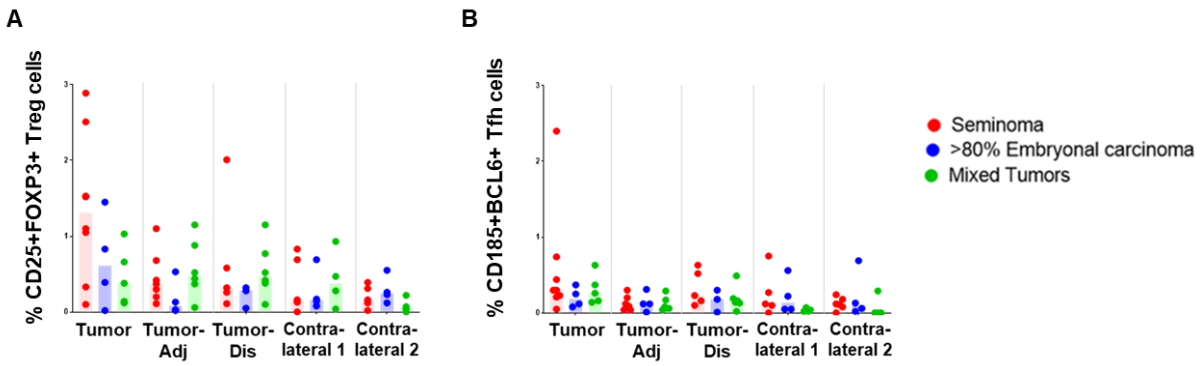

Figure 3.8 Flow cytometric analysis of CD25+FOXP3+ Treg and CXCR5+BCL6+Tfh cells in human testicular tissues. A-B: Respective percentages of CD25+FOXP3+Treg and CXCR5+BCL6+ Tfh cells in total live cells [seminoma: Tumor n=8; Tumor-Adj n=7; Tumor-Dis n=5; Contralateral 1 n= 5; Contralateral 2 n= 6; embryonal carcinoma: Tumor n=4; Tumor-Adj n=4; Tumor-Dis n=3; Contralateral 1 n=4; Contralateral 2 n=4; mixed TGCT: Tumor n=5; Tumor-Adj n=6; Tumor-Dis n= 6; Contralateral 1 n=4; Contralateral 2 n= 4].

Additionally, Treg and Tfh were also detected in other locations of tumor-bearing testis. For example, the median percentage of Treg were 0.37% (0.11-1.10%), 0.08% (0.02-0.53%) and 0.48% (0.06-1.15%) of the total live cells in Tumor-Adj sites of seminoma, embryonal carcinoma (≥80%) and mixed tumors, resp. (Figure 3.8A-B and Table 3.2). While Tfh accounted for 0.04-0.30% (median 0.09%), 0.01-0.31% (median 0.12%), and 0.04-0.29% (median 0.07%) of the total live cells in Tumor-Adj sites of seminoma, embryonal carcinoma (≥80%) and mixed tumors, resp. (Figure 3.8A-B and Table 3.2).

Similarly, in Tumor-Dis sites of seminoma, embryonal carcinoma (≥80%) and mixed Tumors, Treg accounted for 0.11-2.01% (median 0.32%), 0.05-0.32% (median 0.28%), and 0.10-1.15% (median 0.47%) of the total live cells, resp., and Tfh accounted for 0.10-0.63% (median 0.23%), 0.01-0.30% (median 0.18%) and 0.02-0.49% (median 0.15%) of the total live cells, resp. (Figure 3.8A-B and Table 3.2). In addition to the tumor-bearing testis, a very small percentage of Treg and Tfh cells were detectable in contralateral testes of TGCT patients. For example, Treg accounted for 0.00-0.83% (median 0.16%) and 0.02-0.39% (median 0.14%) of the total live cells, and Tfh cells accounted for 0.00-0.75% (median 0.12%) and 0.00-0.24% (median 0.115%) of the total live cells in contralateral 1 and contralateral 2 sites of seminoma, resp. (Figure 3.8A-B and Table 3.2). Whereas Treg accounted for 0.08-0.69% (median 0.155%) and 0.12-0.55% (median 0.245%) of the total live cells, and Tfh cells accounted for 0.05-0.56% (median 0.135%) and 0.02-0.69% (median 0.095%) of the total live cells in contralateral 1 and contralateral 2 sites of embryonal carcinoma (≥80%), resp. (Fig. 3.6 A-B and Table 3.4). In addition, 0.04-0.93% (median 0.375%) and 0.00-0.22% (median 0.055%) of the total live cells were Treg, and 0.02-0.07% (median 0.03%) and 0.00-0.29% (median 0%) of total live cells were Tfh cells found in contralateral 1 and contralateral 2 sites of mixed tumor, resp. (Figure 3.8A-B and Table 3.2). Taken together, Treg and Tfh cells were abundantly found in tumor-bearing testes, mostly in Tumor sites of TGCT.

3.3 Single cell landscape of immune cells in normal human and TGCT

3.3.1 Identification of different cells in human normal and TGCT samples by scRNA-seq

Datasets available from scRNAseq analysis of normal (n=3) and TGCT (n=4) were analysed to investigate the cellular composition of human testis. Following multiple analytical quality control filtering, a total of 10,153 cells were used for subsequent in-depth analysis to reveal the cellular composition of human testis and TGCT. Clustering analysis and visualization by t-distributed stochastic neighbor embedding (tSNE) showed that different samples intermixed in many clusters as well as sample specific clusters represent the underlying biological differences between the analyzed samples

(Figure 3.9). The primary cluster analysis generated a total of 46 individual clusters with cell cluster sizes ranging from 590 cells to the smallest cluster of only 19 cells (Supplementary Figure 2A-B) and calculated the reactive contribution of each cluster by each analyzed sample (Supplementary Figure 2B-C). Individual clusters were identified by expression analysis of cell-specific signature markers (Supplementary Figure 3), allowing to categorize these clusters into T cells (*CD3D, CD3E, CD3G*), B cells (*MS4A1, CD22, PAX5*), macrophages (*CD68, CD14, LYZ*), plasmacells (*CD79A, TNFRSF17, IGHG4*), tumor cells (*NANOG, POU5F1, TFAP2C*), endothelial cells (*CLDN5, RAMP2, VWF*), fibroblasts (*DCN, COL1A1, COL5A1*), germ cells (*PRM2, TNP1, SPATA18*), and undefined cells (Supplementary Figure 3, Supplementary Figure 4). There were multiple clusters representing the same cell type that were merged for better visualization (Supplementary Figure 4), followed by the determination of cellular composition of each sample (Figure 3.9 and Figure 3.10).

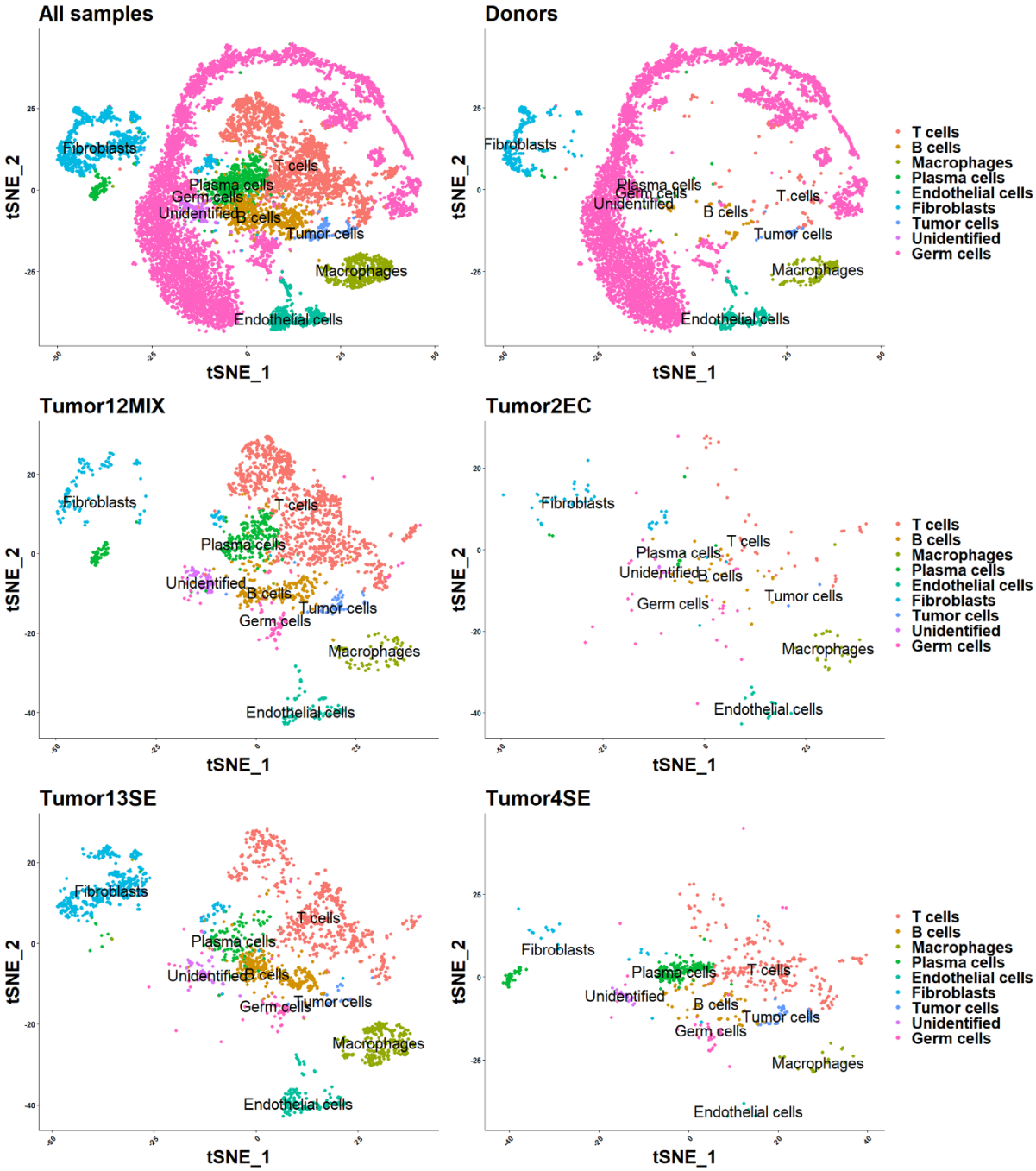

Figure 3.9 scRNA-seq analysis of normal human testis and TGCT identifies distinct cell populations, including immune cell subtypes. tSNE presentation of major cell types and associated clusters in normal donor (n=3; pooled data) and TGCT samples (Tumor12MIX: mixed TGCT, Tumor13SE: seminoma, Tumor4SE: seminoma, Tumor2EC: embryonal carcinoma).

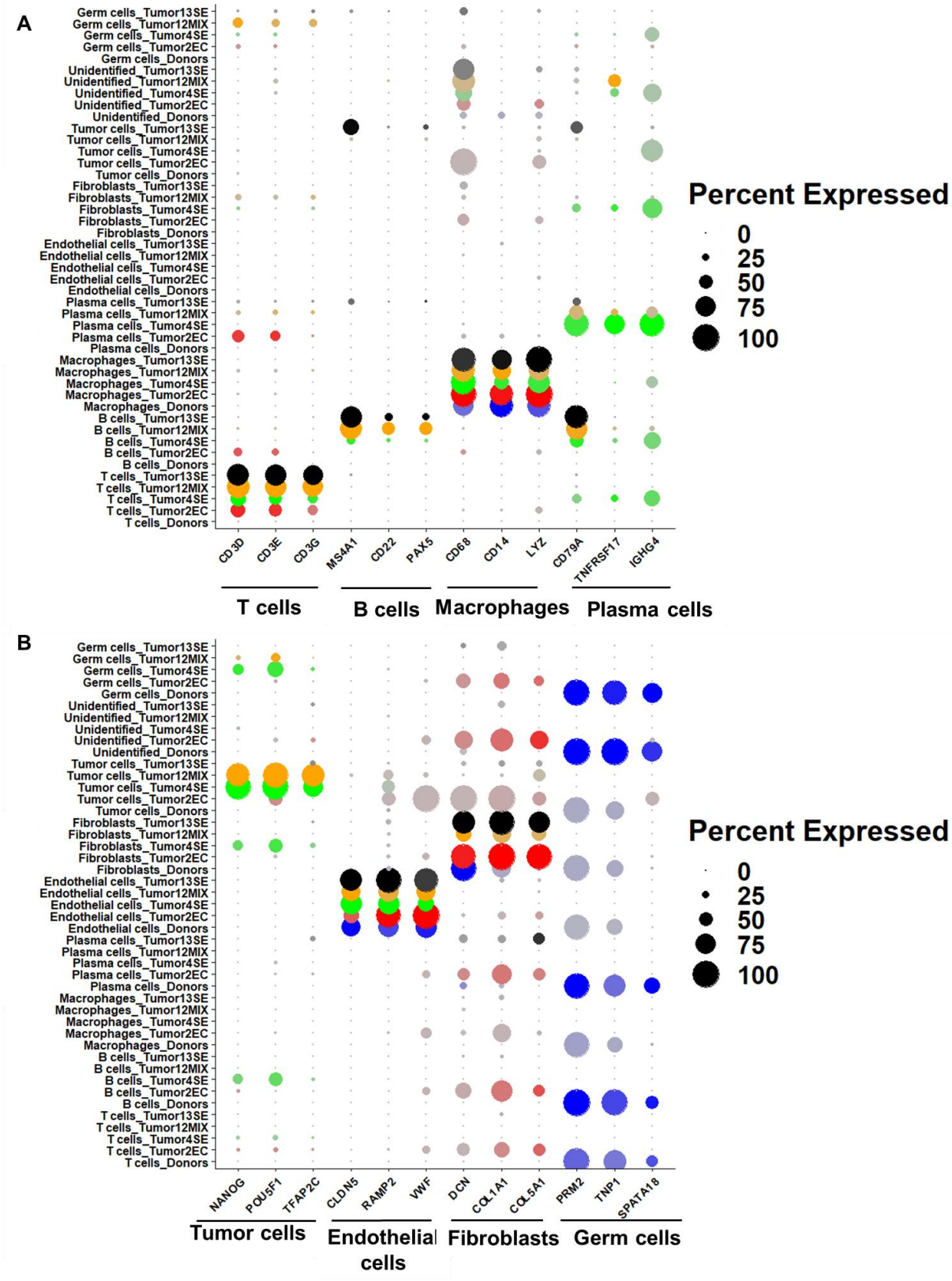

Figure 3.10 Dot Plot shows putative marker genes expressed by immune cells (A) and rest of the cells (B) in individual samples. Dot size encodes the percentage of cells within a cluster expressing the transcript, whereas the color intensity represents the average signal measured in expressing cells.

In addition to that, a DGEs analysis was performed, and top 5 differentially expressed genes of each cell type were identified (Figure 3.11) to understand which genes possibly involved in the regulation of each cell function in the TGCT microenvironment. Finally, proportion of different cells in each analyzed sample were calculated and it showed that normal testes contain mostly germ cells (77.56% of total analyzed cells) and a small proportion of fibroblasts (2.90% of total analyzed cells), and endothelial cells (2.56% of total analyzed cells). In addition, a very low proportion of immune cells, including macrophages (1.82% of total analyzed cells), T cells (0.08% of total analyzed cells) but no B cells were detected in normal human testis (Figure 3.12). Among the various immune cells, macrophages represent the leading immune cell found in these tissue specimens (Figure 3.12).

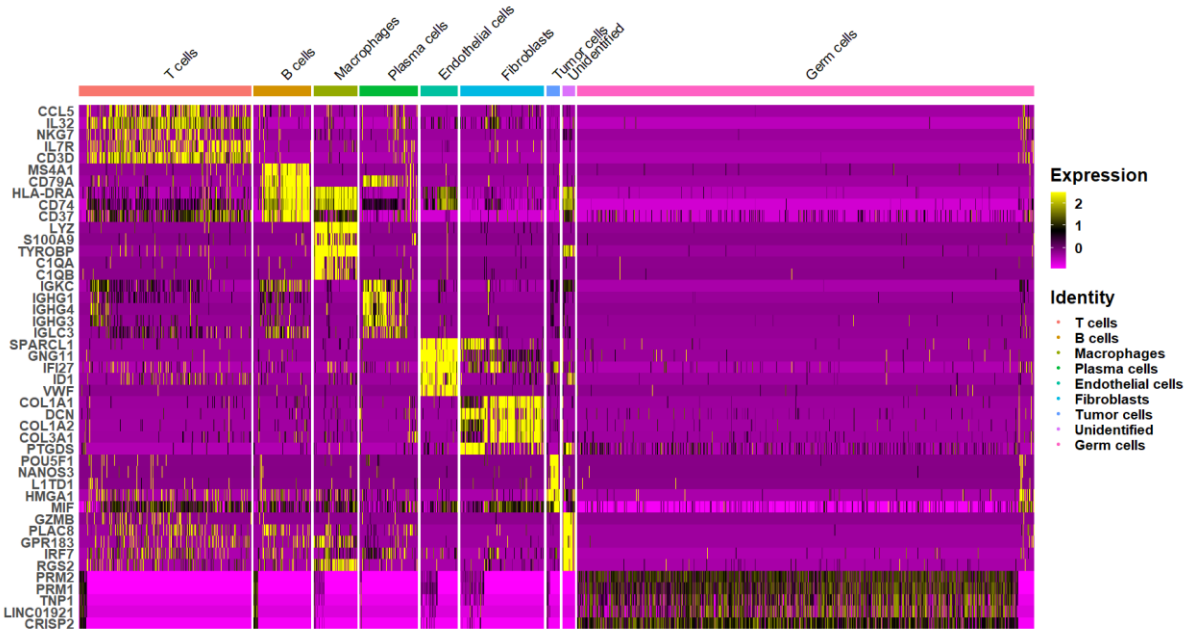

Figure 3.11 Heatmap of the top 5 significantly differentially expressed genes in each cell type analyzed. Each column represents a cell, while each row denotes a gene.

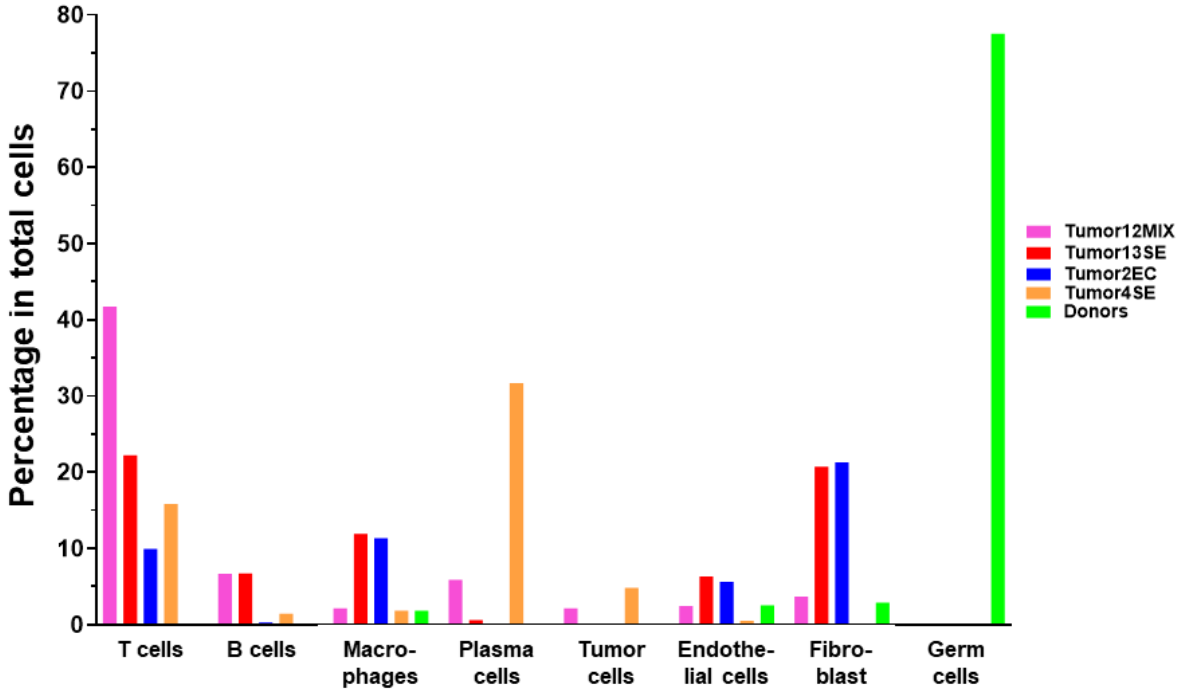

Figure 3.12 The proportion of different cells among pooled healthy donor and individual tumor samples.

In contrast, TGCT samples mainly contained various infiltrating immune cells including T cells, B cells, macrophages, and plasma cells (Figure 3.12). Among them, T cells represented the major component of infiltrating immune cells (9.94-41.73% of total analyzed cells) in TGCT (Figure 3.12), whereas macrophages, B cells and plasma cells accounted for 1.85-11.93%, 0.32-6.75%, and 0.16-31.60% of total analyzed cells in TGCT, resp. However, the proportion of leading immune cells significantly varied from tumor to tumor. For example, macrophages were the leading immune cells (11.37% of total analyzed cells) in embryonal carcinoma (Figure 3.12), while T cells were the leading infiltrating immune cells, accounted for 15.85-22.21% of the total analyzed cells in seminoma and 41.73% of the total analyzed cells in mixed TGCT (Figure 3.12), indicating that T cells are predominantly associated with most of the TGCTs. In addition to the immune cells, a considerable amount of fibroblasts (0.0-20.72% of total analyzed cells), endothelial cells (0.5-6.33% of total analyzed cells), and tumor cells (0.08-4.83% of total analyzed cells) were found in TGCT samples (Figure 3.12), describing the complex testicular microenvironment containing a variety of cells and complicating the functional characterization of a specific cell of interest in the human testis under normal and diseased conditions.

3.3.2 Analysis of T cells and their subtypes in human normal testis and TGCT

Secondary clustering of the T cell population was performed to dissect their heterogeneity. A total of 17 subclusters consisted of cytotoxic T cells (CD8A, CCL5, GZMA), proliferating (activated) T cells (MKI67, TYMS, CDK1), CCR7+ (newly recruited) T cells (CCR7, LEP1, IL7R), Treg cells (FOXP3, CTLA4, TNFRSF18), and other CD4+ T cells (Figure 3.13, Supplementary Figure 5 and Supplementary Figure 6) identified by the expression of the canonical markers in each cluster (Figure 3.14 and Supplementary Figure 6) as well as the enrichment of the differentially expressed gene in each cluster (Figure 3.15). A heatmap was generated depicting the top 5 differentially expressed genes in each T cell subtype (Figure 3.15), giving an indication of which gene regulates T cell subtypes functions in the TGCT microenvironment. There were multiple clusters representing the same cell type that were merged for better visualization (Supplementary Figure 5), followed by the determination of T cell composition of each sample (Figure 3.13 and Figure 3.14).

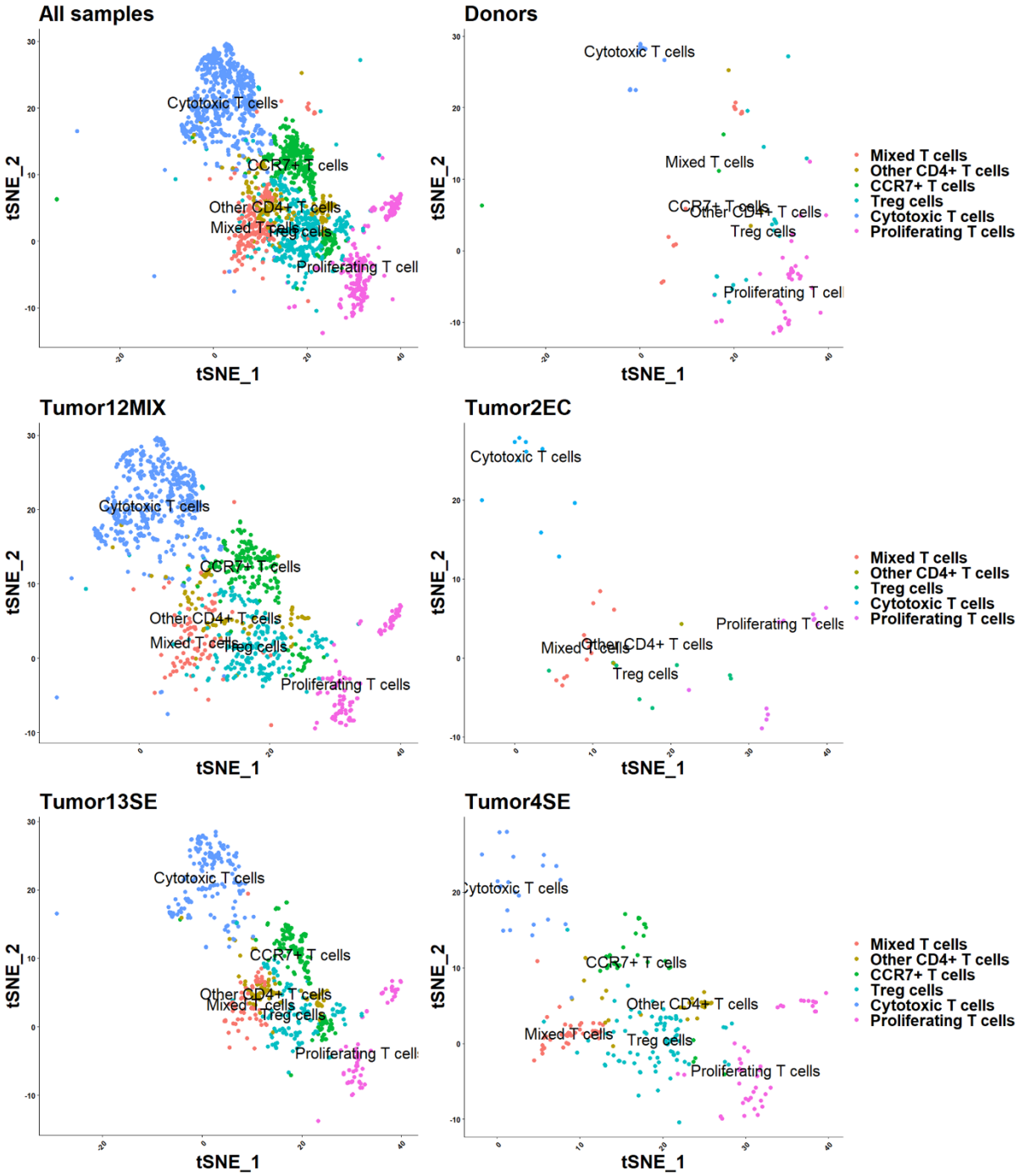

Figure 3.13 Analysis of T cells in normal human testis and TGCT. tSNE plot shows the clustering of T cells in donor (n=3; pooled data) and TGCT samples (Tumor12MIX: mixed TGCT, Tumor13SE: seminoma, Tumor4SE: seminoma, Tumor2EC: embryonal carcinoma).

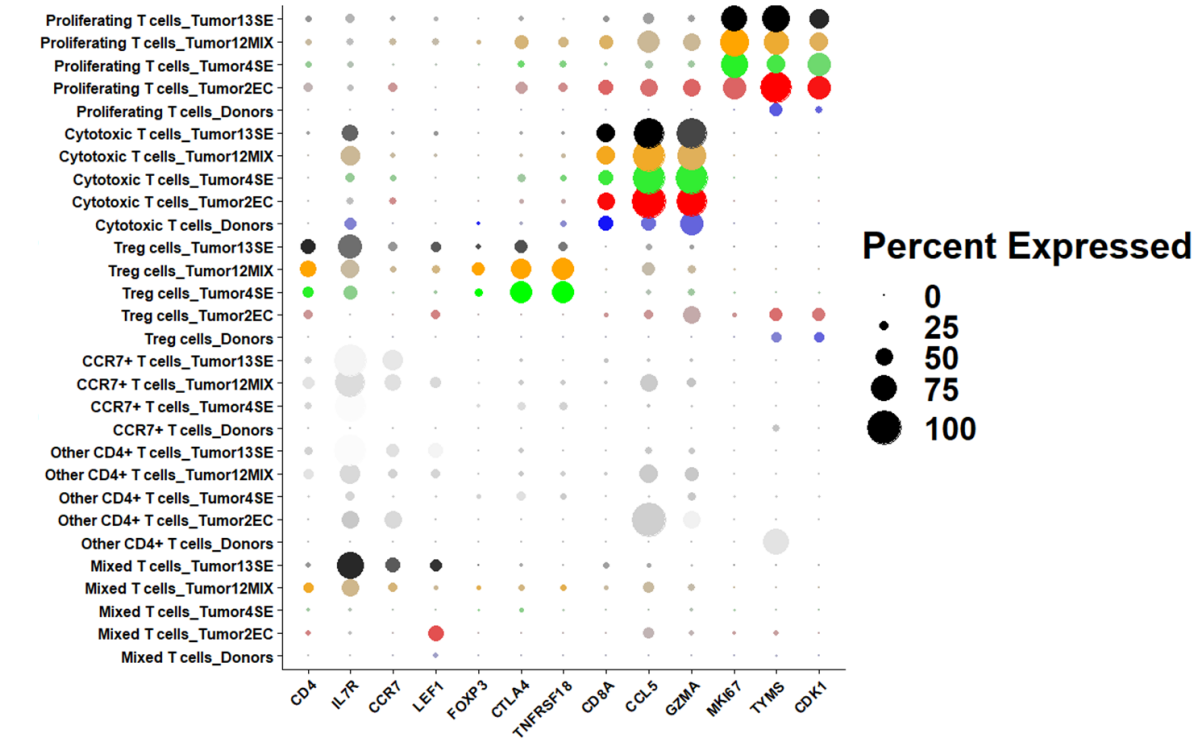

Figure 3.14 Dot plot shows expression levels of immune typing markers in different T cells clusters in a pooled analysis all studied samples. The size of the dot encodes the percentage of cells within a cluster expressing the gene, whereas the colour intensity encodes the average expression level of expressing cells.

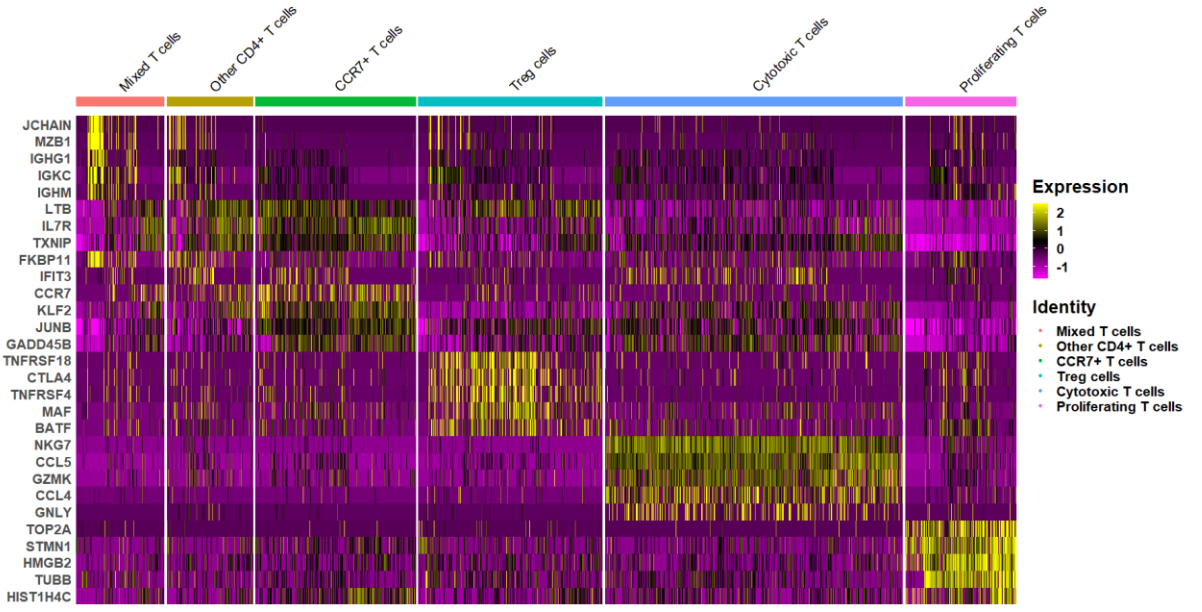

Figure 3.15 Heatmap shows the top 5 differentially expressed genes by various T cell clusters in the studied samples. Each row denotes a gene, while each column represents a cell.

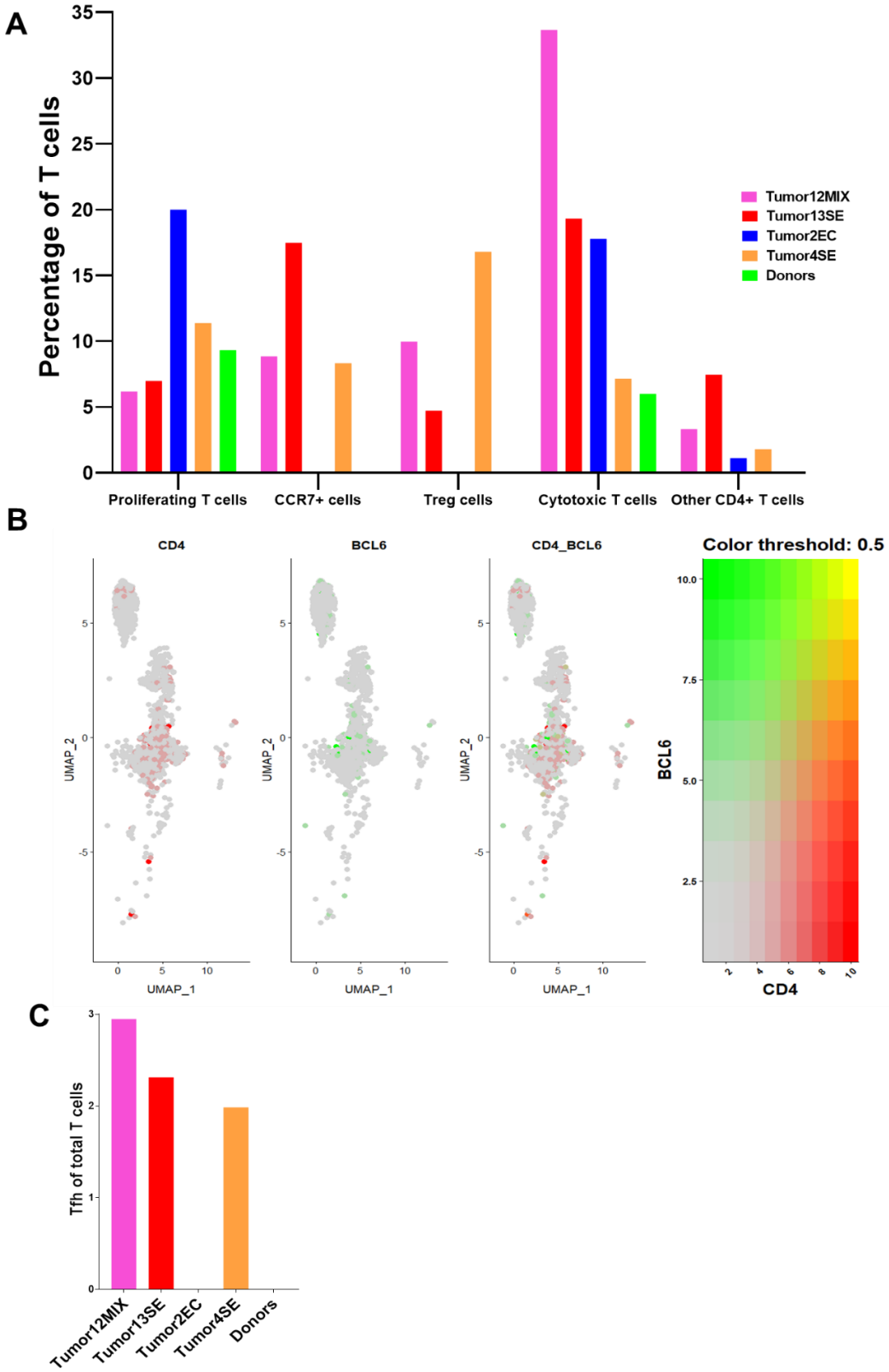

Figure 3.16 T cell subtypes in normal human testis and TGCT. A. Bar plot shows the proportion of different T cell subtypes among donors and TGCT. B: Co-expression of Tfh cell markers (CD4 and BCL6) in total T cell population. C: Proportion of Tfh cells in individual samples.

Analysis of T cell subpopulations in human testicular specimens showed that in addition to cytotoxic T cells, proliferating (activated) T cells, CCR7+ (newly recruited) T cells, and other CD4+ T cells accounted for 6.17-33.67%, 6.17-20%, 0.00-17.49% and 0.00-7.44% of CD3+ T cells, resp. (Figure 3.16A). Importantly, individual clusters representing Treg cells were also detected in the secondary clustering analysis, accounted for 0.00- 16.80% of CD3+ T cells (Figure 3.16A), but no individual cluster was found representing Tfh cells. Therefore, a newly developed analytical option in Seurat was employed to visualize and quantify the co-expression of CD4 and BCL6 simultaneously to confirm the presence of Tfh in human testicular samples (Figure 3.16B). Using the extended analysis, it was shown that Tfh cells were found in the analyzed TGCT samples and accounted for 0.00–2.95% of the CD3+ T cells (Figure 3.16C).

3.3.3 Cross-validation of the Treg-associated gene expression and putative mechanisms of Treg cell function in human TGCT

A set of well-studied signature molecules of Treg cells were selected by extensive literature review and their expression profiles were cross validated from different perspectives. Here, a total of 11 most functional molecules of Treg such as *BATF, CCL5, CTLA4 (CD152), CXCR4 (CD184), FOXP3, GITR (TNFRSF18), ICOS (CD278), CD25 (IL2RA), TIGIT, TNFRSF4 (OX40),* and *TNF-α (TNF)* were selected based on their intimate involvement in the functions of Treg cells. The expression levels of selected Treg-signature molecules were evaluated in different settings, such as in all identified cells the tissue microenvironment (Figure 3.17), in only T cells from different TGCT compared to normal testis (Figure 3.18), and in only Treg cells from different TGCT compared to normal testis (Figure 3.19).

Firstly, differential expression analysis of selected Treg-specific markers in the tissue microenvironment composed of different cells, illustrated that they were highly expressed mainly in T cells compared to the other cells (Figure 3.17), preliminary confirming the presence of Treg cells in the total T cell population. However, it should be noted that the selected markers were also expressed by other cells, indicating the complexity of targeting individual cells of interest in the tissue microenvironment. Next,

differential expression analysis of selected genes was performed in only T cells from different TGCT compared to normal testis, and it showed that all selected markers of Treg cells are highly expressed in TGCT compared to normal testis, further confirming the presence of Treg and indicating their possible involvement in TGCT (Figure 3.18). Finally, we performed differential expression analysis of Treg specific selected genes in Treg cell populations and revealed that Treg-specific markers are mainly expressed in seminoma and mixed TGCT but not prominently in embryonal carcinoma (Figure 3.19), which is matched with identification and quantification of T cells subtypes in above analysis (Figure 3.16A).

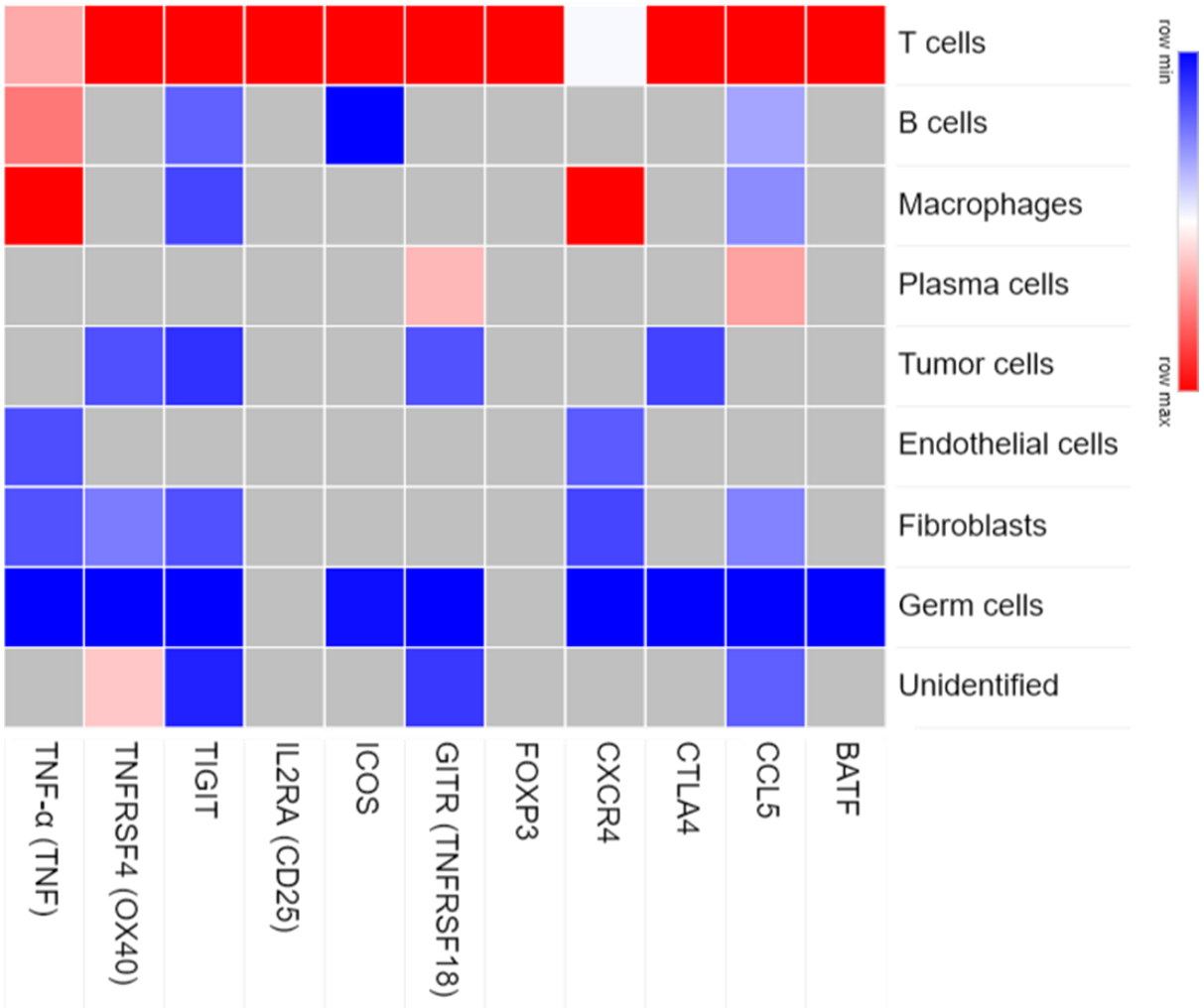

Figure 3.17 Differential expression of Treg-associated genes in different cells found in human testicular tissue microenvironment. A relative color scheme uses the minimum and maximum values in each row to convert values to colors. Gray color represents the absence of gene expression.

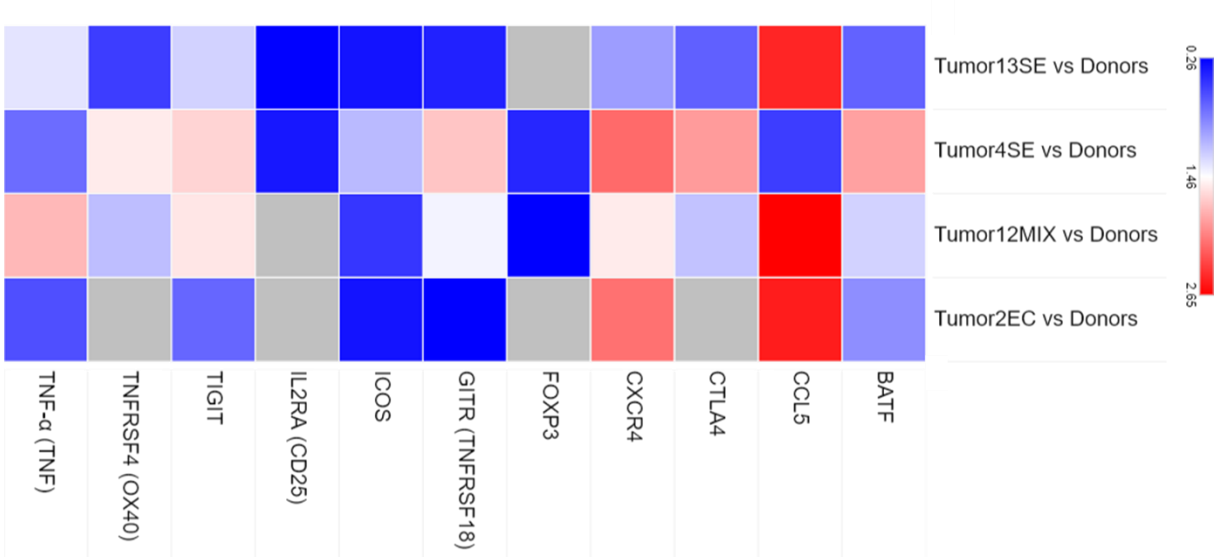

Figure 3.18 Differential expression analysis of Treg-associated genes in T cells of different TCGT vs Donors. Color schemes (blue to red) represent the log2fold change. Gray color represents the absence of gene expression.

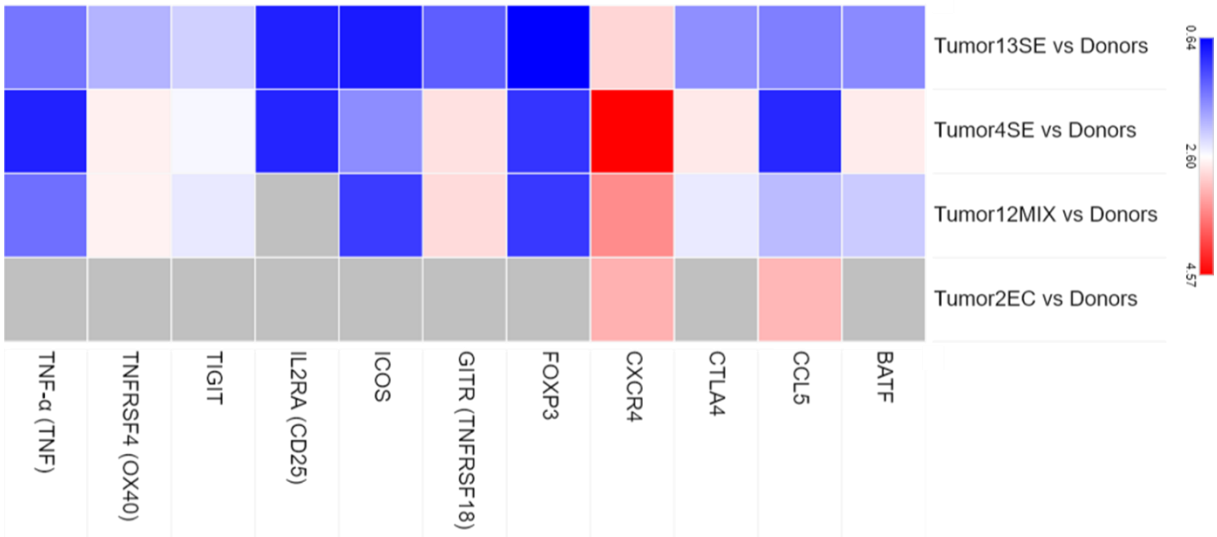

Figure 3.19 Differential expression analysis of Treg-associated signature genes in Treg cells of different TCGT vs Donors. Color schemes (blue to red) represent the log2fold change. Gray color represents the absence of gene expression.

Subsequently, the expression of the selected genes was further validated with publicly available TCGA (The Cancer Genome Atlas)-TGCT data (seminoma n=63 and non-seminoma n=70) to re-validate the dominance of Treg cells in seminoma compared to non-seminoma, including embryonal carcinoma. The TCGA gene expression analysis showed that the selected markers of Treg cell expressions were significantly upregulated in seminoma compared to non-seminoma that fully matched with our study results (Figure 3.20). In addition, a co-expression analysis of selected Treg genes was performed using TCGA-TGCT dataset (n=156 samples) in cBioPortal to identify groups of genes with similar expression patterns and involvement in the same biological process, ranked by Pearson's correlation coefficient and Spearman's Correlation Coefficient (Supplementary Figure 6 and Table 3.3). The value of the correlation coefficient ranges from +1 to -1, with positive values representing higher levels of one variable associated with higher levels of the other, and negative values representing higher levels of one variable associated with lower levels of the other. In particular, the sign of the correlation coefficient indicates the direction of the association, while the magnitude of the correlation coefficient indicates the strength of the association. Among the selected genes, a high-level correlation between BATF vs. CCL5 was found. In addition, there are 18 other interactions between the selected genes whose correlation coefficient was >0.8, indicating a strong correlation between genes potentially involved in Treg cell recruitment and functions (Supplementary Figure 6 and Table 3.3). Furthermore, a PPIs network of Treg cell-specific selected proteins was generated by STRING (https://string-db.org/) to understand the function and behavior of proteins and their biological processes and pathways. The PPI network shows that the selected proteins are highly interconnected to exhibit the functions of the Treg cells (Figure 3.21). Nevertheless, CD25 (IL2RA), CTLA4, and FOXP3 seem to be leading proteins to regulate Treg cells in human testis.

Table 3.3 Co-expression analysis of Treg-associated signature genes in TGCT samples (150 patients / 156 samples) with Spearman and Pearson coefficient value. The correlation coefficient ranges between +1 to -1 represent the positive and negative correlation between the selected genes. Correlation coefficient values >0.8 are in bold.

Genes	Spearman coefficient	Pearson coefficient
CXCR4 vs TNFRSF18	0.30	0.25
CXCR4 vs CTLA4	0.40	0.37
CXCR4 vs CCL5	0.38	0.33
CXCR4 vs BATF	0.40	0.41
CXCR4 vs TNFRSF4	0.49	0.51
CXCR4 vs IL2RA	0.26	0.25
CXCR4 vs TIGIT	0.37	0.31
CXCR4 vs ICOS	0.31	0.29
CXCR4 vs TNF	0.36	0.37
CXCR4 vs FOXP3	0.27	0.25
TNFRSF18 vs CTLA4	0.79	0.75
TNFRSF18 vs TIGIT	0.68	0.71
TNFRSF18 vs FOXP3	0.70	0.66
TNFRSF18 vs BATF	**0.86**	**0.85**
TNFRSF18 vs ICOS	0.71	0.70
TNFRSF18 vs CLL6	0.78	0.77
TNFRSF18 vs TNFRSF4	0.74	0.77
TNFRSF18 vs IL2RA	0.65	0.65
TNFRSF18 vs TNF	0.73	0.71
CTLA4 vs BATF	**0.87**	**0.86**
CTLA4 vs TNFRSF4	0.62	0.58
CTLA4 vs ICOS	**0.88**	**0.90**
CTLA4 vs CCL5	**0.88**	**0.89**
CTLA4 vs TIGIT	**0.88**	**0.90**
CTLA4 vs IL2RA	**0.80**	**0.79**
CTLA4 vs FOXP3	**0.85**	**0.81**
CTLA4 vs TNF	**0.82**	**0.79**
BATF vs TNFRSF4	0.75	0.74
BATF vs TIGIT	**0.83**	**0.82**
BATF vs IL2RA	0.76	0.79
BATF vs FOXP3	0.77	0.74
BATF vs TNF	**0.82**	**0.79**
BATF vs ICOS	**0.82**	**0.84**
BATF vs CCL5	**0.92**	**0.92**
TNFRSF4 vs TIGIT	0.50	0.49
TNFRSF4 vs FOXP3	0.57	0.50
TNFRSF4 vs TNF	0.64	0.64
TNFRSF4 vs ICOS	0.57	0.54
TNFRSF4 vs CCL5	0.66	0.64
TNFRSF4 vs IL2RA	0.59	0.59
TNFRSF4 vs CCL5	**0.87**	**0.89**
TIGIT vs IL2RA	0.77	0.78
TIGIT vs FOXP3	**0.81**	**0.81**
TIGIT vs TNF	0.73	0.71
ICOS vs CCL5	**0.84**	**0.87**
ICOS vs TNF	0.76	0.76
ICOS vs FOXP3	**0.86**	**0.83**

Table 3.3		
Genes	**Spearman coefficient**	**Pearson coefficient**
ICOS vs IL2RA	**0.81**	**0.84**
FOXP3 vs CCL5	0.76	0.74
FOXP3 vs IL2RA	0.76	0.78
FOXP3 vs TNF	0.75	0.73
CCL5 vs IL2RA	0.78	0.79
IL2RA vs TNF	**0.82**	**0.79**
CCL5 vs TNF	**0.81**	**0.78**

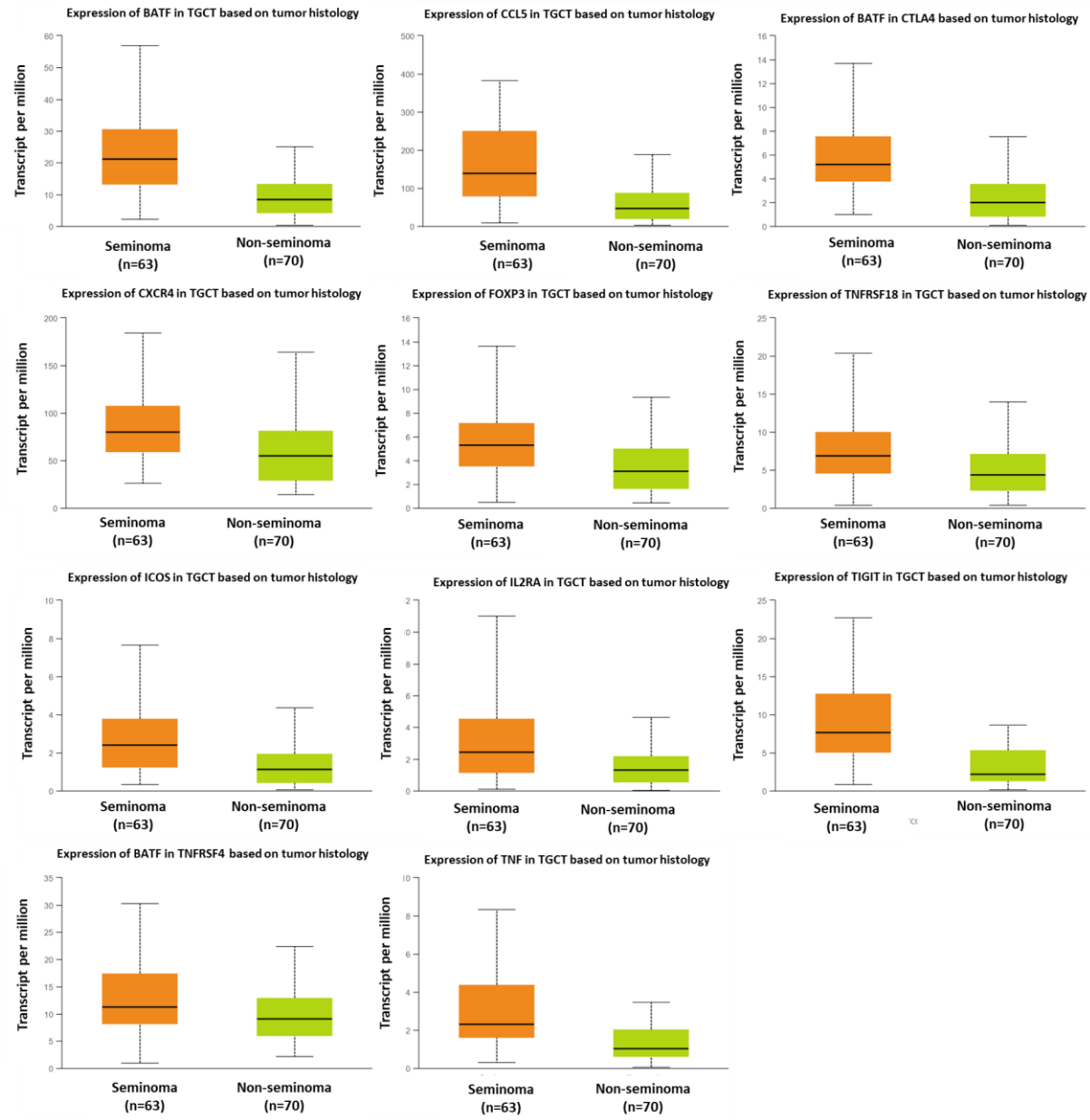

Figure 3.20 Cross-validation of Treg-associated selected gene using UALCAN for analyzing TGCT OMICS data. The expressions of the selected genes were extracted from TCGA-TGCT dataset. Number of seminomas (n=63) and non-seminomas (n=70). The orange color represents seminoma, and the green color represents no seminoma. All comparisons are statistically significant ($p<0.05$)

Besides the PPIs among the Treg-specific selected genes, the interactions between other cell markers used to identify different cell populations in testicular tissues and Treg-specific selected genes were also generated by STRING (Supplementary Figure 7). Various PPIs of different cell-specific proteins were detected, including an experimentally identified known interaction between NANOG and CXCR4 that might regulate Treg in TGCT, which requires further experimental evidence. In addition, several tight interactions between Treg cells and other cell-specific proteins have also been observed, indicating the cellular and functional complexity of testes.

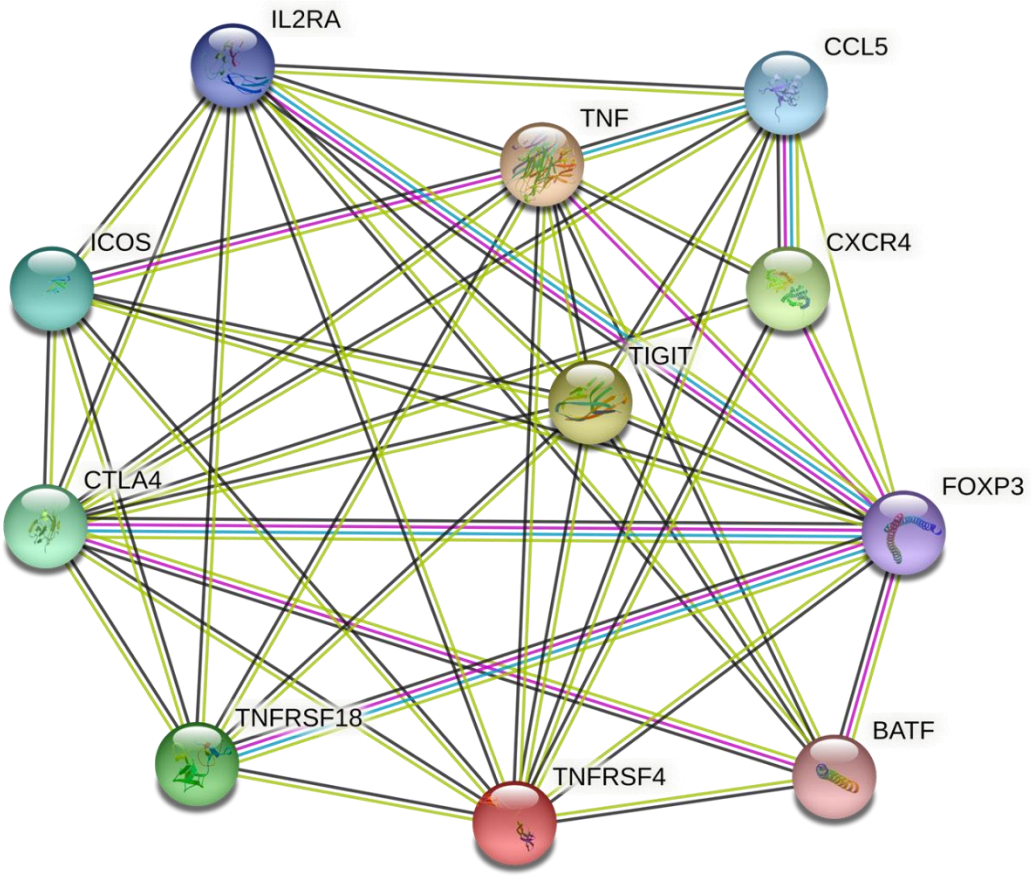

Figure 3.21 The protein-protein interaction (PPI) network of Treg-selected protein was generated by STRING. Colored nodes indicate query proteins and first shell of interaction, filled nodes represent known or predicted 3D structure. Pastel color edges represent the known interactions from curated databases, pink color edges represent known interactions determined experimentally, green color edges represent predicted interactions between neighboring genes, red color edges represent the predicted gene fusion interaction, blue color edges represent the predicted co-occurrence of gene interaction. Other color edges, for example olive color represents textmining, black color represents co-expression and purple color represents protein homology.

3.3.4 Cross-validation of the Tfh-associated gene and putative mechanism of Tfh cells in human TGCT

Similar to Treg cells, a set of Tfh cell-associated genes were selected and their expression profiles cross-validated from different perspectives. A total of 8 most functional Tfh molecules of Tfh cells including *BCL6, CXCR3, ICOS, CXCL13, IRF4, SATA3*, and *CD40LG* were selected based on their involvement in Tfh cell functions. The expression levels of selected Tfh-signature molecules were evaluated in the tissue microenvironment (Figure 3.22) and in only T cells from different TGCT compared to normal testis (Figure 3.23). In the tissue microenvironment, selected Tfh-specific markers are highest expressed in T cells compared to the other cells (Figure 3.22), preliminarily confirming the presence of Tfh cells in the total T cell population. However, it should be noted that selected markers might also be expressed by cells other than T cells, indicating the complexity of targeting individual cells of interest in the testicular tissue microenvironment. Then, differential gene expression analysis of selected Tfh-specific markers in T cells from different TGCT compared to normal testis was performed and it was shown that all selected markers are highly expressed by T cells in TGCT compared to normal testis, further indicating the presence of Tfh and points to their possible involvement in TGCT (Figure 3.23). Furthermore, selected Tfh-specific markers are highly expressed in seminoma and mixed tumor compared to embryonal carcinoma which is matched with identification and quantification of T cells subtypes in above analysis (Figure 3.16C). Since no cluster representing exclusively Tfh cells was identified, it was not possible to analyze selected gene expression only in Tfh cells from testicular tumors compared to donors. Furthermore, the expression of selected Tfh genes was cross-validated with publicly available TCGA-TGCT data (seminoma n=63 and non-seminoma n=70). TCGA gene expression analysis showed that selected most Tfh-specific genes are upregulated in seminoma compared to non-seminoma, with the exception of BCL6, STAT3 and CXCL13, which could be due to the heterogeneity of the samples (Figure 3.24).

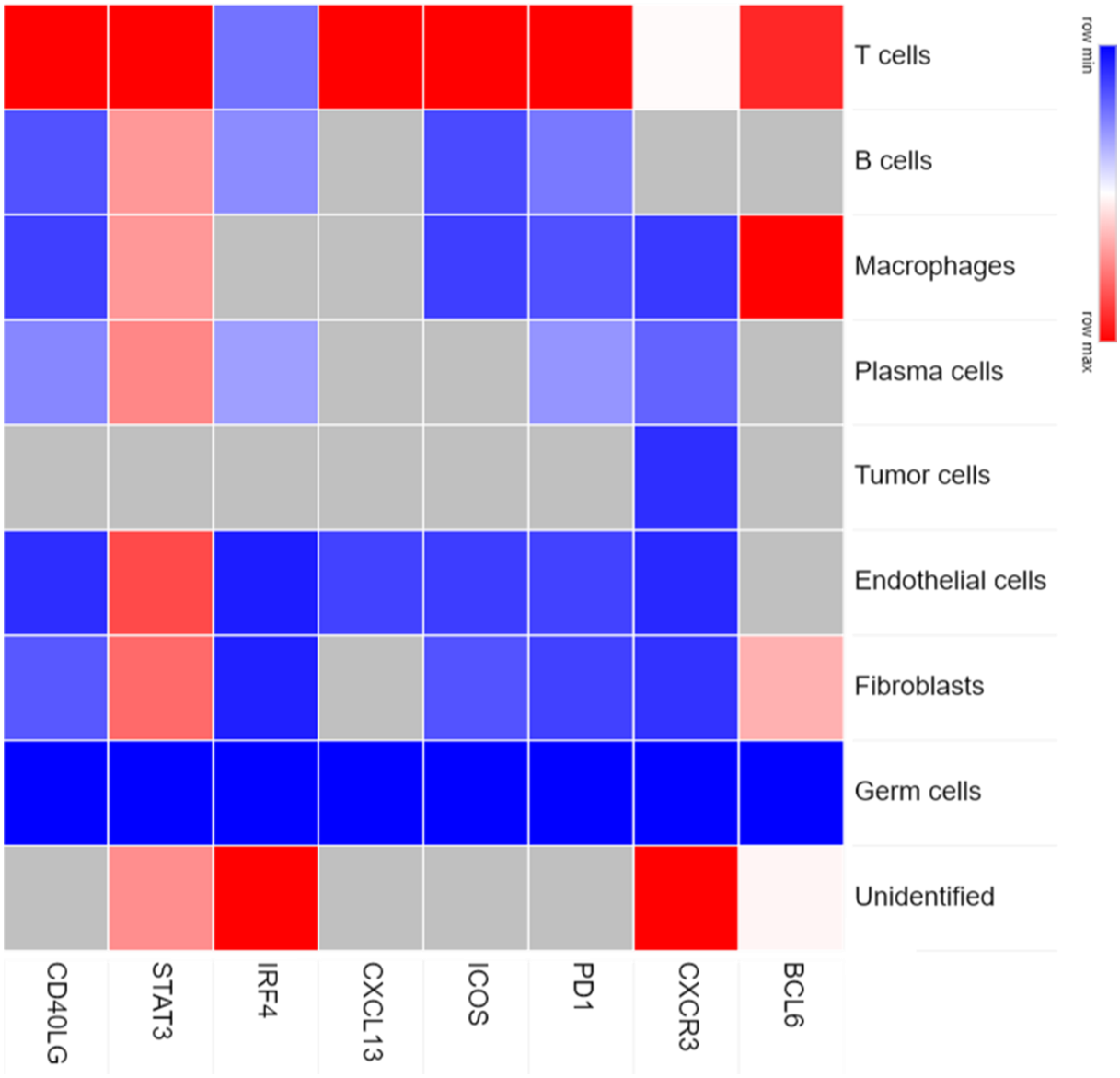

Figure 3.22 Differential expression of Tfh-associated genes in different cells found in human testicular tissue microenvironment. A relative color scheme uses the minimum and maximum values in each row to convert values to colors. Gray color represents the absence of gene expression.

In addition, similar to the Treg analysis, a co-expression analysis of selected Tfh-specifc genes was performed using TCGA-TGCT dataset (n=156 samples) in cBioPortal to identify groups of genes with similar expression patterns and involvement in the same biological process, ranked by Pearson's correlation coefficient and Spearman's Correlation Coefficient (Supplementary Figure 13 and Table 3.4). The height level of correlation between CXCR3 and ICOS was observed, suggesting that

Tfh cells may play an important role in human TGCT via the interaction between CXCR3 and ICOS which need to be experimentally proven. Besides, there are 6 other interactions between the selected genes whose correlation coefficient was >0.8, indicating a strong correlation between genes potentially involved in Tfh cell in the recruitment and functions of human TGCT (Supplementary Figure 13 and Table 3.4). In addition to co-expression analysis, PPIs of Tfh cell-specific molecules were generated by STRING (https://string-db.org/) to understand the function and behavior of proteins and their biological processes and pathways. PPIs networkers showed that the selected proteins are linked together to reveal the functions of the Tfh cells in human TGCT (Figure 3.25). Furthermore, the interactions between other cell markers used to identify different cell populations in testicular tissues and Tfh-specific selected genes were also generated by STRING (Supplementary Figure 14), and a close interaction between BCL6 and NANOG was confirmed along with the interactions between BCL6 and other cell-specific proteins, indicating the importance of BCL6 in Tfh cell biology in testicular biology.

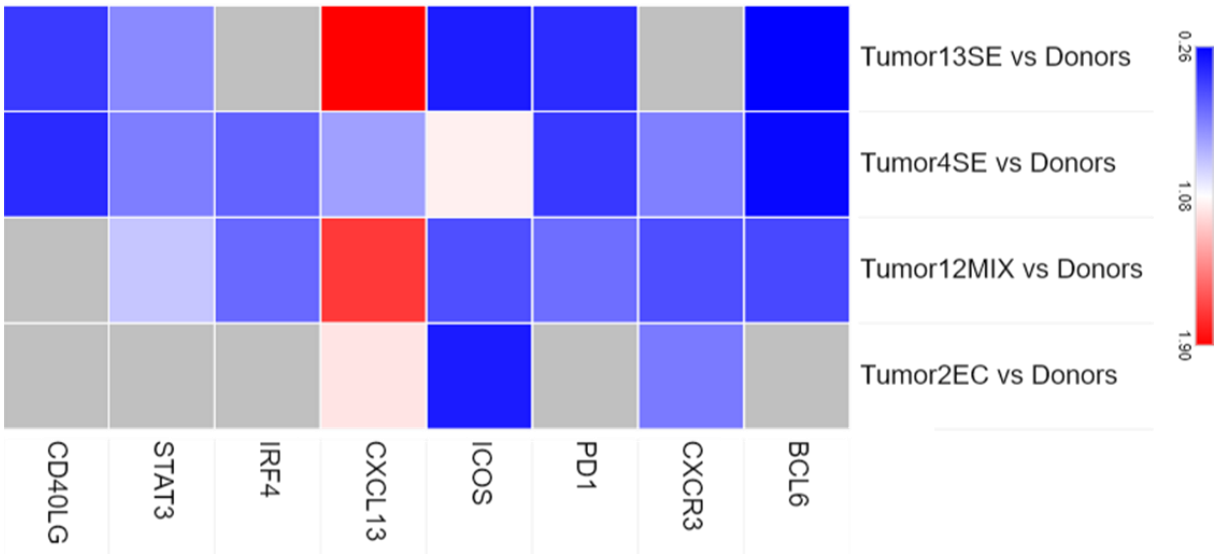

Figure 3.23 Differential expression analysis of Tfh-associated genes in T cells of different TCGT vs Donors. Color schemes (blue to red) represent the log2fold change. Gray color represents the absence of gene expression.

Table 3.4 Co-expression analysis of Tfh-associated signature genes in TGCT samples (150 patients / 156 samples) with Spearman and Pearson coefficient value. The correlation coefficient ranges between +1 to -1 represent the positive and negative correlation between the selected genes. Correlation coefficient values >0.8 are in bold.

Genes	Spearman coefficient	Pearson coefficient
BCL6 vs CXCR3	0.20	0.14
BCL6 vs PDCD1	0.16	0.08
BCL6 vs ICOS	0.09	0.03
BCL6 vs CXCL13	0.20	0.15
BCL6 vs IRF4	0.05	0.02
BCL6 vs STAT3	0.43	0.43
BCL6 vs CD40LG	0.26	0.23CXCR3
CXCR3 vs ICOS	**0.87**	**0.90**
CXCR3 vs CXCL13	0.59	0.70
CXCR3 vs IRF4	**0.84**	**0.87**
CXCR3 vs STAT3	-0.03	0.06
CXCR3 vs CD40LG	**0.89**	**0.88**
PDCD1 vs ICOS	**0.85**	**0.73**
PDCD1 vs CXCL13	0.65	0.73
PDCD1 vs IRF4	**0.83**	**0.86**
PDCD1 vs STAT3	-0.12	-0.04
PDCD1 vs CD40LG	**0.85**	**0.80**
ICOS vs CXCL13	0.60	0.71
ICOS vs IRF4	0.74	0.79
ICOS vs STAT3	0.05	0.09
ICOS vs CD40LG	**0.80**	**0.81**
CXCL13 vs IRF4	0.51	0.63
CXCL13 vs STAT3	0.05	0.11
CXCL13 vs CD40LG	0.41	0.54
IRF4 vs STAT3	-0.09	-0.01
IRF4 vs CD40LG	0.78	0.77
CD40LG vs STAT3	0.02	0.11

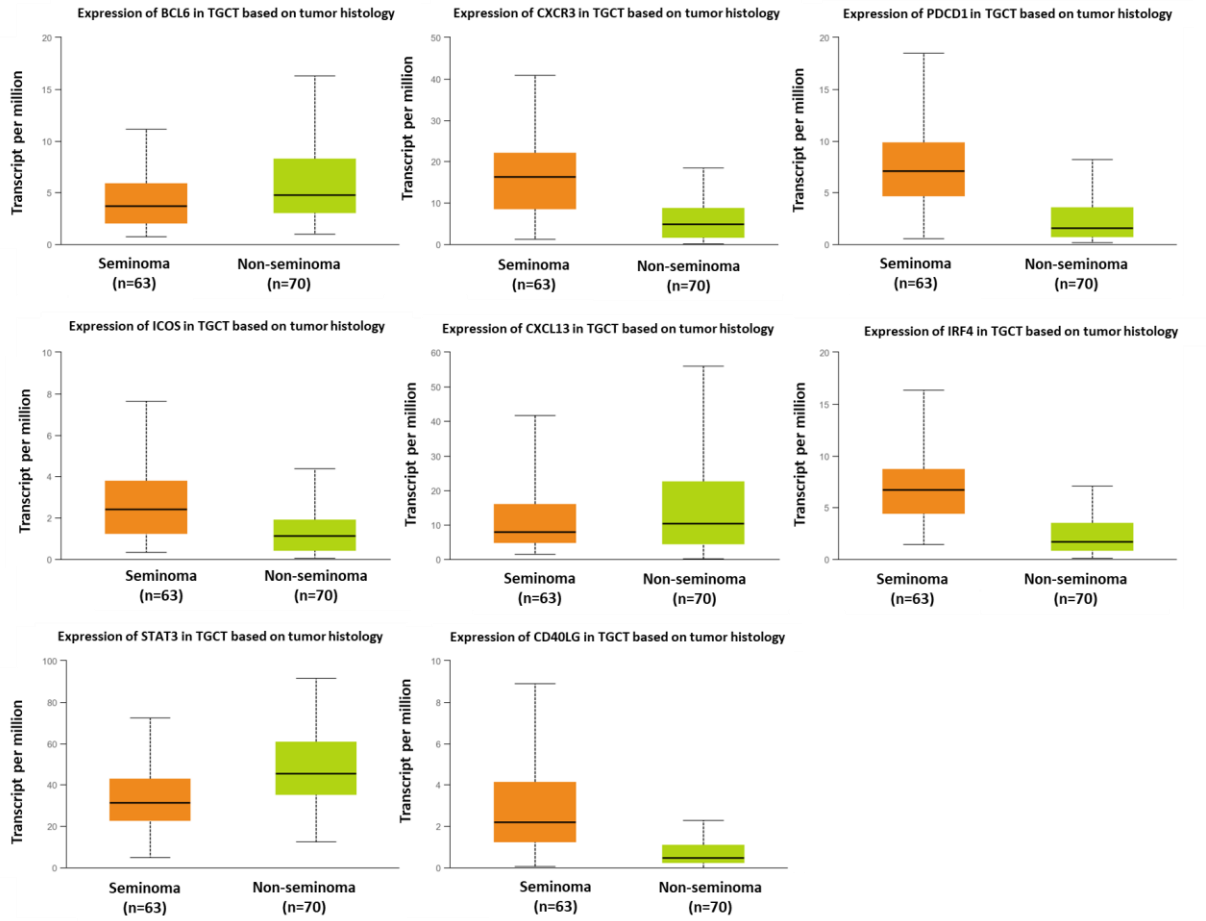

Figure 3.24 Cross-validation of Tfh-associated selected gene using UALCAN for analyzing TGCT OMICS data. The expressions of the selected genes were extracted from TCGA-TGCT dataset. Number of seminoma (n=63) and non-seminoma (n=70). The orange color represents seminoma, and the green color represents no seminoma. All comparisons are statistically significant ($p<0.05$)

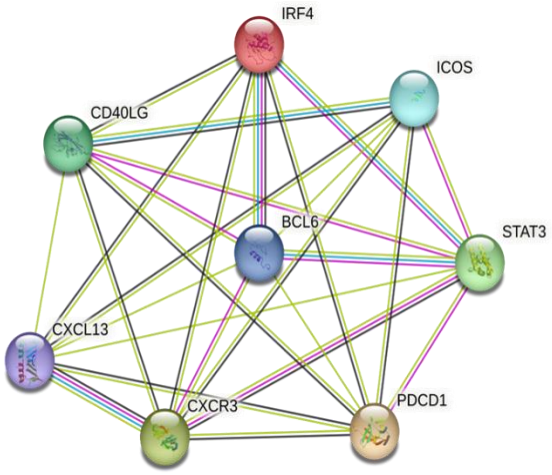

Figure 3.25 The protein-protein interaction (PPI) network of Tfh-selected protein was generated by STRING. Colored nodes indicate query proteins and first shell of interaction, filled nodes represent known or predicted 3D structure. Pastel color edges represent the known interactions from curated databases, pink color edges represent known interactions determined experimentally, green color edges represent predicted interactions between neighboring genes, red color edges represent the predicted gene fusion interaction, blue color edges represent the predicted co-occurrence of gene interaction. Other color edges, for example olive color represents textmining, black color represents co-expression and purple color represents protein homology.

3.3.5 Differential gene expression analysis of different cells found in the microenvironment of testicular tissue

As shown above, the analyzed human testicular tissue microenvironment consists of various cells, including T cells, B cells, macrophages, plasma cells, tumor cells, endothelial cells, fibroblasts, germ cells, and undefined cells, forming a dynamic, multi-faceted regulatory network that is responsible for maintenance of human testicular homeostasis and the development and progression of human TGCT. However, the underlying mechanism of how different cells incorporate each other into the tissue microenvironment to facilitate the normal functions of the human testis as well as the development and progression of human testicular diseases, specially TGCT, remains unknown to date. Therefore, DGEs of a single cell compared to the rest of the cells in the analyzed tissue microenvironment was performed to get an overview of identical and non-identical genes in the different cells found in the testicular tissue microenvironment (Supplementary Figure 15) to open a new window for functional studies of specific cells in human testicular tissue as well as to improve the targeted therapy of human TGCT. The broad spectrum DGEs analysis (Supplementary Figure

15) revealed the number and percentage of identical (40.8-71.6%) and non-identical genes in all cells, reflecting the complexity and challenges of functional study of a particular cell in the tissue microenvironment either in normal physiological and/or pathological condition.

In line with our study objective, only T cells are described in comparison to the rest of the identified cells in human testicular tissue. A total of 4629 differentially expressed genes were detected in the DGEs analysis between T cells and rest of the cells in the human testis (Supplementary Figure 7), gene list was filtered by log2 fold change of >0.58, P-value (<0.05) and pct >0.5 (the percentage of cells where the feature is detected). Followed by top 20 upregulated and downregulated genes have been separately analyzed for GSEA-GO and GSEA-pathway analysis using a functional enrichment analysis datasets named “Enrichr” (Figure 3.26 and Figure 3.27).

The Enrichr GO biological process function of top 20 up-expressed genes showed significantly altered genes in T cells compared to the other cells enriched for different biological functions, and the top 10 GO biological process terms were ranked by P value (Figure 3.26A). Among them, there are some significant GO terms for biological processes such as T cell activation (where mature or immature T cells undergo morphological and behavioral changes resulting from exposure to a mitogen, cytokine, chemokine, or cellular ligand for which they are specific), T cell receptor signaling pathway (the series of molecular signals initiated by the cross-linking of an antigen receptor on a T cell), positive regulation of T cell proliferation (any process that activates or increases the rate or extent of T cell proliferation) were observed. Whereas the top 10 GO biological process of top 20 down-expressed genes showed different significant GO terms for biological processes, including spermatid development (the process whose specific outcome is the progression of a spermatid over time, from its formation to the mature structure) (Figure 3.26A).

Enrichr GO molecular function of to 20 up-expressed genes revealed significantly altered genes in T cells enriched for various molecular functions such as different chemokine receptor binging and activity, while top 20-downexpressd genes showed significantly altered genes in T cells enriched for DNA binding, bending etc. (Figure 3.26B).

In addition to the GO biological and molecular functions, the GO interpretation of the cellular component of top 20 up-expressed genes revealed that most of the differentially expressed genes are associated with the alpha-beta T cell receptor complex, T cell receptor complex, while the GO interpretation of the cellular component of top 20 down-expressed genes revealed that most of the differentially expressed genes are associated with the rough endoplasmic reticulum (Figure 3.26C).

Furthermore, a GSEA pathway analysis was performed using the same 20 up-expressed and 20 down-expressed differentially expressed genes (separately) to determine their association with different signaling pathways by Enrichr using multiple functional databases such as BioPlanet, WikiPathways, KEGG and different gene sets associated with different signaling pathways have been identified (Figure 3.27 A-C).For example, among the top 20 up-expressed gene, different gene set associated with PD-1 signaling, IL-2 signaling pathways etc. were identified using the BioPlanet Pathway Functional Database (Figure 3.27A). Similarly, using the WikiPathway database and KEGG pathway database, different sets of genes associated with different pathways were found including a gene set associated with T cell receptor pathway (Figure 3.27B, C). On the contrary, GSEA pathway analysis with top 20 down-expressed differentially expressed genes showed a gene set associated with male infertility using the WikiPathway Functional Database (Figure 3.27B).

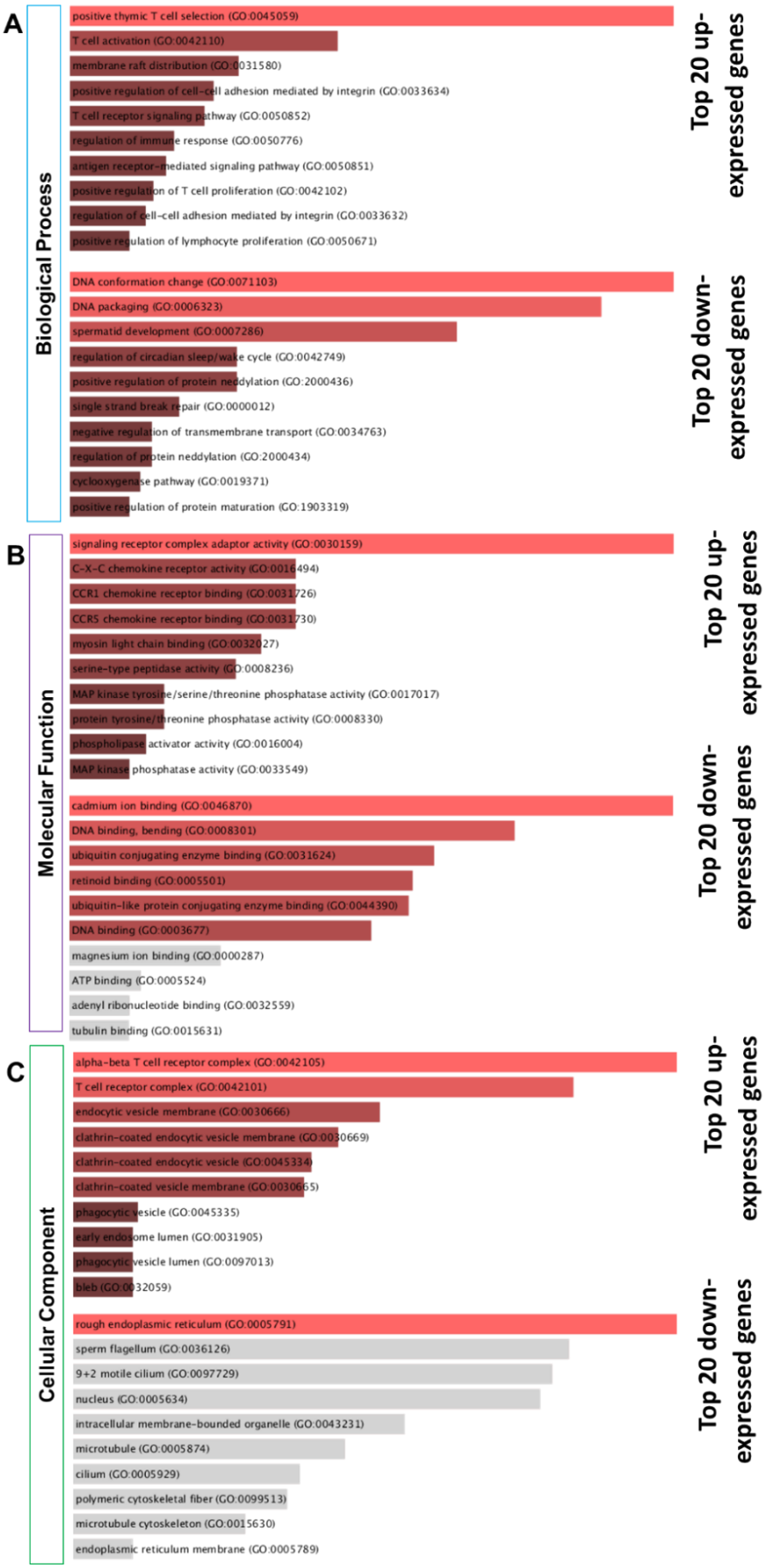

Figure 3.26 See next page for caption.

Figure 3.26 Gene set enrichment analysis- Geneontology (GO) analysis of top genes 20 (20 up expressed and 20 down expressed) genes in T cells compared to the other cells in the human testicular tissue microenvironment by Enrichr. Bar chart showed the top 10 GO terms for biological process (A), molecular function (B) and cellular component (C) respectively between T cells vs rest of the cells in primary clusters. Bar charts length and color represent the significance of respective term.

3.3.6 Differential gene expression analysis of T cells from different TGCT compared to normal testis

DGEs analysis of T cells derived from different TGCTs compared to normal testes was performed to identify the functional genes involved in T cell biology in testicular cancer. A range of 5,882-6,462 genes were detected in different TGCTs compared to normal testes (Supplementary Figure 8A-D), and a variety of genes that were identical and non-identical between the TGCTs patients were observed (Supplementary Figure 16). Although the highest number of differentially expressed genes was detected in embryonic carcinoma compared to normal testes, a relatively low number of genes were statistically significant with a log2-fold change of $\geq$0.58 (Supplementary Figure 8D). Notably, the identical and non-identical genes in T cells across the different TGCT compared to donors can serve as new diagnostic markers as well as help to develop personalized immunotherapies. Nevertheless, top 300 (150 up-expressed and 150 down-expressed) differentially expressed genes from different TGCTs compared to donors were used to perform a GSEA-GO analysis to classify the genes according to their respective GO terms by WebGestalt (Supplementary Figure 17A-D).

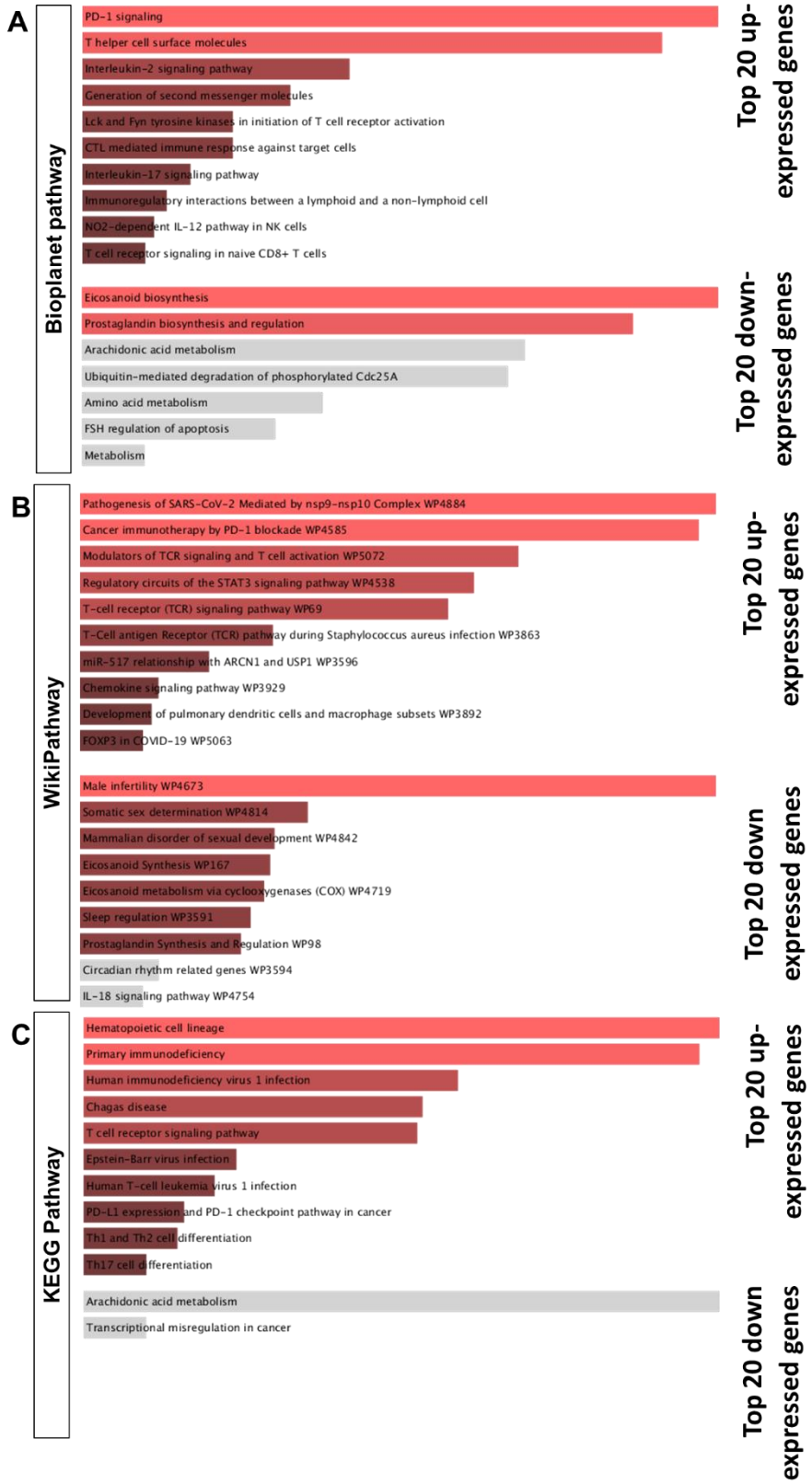

Figure 3.27 See next page for caption.

Figure 3.27 Gene set enrichment analysis- Pathway analysis of top 300 (150 up expressed and 150 down expressed) gene in T cells compared to the other cells in the human testicular tissue microenvironment by Enrichr. Bar chart showed the top 10 pathways analysis by Bioplanet pathway (A), WikiPathway (B) and KEGG pathway (C). Bar charts length and color represent the significance of respective term.

There were several identical positive and negative GO biological processes, molecular processes and cellular compartments observed in the different tumors A-D). Nonetheless, there are some interesting sets of genes that are positively associated with various biological processes, including T-cell activation, adaptive immune response, lymphocyte-mediated immunity, regulation of cytokine stimulus Supplementary Figure 17A-D). Interestingly, a couple of gene sets were also detected responsible for sperm motility, fertilization in GSEA-GO analysis (Supplementary Figure 17A-D). Apart from the biological processes, a set of genes responsible for cell adhesion molecule binding was identical across all tumor datasets (Supplementary Figure 17A-D). In addition to the biological processes and molecular functions, the cellular component of the selected genes was also assessed in order to develop a cellular targeting strategy.

In addition, the same top 300 (150 unexpressed and 150 down-expressed) differentially expressed genes from different TGCTs were used to perform a GSEA pathway analysis to determine their association with different signaling pathways through WebGestalt using multiple functional databases including WikiPathways, Panther Pathways, and KEGG, and to determine different associated gene sets with different signaling pathways were identified (Supplementary Figure 18A-D). Remarkably, several interesting gene sets related to T cell receptor signaling pathway, TGF signaling pathway, cancer immunotherapy by PD-1 blockade, differentiation of Th17, Th1 and Th2, etc. were found that might be interesting for the functional study of T cells, including Treg cells in human TGCTs (Supplementary Figure 18A-D).

3.4 Hanging drop cultures of human testicular tissue samples to study immune cells in a preserved niche

As previously mentioned, the functional study of immune cells in testicular cancer development and progression is limited due to the lack of suitable animal models, hence an alternative model for testicular immune cell functions is urgently needed. Therefore, we employed an established *ex vivo* model that was successfully tested in human testicular tissue where germ cells and somatic cell phenotypes were unaffected. However, it is still limited to study immune cells in hanging drop cultures of testicular tissue yet. Therefore, this study first attempted to optimize the condition suitable for immune cell survival with unaltered germ cells and other testicular somatic cells. Human testicular tissues from the different localizations were cultured for 3 days (n=4) and 7 days (n=2), and cultured tissue fragments were used to perform flow cytometric analysis of overall immune cell survival with a particular focus on T cells (Table 3.5). Two samples, one presenting 95% embryonal carcinoma with 5% post-pubertal teratoma, the other 30% seminoma with 70% post-pubertal teratoma were cultured for 7 days. Flow cytometric analysis was then performed and at the Tumor sites of these two patient samples, 16.3% and 26.9% of the total events analyzed (median 21.6%) were live cells and 3.34-6.46% (median 4.9 %) and 1.67–2.05% (median 1.86 %) of the total living cells were CD45+ total immune cells and CD3+ T cells, resp. (Table 3.5).

Other four samples, three representing pure seminomas and one sample representing mixed tumors (50% seminomas and 50% embryonic carcinomas), were cultured for 3 days. At Tumor sites of seminoma, 2.93-26% (median 14.466%) of the total events analyzed were live cells, and 3.15-9.15% (median 6.15) and 1.45-5.75% (median 3.6%) of the total live cells were CD45+ immune cells and CD3+ T cells, respectively (Table 3.5). Whereas, in Tumor-Adj and Tumor-Dis sites of seminoma, live cells accounted for 1.99-57.3% (median 29.645%) and 28.2-82.5% (median 55.35%) of total analyzed events, CD45+ immune cells accounted for 3.88-7.06% (median 5.47%) and 7.94-13.7% (median 10.82) of total live cells, and CD3+T cells accounted for 0.88-1.18 (median 1.03) and 0.95-4.08% (median 2.515) of total live cells. Notably, highest percentage of live cells (58.5% and 69.2%) were found in the contralateral sites of seminoma patient (Table 3.5). A relatively high percentage of single viable cells (1.99-

82.5% of total analyzed events, median) was observed in tissue cultured for 3 days compared to tissue cultured for 7 days (16.3-58% of total analyzed events, median 42.45%). However, no major difference in viable immune cells was observed between 3-day cultured tissue versus 7-day cultured tissue (Table 3.5). Since only a low percentage of the immune cells was alive after 3 and 7 days of culture, further medication in medium composition is needed that favor immune cells survival.

Table 3.5 Analysis of immune cells in hanging drop-cultured human testis cancer samples by flow cytometry.

Internal patient number	Age (years)	Tumor and Contralateral side (1= left; 2= right)	Tissue sample location	Culture time	Overall clinical histopathological assessment (Primary tumor histology %)	Histological assessment (in-house) of each section BEFORE hanging drop culture	Histological assessment (in-house) of each section AFTER hanging drop culture	Total number of single live cells	% Single total live cells	% Of CD45+ cells in total single live cells	% Of CD3+ cells in total single live cells
Hoca-60	34	2	Tumor	7 days	95% EC+ 5% Post-pubertal Teratoma	EC, Ly	Seems EC, Ly	2339	16.3	6.46	2.05
HoCa-64	30	1	Tumor		30% SE+70% Post-pubertal Teratoma	SE, LY, TS, FSC	SE, GCNIS, ly	2812	26.9	3.34	1.67
			Tumor-Adj			GCNIS, Ly, TS, SE (few)	GCNIS, Ly, TS, SE (few)	3388	58	5.99	3.63
			Tumor-Dis			GCNIS, Ly, TS	GCNIS, Ly, TS	5126	61	13.7	10.3
HoCa-66	33	2	Tumor	3 days	50% SE+ 50%EC (Hematoma + scarring)	FSC, Ly, SCO	hard to do histological evolution	3405	76.8	4.17	3.20
			Tumor-Adj			GCNIS, TS		45003	80.2	9.78	0.93
			Tumor-Dis			GCNIS, Ly		6972	76.8	4.55	3.18
HoCa-82	56	2	Tumor		100% SE	SE	SE	1238	26	3.15	1.45
			Tumor-Adj			TS	TS	800	57.3	3.88	0.88
			Tumor-Dis			TS, FSC, GCNIS	TS, FSC, GCNIS	1688	82.5	7.94	0.95
HoCa-83	39	2	Tumor-Adj			FSC, TS	-	1629	66.2	1.66	0.98
			Tumor-Dis			SCO, TS	-	1651	70.5	7.15	3.69
HoCa-84	52	1	Tumor			SE/EC, Ly, HYP	-	1147	12.93	9.15	5.75
			Tumor-Adj			HYP+Ly	-	85	1.99	7.06	1.18
			Tumor-Dis			HYP	-	1200	28.2	13.7	4.08
		2	Contralateral 1			hyp	-	1512	58.5	5.89	3.57
			Contralateral 2			Dv, hyp	-	1928	69.2	1.97	1.35

4 DISCUSSIONS

Despite TGCT is the most curable cancer with a survival rate of >95% (Hanna and Einhorn, 2014, Gaddam and Chesnut, 2022), it still presents numerous challenges, including an increasing incidence rate, an increased risk of developing secondary malignancies and long-lasting adverse effects such as infertility, hypogonadism, osteoporosis, metabolic or cardiovascular diseases which represent the most relevant life-threatening consequences of available TGCT therapy (De Toni et al., 2019, Gaddam and Chesnut, 2022). To minimize these adverse upshots, this study has focused on investigating the immune contexture of TGCT, which could help to improve the current understanding of TGCT pathogenesis and immune surveillance, with the main goal of developing an effective immunotherapy for TGCT.

As mentioned above, testes are an immune-privileged organ that protects germ cells from autoimmune attacks and reacts to invading pathogens by eliciting a finely balanced immune response (Kaur et al., 2013, Fijak et al., 2018, Kaur et al., 2021). Although the successful progression of spermatogenesis is the fundamental role of testicular immune privilege, the correlation between testicular immune privilege and the development of TGCT is still poorly understood (Kalavska et al., 2020). Nevertheless, several studies examined the response of immune cells to the presence of pre-invasive GCNIS and TGCT by characterizing immune cells as well as cytokine profiles. Hvarness et al. (Hvarness et al., 2013) and Klein et al. (Klein et al., 2016) described a significantly different pattern of immune cells infiltration and distribution in human testicular tissues presenting TGCT, pre-invasive GCNIS, HYP+ly compared to normal testis. In both studies, T cells were found in all analyzed samples and the highest number of T cells was found in human TGCT as the major component of tumor infiltrating lymphocytes, while macrophages represent the leading resident immune cells in normal testes. In addition, Klein et al. (Klein et al., 2016) uniquely characterized the TGCT microenvironment by the presence of B cells. These results suggest an association between different immune cells and TGCT development and progression. However, the functional characterization of infiltrating immune cell landscape in human normal testis and TGCT is not yet well defined due to several limitations, including precious clinical specimens, lack of TGCT animal models and strict ethical rules and regulations. Notwithstanding these limitations, further studies are needed to improve

our understanding of immune surveillance and/or inflammatory immune response and/or autoimmune response of infiltrating immune cells particularly in human TGCT.

This study performed an in-depth analysis of immune cells in independent human testis samples by different techniques to get a broader view of the immune environment of human TGCT as well as normal testis. Interestingly, in spite of high inter-individual variation and sample heterogeneity, all applied techniques using different sample types (archive and fresh material) and cohorts (retrospective and prospective) yielded a similar composition of immune cells in human testis with an overall increase of immune cells in testicular pathologies, especially in seminoma compared to other conditions.

Briefly, phenotypic characterization of immune cell infiltrates in retrospective archive testis samples by IHC revealed that T cells represent the major component of infiltrating immune cells in human testicular pathological conditions and the highest number of T cells was found in seminoma, whereas a small number of T cells were found in normal testis, suggesting the involvement of T cells in the regulation of normal testicular function as well as in the development and progression of TGCT, mostly seminoma. In addition, the major subtypes of T cells, CD4+ Th and CD8+ Tc cells, were also found in all studied samples with different infiltration density and distribution, but the highest number of both T cells was found in seminomas compared to other samples, suggesting that these cells are closely associated with seminoma, but could also play an important role in normal testicular function. Although the overall T cell presence in human TGCT is basically known, very few studies have focused on examining the significance of rare T cells in human testes. Therefore, this study paid particular attention to the two most common rare T cell subtypes, Treg and Tfh, which are involved in the prognosis estimation in other cancers (Togashi et al., 2019, Crotty, 2019), but only to a limited extent in human testes. Here, a significantly increased number of Treg and Tfh cells was observed in testicular pathologies, mostly in seminoma compared to other pathological conditions and normal testis, suggesting that Treg and Tfh might have an impact on TGCT biology, mainly in seminoma. Treg cells were also found in infertile testes and pre-invasive GCNIS+ly and rarely in normal testes with different infiltration densities, providing preliminary evidence that Treg cells may be involved in the regulation of spermatogenesis but mostly in the development

and progression of human TGCT. Whereas Tfh cells were uniquely detected in seminoma with FLS but not in other samples, suggesting a very specific correlation between Tfh and seminoma. FLS are defined as structures containing B cells, plasma cells, follicular DCs, Th and Tc, in which each cell interacts with each other and influences the humoral response and cell-mediated immunity in the pathogenesis of various diseases. To our knowledge, this is the first time that Tfh cells have been studied in human TGCT. This new finding suggests that recruitment of Tfh cells depends on the presence of a very specific environment FLS, and Tfh cells are closely associated with human TGCT, mostly seminoma in special circumstance.

In addition to T cells, consistent with previous studies (Hvarness et al., 2013, Klein et al., 2016), macrophages represent the leading resident immune cells in normal testis and the second highest infiltrating immune cells in seminoma, suggesting that macrophages may play dual role in the regulation of testicular function as well as in the pathological condition. Interestingly, B cells were absent in normal testis but uniquely found in seminoma, suggesting that B cells are exclusively associated with advantage stages of TGCT, but probably have no involvement in the regulation of normal testicular function. Furthermore, DCs were rarely observed in NSP but abundantly found in infertile testis, GCNIS±ly and seminoma. The highest number of DCs was found in seminomas compared to other specimens, suggesting that DCs recruitment might be directly correlated with human TGCT development and progression.

Yet, tumor heterogeneity and intra-tumoral heterogeneity are the main challenges for the development of personalized oncological medicine in different cancers, including TGCT. Recently, Nestler et al. performed transcriptome analysis using different regions of TGCT and showed clear heterogeneity of differentially expressed genes in Tumor and Tumor-Adj regions (Nestler et al., 2022). Particularly, a list of significantly expressed genes in Tumor-Adj compared to Tumor were detected which are associated with TGCT progression and metastatic spread, while genes highly expressed in Tumor are mainly associated with cancer-related signaling pathways (Nestler et al., 2022). The regional differences in gene expression correspond to inter-tumoral and intra-tumoral heterogeneity. With a similar perception, this study

investigated regional immune cell composition in fresh prospective human testicular tissue by flow cytometry and observed a marked difference in immune cell composition in different areas of tumor-bearing and unaffected contralateral testis.

Consistent with IHC phenotypic analysis, flow cytometric analysis of prospective fresh human testicular specimens showed that T cells are the leading infiltrating immune cells in TGCT, with the highest number of T cells at Tumor sites of seminoma compared to other sites of seminoma and other TGCT, reflecting the important association between T cells and TGCT. In addition, subtyping T cells, CD4+ Th cells and CD8+ Tc cells are also abundantly found in Tumor sites of seminoma compared to other TGCT. Further analysis of immune cell composition in different localizations of testes showed that rare T cell subtypes, Treg and Tfh cells, are found in all the locations of human testes and the highest number of Treg and Tfh cells are in Tumor site of seminoma compared to other samples, suggesting the importance of rare T cells in TGCT biology, particularly in seminoma. In addition to T cells, other immune cells such as macrophages and B cells are also abundantly found in the Tumor sites of TGCT compared to other sites of different TGCT and contralateral testis, further suggesting that the recruitment of immune cells probably regulated by the advanced stage of TGCT. Interestingly, highest number of T cells and B cells was found in seminoma whereas highest numbers of macrophages were found in Tumor sites of embryonic carcinomas, while the highest numbers of other immune cells were found in Tumor sites of seminoma and mixed tumors, suggesting that macrophages have a distinct association with embryonal carcinoma compared to other TGCT. In addition, macrophages were the leading immune cells in the contralateral testes, representing normal or infertile testes.

Finally, to gain insight into the cell populations that may contribute to human TGCT, this study assessed the composition of cells with a special focus on the immune cell landscape in human normal and TGCT by scRNA-seq. Even with the sample heterogeneity, human testis scRNA-seq showed identical results as IHC and flow cytometric analysis of immune cells using retrospective archive and fresh testicular tissue samples. Consistent with the retrospective and prospective sample cohorts, T cells were the most abundant infiltrating immune cells in human TGCT, while macrophages were the leading resident immune cells in normal testes. Further

analysis of T cells was performed to investigate their subtypes. In addition to CD8+Tc cells, secondary clustering identified increased number of proliferating (activated) T cells, CCR7+ (newly recruited) T cells, and other CD4+ T cells, Treg and Tfh with variable frequencies in TCGT compared to normal testis, further suggesting their important association with TGCT. Cellular quantification analysis showed that both Treg and Tfh cells were abundant in seminoma and mixed tumor compared to embryonic carcinoma and normal testis. This further indicates the functional involvement of Treg and Tfh cells with a specific TGCT. In addition to T cells, B cells, plasma cells and macrophages were also abundantly observed in TGCT compared to normal testes, further indicating their association with TGCT.

Even though the sample heterogeneity, all approaches used in this study showed an increased number of Treg and Tfh cells in TGCT, which is in completely contrast to Siska et al. (Siska et al., 2017a) where they showed that human TGCT, particularly seminoma, is associated with reduced infiltration of Treg cells. This could be due to the different sample groups and comparison methods. Still, there were several challenges observed in this study. The selection of a specific marker for investigating immune cells is a universal challenge that this study also had to face. For example, CD4 is a core marker for Th cells but can also be expressed by macrophages (Guo et al., 2021), which somehow confounds the quantification of CD4+ Th cells in the study groups. Similarly, CD11c is a well-known marker for DCs, but is also used to distinguish different origins of macrophages (Lu et al., 2022). Furthermore, CD4+ T cells and CD8+ T cells are considered helper and cytotoxic T cells, resp., but these two cells may also exhibit contrasting properties (Oh and Fong, 2021), making it difficult to provide a constructive summary of the study.

Nevertheless, taken together, even with analyzing different groups of samples by different techniques, a similar composition of immune cells was observed in human testes presenting different phenotypes. Compared to the normal testis or other pathologies, immune cells were overall abundantly found in TGCT, mostly in seminoma, where T cells were the leading infiltrating immune cells. However, the underlying mechanism of immune cell recruitment in TGCT remains to be elucidated. Primarily, this study hypothesized that human testes provide a special environment under pathological conditions by secreting various cytokines and chemokines that

predominantly attract T cells, including their rare Treg and Tfh cells, towards the testicular microenvironment, however, additional analysis needs to be performed to support this hypothesis.

Last but not least, this study has analytically elucidated the possible mechanism how Treg and Tfh cells recruit and are functionally involved in TGCT by extended bioinformatical analysis of scRNA-seq datasets and publicly available databases. A set of known signature molecules that regulate Treg and Tfh cell function were selected, and their expression profiles were cross validated from different perspectives. Selected molecules are known with their special function in Treg cells. For example, BATF belongs to the AP-1 family of transcription factor and plays a critical role in regulating the differentiation and maintenance of non-lymphoid tissue resident Treg cells through direct regulation of ST2 (Vasanthakumar et al., 2015, Delacher et al., 2020). CCL5 is a chemokine that can be transactivated by cancer-FOXP3 and promotes the recruitment of Tregs from peripheral blood to the tumor site (Wang et al., 2017c). CTLA4-dependent and /or high-affinity IL2R-dependent suppression of T cell activity seems to be key to the immunosuppressive function of Treg as -Treg-specific CTLA4 lacking impairs Treg-mediated immune suppression and systematic hyperproliferation of naive conventional CD4+ T cells (Wing et al., 2008), mutations in CTLA4 are associated with impairment in the immunosuppressive activity of Treg cells (Schubert et al., 2014, Kuehn et al., 2014), FOXP3 mediated upregulation of CTLA4 and CD25 (IL2RA) transcription stimulates immunosuppression activities of Treg cells (Hori et al., 2003, Birzele et al., 2011, Morikawa and Sakaguchi, 2014). CXCR4 is activated by CXCL12, that regulates T cell access and recruits immunosuppressive population into TME including IL-10 producing Treg cells (Santagata et al., 2021). CXCR4 antagonism has also been shown to reverse Treg suppression function (Santagata et al., 2021). FOXP3 is a lineage-specifying transcription factor and master regulator of Treg cell phenotypes and immunosuppressive functions (Colamatteo et al., 2019, Togashi et al., 2019). FOXP3 has been shown to directly suppress transcription of the IL2 and to upregulate CTLA4 and IL2RA transcription (Togashi et al., 2019). GITR (TNFRSF18) is upregulated in tumor infiltrating Treg cells and mainly responsible for Treg activation in the tumor microenvironment and stimulates immunosuppressive capacity of Treg cells (De Simone et al., 2016). ICOS (CD278) promotes the generation, proliferation,

survival, and suppressive ability of Treg through complex signaling pathways. For example, ICOS promotes FOXP3 transcription, favoring nuclear factor of activated T cells binding to FOXP3 over AP1 and upregulating IL-10, TGF-β (Chen et al., 2018, Li and Xiong, 2020b). ICOS stimulates PI3K recruitment to the YMFM motif at the cytoplasmic tail and phosphorylation of AKT, which induces BCL-2 expression and inhibits proapoptotic BCL-2 protein production, thereby enhancing Treg cell survival (Li and Xiong, 2020b). In addition, ICOS expression increases CXCR3 expression, which stimulates the migration of Tregs to inflammatory tissues (Li and Xiong, 2020b). CD25 (IL2RA) is another master regulators for the differentiation and proliferation of Treg cells (Plitas and Rudensky, 2016), and highly expressed CD25 (IL2RA) by Treg deprive the milieu in IL-2, reducing the expansion of conventional CD4+ T cells and memory CD8+ T cells and their differentiation into effectors (Cinier et al., 2021). TIGIT can act primarily in Tregs to impede anti-tumor CD8+ T cell responses and promote tumor growth. TIGIT+ Tregs upregulates the expression of HAVCR2 in tumor, and HAVCR2 and TIGIT synergize to suppress anti-tumor immune responses (Kurtulus et al., 2015, Chauvin and Zarour, 2020). TNFRSF4 (OX40) is highly expressed in Treg and mainly responsible for Treg activation in the TME and boosts Treg proliferation and immunosuppressive activity (Aspeslagh et al., 2016). TNFα plays dual roles in Treg cells. For example, some studies discovered that the highly expressed TNFα enhances proliferation, and suppressive capabilities of Treg cells (Chen et al., 2007, Zaragoza et al., 2016, Yang et al., 2019). In contrast, other studies demonstrated that TNFα negatively regulates the suppressive function of Treg cells (Nie et al., 2013, Nie et al., 2016, Yang et al., 2019).

All of these Treg signature molecules were highly expressed in scRNA-seq datasets from human TGCT samples (mostly in seminoma) compared to normal testes, which was also consistent in the publicly available TCGA-TGCT data in UALCAN, strongly advocating possible involvement of Treg cells in TGCT. Followed by a co-expression analysis of selected Treg functional molecules was performed using public omics datasets and a high-level correlation was found between BATF and CCL5, suggesting that the increase of Treg cells in human TGCT may be regulated by the cooperation between BATF and CCL5. In addition, there are 18 other interactions between the selected genes whose correlation coefficient was >0.8, indicating a strong association of genes potentially involved in Treg cell recruitment and function. In addition to co-

expression analysis, a PPIs network was created showing that CD25 (IL2RA), CTLA4, and FOXP3 appear to be leading proteins to regulate Treg cells in human TGCT. In addition, PPIs were also constructed between Treg-specific genes and other cellular markers used to identify different cell populations in the testicular microenvironment, and an interaction between NANOG and CXCR4 was demonstrated. Since it is known that NANOG is one of the common markers for GCNIS and TGCT and CXCR4 is an enhancer of Treg recruitment to the TME, it can be assumed that these NANOG-CXCR4 interactions might be interesting for understanding the underlying mechanisms of Treg in TGCT. Interestingly, recent evidence shows that NANOG regulates glioblastoma cell migration via the SDF1/CXCR4 pathway (Sánchez-Sánchez et al., 2021). In view of this evidence, it can be strongly state that the interaction between NANOG and CXCR4 can regulate Treg recruitment and functions in TGCT in our case.

Similar to Treg cells, a set of Tfh cell-associated genes were selected, and each of these molecules plays a crucial functional role in Tfh cells. For example, BCL6 is the central regulator of Tfh cell differentiation and function (Choi and Crotty, 2021b). As previously mentioned, BCL6 acts on several aspects of Tfh cell differentiation, maintenance and function. CXCR3 is a signature molecule of Th1 cells but can also be expressed by Tfh cells and turns out to be a poor helper of B cells. CXCR3 may help change the localization of Tfh cells from the GC to the T:B border (Crotty, 2019). ICOS is one of the main factors for the differentiation of Tfh cells and also acts as a co-stimulatory molecule and a migratory receptor for Tfh cells (Xu et al., 2013, Pedros et al., 2016). CXCL13 is exclusively expressed by human Tfh cells, but not by mice. The strongest correlation with the immunoprotected function of Tfh is mainly regulated by CXCL13 (Crotty, 2019). IRF4 involved in the differentiation of Tfh cells through incorporating with other transcriptions factors including BCL6 (Vinuesa et al., 2016). IL-21-mediated Tfh differentiation is primarily regulated by STAT3. Additionally, SATA3 stimulates IL-6-mediated BCL6 expression and TGF-mediated differentiation of Tfh cells (Schmitt et al., 2014, Vinuesa et al., 2016). CD40LG contributes to the migration of Tfh cells and stimulates Tfh cells interaction with B cells (Mayberry et al., 2022).

The expression profiles were also cross validated from different perspectives to unveil the possible mechanism how Tfh cells are involved in human TGCT. All of these Tfh signature molecules were highly expressed in human TGCT samples (mainly in seminoma) compared to normal testis in scRNA-seq datasets, and a similar expression pattern of these genes was also observed in the publicly available omics data, suggesting a possible involvement of Tfh cells in TGCT. In addition, co-expression analysis of selected Tfh-specific genes was performed using TCGA-TGCT datasets and a high level of correlation between CXCR3 and ICOS was observed, suggesting that Tfh cells may play an important role in human TGCT via the interaction between CXCR3 and ICOS. Besides, there are 6 other interactions between the selected genes whose correlation coefficient was >0.8, indicating a strong correlation between genes potentially involved in Tfh cell in the recruitment and functions of human TGCT. Likewise, a PPI network was created that shows a close interaction between the Tfh-selected proteins. Furthermore, the interactions between other cell markers used to identify different cell populations in the testicular microenvironment and Tfh-specific selected protein were also generated, and a tight interaction between BCL6 and NANOG was observed, strongly suggesting the possible mechanism how Tfh cells are involved in TGCT.

Besides, a downstream analysis of scRNA-seq datasets was performed in multiple perspectives. The top 20 up-expressed and 20 down-expressed genes in T cells compared to the rest of the cells in the testis microenvironment were used to perform GSEA-GO and GSEA pathway analysis to identify possible mechanisms how T cells involved in TGCT. Interestingly, different set of genes involved in the PD-1 signaling, IL-2 signaling pathway which are already a well-established signaling mechanism in tumor progression, has been identified (Jiang et al., 2016, Han et al., 2020), therefore it can be hypothesized that different genes from T cells play an important role in TGCT progression via PD-1 signaling and IL-2 signaling pathway. Furthermore, analysis of GSEA signaling pathways revealed different signaling pathways including T cell receptor signaling pathway, which is an important mechanism of T cells function in general and might be in human TGCT.

Later, a DGEs analysis of T cells from different TGCTs compared to normal testes was performed and the top 300 genes from each tumor compared to normal testes were used to perform GSEA in different contexts. GSEA-GO analysis showed that different sets of genes regulate T cell activation, adaptive immune response, leukocyte differentiation, etc., while GSEA signaling analysis showed different sets of genes may regulate different signaling pathways including T cell antigen receptor signaling pathways, TGF-β, cancer immunotherapy by PD-1 blockades etc. suggesting the possible signaling pathways how T cells exhibit their role in TGCT. In addition, it was also found that certain gene sets are involved in the regulation of various CD4+Th cell differentiations such as Th1, Th2 and Th17 cells. This study strongly believes that the functional characterization of these genes would have a positive impact on the understanding of T cell biology in general as well as in human TGCT. However, all these analytical findings have to be proven experimentally.

As the functional analysis of infiltrating immune cells in human TGCT remains a challenge due to the limitation of precious samples and the lack of a suitable animal model, there is an urgent need to establish alternative models (*ex vivo* and/or animal model) for the functional analysis of the infiltration Immune cells in normal and diseased testicles. Therefore, this study also focused on the establishment of a suitable *ex vivo* culture for immune cells study, known as hanging drop, using human testicular tissue, which requires further work to establish. Nonetheless, our previous study used a human TGCT cell line (TCam-2) to analyze the possible mechanisms of various immune cells recruitment into human TGCT and showed that TCam-2 cells could release a pro-inflammatory cytokine IL-6 that can attract B cells toward them (Klein et al., 2017). Furthermore, a recent study also showed that IL-6 is highly expressed in TGCT (Nestler et al., 2022). Previous studies showed that multifunctional IL-6 regulates the differentiation, proliferation and activation of various immune cells including B cells, DCs and T cells with their subtypes (Tanaka et al., 2014), hence IL-6 can be considered as a potential immunotherapeutic target for TGCT.

In conclusion, this study showed for the first time a consistent pattern of immune cell infiltration in TGCT compared to normal testicular tissue assessed by different techniques and in independent sample sets. Even though high inter-individual

variation and sample heterogeneity, all approaches show a similar composition of immune cells in the human testis with an overall increase of immune cells in testicular pathologies, especially in TGCT compared to other conditions. In addition, it clearly showed that the predominance of resident macrophages in normal testis is shifted to T cells as major component of TIL in TGCT. Furthermore, a significantly increased number of rare T cell subtypes, particularly Treg and Tfh, was observed in TGCT compared to other pathological conditions and normal testis, providing first evidence that Treg and Tfh may be involved in TGCT biology (Figure 4.1). With these first indications of the potential importance of T cells and their rarer subtypes in the immune environment of TGCT, further experiments, including downstream analysis of transcriptome data from different immune cells, are underway to interrogate their functions to identify novel prognostic factors and/or immunotherapeutic concepts.

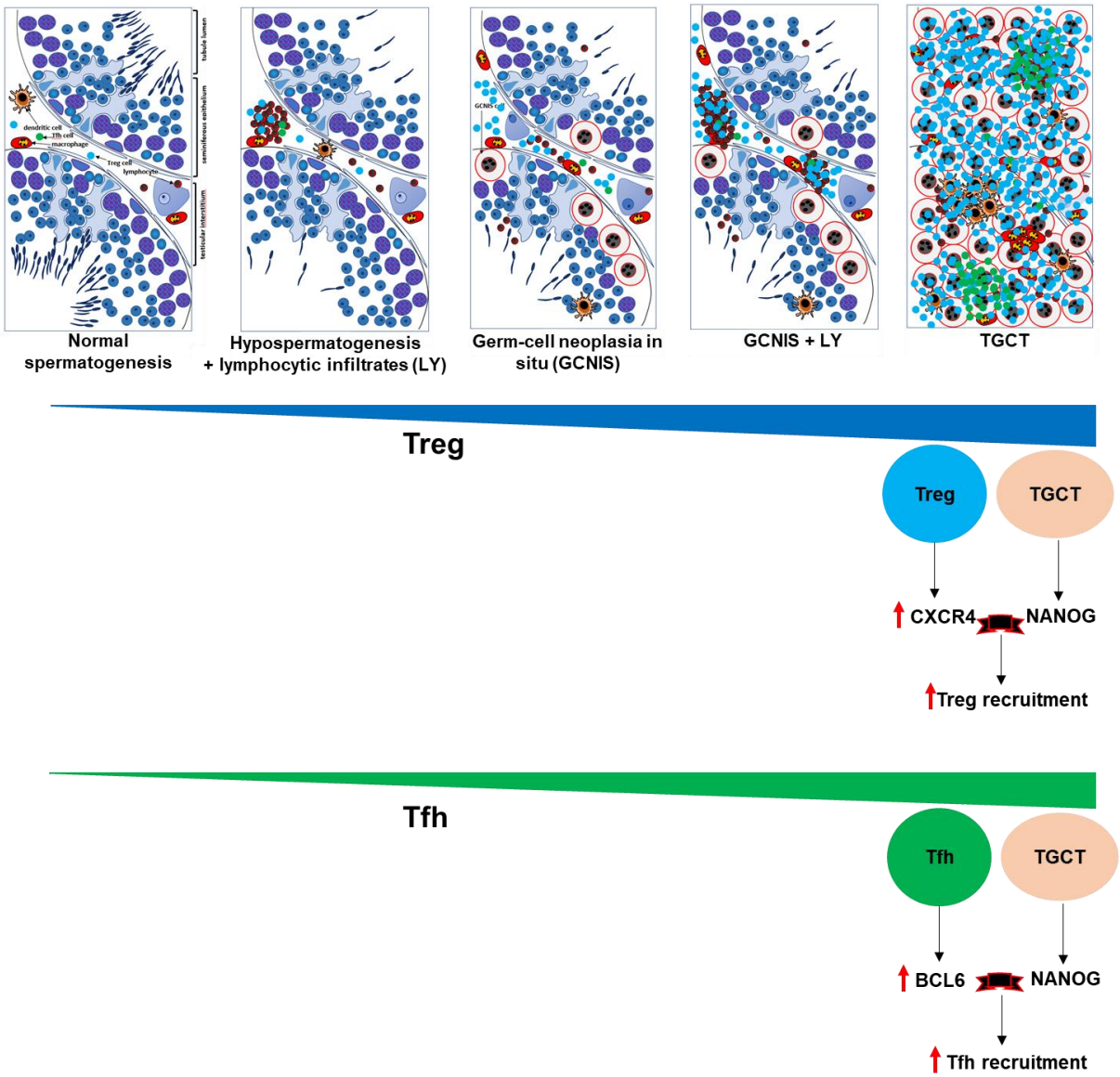

Figure 4.1 Schematic summary of key outcomes. Rare T cell subtypes Treg and Tfh are highly infiltrated in TCGT compared to the other group of samples through interacting with NANOG of TGCT cells. The upper part of this figure was modified from Loveland et al. (2017) Front Endocrinol 8:307.

5 OUTLOOK OF THE STUDY

This study will be continuing to experimentally demonstrate the possible mechanisms of Treg and Tfh cells involvement in TGCT. First, customized microarray or RT-qPCR will be used to perform expression analysis of Treg and Tfh cell-associated molecules, including cytokines, chemokines and other functional genes in human seminoma and embryonal carcinoma tissue compared to normal testicular tissue to support the obtained scRNA-seq data.

Due to the unavailability of proper in vivo model for seminoma study, an in vitro co-culture of seminoma cell line Tcam2 and Treg or Tfh (isolated from PBMC) will be being used to study these rare T cells functional mechanisms. Treg or Tfh will be being co-cultured with Tcam2 cells for different time periods and supernatant will be collected for ELISA analysis and cell pellets will be collected for RNA extraction and RT-qPCR. Additionally, a hanging drop culture of human testis tissue bearing tumor and normal phenotype will be perform to study Treg and Tfh functions. Different drugs such as Daclizumab, Ipilimumab, Mogamulizumab, Parsaclisib, Dasatinib, Galunisertib, Bevacizumab etc will be used in the co-culture to target Treg receptors, intracellular signaling and the tumor microenvironment. Followed by ELISA, RTqPCR will be performed.

6. REFERENCES

ABBAS, A. K., TROTTA, E., D, R. S., MARSON, A. & BLUESTONE, J. A. 2018. Revisiting IL-2: Biology and therapeutic prospects. *Sci Immunol,* 3.

ABBOTT, R. K., LEE, J. H., MENIS, S., SKOG, P., ROSSI, M., OTA, T., KULP, D. W., BHULLAR, D., KALYUZHNIY, O., HAVENAR-DAUGHTON, C., SCHIEF, W. R., NEMAZEE, D. & CROTTY, S. 2018. Precursor Frequency and Affinity Determine B Cell Competitive Fitness in Germinal Centers, Tested with Germline-Targeting HIV Vaccine Immunogens. *Immunity,* 48**,** 133-146.e6.

AHMADZADEH, M., PASETTO, A., JIA, L., DENIGER, D. C., STEVANOVIĆ, S., ROBBINS, P. F. & ROSENBERG, S. A. 2019. Tumor-infiltrating human CD4(+) regulatory T cells display a distinct TCR repertoire and exhibit tumor and neoantigen reactivity. *Sci Immunol,* 4.

AKKAYA, M., TRABA, J., ROESLER, A. S., MIOZZO, P., AKKAYA, B., THEALL, B. P., SOHN, H., PENA, M., SMELKINSON, M., KABAT, J., DAHLSTROM, E., DORWARD, D. W., SKINNER, J., SACK, M. N. & PIERCE, S. K. 2018. Second signals rescue B cells from activation-induced mitochondrial dysfunction and death. *Nat Immunol,* 19**,** 871-884.

ALDINUCCI, D., BORGHESE, C. & CASAGRANDE, N. 2020. The CCL5/CCR5 Axis in Cancer Progression. *Cancers (Basel),* 12.

ALGERMISSEN, B., HERMES, B., FELDMANN-BOEDDEKER, I., BAUER, F. & HENZ, B. 1999. Mast cell chymase and tryptase during tissue turnover: analysis on in vitro mitogenesis of fibroblasts and keratinocytes and alterations in cutaneous scars. *Experimental dermatology,* 8**,** 193-198.

AMOOZGAR, Z., KLOEPPER, J., REN, J., TAY, R. E., KAZER, S. W., KINER, E., KRISHNAN, S., POSADA, J. M., GHOSH, M. & MAMESSIER, E. 2021. Targeting Treg cells with GITR activation alleviates resistance to immunotherapy in murine glioblastomas. *Nature Communications,* 12**,** 1-16.

ANDREASSEN, K., KRISTIANSEN, W., KARLSSON, R., ASCHIM, E., DAHL, O., FOSSÅ, S., ADAMI, H.-O., WIKLUND, F., HAUGEN, T. & GROTMOL, T. 2013. Genetic variation in AKT1, PTEN and the 8q24 locus, and the risk of testicular germ cell tumor. *Human Reproduction,* 28**,** 1995-2002.

ANICHINI, A., MORTARINI, R., ROMAGNOLI, L., BALDASSARI, P., CABRAS, A., CARLO-STELLA, C., GIANNI, A. M. & DI NICOLA, M. 2006. Skewed T-cell differentiation in patients with indolent non-Hodgkin lymphoma reversed by ex vivo T-cell culture with gammac cytokines. *Blood,* 107**,** 602-9.

ANNUNZIATO, F., COSMI, L., LIOTTA, F., MAGGI, E. & ROMAGNANI, S. 2014. Human Th1 dichotomy: origin, phenotype and biologic activities. *Immunology,* 144**,** 343-51.

ANNUNZIATO, F., COSMI, L., SANTARLASCI, V., MAGGI, L., LIOTTA, F., MAZZINGHI, B., PARENTE, E., FILÌ, L., FERRI, S., FROSALI, F., GIUDICI, F., ROMAGNANI, P., PARRONCHI, P., TONELLI, F., MAGGI, E. & ROMAGNANI, S. 2007. Phenotypic and functional features of human Th17 cells. *J Exp Med,* 204**,** 1849-61.

ARCE VARGAS, F., FURNESS, A. J. S., LITCHFIELD, K., JOSHI, K., ROSENTHAL, R., GHORANI, E., SOLOMON, I., LESKO, M. H., RUEF, N., RODDIE, C., HENRY, J. Y., SPAIN, L., BEN AISSA, A., GEORGIOU, A., WONG, Y. N. S., SMITH, M., STRAUSS, D., HAYES, A., NICOL, D., O'BRIEN, T., MÅRTENSSON, L., LJUNGARS, A., TEIGE, I., FRENDÉUS, B., PULE, M., MARAFIOTI, T., GORE, M., LARKIN, J., TURAJLIC, S., SWANTON, C., PEGGS, K. S. & QUEZADA, S. A. 2018. Fc Effector Function Contributes to the Activity of Human Anti-CTLA-4 Antibodies. *Cancer Cell,* 33**,** 649-663.e4.

ASADZADEH, Z., MOHAMMADI, H., SAFARZADEH, E., HEMMATZADEH, M., MAHDIAN-SHAKIB, A., JADIDI-NIARAGH, F., AZIZI, G. & BARADARAN, B. 2017. The paradox of Th17 cell functions in tumor immunity. *Cell Immunol,* 322**,** 15-25.

ASPESLAGH, S., POSTEL-VINAY, S., RUSAKIEWICZ, S., SORIA, J. C., ZITVOGEL, L. & MARABELLE, A. 2016. Rationale for anti-OX40 cancer immunotherapy. *Eur J Cancer,* 52**,** 50-66.

AYERS, M., LUNCEFORD, J., NEBOZHYN, M., MURPHY, E., LOBODA, A., KAUFMAN, D. R., ALBRIGHT, A., CHENG, J. D., KANG, S. P., SHANKARAN, V., PIHA-PAUL, S. A., YEARLEY, J., SEIWERT, T. Y., RIBAS, A. & MCCLANAHAN, T. K. 2017. IFN-γ-related mRNA profile predicts clinical response to PD-1 blockade. *J Clin Invest,* 127**,** 2930-2940.

BADELL, I. R., LA MURAGLIA, G. M., 2ND, LIU, D., WAGENER, M. E., DING, G. & FORD, M. L. 2018. Selective CD28 Blockade Results in Superior Inhibition of Donor-Specific T Follicular Helper Cell and Antibody Responses Relative to CTLA4-Ig. *Am J Transplant,* 18**,** 89-101.

BAIRD, D., MEYERS, G. J. & HU, J. S. 2018. Testicular cancer: Diagnosis and treatment. *American family physician,* 97**,** 261-268.

BALLESTEROS-TATO, A., LEÓN, B., GRAF, B. A., MOQUIN, A., ADAMS, P. S., LUND, F. E. & RANDALL, T. D. 2012. Interleukin-2 inhibits germinal center formation by limiting T follicular helper cell differentiation. *Immunity,* 36**,** 847-56.

BANEK, L., HITTMAIR, A., PEZEROVIĆ-PANIJAN, R., GOLUŽA, T. & SCHULZE, W. 1999. Mast cells in testicular biopsies of infertile men with 'mixed atrophy'of seminiferous tubules. *Andrologia,* 31**,** 203-210.

BARNES, T. A. & AMIR, E. 2018. HYPE or HOPE: the prognostic value of infiltrating immune cells in cancer. *Br J Cancer,* 118**,** e5.

BARONI, T., ARATO, I., MANCUSO, F., CALAFIORE, R. & LUCA, G. 2019. On the Origin of Testicular Germ Cell Tumors: From Gonocytes to Testicular Cancer. *Front Endocrinol (Lausanne),* 10**,** 343.

BARSHESHET, Y., WILDBAUM, G., LEVY, E., VITENSHTEIN, A., AKINSEYE, C., GRIGGS, J., LIRA, S. A. & KARIN, N. 2017. CCR8(+)FOXp3(+) T(reg) cells as master drivers of immune regulation. *Proc Natl Acad Sci U S A,* 114**,** 6086-6091.

BASU, A., RAMAMOORTHI, G., ALBERT, G., GALLEN, C., BEYER, A., SNYDER, C., KOSKI, G., DISIS, M. L., CZERNIECKI, B. J. & KODUMUDI, K. 2021. Differentiation and Regulation of T(H) Cells: A Balancing Act for Cancer Immunotherapy. *Front Immunol,* 12**,** 669474.

BATOOL, A., KARIMI, N., WU, X.-N., CHEN, S.-R. & LIU, Y.-X. 2019. Testicular germ cell tumor: a comprehensive review. *Cellular and Molecular Life Sciences,* 76**,** 1713-1727.

BAUMANN, S., KRUEGER, A., KIRCHHOFF, S. & KRAMMER, P. H. 2002. Regulation of T cell apoptosis during the immune response. *Current molecular medicine,* 2**,** 257-272.

BAUMJOHANN, D. & BROSSART, P. 2021. T follicular helper cells: linking cancer immunotherapy and immune-related adverse events. *J Immunother Cancer,* 9.

BAUQUET, A. T., JIN, H., PATERSON, A. M., MITSDOERFFER, M., HO, I. C., SHARPE, A. H. & KUCHROO, V. K. 2009. The costimulatory molecule ICOS regulates the expression of c-Maf and IL-21 in the development of follicular T helper cells and TH-17 cells. *Nat Immunol,* 10**,** 167-75.

BÉGUELIN, W., TEATER, M., GEARHART, M. D., CALVO FERNÁNDEZ, M. T., GOLDSTEIN, R. L., CÁRDENAS, M. G., HATZI, K., ROSEN, M., SHEN, H., CORCORAN, C. M., HAMLINE, M. Y., GASCOYNE, R. D., LEVINE, R. L., ABDEL-WAHAB, O., LICHT, J. D., SHAKNOVICH, R., ELEMENTO, O., BARDWELL, V. J. & MELNICK, A. M. 2016. EZH2 and BCL6 Cooperate to Assemble CBX8-BCOR Complex to Repress Bivalent Promoters, Mediate Germinal Center Formation and Lymphomagenesis. *Cancer Cell,* 30**,** 197-213.

BELL, D. A., FLOTTE, T. J. & BHAN, A. K. 1987. Immunohistochemical characterization of seminoma and its inflammatory cell infiltrate. *Hum Pathol,* 18**,** 511-20.

BENEVIDES, L., DA FONSECA, D. M., DONATE, P. B., TIEZZI, D. G., DE CARVALHO, D. D., DE ANDRADE, J. M., MARTINS, G. A. & SILVA, J. S. 2015. IL17 Promotes Mammary Tumor Progression by Changing the Behavior of Tumor Cells and Eliciting Tumorigenic Neutrophils Recruitment. *Cancer Res,* 75**,** 3788-99.

BENTEBIBEL, S. E., SCHMITT, N., BANCHEREAU, J. & UENO, H. 2011. Human tonsil B-cell lymphoma 6 (BCL6)-expressing CD4+ T-cell subset specialized for B-cell help outside germinal centers. *Proc Natl Acad Sci U S A,* 108**,** E488-97.

BERGMANN, M. & KLIESCH, S. 2010. Testicular biopsy and histology. *Andrology.* Springer.

BERNEY, D. M., CREE, I., RAO, V., MOCH, H., SRIGLEY, J. R., TSUZUKI, T., AMIN, M. B., COMPERAT, E. M., HARTMANN, A. & MENON, S. 2022. An introduction to the WHO 5th edition 2022 classification of testicular tumours. *Histopathology,* 81**,** 459-466.

BETZ, B. C., JORDAN-WILLIAMS, K. L., WANG, C., KANG, S. G., LIAO, J., LOGAN, M. R., KIM, C. H. & TAPAROWSKY, E. J. 2010. Batf coordinates multiple aspects of B and T cell function required for normal antibody responses. *J Exp Med,* 207**,** 933-42.

BHUSHAN, S. & MEINHARDT, A. 2017. The macrophages in testis function. *Journal of reproductive immunology,* 119**,** 107-112.

BHUSHAN, S., TCHATALBACHEV, S., LU, Y., FRÖHLICH, S., FIJAK, M., VIJAYAN, V., CHAKRABORTY, T. & MEINHARDT, A. 2015. Differential activation of inflammatory pathways in testicular macrophages provides a rationale for their subdued inflammatory capacity. *J Immunol,* 194**,** 5455-64.

BHUSHAN, S., THEAS, M. S., GUAZZONE, V. A., JACOBO, P., WANG, M., FIJAK, M., MEINHARDT, A. & LUSTIG, L. 2020. Immune cell subtypes and their function in the testis. *Frontiers in Immunology,* 11**,** 583304.

BINDEA, G., MLECNIK, B., TOSOLINI, M., KIRILOVSKY, A., WALDNER, M., OBENAUF, A. C., ANGELL, H., FREDRIKSEN, T., LAFONTAINE, L., BERGER, A., BRUNEVAL, P., FRIDMAN, W. H., BECKER, C., PAGÈS, F., SPEICHER, M. R., TRAJANOSKI, Z. & GALON, J. 2013. Spatiotemporal dynamics of intratumoral immune cells reveal the immune landscape in human cancer. *Immunity,* 39**,** 782-95.

BIRZELE, F., FAUTI, T., STAHL, H., LENTER, M. C., SIMON, E., KNEBEL, D., WEITH, A., HILDEBRANDT, T. & MENNERICH, D. 2011. Next-generation insights into regulatory T cells: expression profiling and FoxP3 occupancy in Human. *Nucleic Acids Res,* 39**,** 7946-60.

BLIGHE, K., RANA, S. & LEWIS, M. 2019. EnhancedVolcano: Publication-ready volcano plots with enhanced colouring and labeling. *R package version,* 1.

BOBZIEN, B., YASUNAMI, Y., MAJERCIK, M., LACY, P. E. & DAVIE, J. M. 1983. Intratesticular transplants of islet xenografts (rat to mouse). *Diabetes,* 32**,** 213-216.

BOLLIG, N., BRÜSTLE, A., KELLNER, K., ACKERMANN, W., ABASS, E., RAIFER, H., CAMARA, B., BRENDEL, C., GIEL, G., BOTHUR, E., HUBER, M., PAUL, C., ELLI, A., KROCZEK, R. A., NURIEVA, R., DONG, C., JACOB, R., MAK, T. W. & LOHOFF, M. 2012. Transcription factor IRF4 determines germinal center formation through follicular T-helper cell differentiation. *Proc Natl Acad Sci U S A,* 109**,** 8664-9.

BOLS, B., JENSEN, L., JENSEN, A. & BRAENDSTRUP, O. 2000. Immunopathology of in situ seminoma. *Int J Exp Pathol,* 81**,** 211-7.

BORST, J., AHRENDS, T., BĄBAŁA, N., MELIEF, C. J. & KASTENMÜLLER, W. 2018. CD4+ T cell help in cancer immunology and immunotherapy. *Nature Reviews Immunology,* 18**,** 635-647.

BROWN, P. R., MIKI, K., HARPER, D. B. & EDDY, E. M. 2003. A-kinase anchoring protein 4 binding proteins in the fibrous sheath of the sperm flagellum. *Biology of reproduction,* 68**,** 2241-2248.

BRYANT, V. L., MA, C. S., AVERY, D. T., LI, Y., GOOD, K. L., CORCORAN, L. M., DE WAAL MALEFYT, R. & TANGYE, S. G. 2007. Cytokine-mediated regulation of human B cell differentiation into Ig-secreting cells: predominant role of IL-21 produced by CXCR5+ T follicular helper cells. *J Immunol,* 179**,** 8180-90.

BUISSERET, L., GARAUD, S., DE WIND, A., VAN DEN EYNDEN, G., BOISSON, A., SOLINAS, C., GU-TRANTIEN, C., NAVEAUX, C., LODEWYCKX, J. N., DUVILLIER, H., CRACIUN, L., VEYS, I., LARSIMONT, D., PICCART-GEBHART, M., STAGG, J., SOTIRIOU, C. & WILLARD-GALLO, K. 2017. Tumor-infiltrating lymphocyte composition, organization and PD-1/ PD-L1 expression are linked in breast cancer. *Oncoimmunology,* 6**,** e1257452.

BULLIARD, Y., JOLICOEUR, R., WINDMAN, M., RUE, S. M., ETTENBERG, S., KNEE, D. A., WILSON, N. S., DRANOFF, G. & BROGDON, J. L. 2013. Activating Fc γ receptors contribute to the antitumor activities of immunoregulatory receptor-targeting antibodies. *J Exp Med,* 210**,** 1685-93.

BURRIS, H. A., CALLAHAN, M. K., TOLCHER, A. W., KUMMAR, S., FALCHOOK, G. S., PACHYNSKI, R. K., TYKODI, S. S., GIBNEY, G. T., SEIWERT, T. Y. & GAINOR, J. F. 2017. Phase 1 safety of ICOS agonist antibody JTX-2011 alone and with nivolumab (nivo) in advanced solid tumors; predicted vs observed pharmacokinetics (PK) in ICONIC. American Society of Clinical Oncology.

BUTT, D., CHAN, T. D., BOURNE, K., HERMES, J. R., NGUYEN, A., STATHAM, A., O'REILLY, L. A., STRASSER, A., PRICE, S., SCHOFIELD, P., CHRIST, D., BASTEN, A., MA, C. S., TANGYE, S. G., PHAN, T. G., RAO, V. K. & BRINK, R. 2015. FAS Inactivation Releases Unconventional Germinal Center B Cells that Escape Antigen Control and Drive IgE and Autoantibody Production. *Immunity,* 42**,** 890-902.

BUZZATTI, G., DELLEPIANE, C. & DEL MASTRO, L. 2019. New emerging targets in cancer immunotherapy: the role of GITR. *ESMO open,* 4**,** e000738.

BYSTROM, J., CLANCHY, F. I. L., TAHER, T. E., AL-BOGAMI, M., ONG, V. H., ABRAHAM, D. J., WILLIAMS, R. O. & MAGEED, R. A. 2019. Functional and phenotypic heterogeneity of Th17 cells in health and disease. *Eur J Clin Invest,* 49**,** e13032.

CAI, G., NIE, X., ZHANG, W., WU, B., LIN, J., WANG, H., JIANG, C. & SHEN, Q. 2012. A regulatory role for IL-10 receptor signaling in development and B cell help of T follicular helper cells in mice. *J Immunol,* 189**,** 1294-302.

CANNONS, J. L., QI, H., LU, K. T., DUTTA, M., GOMEZ-RODRIGUEZ, J., CHENG, J., WAKELAND, E. K., GERMAIN, R. N. & SCHWARTZBERG, P. L. 2010. Optimal germinal center responses require a multistage T cell: B cell adhesion process involving integrins, SLAM-associated protein, and CD84. *Immunity,* 32**,** 253-265.

CANNONS, J. L., TANGYE, S. G. & SCHWARTZBERG, P. L. 2011. SLAM family receptors and SAP adaptors in immunity. *Annual review of immunology,* 29**,** 665-705.

CAO, L., HU, X., ZHANG, J., HUANG, G. & ZHANG, Y. 2014. The role of the CCL22-CCR4 axis in the metastasis of gastric cancer cells into omental milky spots. *J Transl Med,* 12**,** 267.

CASTELLINO, F. & GERMAIN, R. N. 2006. Cooperation between CD4+ and CD8+ T cells: when, where, and how. *Annu. Rev. Immunol.,* 24**,** 519-540.

CHAN, W. L., PEJNOVIC, N., LEE, C. A. & AL-ALI, N. A. 2001. Human IL-18 receptor and ST2L are stable and selective markers for the respective type 1 and type 2 circulating lymphocytes. *J Immunol,* 167**,** 1238-44.

CHANDRASHEKAR, D. S., KARTHIKEYAN, S. K., KORLA, P. K., PATEL, H., SHOVON, A. R., ATHAR, M., NETTO, G. J., QIN, Z. S., KUMAR, S., MANNE, U., CREIGHTON, C. J. & VARAMBALLY, S. 2022. UALCAN: An update to the integrated cancer data analysis platform. *Neoplasia,* 25**,** 18-27.

CHAUDHRY, A., RUDRA, D., TREUTING, P., SAMSTEIN, R. M., LIANG, Y., KAS, A. & RUDENSKY, A. Y. 2009. CD4+ regulatory T cells control TH17 responses in a Stat3-dependent manner. *Science,* 326**,** 986-91.

CHAUVIN, J.-M. & ZAROUR, H. M. 2020. TIGIT in cancer immunotherapy. *Journal for immunotherapy of cancer,* 8.

CHAVELE, K. M., MERRY, E. & EHRENSTEIN, M. R. 2015. Cutting edge: circulating plasmablasts induce the differentiation of human T follicular helper cells via IL-6 production. *J Immunol,* 194**,** 2482-5.

CHELLAPPA, S., HUGENSCHMIDT, H., HAGNESS, M., SUBRAMANI, S., MELUM, E., LINE, P. D., LABORI, K. J., WIEDSWANG, G., TASKÉN, K. & AANDAHL, E. M. 2017. CD8+ T Cells That Coexpress RORγt and T-bet Are Functionally Impaired and Expand in Patients with Distal Bile Duct Cancer. *J Immunol,* 198**,** 1729-1739.

CHEN, B. J., ZHAO, J. W., ZHANG, D. H., ZHENG, A. H. & WU, G. Q. 2022. Immunotherapy of Cancer by Targeting Regulatory T cells. *Int Immunopharmacol,* 104**,** 108469.

CHEN, J., YAO, Y., GONG, C., YU, F., SU, S., CHEN, J., LIU, B., DENG, H., WANG, F., LIN, L., YAO, H., SU, F., ANDERSON, K. S., LIU, Q., EWEN, M. E., YAO, X. & SONG, E. 2011. CCL18 from tumor-associated macrophages promotes breast cancer metastasis via PITPNM3. *Cancer Cell,* 19**,** 541-55.

CHEN, Q., MO, L., CAI, X., WEI, L., XIE, Z., LI, H., LI, J. & HU, Z. 2018. ICOS signal facilitates Foxp3 transcription to favor suppressive function of regulatory T cells. *Int J Med Sci,* 15**,** 666-673.

CHEN, X., BÄUMEL, M., MÄNNEL, D. N., HOWARD, O. Z. & OPPENHEIM, J. J. 2007. Interaction of TNF with TNF receptor type 2 promotes expansion and function of mouse CD4+ CD25+ T regulatory cells. *The Journal of Immunology,* 179**,** 154-161.

CHENG, L., ALBERS, P., BERNEY, D. M., FELDMAN, D. R., DAUGAARD, G., GILLIGAN, T. & LOOIJENGA, L. H. J. 2018. Testicular cancer. *Nat Rev Dis Primers,* 4**,** 29.

CHEVALIER, N., JARROSSAY, D., HO, E., AVERY, D. T., MA, C. S., YU, D., SALLUSTO, F., TANGYE, S. G. & MACKAY, C. R. 2011. CXCR5 expressing human central memory CD4 T cells and their relevance for humoral immune responses. *J Immunol,* 186**,** 5556-68.

CHOI, J. & CROTTY, S. 2021a. Bcl6-Mediated Transcriptional Regulation of Follicular Helper T cells (T(FH)). *Trends Immunol,* 42**,** 336-349.

CHOI, J. & CROTTY, S. 2021b. Bcl6-mediated transcriptional regulation of follicular helper T cells (TFH). *Trends in immunology,* 42**,** 336-349.

CHOI, J., DIAO, H., FALITI, C. E., TRUONG, J., ROSSI, M., BÉLANGER, S., YU, B., GOLDRATH, A. W., PIPKIN, M. E. & CROTTY, S. 2020. Bcl-6 is the nexus transcription factor of T follicular helper cells via repressor-of-repressor circuits. *Nat Immunol,* 21**,** 777-789.

CHOI, Y. S., ETO, D., YANG, J. A., LAO, C. & CROTTY, S. 2013. Cutting edge: STAT1 is required for IL-6-mediated Bcl6 induction for early follicular helper cell differentiation. *J Immunol,* 190**,** 3049-53.

CHOI, Y. S., GULLICKSRUD, J. A., XING, S., ZENG, Z., SHAN, Q., LI, F., LOVE, P. E., PENG, W., XUE, H. H. & CROTTY, S. 2015. LEF-1 and TCF-1 orchestrate T(FH) differentiation by regulating differentiation circuits upstream of the transcriptional repressor Bcl6. *Nat Immunol,* 16**,** 980-90.

CHRAA, D., NAIM, A., OLIVE, D. & BADOU, A. 2019. T lymphocyte subsets in cancer immunity: Friends or foes. *J Leukoc Biol,* 105**,** 243-255.

CHTANOVA, T., TANGYE, S. G., NEWTON, R., FRANK, N., HODGE, M. R., ROLPH, M. S. & MACKAY, C. R. 2004. T follicular helper cells express a distinctive transcriptional profile, reflecting their role as non-Th1/Th2 effector cells that provide help for B cells. *J Immunol,* 173**,** 68-78.

CHUNG, Y., TANAKA, S., CHU, F., NURIEVA, R. I., MARTINEZ, G. J., RAWAL, S., WANG, Y. H., LIM, H., REYNOLDS, J. M., ZHOU, X. H., FAN, H. M., LIU, Z. M., NEELAPU, S. S. & DONG, C. 2011. Follicular regulatory T cells expressing Foxp3 and Bcl-6 suppress germinal center reactions. *Nat Med,* 17**,** 983-8.

CINIER, J., HUBERT, M., BESSON, L., DI ROIO, A., RODRIGUEZ, C., LOMBARDI, V., CAUX, C. & MÉNÉTRIER-CAUX, C. 2021. Recruitment and Expansion of Tregs Cells in the Tumor Environment-How to Target Them? *Cancers (Basel),* 13.

COLAMATTEO, A., CARBONE, F., BRUZZANITI, S., GALGANI, M., FUSCO, C., MANISCALCO, G. T., DI RELLA, F., DE CANDIA, P. & DE ROSA, V. 2019. Molecular Mechanisms Controlling Foxp3 Expression in Health and Autoimmunity: From Epigenetic to Post-translational Regulation. *Front Immunol,* 10**,** 3136.

COOMBES, J. L., SIDDIQUI, K. R., ARANCIBIA-CÁRCAMO, C. V., HALL, J., SUN, C. M., BELKAID, Y. & POWRIE, F. 2007. A functionally specialized population of mucosal CD103+ DCs induces Foxp3+ regulatory T cells via a TGF-beta and retinoic acid-dependent mechanism. *J Exp Med,* 204**,** 1757-64.

CORGNAC, S., MALENICA, I., MEZQUITA, L., AUCLIN, E., VOILIN, E., KACHER, J., HALSE, H., GRYNSZPAN, L., SIGNOLLE, N., DAYRIS, T., LECLERC, M., DROIN, N., DE MONTPRÉVILLE, V., MERCIER, O., VALIDIRE, P., SCOAZEC, J. Y., MASSARD, C.,

CHOUAIB, S., PLANCHARD, D., ADAM, J., BESSE, B. & MAMI-CHOUAIB, F. 2020. CD103(+)CD8(+) T(RM) Cells Accumulate in Tumors of Anti-PD-1-Responder Lung Cancer Patients and Are Tumor-Reactive Lymphocytes Enriched with Tc17. *Cell Rep Med,* 1**,** 100127.

CREMONESI, E., GOVERNA, V., GARZON, J. F. G., MELE, V., AMICARELLA, F., MURARO, M. G., TRELLA, E., GALATI-FOURNIER, V., OERTLI, D., DÄSTER, S. R., DROESER, R. A., WEIXLER, B., BOLLI, M., ROSSO, R., NITSCHE, U., KHANNA, N., EGLI, A., KECK, S., SLOTTA-HUSPENINA, J., TERRACCIANO, L. M., ZAJAC, P., SPAGNOLI, G. C., EPPENBERGER-CASTORI, S., JANSSEN, K. P., BORSIG, L. & IEZZI, G. 2018. Gut microbiota modulate T cell trafficking into human colorectal cancer. *Gut,* 67**,** 1984-1994.

CROTTY, S. 2014. T follicular helper cell differentiation, function, and roles in disease. *Immunity,* 41**,** 529-42.

CROTTY, S. 2015. A brief history of T cell help to B cells. *Nat Rev Immunol,* 15**,** 185-9.

CROTTY, S. 2019. T follicular helper cell biology: a decade of discovery and diseases. *Immunity,* 50**,** 1132-1148.

CROTTY, S., KERSH, E. N., CANNONS, J., SCHWARTZBERG, P. L. & AHMED, R. 2003. SAP is required for generating long-term humoral immunity. *Nature,* 421**,** 282-287.

CUCAK, H., YRLID, U., REIZIS, B., KALINKE, U. & JOHANSSON-LINDBOM, B. 2009. Type I interferon signaling in dendritic cells stimulates the development of lymph-node-resident T follicular helper cells. *Immunity,* 31**,** 491-501.

CURIEL, T. J., COUKOS, G., ZOU, L., ALVAREZ, X., CHENG, P., MOTTRAM, P., EVDEMON-HOGAN, M., CONEJO-GARCIA, J. R., ZHANG, L., BUROW, M., ZHU, Y., WEI, S., KRYCZEK, I., DANIEL, B., GORDON, A., MYERS, L., LACKNER, A., DISIS, M. L., KNUTSON, K. L., CHEN, L. & ZOU, W. 2004. Specific recruitment of regulatory T cells in ovarian carcinoma fosters immune privilege and predicts reduced survival. *Nat Med,* 10**,** 942-9.

CURTI, B. D., KOVACSOVICS-BANKOWSKI, M., MORRIS, N., WALKER, E., CHISHOLM, L., FLOYD, K., WALKER, J., GONZALEZ, I., MEEUWSEN, T., FOX, B. A., MOUDGIL, T., MILLER, W., HALEY, D., COFFEY, T., FISHER, B., DELANTY-MILLER, L., RYMARCHYK, N., KELLY, T., CROCENZI, T., BERNSTEIN, E., SANBORN, R., URBA, W. J. & WEINBERG, A. D. 2013. OX40 is a potent immune-stimulating target in late-stage cancer patients. *Cancer Res,* 73**,** 7189-7198.

DAL SECCO, V., RICCIOLI, A., PADULA, F., ZIPARO, E. & FILIPPINI, A. 2008. Mouse Sertoli cells display phenotypical and functional traits of antigen-presenting cells in response to interferon gamma. *Biology of reproduction,* 78**,** 234-242.

DANNULL, J., SU, Z., RIZZIERI, D., YANG, B. K., COLEMAN, D., YANCEY, D., ZHANG, A., DAHM, P., CHAO, N., GILBOA, E. & VIEWEG, J. 2005. Enhancement of vaccine-mediated antitumor immunity in cancer patients after depletion of regulatory T cells. *J Clin Invest,* 115**,** 3623-33.

DE ROSE, R., FERNANDEZ, C. S., HEDGER, M. P., KENT, S. J. & WINNALL, W. R. 2013. Characterisation of macaque testicular leucocyte populations and T-lymphocyte immunity. *Journal of Reproductive Immunology,* 100**,** 146-156.

DE SIMONE, M., ARRIGONI, A., ROSSETTI, G., GRUARIN, P., RANZANI, V., POLITANO, C., BONNAL, R. J. P., PROVASI, E., SARNICOLA, M. L., PANZERI, I., MORO, M., CROSTI, M., MAZZARA, S., VAIRA, V., BOSARI, S., PALLESCHI, A., SANTAMBROGIO, L., BOVO, G., ZUCCHINI, N., TOTIS, M., GIANOTTI, L., CESANA, G., PEREGO, R. A., MARONI, N., PISANI CERETTI, A., OPOCHER, E., DE FRANCESCO, R., GEGINAT, J., STUNNENBERG, H. G., ABRIGNANI, S. & PAGANI, M. 2016. Transcriptional Landscape of Human Tissue Lymphocytes Unveils Uniqueness of Tumor-Infiltrating T Regulatory Cells. *Immunity,* 45**,** 1135-1147.

DE TONI, L., ŠABOVIC, I., COSCI, I., GHEZZI, M., FORESTA, C. & GAROLLA, A. 2019. Testicular cancer: Genes, environment, hormones. *Frontiers in endocrinology,* 10**,** 408.

DE VRIES, G., ROSAS-PLAZA, X., VAN VUGT, M., GIETEMA, J. A. & DE JONG, S. 2020. Testicular cancer: Determinants of cisplatin sensitivity and novel therapeutic opportunities. *Cancer Treat Rev,* 88**,** 102054.

DEAGLIO, S., DWYER, K. M., GAO, W., FRIEDMAN, D., USHEVA, A., ERAT, A., CHEN, J. F., ENJYOJI, K., LINDEN, J., OUKKA, M., KUCHROO, V. K., STROM, T. B. & ROBSON, S. C. 2007. Adenosine generation catalyzed by CD39 and CD73 expressed on regulatory T cells mediates immune suppression. *J Exp Med,* 204**,** 1257-65.

DEFALCO, T., BHATTACHARYA, I., WILLIAMS, A. V., SAMS, D. M. & CAPEL, B. 2014. Yolk-sac-derived macrophages regulate fetal testis vascularization and morphogenesis. *Proc Natl Acad Sci U S A,* 111**,** E2384-93.

DEFALCO, T., POTTER, S. J., WILLIAMS, A. V., WALLER, B., KAN, M. J. & CAPEL, B. 2015. Macrophages Contribute to the Spermatogonial Niche in the Adult Testis. *Cell Rep,* 12**,** 1107-19.

DEL RISCO KOLLERUD, R., RUUD, E., HAUGNES, H. S., CANNON-ALBRIGHT, L. A., THORESEN, M., NAFSTAD, P., VLATKOVIC, L., BLAASAAS, K. G., NÆSS, Ø. & CLAUSSEN, B. 2019. Family history of cancer and risk of paediatric and young adult's testicular cancer: A Norwegian cohort study. *Br J Cancer,* 120**,** 1007-1014.

DELACHER, M., IMBUSCH, C. D., HOTZ-WAGENBLATT, A., MALLM, J. P., BAUER, K., SIMON, M., RIEGEL, D., RENDEIRO, A. F., BITTNER, S., SANDERINK, L., PANT, A., SCHMIDLEITHNER, L., BRABAND, K. L., ECHTENACHTER, B., FISCHER, A., GIUNCHIGLIA, V., HOFFMANN, P., EDINGER, M., BOCK, C., REHLI, M., BRORS, B., SCHMIDL, C. & FEUERER, M. 2020. Precursors for Nonlymphoid-Tissue Treg Cells Reside in Secondary Lymphoid Organs and Are Programmed by the Transcription Factor BATF. *Immunity,* 52**,** 295-312.e11.

DING, P., ZHU, R., CAI, B., ZHANG, J., BU, Q. & SUN, D. W. 2019a. IL-9-producing CD8(+) T cells represent a distinctive subset with different transcriptional characteristics from conventional CD8(+) T cells, and partially infiltrate breast tumors. *Int J Biochem Cell Biol,* 115**,** 105576.

DING, Z. Y., LI, R., ZHANG, Q. J., WANG, Y., JIANG, Y., MENG, Q. Y., XI, Q. L. & WU, G. H. 2019b. Prognostic role of cyclin D2/D3 in multiple human malignant neoplasms: A systematic review and meta-analysis. *Cancer medicine,* 8**,** 2717-2729.

DISIS, M. L. 2010. Immune regulation of cancer. *J Clin Oncol,* 28**,** 4531-8.

DITORO, D., WINSTEAD, C. J., PHAM, D., WITTE, S., ANDARGACHEW, R., SINGER, J. R., WILSON, C. G., ZINDL, C. L., LUTHER, R. J., SILBERGER, D. J., WEAVER, B. T., KOLAWOLE, E. M., MARTINEZ, R. J., TURNER, H., HATTON, R. D., MOON, J. J., WAY, S. S., EVAVOLD, B. D. & WEAVER, C. T. 2018. Differential IL-2 expression defines developmental fates of follicular versus nonfollicular helper T cells. *Science,* 361.

DOBRZANSKI, M. J. 2013. Expanding roles for CD4 T cells and their subpopulations in tumor immunity and therapy. *Front Oncol,* 3**,** 63.

DOBRZANSKI, M. J., REOME, J. B. & DUTTON, R. W. 2000. Type 1 and type 2 CD8+ effector T cell subpopulations promote long-term tumor immunity and protection to progressively growing tumor. *J Immunol,* 164**,** 916-25.

DOI, T., MURO, K., ISHII, H., KATO, T., TSUSHIMA, T., TAKENOYAMA, M., OIZUMI, S., GEMMOTO, K., SUNA, H., ENOKITANI, K., KAWAKAMI, T., NISHIKAWA, H. & YAMAMOTO, N. 2019. A Phase I Study of the Anti-CC Chemokine Receptor 4 Antibody, Mogamulizumab, in Combination with Nivolumab in Patients with Advanced or Metastatic Solid Tumors. *Clin Cancer Res,* 25**,** 6614-6622.

DONNER, J., KLIESCH, S., BREHM, R. & BERGMANN, M. 2004. From carcinoma in situ to testicular germ cell tumour. *Apmis,* 112**,** 79-88.

DUAN, Y. G., YU, C. F., NOVAK, N., BIEBER, T., ZHU, C. H., SCHUPPE, H. C., HAIDL, G. & ALLAM, J. P. 2011. Immunodeviation towards a Th17 immune response associated with testicular damage in azoospermic men. *Int J Androl,* 34**,** e536-45.

DUHEN, T., GEIGER, R., JARROSSAY, D., LANZAVECCHIA, A. & SALLUSTO, F. 2009. Production of interleukin 22 but not interleukin 17 by a subset of human skin-homing memory T cells. *Nat Immunol,* 10**,** 857-63.

EHI, K., ISHIGAMI, S., MASAMOTO, I., UENOSONO, Y., NATSUGOE, S., ARIGAMI, T., ARIMA, H., KIJIMA, Y., YOSHINAKA, H., YANAGITA, S., KOZONO, T., FUNASAKO, Y., MARUYAMA, I. & AIKOU, T. 2008. Analysis of T-helper type 1 and 2 cells and T-cytotoxic type 1 and 2 cells of sentinel lymph nodes in breast cancer. *Oncol Rep,* 19**,** 601-7.

EKSTEEN, B., MILES, A., CURBISHLEY, S. M., TSELEPIS, C., GRANT, A. J., WALKER, L. S. & ADAMS, D. H. 2006. Epithelial inflammation is associated with CCL28 production and the recruitment of regulatory T cells expressing CCR10. *J Immunol,* 177**,** 593-603.

EL-DEMIRY, M. I., HARGREAVE, T. B., BUSUTTIL, A., ELTON, R., JAMES, K. & CHISHOLM, G. D. 1987. Immunocompetent cells in human testis in health and disease. *Fertil Steril,* 48**,** 470-9.

ELLER, K., WOLF, D., HUBER, J. M., METZ, M., MAYER, G., MCKENZIE, A. N., MAURER, M., ROSENKRANZ, A. R. & WOLF, A. M. 2011. IL-9 production by regulatory T cells recruits mast cells that are essential for regulatory T cell-induced immune suppression. *The Journal of Immunology,* 186**,** 83-91.

ELLYARD, J. I., SIMSON, L. & PARISH, C. R. 2007. Th2-mediated anti-tumour immunity: friend or foe? *Tissue Antigens,* 70**,** 1-11.

ERSCHING, J., EFEYAN, A., MESIN, L., JACOBSEN, J. T., PASQUAL, G., GRABINER, B. C., DOMINGUEZ-SOLA, D., SABATINI, D. M. & VICTORA, G. D. 2017. Germinal Center Selection and Affinity Maturation Require Dynamic Regulation of mTORC1 Kinase. *Immunity,* 46**,** 1045-1058.e6.

ETO, D., LAO, C., DITORO, D., BARNETT, B., ESCOBAR, T. C., KAGEYAMA, R., YUSUF, I. & CROTTY, S. 2011. IL-21 and IL-6 are critical for different aspects of B cell immunity and redundantly induce optimal follicular helper CD4 T cell (Tfh) differentiation. *PLoS One,* 6**,** e17739.

FACCIABENE, A., PENG, X., HAGEMANN, I. S., BALINT, K., BARCHETTI, A., WANG, L. P., GIMOTTY, P. A., GILKS, C. B., LAL, P., ZHANG, L. & COUKOS, G. 2011. Tumour hypoxia promotes tolerance and angiogenesis via CCL28 and T(reg) cells. *Nature,* 475**,** 226-30.

FAGHIH, Z., REZAEIFARD, S., SAFAEI, A., GHADERI, A. & ERFANI, N. 2013. IL-17 and IL-4 producing CD8+ T cells in tumor draining lymph nodes of breast cancer patients: positive association with tumor progression. *Iran J Immunol,* 10**,** 193-204.

FEHERVARI, Z. 2017. Testicular macrophage origin. *Nature Immunology,* 18**,** 1067-1067.

FERGUSON, L. & AGOULNIK, A. I. 2013. Testicular cancer and cryptorchidism. *Frontiers in endocrinology,* 4**,** 32.

FERLIN, A., PENGO, M., PIZZOL, D., CARRARO, U., FRIGO, A. C. & FORESTA, C. 2012. Variants in KITLG predispose to testicular germ cell cancer independently from spermatogenic function. *Endocrine-related cancer,* 19**,** 101-108.

FIETZ, D. & KLIESCH, S. 2022. Biopsie und Histologie des Hodens. *Andrologie: Grundlagen und Klinik der reproduktiven Gesundheit des Mannes.* Springer.

FIETZ, D., SCHUPPE, H.-C. & LOVELAND, K. L. 2022. Immunobiology of Testicular Cancer. Springer.

FIJAK, M., BHUSHAN, S. & MEINHARDT, A. 2017. The immune privilege of the testis. *Immune infertility.* Springer.

FIJAK, M., DAMM, L. J., WENZEL, J. P., ASLANI, F., WALECKI, M., WAHLE, E., EISEL, F., BHUSHAN, S., HACKSTEIN, H. & BAAL, N. 2015. Influence of testosterone on inflammatory response in testicular cells and expression of transcription factor Foxp3 in T cells. *American journal of reproductive immunology,* 74**,** 12-25.

FIJAK, M., PILATZ, A., HEDGER, M. P., NICOLAS, N., BHUSHAN, S., MICHEL, V., TUNG, K. S. K., SCHUPPE, H. C. & MEINHARDT, A. 2018. Infectious, inflammatory and 'autoimmune' male factor infertility: how do rodent models inform clinical practice? *Hum Reprod Update,* 24**,** 416-441.

FONSEKA, P., PATHAN, M., CHITTI, S. V., KANG, T. & MATHIVANAN, S. 2021. FunRich enables enrichment analysis of OMICs datasets. *J Mol Biol,* 433**,** 166747.
FONTENOT, J. D., GAVIN, M. A. & RUDENSKY, A. Y. 2003. Foxp3 programs the development and function of CD4+CD25+ regulatory T cells. *Nat Immunol,* 4**,** 330-6.
FOSS, F. 2006. Clinical experience with denileukin diftitox (ONTAK). *Semin Oncol,* 33**,** S11-6.
FRIDMAN, W. H., PAGÈS, F., SAUTÈS-FRIDMAN, C. & GALON, J. 2012. The immune contexture in human tumours: impact on clinical outcome. *Nat Rev Cancer,* 12**,** 298-306.
FUJIMURA, T., KAMBAYASHI, Y., FUJISAWA, Y., HIDAKA, T. & AIBA, S. 2018. Tumor-Associated Macrophages: Therapeutic Targets for Skin Cancer. *Front Oncol,* 8**,** 3.
GABRILOVICH, D. I. 2017. Myeloid-Derived Suppressor Cells. *Cancer Immunol Res,* 5**,** 3-8.
GADDAM, S. J. & CHESNUT, G. T. 2022. Testicle Cancer. *StatPearls.* Treasure Island (FL): StatPearls Publishing

GALAN, J., DE FELICI, M., BUCH, B., RIVERO, M., SEGURA, A., ROYO, J., CRUZ, N., REAL, L. & RUIZ, A. 2006. Association of genetic markers within the KIT and KITLG genes with human male infertility. *Human Reproduction,* 21**,** 3185-3192.
GALGANI, M., BRUZZANITI, S., LA ROCCA, C., MICILLO, T., DE CANDIA, P., BIFULCO, M. & MATARESE, G. 2021. Immunometabolism of regulatory T cells in cancer. *Mol Aspects Med,* 77**,** 100936.
GALLUZZI, L., BUQUÉ, A., KEPP, O., ZITVOGEL, L. & KROEMER, G. 2015. Immunological Effects of Conventional Chemotherapy and Targeted Anticancer Agents. *Cancer Cell,* 28**,** 690-714.
GAO, J., AKSOY, B. A., DOGRUSOZ, U., DRESDNER, G., GROSS, B., SUMER, S. O., SUN, Y., JACOBSEN, A., SINHA, R., LARSSON, E., CERAMI, E., SANDER, C. & SCHULTZ, N. 2013. Integrative analysis of complex cancer genomics and clinical profiles using the cBioPortal. *Sci Signal,* 6**,** pl1.
GAO, J., WANG, X., WANG, Y., HAN, F., CAI, W., ZHAO, B., LI, Y., HAN, S., WU, X. & HU, D. 2016. Murine Sertoli cells promote the development of tolerogenic dendritic cells: a pivotal role of galectin-1. *Immunology,* 148**,** 253-65.
GARAUD, S., ZAYAKIN, P., BUISSERET, L., RULLE, U., SILINA, K., DE WIND, A., VAN DEN EYDEN, G., LARSIMONT, D., WILLARD-GALLO, K. & LINĒ, A. 2018. Antigen Specificity and Clinical Significance of IgG and IgA Autoantibodies Produced in situ by Tumor-Infiltrating B Cells in Breast Cancer. *Front Immunol,* 9**,** 2660.
GARZA, K. M., AGERSBORG, S. S., BAKER, E. & TUNG, K. S. 2000. Persistence of physiological self antigen is required for the regulation of self tolerance. *The Journal of Immunology,* 164**,** 3982-3989.
GEVA, R., VOSKOBOYNIK, M., DOBRENKOV, K., MAYAWALA, K., GWO, J., WNEK, R., CHARTASH, E. & LONG, G. V. 2020. First-in-human phase 1 study of MK-1248, an anti–glucocorticoid-induced tumor necrosis factor receptor agonist monoclonal antibody, as monotherapy or with pembrolizumab in patients with advanced solid tumors. *Cancer,* 126**,** 4926-4935.
GHAZARIAN, A. A., TRABERT, B., DEVESA, S. S. & MCGLYNN, K. A. 2015. Recent trends in the incidence of testicular germ cell tumors in the United States. *Andrology,* 3**,** 13-18.
GHIRINGHELLI, F., PUIG, P. E., ROUX, S., PARCELLIER, A., SCHMITT, E., SOLARY, E., KROEMER, G., MARTIN, F., CHAUFFERT, B. & ZITVOGEL, L. 2005. Tumor cells convert immature myeloid dendritic cells into TGF-beta-secreting cells inducing CD4+CD25+ regulatory T cell proliferation. *J Exp Med,* 202**,** 919-29.
GIANCHECCHI, E. & FIERABRACCI, A. 2018. Inhibitory receptors and pathways of lymphocytes: the role of PD-1 in Treg development and their involvement in autoimmunity onset and cancer progression. *Frontiers in immunology,* 9**,** 2374.

GIANNATEMPO, P., GRECO, T., MARIANI, L., NICOLAI, N., TANA, S., FARÈ, E., RAGGI, D., PIVA, L., CATANZARO, M. & BIASONI, D. 2015. Radiotherapy or chemotherapy for clinical stage IIA and IIB seminoma: a systematic review and meta-analysis of patient outcomes. *Annals of Oncology,* 26**,** 657-668.

GILLIGAN, T., LIN, D. W., AGGARWAL, R., CHISM, D., COST, N., DERWEESH, I. H., EMAMEKHOO, H., FELDMAN, D. R., GEYNISMAN, D. M. & HANCOCK, S. L. 2019. Testicular cancer, version 2.2020, NCCN clinical practice guidelines in oncology. *Journal of the National Comprehensive Cancer Network,* 17**,** 1529-1554.

GITLIN, A. D., SHULMAN, Z. & NUSSENZWEIG, M. C. 2014. Clonal selection in the germinal centre by regulated proliferation and hypermutation. *Nature,* 509**,** 637-40.

GOBERT, M., TREILLEUX, I., BENDRISS-VERMARE, N., BACHELOT, T., GODDARD-LEON, S., ARFI, V., BIOTA, C., DOFFIN, A. C., DURAND, I., OLIVE, D., PEREZ, S., PASQUAL, N., FAURE, C., RAY-COQUARD, I., PUISIEUX, A., CAUX, C., BLAY, J. Y. & MÉNÉTRIER-CAUX, C. 2009. Regulatory T cells recruited through CCL22/CCR4 are selectively activated in lymphoid infiltrates surrounding primary breast tumors and lead to an adverse clinical outcome. *Cancer Res,* 69**,** 2000-9.

GOLUBOVSKAYA, V. & WU, L. 2016. Different subsets of T cells, memory, effector functions, and CAR-T immunotherapy. *Cancers,* 8**,** 36.

GONG, F., QIAN, C., ZHU, H., ZHU, J., PAN, Y., DONG, Q. & JIANG, D. 2016. Circulating follicular T-helper cell subset distribution in patients with asthma. *Allergy Asthma Proc,* 37**,** 154-161.

GONG, J., ZENG, Q., YU, D. & DUAN, Y. G. 2020. T Lymphocytes and Testicular Immunity: A New Insight into Immune Regulation in Testes. *Int J Mol Sci,* 22.

GRISWOLD, M. D. 1998. The central role of Sertoli cells in spermatogenesis. *Semin Cell Dev Biol,* 9**,** 411-6.

GROHMANN, U., ORABONA, C., FALLARINO, F., VACCA, C., CALCINARO, F., FALORNI, A., CANDELORO, P., BELLADONNA, M. L., BIANCHI, R., FIORETTI, M. C. & PUCCETTI, P. 2002. CTLA-4-Ig regulates tryptophan catabolism in vivo. *Nat Immunol,* 3**,** 1097-101.

GROSSMAN, W. J., VERBSKY, J. W., BARCHET, W., COLONNA, M., ATKINSON, J. P. & LEY, T. J. 2004. Human T regulatory cells can use the perforin pathway to cause autologous target cell death. *Immunity,* 21**,** 589-601.

GU-TRANTIEN, C., LOI, S., GARAUD, S., EQUETER, C., LIBIN, M., DE WIND, A., RAVOET, M., LE BUANEC, H., SIBILLE, C., MANFOUO-FOUTSOP, G., VEYS, I., HAIBE-KAINS, B., SINGHAL, S. K., MICHIELS, S., ROTHÉ, F., SALGADO, R., DUVILLIER, H., IGNATIADIS, M., DESMEDT, C., BRON, D., LARSIMONT, D., PICCART, M., SOTIRIOU, C. & WILLARD-GALLO, K. 2013. $CD4^+$ follicular helper T cell infiltration predicts breast cancer survival. *J Clin Invest,* 123**,** 2873-92.

GU-TRANTIEN, C., MIGLIORI, E., BUISSERET, L., DE WIND, A., BROHÉE, S., GARAUD, S., NOËL, G., DANG CHI, V. L., LODEWYCKX, J. N., NAVEAUX, C., DUVILLIER, H., GORIELY, S., LARSIMONT, D. & WILLARD-GALLO, K. 2017. CXCL13-producing TFH cells link immune suppression and adaptive memory in human breast cancer. *JCI Insight,* 2.

GUAZZONE, V. A., HOLLWEGS, S., MARDIROSIAN, M., JACOBO, P., HACKSTEIN, H., WYGRECKA, M., SCHNEIDER, E., MEINHARDT, A., LUSTIG, L. & FIJAK, M. 2011. Characterization of dendritic cells in testicular draining lymph nodes in a rat model of experimental autoimmune orchitis. *Int J Androl,* 34**,** 276-89.

GUO, J., GROW, E. J., MLCOCHOVA, H., MAHER, G. J., LINDSKOG, C., NIE, X., GUO, Y., TAKEI, Y., YUN, J., CAI, L., KIM, R., CARRELL, D. T., GORIELY, A., HOTALING, J. M. & CAIRNS, B. R. 2018. The adult human testis transcriptional cell atlas. *Cell Research,* 28**,** 1141-1157.

GURNEY, J. K., FLORIO, A. A., ZNAOR, A., FERLAY, J., LAVERSANNE, M., SARFATI, D., BRAY, F. & MCGLYNN, K. A. 2019. International Trends in the Incidence of Testicular Cancer: Lessons from 35 Years and 41 Countries. *European urology,* 76**,** 615-623.

HACIOGLU, B. M., KODAZ, H., ERDOGAN, B., CINKAYA, A., TASTEKIN, E., HACIBEKIROGLU, I., TURKMEN, E., KOSTEK, O., GENC, E. & UZUNOGLU, S. 2017. K-RAS and N-RAS mutations in testicular germ cell tumors. *Bosnian Journal of Basic Medical Sciences,* 17**,** 159.

HADRUP, S. R., BRAENDSTRUP, O., JACOBSEN, G. K., MORTENSEN, S., PEDERSEN, L., SEREMET, T., ANDERSEN, M. H., BECKER, J. C. & STRATEN, P. T. 2006. Tumor infiltrating lymphocytes in seminoma lesions comprise clonally expanded cytotoxic T cells. *Int J Cancer,* 119**,** 831-8.

HALES, D. B. 2002. Testicular macrophage modulation of Leydig cell steroidogenesis. *J Reprod Immunol,* 57**,** 3-18.

HAMID, O., THOMPSON, J. A., DIAB, A., ROS, W., ESKENS, F., BERMINGHAM, C., KONTO, C., LONG, H., LIAO, K. & GANGULY, B. J. 2016. First in human (FIH) study of an OX40 agonist monoclonal antibody (mAb) PF-04518600 (PF-8600) in adult patients (pts) with select advanced solid tumors: Preliminary safety and pharmacokinetic (PK)/pharmacodynamic results. American Society of Clinical Oncology.

HAN, Y., LIU, D. & LI, L. 2020. PD-1/PD-L1 pathway: current researches in cancer. American journal of cancer research, 10, 727.

HANNA, N. & EINHORN, L. H. 2014. Testicular cancer: a reflection on 50 years of discovery. *Journal of Clinical Oncology,* 32**,** 3085-3092.

HANSON, A., ELPEK, K., DUONG, E., SHALLBERG, L., FAN, M., JOHNSON, C., WALLACE, M., MABRY, G. R., SAZINSKY, S. & PEPPER, L. 2020. ICOS agonism by JTX-2011 (vopratelimab) requires initial T cell priming and Fc cross-linking for optimal T cell activation and anti-tumor immunity in preclinical models. *Plos one,* 15**,** e0239595.

HATZI, K., JIANG, Y., HUANG, C., GARRETT-BAKELMAN, F., GEARHART, M. D., GIANNOPOULOU, E. G., ZUMBO, P., KIROUAC, K., BHASKARA, S., POLO, J. M., KORMAKSSON, M., MACKERELL, A. D., JR., XUE, F., MASON, C. E., HIEBERT, S. W., PRIVE, G. G., CERCHIETTI, L., BARDWELL, V. J., ELEMENTO, O. & MELNICK, A. 2013. A hybrid mechanism of action for BCL6 in B cells defined by formation of functionally distinct complexes at enhancers and promoters. *Cell Rep,* 4**,** 578-88.

HATZI, K., NANCE, J. P., KROENKE, M. A., BOTHWELL, M., HADDAD, E. K., MELNICK, A. & CROTTY, S. 2015. BCL6 orchestrates Tfh cell differentiation via multiple distinct mechanisms. *J Exp Med,* 212**,** 539-53.

HAVENAR-DAUGHTON, C., LINDQVIST, M., HEIT, A., WU, J. E., REISS, S. M., KENDRIC, K., BÉLANGER, S., KASTURI, S. P., LANDAIS, E., AKONDY, R. S., MCGUIRE, H. M., BOTHWELL, M., VAGEFI, P. A., SCULLY, E., TOMARAS, G. D., DAVIS, M. M., POIGNARD, P., AHMED, R., WALKER, B. D., PULENDRAN, B., MCELRATH, M. J., KAUFMANN, D. E. & CROTTY, S. 2016. CXCL13 is a plasma biomarker of germinal center activity. *Proc Natl Acad Sci U S A,* 113**,** 2702-7.

HAYNES, N. M., ALLEN, C. D., LESLEY, R., ANSEL, K. M., KILLEEN, N. & CYSTER, J. G. 2007. Role of CXCR5 and CCR7 in follicular Th cell positioning and appearance of a programmed cell death gene-1high germinal center-associated subpopulation. *J Immunol,* 179**,** 5099-108.

HE, D., LI, H., YUSUF, N., ELMETS, C. A., LI, J., MOUNTZ, J. D. & XU, H. 2010. IL-17 promotes tumor development through the induction of tumor promoting microenvironments at tumor sites and myeloid-derived suppressor cells. *J Immunol,* 184**,** 2281-8.

HEAD, J. R., NEAVES, W. B. & BILLINGHAM, R. E. 1983. Immune privilege in the testis. I. Basic parameters of allograft survival. *Transplantation,* 36**,** 423-31.

HEDGER, M. P. 2011. Immunophysiology and pathology of inflammation in the testis and epididymis. *J Androl,* 32**,** 625-40.

HEDGER, M. P. 2015. The immunophysiology of male reproduction. *Knobil and Neill's physiology of reproduction***,** 805.

HEDGER, M. P., NIKOLIC-PATERSON, D. J., HUTCHINSON, P., ATKINS, R. C. & DE KRETSER, D. M. 1998. Immunoregulatory activity in adult rat testicular interstitial fluid: roles of interleukin-1 and transforming growth factor beta. *Biol Reprod,* 58**,** 927-34.

HEESTERS, B. A., CHATTERJEE, P., KIM, Y. A., GONZALEZ, S. F., KULIGOWSKI, M. P., KIRCHHAUSEN, T. & CARROLL, M. C. 2013. Endocytosis and recycling of immune complexes by follicular dendritic cells enhances B cell antigen binding and activation. *Immunity,* 38**,** 1164-75.

HEESTERS, B. A., VAN DER POEL, C. E., DAS, A. & CARROLL, M. C. 2016. Antigen Presentation to B Cells. *Trends Immunol,* 37**,** 844-854.

HEMMINKI, K. & CHEN, B. 2006. Familial risks in testicular cancer as aetiological clues. *Int J Androl,* 29**,** 205-10.

HILVERING, B., HINKS, T. S. C., STÖGER, L., MARCHI, E., SALIMI, M., SHRIMANKER, R., LIU, W., CHEN, W., LUO, J., GO, S., POWELL, T., CANE, J., THULBORN, S., KURIOKA, A., LENG, T., MATTHEWS, J., CONNOLLY, C., BORG, C., BAFADHEL, M., WILLBERG, C. B., RAMASAMY, A., DJUKANOVIĆ, R., OGG, G., PAVORD, I. D., KLENERMAN, P. & XUE, L. 2018. Synergistic activation of pro-inflammatory type-2 CD8(+) T lymphocytes by lipid mediators in severe eosinophilic asthma. *Mucosal Immunol,* 11**,** 1408-1419.

HINRICHS, C. S., KAISER, A., PAULOS, C. M., CASSARD, L., SANCHEZ-PEREZ, L., HEEMSKERK, B., WRZESINSKI, C., BORMAN, Z. A., MURANSKI, P. & RESTIFO, N. P. 2009. Type 17 CD8+ T cells display enhanced antitumor immunity. *Blood,* 114**,** 596-9.

HIRST, C. E., BUZZA, M. S., SUTTON, V. R., TRAPANI, J. A., LOVELAND, K. L. & BIRD, P. I. 2001. Perforin-independent expression of granzyme B and proteinase inhibitor 9 in human testis and placenta suggests a role for granzyme B-mediated proteolysis in reproduction. *Mol Hum Reprod,* 7**,** 1133-42.

HO, W., NASRAH, N. & JOHNSON, D. 2019. Phase I/II dose escalation and expansion study of FLX475 alone and in combination with pembrolizumab in advanced cancer. American Society of Clinical Oncology.

HOLLISTER, K., KUSAM, S., WU, H., CLEGG, N., MONDAL, A., SAWANT, D. V. & DENT, A. L. 2013. Insights into the role of Bcl6 in follicular Th cells using a new conditional mutant mouse model. *J Immunol,* 191**,** 3705-11.

HONG, S., ZHANG, Z., LIU, H., TIAN, M., ZHU, X., ZHANG, Z., WANG, W., ZHOU, X., ZHANG, F., GE, Q., ZHU, B., TANG, H., HUA, Z. & HOU, B. 2018. B Cells Are the Dominant Antigen-Presenting Cells that Activate Naive CD4(+) T Cells upon Immunization with a Virus-Derived Nanoparticle Antigen. *Immunity,* 49**,** 695-708.e4.

HORI, S., NOMURA, T. & SAKAGUCHI, S. 2003. Control of regulatory T cell development by the transcription factor Foxp3. *Science,* 299**,** 1057-61.

HORVATH, A. J., IRVING, J. A., ROSSJOHN, J., LAW, R. H., BOTTOMLEY, S. P., QUINSEY, N. S., PIKE, R. N., COUGHLIN, P. B. & WHISSTOCK, J. C. 2005. The murine orthologue of human antichymotrypsin: a structural paradigm for clade A3 serpins. *Journal of Biological Chemistry,* 280**,** 43168-43178.

HSU, A. T., LUPANCU, T. J., LEE, M. C., FLEETWOOD, A. J., COOK, A. D., HAMILTON, J. A. & ACHUTHAN, A. 2018. Epigenetic and transcriptional regulation of IL4-induced CCL17 production in human monocytes and murine macrophages. *J Biol Chem,* 293**,** 11415-11423.

HUANG, J., CHAN, S. C., TIN, M. S., LIU, X., LOK, V. T., NGAI, C. H., ZHANG, L., LUCERO-PRISNO, D. E., 3RD, XU, W., ZHENG, Z. J., CHIU, P. K., NG, A. C., ENIKEEV, D., NICOL, D., SPIESS, P. E., LAGUNA, P., TEOH, J. Y. & WONG, M. C. S. 2022. Worldwide Distribution, Risk Factors, and Temporal Trends of Testicular Cancer Incidence and Mortality: A Global Analysis. *Eur Urol Oncol,* 5**,** 566-576.

HUANG, R., GRISHAGIN, I., WANG, Y., ZHAO, T., GREENE, J., OBENAUER, J. C., NGAN, D., NGUYEN, D.-T., GUHA, R. & JADHAV, A. 2019a. The NCATS BioPlanet–an integrated platform for exploring the universe of cellular signaling pathways for toxicology, systems biology, and chemical genomics. *Frontiers in pharmacology***,** 445.

HUANG, Y. H., CHANG, C. Y., KUO, Y. Z., FANG, W. Y., KAO, H. Y., TSAI, S. T. & WU, L. W. 2019b. Cancer-associated fibroblast-derived interleukin-1β activates protumor C-C motif chemokine ligand 22 signaling in head and neck cancer. *Cancer Sci,* 110**,** 2783-2793.

HUBER, M., HEINK, S., GROTHE, H., GURALNIK, A., REINHARD, K., ELFLEIN, K., HÜNIG, T., MITTRÜCKER, H. W., BRÜSTLE, A., KAMRADT, T. & LOHOFF, M. 2009. A Th17-like developmental process leads to CD8(+) Tc17 cells with reduced cytotoxic activity. *Eur J Immunol,* 39**,** 1716-25.

HUI, E., CHEUNG, J., ZHU, J., SU, X., TAYLOR, M. J., WALLWEBER, H. A., SASMAL, D. K., HUANG, J., KIM, J. M. & MELLMAN, I. 2017. T cell costimulatory receptor CD28 is a primary target for PD-1–mediated inhibition. *Science,* 355**,** 1428-1433.

HURTENBACH, U. & SHEARER, G. 1982. Germ cell-induced immune suppression in mice. Effect of inoculation of syngeneic spermatozoa on cell-mediated immune responses. *The Journal of experimental medicine,* 155**,** 1719-1729.

HUSSEIN, M. R., ABOU-DEIF, E. S., BEDAIWY, M. A., SAID, T. M., MUSTAFA, M. G., NADA, E., EZAT, A. & AGARWAL, A. 2005. Phenotypic characterization of the immune and mast cell infiltrates in the human testis shows normal and abnormal spermatogenesis. *Fertility and sterility,* 83**,** 1447-1453.

HVARNESS, T., NIELSEN, J. E., ALMSTRUP, K., SKAKKEBAEK, N. E., RAJPERT-DE MEYTS, E. & CLAESSON, M. H. 2013. Phenotypic characterisation of immune cell infiltrates in testicular germ cell neoplasia. *J Reprod Immunol,* 100**,** 135-45.

IELLEM, A., MARIANI, M., LANG, R., RECALDE, H., PANINA-BORDIGNON, P., SINIGAGLIA, F. & D'AMBROSIO, D. 2001. Unique chemotactic response profile and specific expression of chemokine receptors CCR4 and CCR8 by CD4(+)CD25(+) regulatory T cells. *J Exp Med,* 194**,** 847-53.

IMAI, T., NAGIRA, M., TAKAGI, S., KAKIZAKI, M., NISHIMURA, M., WANG, J., GRAY, P. W., MATSUSHIMA, K. & YOSHIE, O. 1999. Selective recruitment of CCR4-bearing Th2 cells toward antigen-presenting cells by the CC chemokines thymus and activation-regulated chemokine and macrophage-derived chemokine. *Int Immunol,* 11**,** 81-8.

ISE, W., FUJII, K., SHIROGUCHI, K., ITO, A., KOMETANI, K., TAKEDA, K., KAWAKAMI, E., YAMASHITA, K., SUZUKI, K., OKADA, T. & KUROSAKI, T. 2018. T Follicular Helper Cell-Germinal Center B Cell Interaction Strength Regulates Entry into Plasma Cell or Recycling Germinal Center Cell Fate. *Immunity,* 48**,** 702-715.e4.

ITO, N., SUZUKI, Y., TANIGUCHI, Y., ISHIGURO, K., NAKAMURA, H. & OHGI, S. 2005. Prognostic significance of T helper 1 and 2 and T cytotoxic 1 and 2 cells in patients with non-small cell lung cancer. *Anticancer Res,* 25**,** 2027-31.

JABEEN, R. & KAPLAN, M. H. 2012. The symphony of the ninth: the development and function of Th9 cells. *Curr Opin Immunol,* 24**,** 303-7.

JACKSON, J. J., KETCHAM, J. M., YOUNAI, A., ABRAHAM, B., BIANNIC, B., BECK, H. P., BUI, M. H. T., CHIAN, D., CUTLER, G., DIOKNO, R., HU, D. X., JACOBSON, S., KARBARZ, E., KASSNER, P. D., MARSHALL, L., MCKINNELL, J., MELEZA, C., OKAL, A., POOKOT, D., REILLY, M. K., ROBLES, O., SHUNATONA, H. P., TALAY, O., WALKER, J. R., WADSWORTH, A., WUSTROW, D. J. & ZIBINSKY, M. 2019. Discovery of a Potent and Selective CCR4 Antagonist That Inhibits T(reg) Trafficking into the Tumor Microenvironment. *J Med Chem,* 62**,** 6190-6213.

JACOBO, P., GUAZZONE, V. A., JARAZO-DIETRICH, S., THEAS, M. S. & LUSTIG, L. 2009. Differential changes in CD4+ and CD8+ effector and regulatory T lymphocyte subsets in the testis of rats undergoing autoimmune orchitis. *Journal of reproductive immunology,* 81**,** 44-54.

JACOBO, P., GUAZZONE, V. A., PÉREZ, C. V. & LUSTIG, L. 2015. CD 4+ F oxp3+ R egulatory T Cells in Autoimmune O rchitis: Phenotypic and Functional Characterization. *American Journal of Reproductive Immunology,* 73**,** 109-125.

JACOBO, P., PÉREZ, C. V., THEAS, M. S., GUAZZONE, V. A. & LUSTIG, L. 2011. CD4+ and CD8+ T cells producing Th1 and Th17 cytokines are involved in the pathogenesis of autoimmune orchitis. *Reproduction,* 141**,** 249-58.

JACOBS, J. F., PUNT, C. J., LESTERHUIS, W. J., SUTMULLER, R. P., BROUWER, H. M., SCHARENBORG, N. M., KLASEN, I. S., HILBRANDS, L. B., FIGDOR, C. G., DE VRIES, I. J. & ADEMA, G. J. 2010. Dendritic cell vaccination in combination with anti-CD25 monoclonal antibody treatment: a phase I/II study in metastatic melanoma patients. *Clin Cancer Res,* 16**,** 5067-78.

JAHNUKAINEN, K., JØRGENSENN, PÖLLÄNEN, P., GIWERCMAN, A. & SKAKKEBAEK, N. E. 1995. Incidence of testicular mononuclear cell infiltrates in normal human males and in patients with germ cell neoplasia. *Int J Androl,* 18**,** 313-20.

JENSEN, S. M., MASTON, L. D., GOUGH, M. J., RUBY, C. E., REDMOND, W. L., CRITTENDEN, M., LI, Y., PURI, S., POEHLEIN, C. H., MORRIS, N., KOVACSOVICS-BANKOWSKI, M., MOUDGIL, T., TWITTY, C., WALKER, E. B., HU, H. M., URBA, W. J., WEINBERG, A. D., CURTI, B. & FOX, B. A. 2010. Signaling through OX40 enhances antitumor immunity. *Semin Oncol,* 37**,** 524-32.

JIA, Y., KODUMUDI, K. N., RAMAMOORTHI, G., BASU, A., SNYDER, C., WIENER, D., PILON-THOMAS, S., GROVER, P., ZHANG, H., GREENE, M. I., MO, Q., TONG, Z., CHEN, Y. Z., COSTA, R. L. B., HAN, H., LEE, C., SOLIMAN, H., CONEJO-GARCIA, J. R., KOSKI, G. & CZERNIECKI, B. J. 2021. Th1 cytokine interferon gamma improves response in HER2 breast cancer by modulating the ubiquitin proteasomal pathway. *Mol Ther,* 29**,** 1541-1556.

JIANG, T., ZHOU, C. & REN, S. 2016. Role of IL-2 in cancer immunotherapy. Oncoimmunology, 5, e1163462.

JOGDAND, G. M., MOHANTY, S. & DEVADAS, S. 2016. Regulators of Tfh Cell Differentiation. *Front Immunol,* 7**,** 520.

JOHNSTON, R. J., CHOI, Y. S., DIAMOND, J. A., YANG, J. A. & CROTTY, S. 2012. STAT5 is a potent negative regulator of TFH cell differentiation. *J Exp Med,* 209**,** 243-50.

JOHNSTON, R. J., POHOLEK, A. C., DITORO, D., YUSUF, I., ETO, D., BARNETT, B., DENT, A. L., CRAFT, J. & CROTTY, S. 2009. Bcl6 and Blimp-1 are reciprocal and antagonistic regulators of T follicular helper cell differentiation. *Science,* 325**,** 1006-10.

JØRGENSEN, A., JOHANSEN, M. L., JUUL, A., SKAKKEBAEK, N. E., MAIN, K. M. & RAJPERT-DE MEYTS, E. Pathogenesis of germ cell neoplasia in testicular dysgenesis and disorders of sex development. Seminars in cell & developmental biology, 2015. Elsevier, 124-137.

KALAVSKA, K., KUCEROVA, L., SCHMIDTOVA, S., CHOVANEC, M. & MEGO, M. 2020. Cancer stem cell niche and immune-active tumor microenvironment in testicular germ cell tumors. *Tumor Microenvironments in Organs***,** 111-121.

KALAVSKA, K., SESTAKOVA, Z., MLCAKOVA, A., KOZICS, K., GRONESOVA, P., HURBANOVA, L., MISKOVSKA, V., REJLEKOVA, K., SVETLOVSKA, D., SYCOVA-MILA, Z., OBERTOVA, J., PALACKA, P., MARDIAK, J., CHOVANEC, M., CHOVANEC, M. & MEGO, M. 2021. Are Changes in the Percentage of Specific Leukocyte Subpopulations Associated with Endogenous DNA Damage Levels in Testicular Cancer Patients? *Int J Mol Sci,* 22.

KAMPHORST, A. O., WIELAND, A., NASTI, T., YANG, S., ZHANG, R., BARBER, D. L., KONIECZNY, B. T., DAUGHERTY, C. Z., KOENIG, L. & YU, K. 2017. Rescue of exhausted CD8 T cells by PD-1–targeted therapies is CD28-dependent. *Science,* 355**,** 1423-1427.

KANEHISA, M., FURUMICHI, M., TANABE, M., SATO, Y. & MORISHIMA, K. 2017. KEGG: new perspectives on genomes, pathways, diseases and drugs. *Nucleic Acids Res,* 45**,** D353-d361.

KARNOWSKI, A., CHEVRIER, S., BELZ, G. T., MOUNT, A., EMSLIE, D., D'COSTA, K., TARLINTON, D. M., KALLIES, A. & CORCORAN, L. M. 2012. B and T cells collaborate in antiviral responses via IL-6, IL-21, and transcriptional activator and coactivator, Oct2 and OBF-1. *J Exp Med,* 209**,** 2049-64.

KAUR, G., MITAL, P. & DUFOUR, J. 2013. Testisimmune privilege-Assumptions versus facts. *Animal reproduction/Colegio Brasileiro de Reproducao Animal,* 10**,** 3.

KAUR, G., THOMPSON, L. A. & DUFOUR, J. M. Sertoli cells–immunological sentinels of spermatogenesis. Seminars in cell & developmental biology, 2014. Elsevier, 36-44.
KAUR, G., WRIGHT, K., VERMA, S., HAYNES, A. & DUFOUR, J. M. 2021. The Good, the Bad and the Ugly of Testicular Immune Regulation: A Delicate Balance Between Immune Function and Immune Privilege. *Adv Exp Med Biol,* 1288**,** 21-47.
KEKÄLÄINEN, E., TUOVINEN, H., JOENSUU, J., GYLLING, M., FRANSSILA, R., PÖNTYNEN, N., TALVENSAARI, K., PERHEENTUPA, J., MIETTINEN, A. & ARSTILA, T. P. 2007. A defect of regulatory T cells in patients with autoimmune polyendocrinopathy-candidiasis-ectodermal dystrophy. *The Journal of Immunology,* 178**,** 1208-1215.
KEMP, R. A. & RONCHESE, F. 2001. Tumor-specific Tc1, but not Tc2, cells deliver protective antitumor immunity. *J Immunol,* 167**,** 6497-502.
KENNEDY, R. & CELIS, E. 2008. Multiple roles for CD4+ T cells in anti-tumor immune responses. *Immunological reviews,* 222**,** 129-144.
KERDILES, Y. M., BEISNER, D. R., TINOCO, R., DEJEAN, A. S., CASTRILLON, D. H., DEPINHO, R. A. & HEDRICK, S. M. 2009. Foxo1 links homing and survival of naive T cells by regulating L-selectin, CCR7 and interleukin 7 receptor. *Nature immunology,* 10**,** 176-184.
KERFOOT, S. M., YAARI, G., PATEL, J. R., JOHNSON, K. L., GONZALEZ, D. G., KLEINSTEIN, S. H. & HABERMAN, A. M. 2011. Germinal center B cell and T follicular helper cell development initiates in the interfollicular zone. *Immunity,* 34**,** 947-60.
KIDANI, Y., NOGAMI, W., YASUMIZU, Y., KAWASHIMA, A., TANAKA, A., SONODA, Y., TONA, Y., NASHIKI, K., MATSUMOTO, R., HAGIWARA, M., OSAKI, M., DOHI, K., KANAZAWA, T., UEYAMA, A., YOSHIKAWA, M., YOSHIDA, T., MATSUMOTO, M., HOJO, K., SHINONOME, S., YOSHIDA, H., HIRATA, M., HARUNA, M., NAKAMURA, Y., MOTOOKA, D., OKUZAKI, D., SUGIYAMA, Y., KINOSHITA, M., OKUNO, T., KATO, T., HATANO, K., UEMURA, M., IMAMURA, R., YOKOI, K., TANEMURA, A., SHINTANI, Y., KIMURA, T., NONOMURA, N., WADA, H., MORI, M., DOKI, Y., OHKURA, N. & SAKAGUCHI, S. 2022. CCR8-targeted specific depletion of clonally expanded Treg cells in tumor tissues evokes potent tumor immunity with long-lasting memory. *Proc Natl Acad Sci U S A,* 119.
KIM, C. H., LIM, H. W., KIM, J. R., ROTT, L., HILLSAMER, P. & BUTCHER, E. C. 2004. Unique gene expression program of human germinal center T helper cells. *Blood,* 104**,** 1952-60.
KIM, H. J. & CANTOR, H. 2014. CD4 T-cell subsets and tumor immunity: the helpful and the not-so-helpful. *Cancer Immunol Res,* 2**,** 91-8.
KIM, J. M., RASMUSSEN, J. P. & RUDENSKY, A. Y. 2007. Regulatory T cells prevent catastrophic autoimmunity throughout the lifespan of mice. *Nat Immunol,* 8**,** 191-7.
KLEIN, B., HAGGENEY, T., FIETZ, D., INDUMATHY, S., LOVELAND, K. L., HEDGER, M., KLIESCH, S., WEIDNER, W., BERGMANN, M. & SCHUPPE, H. C. 2016. Specific immune cell and cytokine characteristics of human testicular germ cell neoplasia. *Hum Reprod,* 31**,** 2192-202.
KLEIN, B., SCHUPPE, H. C., BERGMANN, M., HEDGER, M., LOVELAND, B. & LOVELAND, K. 2017. An in vitro model demonstrates the potential of neoplastic human germ cells to influence the tumour microenvironment. *Andrology,* 5**,** 763-770.
KNEE, D. A., HEWES, B. & BROGDON, J. L. 2016. Rationale for anti-GITR cancer immunotherapy. *European journal of cancer,* 67**,** 1-10.
KNUTSON, K. L. & DISIS, M. L. 2005. Tumor antigen-specific T helper cells in cancer immunity and immunotherapy. *Cancer Immunol Immunother,* 54**,** 721-8.
KOBAYASHI, S., MURATA, K., SHIBUYA, H., MORITA, M., ISHIKAWA, M., FURU, M., ITO, H., ITO, J., MATSUDA, S., WATANABE, T. & YOSHITOMI, H. 2013. A distinct human CD4+ T cell subset that secretes CXCL13 in rheumatoid synovium. *Arthritis Rheum,* 65**,** 3063-72.

KOCH, M. A., TUCKER-HEARD, G., PERDUE, N. R., KILLEBREW, J. R., URDAHL, K. B. & CAMPBELL, D. J. 2009. The transcription factor T-bet controls regulatory T cell homeostasis and function during type 1 inflammation. *Nat Immunol,* 10**,** 595-602.

KONDO, T., TAKATA, H. & TAKIGUCHI, M. 2007. Functional expression of chemokine receptor CCR6 on human effector memory CD8+ T cells. *Eur J Immunol,* 37**,** 54-65.

KRÄUTLER, N. J., SUAN, D., BUTT, D., BOURNE, K., HERMES, J. R., CHAN, T. D., SUNDLING, C., KAPLAN, W., SCHOFIELD, P., JACKSON, J., BASTEN, A., CHRIST, D. & BRINK, R. 2017. Differentiation of germinal center B cells into plasma cells is initiated by high-affinity antigen and completed by Tfh cells. *J Exp Med,* 214**,** 1259-1267.

KREYDIN, E. I., BARRISFORD, G. W., FELDMAN, A. S. & PRESTON, M. A. 2013. Testicular cancer: what the radiologist needs to know. *American Journal of Roentgenology,* 200**,** 1215-1225.

KROENKE, M. A., ETO, D., LOCCI, M., CHO, M., DAVIDSON, T., HADDAD, E. K. & CROTTY, S. 2012. Bcl6 and Maf cooperate to instruct human follicular helper CD4 T cell differentiation. *J Immunol,* 188**,** 3734-44.

KRYSTEL-WHITTEMORE, M., DILEEPAN, K. N. & WOOD, J. G. 2016. Mast cell: a multi-functional master cell. *Frontiers in immunology***,** 620.

KUANG, D. M., PENG, C., ZHAO, Q., WU, Y., ZHU, L. Y., WANG, J., YIN, X. Y., LI, L. & ZHENG, L. 2010. Tumor-activated monocytes promote expansion of IL-17-producing CD8+ T cells in hepatocellular carcinoma patients. *J Immunol,* 185**,** 1544-9.

KUEHN, H. S., OUYANG, W., LO, B., DEENICK, E. K., NIEMELA, J. E., AVERY, D. T., SCHICKEL, J. N., TRAN, D. Q., STODDARD, J., ZHANG, Y., FRUCHT, D. M., DUMITRIU, B., SCHEINBERG, P., FOLIO, L. R., FREIN, C. A., PRICE, S., KOH, C., HELLER, T., SEROOGY, C. M., HUTTENLOCHER, A., RAO, V. K., SU, H. C., KLEINER, D., NOTARANGELO, L. D., RAMPERTAAP, Y., OLIVIER, K. N., MCELWEE, J., HUGHES, J., PITTALUGA, S., OLIVEIRA, J. B., MEFFRE, E., FLEISHER, T. A., HOLLAND, S. M., LENARDO, M. J., TANGYE, S. G. & UZEL, G. 2014. Immune dysregulation in human subjects with heterozygous germline mutations in CTLA4. *Science,* 345**,** 1623-1627.

KUROSE, K., OHUE, Y., WADA, H., IIDA, S., ISHIDA, T., KOJIMA, T., DOI, T., SUZUKI, S., ISOBE, M., FUNAKOSHI, T., KAKIMI, K., NISHIKAWA, H., UDONO, H., OKA, M., UEDA, R. & NAKAYAMA, E. 2015. Phase Ia Study of FoxP3+ CD4 Treg Depletion by Infusion of a Humanized Anti-CCR4 Antibody, KW-0761, in Cancer Patients. *Clin Cancer Res,* 21**,** 4327-36.

KURTULUS, S., SAKUISHI, K., NGIOW, S. F., JOLLER, N., TAN, D. J., TENG, M. W., SMYTH, M. J., KUCHROO, V. K. & ANDERSON, A. C. 2015. TIGIT predominantly regulates the immune response via regulatory T cells. *J Clin Invest,* 125**,** 4053-62.

KUSAM, S., TONEY, L. M., SATO, H. & DENT, A. L. 2003. Inhibition of Th2 differentiation and GATA-3 expression by BCL-6. *J Immunol,* 170**,** 2435-41.

LAGES, C. S., LEWKOWICH, I., SPROLES, A., WILLS-KARP, M. & CHOUGNET, C. 2010. Partial restoration of T-cell function in aged mice by in vitro blockade of the PD-1/PD-L1 pathway. *Aging cell,* 9**,** 785-798.

LAGUNA, M., ALBERS, P., ALGABA, F., BROKEMEYER, C., BOORMANS, J., DI NARDO, D., FISCHER, S., FIZAZI, K., GREMMELS, H., LEAO, R., NICOL, D., NICOLAI, N., OLDERBURG, J., TANDSTAD, T., MAYOR DE CASTRO, J., FANKHAUSER, C., JANISCH, F., MUILWIJK, T., JAIN, Y., SHEPHERD, R. 2022. EAU Guidelines on testicular cancer. In: EAU Guidelines Office (ed) EAU Guidelines. Arnhem, The Netherlands, pp 1–66

LATOUR, S., RONCAGALLI, R., CHEN, R., BAKINOWSKI, M., SHI, X., SCHWARTZBERG, P. L., DAVIDSON, D. & VEILLETTE, A. 2003. Binding of SAP SH2 domain to FynT SH3 domain reveals a novel mechanism of receptor signalling in immune regulation. *Nature cell biology,* 5**,** 149-154.

LECAVALIER-BARSOUM, M., CHAUDARY, N., HAN, K., KORITZINSKY, M., HILL, R. & MILOSEVIC, M. 2018. Targeting the CXCL12/CXCR4 pathway and myeloid cells to

improve radiation treatment of locally advanced cervical cancer. *Int J Cancer,* 143**,** 1017-1028.
LEE, A. Y. S. & KÖRNER, H. 2019. The CCR6-CCL20 axis in humoral immunity and T-B cell immunobiology. *Immunobiology,* 224**,** 449-454.
LEE, J., LOZANO-RUIZ, B., YANG, F. M., FAN, D. D., SHEN, L. & GONZÁLEZ-NAVAJAS, J. M. 2021. The Multifaceted Role of Th1, Th9, and Th17 Cells in Immune Checkpoint Inhibition Therapy. *Front Immunol,* 12**,** 625667.
LEE, J. Y., SKON, C. N., LEE, Y. J., OH, S., TAYLOR, J. J., MALHOTRA, D., JENKINS, M. K., ROSENFELD, M. G., HOGQUIST, K. A. & JAMESON, S. C. 2015. The transcription factor KLF2 restrains $CD4^+$ T follicular helper cell differentiation. *Immunity,* 42**,** 252-264.
LEE, M. H., TUNG-CHIEH CHANG, J., LIAO, C. T., CHEN, Y. S., KUO, M. L. & SHEN, C. R. 2018. Interleukin 17 and peripheral IL-17-expressing T cells are negatively correlated with the overall survival of head and neck cancer patients. *Oncotarget,* 9**,** 9825-9837.
LEE, S. K., RIGBY, R. J., ZOTOS, D., TSAI, L. M., KAWAMOTO, S., MARSHALL, J. L., RAMISCAL, R. R., CHAN, T. D., GATTO, D., BRINK, R., YU, D., FAGARASAN, S., TARLINTON, D. M., CUNNINGHAM, A. F. & VINUESA, C. G. 2011. B cell priming for extrafollicular antibody responses requires Bcl-6 expression by T cells. *J Exp Med,* 208**,** 1377-88.
LEÓN, B., BRADLEY, J. E., LUND, F. E., RANDALL, T. D. & BALLESTEROS-TATO, A. 2014. FoxP3+ regulatory T cells promote influenza-specific Tfh responses by controlling IL-2 availability. *Nat Commun,* 5**,** 3495.
LESLIE, S. W., SAJJAD, H. & VILLANUEVA, C. A. 2022. Cryptorchidism. *StatPearls.* Treasure Island (FL): StatPearls Publishing

LEVINE, A. G., ARVEY, A., JIN, W. & RUDENSKY, A. Y. 2014. Continuous requirement for the TCR in regulatory T cell function. *Nature immunology,* 15**,** 1070-1078.
LI, C., JIANG, P., WEI, S., XU, X. & WANG, J. 2020. Regulatory T cells in tumor microenvironment: new mechanisms, potential therapeutic strategies and future prospects. *Mol Cancer,* 19**,** 116.
LI, D.-Y. & XIONG, X.-Z. 2020a. ICOS+ tregs: A functional subset of tregs in immune diseases. *Frontiers in immunology,* 11**,** 2104.
LI, D. Y. & XIONG, X. Z. 2020b. ICOS(+) Tregs: A Functional Subset of Tregs in Immune Diseases. *Front Immunol,* 11**,** 2104.
LI, H., VAN DER LEUN, A. M., YOFE, I., LUBLING, Y., GELBARD-SOLODKIN, D., VAN AKKOOI, A. C. J., VAN DEN BRABER, M., ROZEMAN, E. A., HAANEN, J., BLANK, C. U., HORLINGS, H. M., DAVID, E., BARAN, Y., BERCOVICH, A., LIFSHITZ, A., SCHUMACHER, T. N., TANAY, A. & AMIT, I. 2019. Dysfunctional CD8 T Cells Form a Proliferative, Dynamically Regulated Compartment within Human Melanoma. *Cell,* 176**,** 775-789.e18.
LI, J., CHEN, S., XIAO, X., ZHAO, Y., DING, W. & LI, X. C. 2017. IL-9 and Th9 cells in health and diseases-From tolerance to immunopathology. *Cytokine Growth Factor Rev,* 37**,** 47-55.
LIANG, Y., PAN, H. F. & YE, D. Q. 2015. IL-17A-producing CD8(+)T cells as therapeutic targets in autoimmunity. *Expert Opin Ther Targets,* 19**,** 651-61.
LIAO, Y., WANG, J., JAEHNIG, E. J., SHI, Z. & ZHANG, B. 2019. WebGestalt 2019: gene set analysis toolkit with revamped UIs and APIs. *Nucleic Acids Res,* 47**,** W199-w205.
LIM, H. W., LEE, J., HILLSAMER, P. & KIM, C. H. 2008. Human Th17 cells share major trafficking receptors with both polarized effector T cells and FOXP3+ regulatory T cells. *J Immunol,* 180**,** 122-9.
LIN, X., YE, L., WANG, X., LIAO, Z., DONG, J., YANG, Y., ZHANG, R., LI, H., LI, P., DING, L., LI, T., ZHANG, W., XU, S., HAN, X., XU, H., WANG, W., GAO, H., YU, X. & LIU, L. 2021. Follicular Helper T Cells Remodel the Immune Microenvironment of Pancreatic Cancer via Secreting CXCL13 and IL-21. *Cancers (Basel),* 13.

LINTERMAN, M. A., DENTON, A. E., DIVEKAR, D. P., ZVETKOVA, I., KANE, L., FERREIRA, C., VELDHOEN, M., CLARE, S., DOUGAN, G., ESPÉLI, M. & SMITH, K. G. 2014. CD28 expression is required after T cell priming for helper T cell responses and protective immunity to infection. *Elife,* 3.

LINTERMAN, M. A., PIERSON, W., LEE, S. K., KALLIES, A., KAWAMOTO, S., RAYNER, T. F., SRIVASTAVA, M., DIVEKAR, D. P., BEATON, L., HOGAN, J. J., FAGARASAN, S., LISTON, A., SMITH, K. G. & VINUESA, C. G. 2011. Foxp3+ follicular regulatory T cells control the germinal center response. *Nat Med,* 17**,** 975-82.

LITCHFIELD, K., LEVY, M., ORLANDO, G., LOVEDAY, C., LAW, P. J., MIGLIORINI, G., HOLROYD, A., BRODERICK, P., KARLSSON, R. & HAUGEN, T. B. 2017. Identification of 19 new risk loci and potential regulatory mechanisms influencing susceptibility to testicular germ cell tumor. *Nature genetics,* 49**,** 1133-1140.

LITCHFIELD, K., THOMSEN, H., MITCHELL, J. S., SUNDQUIST, J., HOULSTON, R. S., HEMMINKI, K. & TURNBULL, C. 2015. Quantifying the heritability of testicular germ cell tumour using both population-based and genomic approaches. *Scientific reports,* 5**,** 1-7.

LITZINGER, M. T., FERNANDO, R., CURIEL, T. J., GROSENBACH, D. W., SCHLOM, J. & PALENA, C. 2007. IL-2 immunotoxin denileukin diftitox reduces regulatory T cells and enhances vaccine-mediated T-cell immunity. *Blood,* 110**,** 3192-201.

LIU, D., XU, H., SHIH, C., WAN, Z., MA, X., MA, W., LUO, D. & QI, H. 2015. T–B-cell entanglement and ICOSL-driven feed-forward regulation of germinal centre reaction. *Nature,* 517**,** 214-218.

LIU, J., ZHANG, N., LI, Q., ZHANG, W., KE, F., LENG, Q., WANG, H., CHEN, J. & WANG, H. 2011. Tumor-associated macrophages recruit CCR6+ regulatory T cells and promote the development of colorectal cancer via enhancing CCL20 production in mice. *PLoS One,* 6**,** e19495.

LIU, S. J., TSAI, J. P., SHEN, C. R., SHER, Y. P., HSIEH, C. L., YEH, Y. C., CHOU, A. H., CHANG, S. R., HSIAO, K. N., YU, F. W. & CHEN, H. W. 2007. Induction of a distinct CD8 Tnc17 subset by transforming growth factor-beta and interleukin-6. *J Leukoc Biol,* 82**,** 354-60.

LIU, X., CHEN, X., ZHONG, B., WANG, A., WANG, X., CHU, F., NURIEVA, R. I., YAN, X., CHEN, P., VAN DER FLIER, L. G., NAKATSUKASA, H., NEELAPU, S. S., CHEN, W., CLEVERS, H., TIAN, Q., QI, H., WEI, L. & DONG, C. 2014. Transcription factor achaete-scute homologue 2 initiates follicular T-helper-cell development. *Nature,* 507**,** 513-8.

LOKKA, E., LINTUKORPI, L., CISNEROS-MONTALVO, S., MÄKELÄ, J. A., TYYSTJÄRVI, S., OJASALO, V., GERKE, H., TOPPARI, J., RANTAKARI, P. & SALMI, M. 2020. Generation, localization and functions of macrophages during the development of testis. *Nat Commun,* 11**,** 4375.

LOVELAND, K. L., KLEIN, B., PUESCHL, D., INDUMATHY, S., BERGMANN, M., LOVELAND, B. E., HEDGER, M. P. & SCHUPPE, H. C. 2017. Cytokines in Male Fertility and Reproductive Pathologies: Immunoregulation and Beyond. *Front Endocrinol (Lausanne),* 8**,** 307.

LOWTHER, D. E., GOODS, B. A., LUCCA, L. E., LERNER, B. A., RADDASSI, K., VAN DIJK, D., HERNANDEZ, A. L., DUAN, X., GUNEL, M. & CORIC, V. 2016. PD-1 marks dysfunctional regulatory T cells in malignant gliomas. *JCI insight,* 1.

LOYHER, P. L., ROCHEFORT, J., BAUDESSON DE CHANVILLE, C., HAMON, P., LESCAILLE, G., BERTOLUS, C., GUILLOT-DELOST, M., KRUMMEL, M. F., LEMOINE, F. M., COMBADIÈRE, C. & BOISSONNAS, A. 2016. CCR2 Influences T Regulatory Cell Migration to Tumors and Serves as a Biomarker of Cyclophosphamide Sensitivity. *Cancer Res,* 76**,** 6483-6494.

LU, L.-F., LIND, E. F., GONDEK, D. C., BENNETT, K. A., GLEESON, M. W., PINO-LAGOS, K., SCOTT, Z. A., COYLE, A. J., REED, J. L. & VAN SNICK, J. 2006. Mast cells are essential intermediaries in regulatory T-cell tolerance. *Nature,* 442**,** 997-1002.

LU, L., KUROISHI, T., TANAKA, Y., FURUKAWA, M., NOCHI, T. & SUGAWARA, S. 2022. Differential expression of CD11c defines two types of tissue-resident macrophages with different origins in steady-state salivary glands. *Scientific reports,* 12**,** 1-14.
LU, Y., HONG, B., LI, H., ZHENG, Y., ZHANG, M., WANG, S., QIAN, J. & YI, Q. 2014. Tumor-specific IL-9-producing CD8+ Tc9 cells are superior effector than type-I cytotoxic Tc1 cells for adoptive immunotherapy of cancers. *Proc Natl Acad Sci U S A,* 111**,** 2265-70.
LU, Y., HONG, S., LI, H., PARK, J., HONG, B., WANG, L., ZHENG, Y., LIU, Z., XU, J., HE, J., YANG, J., QIAN, J. & YI, Q. 2012. Th9 cells promote antitumor immune responses in vivo. *J Clin Invest,* 122**,** 4160-71.
LUCKHEERAM, R. V., ZHOU, R., VERMA, A. D. & XIA, B. 2012. $CD4^+$T cells: differentiation and functions. *Clin Dev Immunol,* 2012**,** 925135.
LÜTHJE, K., KALLIES, A., SHIMOHAKAMADA, Y., BELZ, G. T., LIGHT, A., TARLINTON, D. M. & NUTT, S. L. 2012. The development and fate of follicular helper T cells defined by an IL-21 reporter mouse. *Nat Immunol,* 13**,** 491-8.
LYMPERI, S. & GIWERCMAN, A. 2018. Endocrine disruptors and testicular function. *Metabolism,* 86**,** 79-90.
MA, C.-W., XIU, Z.-L. & ZENG, A.-P. 2012. Discovery of intramolecular signal transduction network based on a new protein dynamics model of energy dissipation. *PLoS One,* 7**,** e31529.
MA, C. S., SURYANI, S., AVERY, D. T., CHAN, A., NANAN, R., SANTNER-NANAN, B., DEENICK, E. K. & TANGYE, S. G. 2009. Early commitment of naïve human CD4(+) T cells to the T follicular helper (T(FH)) cell lineage is induced by IL-12. *Immunol Cell Biol,* 87**,** 590-600.
MA, L., WANG, H., LI, Z., GENG, X. & LI, M. 2019. Chemokine (C-C motif) ligand 18 is highly expressed in glioma tissues and promotes invasion of glioblastoma cells. *J Cancer Res Ther,* 15**,** 358-364.
MA, Y., MATTAROLLO, S. R., ADJEMIAN, S., YANG, H., AYMERIC, L., HANNANI, D., PORTELA CATANI, J. P., DURET, H., TENG, M. W., KEPP, O., WANG, Y., SISTIGU, A., SCHULTZE, J. L., STOLL, G., GALLUZZI, L., ZITVOGEL, L., SMYTH, M. J. & KROEMER, G. 2014. CCL2/CCR2-dependent recruitment of functional antigen-presenting cells into tumors upon chemotherapy. *Cancer Res,* 74**,** 436-45.
MACK, M., CIHAK, J., SIMONIS, C., LUCKOW, B., PROUDFOOT, A. E., PLACHÝ, J., BRÜHL, H., FRINK, M., ANDERS, H. J., VIELHAUER, V., PFIRSTINGER, J., STANGASSINGER, M. & SCHLÖNDORFF, D. 2001. Expression and characterization of the chemokine receptors CCR2 and CCR5 in mice. *J Immunol,* 166**,** 4697-704.
MAHNE, A. E., MAUZE, S., JOYCE-SHAIKH, B., XIA, J., BOWMAN, E. P., BEEBE, A. M., CUA, D. J. & JAIN, R. 2017. Dual roles for regulatory T-cell depletion and costimulatory signaling in agonistic GITR targeting for tumor immunotherapy. *Cancer research,* 77**,** 1108-1118.
MAHNKE, K., SCHÖNFELD, K., FONDEL, S., RING, S., KARAKHANOVA, S., WIEDEMEYER, K., BEDKE, T., JOHNSON, T. S., STORN, V., SCHALLENBERG, S. & ENK, A. H. 2007. Depletion of CD4+CD25+ human regulatory T cells in vivo: kinetics of Treg depletion and alterations in immune functions in vivo and in vitro. *Int J Cancer,* 120**,** 2723-33.
MANTOVANI, A., MARCHESI, F., MALESCI, A., LAGHI, L. & ALLAVENA, P. 2017. Tumour-associated macrophages as treatment targets in oncology. *Nat Rev Clin Oncol,* 14**,** 399-416.
MANZO, A., VITOLO, B., HUMBY, F., CAPORALI, R., JARROSSAY, D., DELL'ACCIO, F., CIARDELLI, L., UGUCCIONI, M., MONTECUCCO, C. & PITZALIS, C. 2008. Mature antigen-experienced T helper cells synthesize and secrete the B cell chemoattractant CXCL13 in the inflammatory environment of the rheumatoid joint. *Arthritis Rheum,* 58**,** 3377-87.
MARSHALL, L. A., MARUBAYASHI, S., JORAPUR, A., JACOBSON, S., ZIBINSKY, M., ROBLES, O., HU, D. X., JACKSON, J. J., POOKOT, D., SANCHEZ, J., BROVARNEY, M., WADSWORTH, A., CHIAN, D., WUSTROW, D., KASSNER, P. D., CUTLER, G.,

WONG, B., BROCKSTEDT, D. G. & TALAY, O. 2020. Tumors establish resistance to immunotherapy by regulating T(reg) recruitment via CCR4. *J Immunother Cancer,* 8.
MARTINEZ-RODRIGUEZ, M., THOMPSON, A. K. & MONTEAGUDO, C. 2017. High CCL27 immunoreactivity in 'supratumoral' epidermis correlates with better prognosis in patients with cutaneous malignant melanoma. *J Clin Pathol,* 70**,** 15-19.
MATEU-JIMENEZ, M., CURULL, V., PIJUAN, L., SÁNCHEZ-FONT, A., RIVERA-RAMOS, H., RODRÍGUEZ-FUSTER, A., AGUILÓ, R., GEA, J. & BARREIRO, E. 2017. Systemic and Tumor Th1 and Th2 Inflammatory Profile and Macrophages in Lung Cancer: Influence of Underlying Chronic Respiratory Disease. *J Thorac Oncol,* 12**,** 235-248.
MAYBERRY, C. L., LOGAN, N. A., WILSON, J. J. & CHANG, C. H. 2022. Providing a Helping Hand: Metabolic Regulation of T Follicular Helper Cells and Their Association With Disease. *Front Immunol,* 13**,** 864949.
MECHLIN, C. & KOGAN, B. 2012. Mast cells, estrogens, and cryptorchidism: a histological based review. *Translational Andrology and Urology,* 1**,** 97.
MEINEKE, V., FRUNGIERI, M. B., JESSBERGER, B., VOGT, H.-J. & MAYERHOFER, A. 2000. Human testicular mast cells contain tryptase: increased mast cell number and altered distribution in the testes of infertile men. *Fertility and sterility,* 74**,** 239-244.
MEINHARDT, A., DEJUCQ-RAINSFORD, N. & BHUSHAN, S. 2022. Testicular macrophages: development and function in health and disease. *Trends in Immunology,* 43**,** 51-62.
MEINHARDT, A., WANG, M., SCHULZ, C. & BHUSHAN, S. 2018. Microenvironmental signals govern the cellular identity of testicular macrophages. *J Leukoc Biol,* 104**,** 757-766.
MELSSEN, M. & SLINGLUFF JR, C. L. 2017. Vaccines targeting helper T cells for cancer immunotherapy. *Current opinion in immunology,* 47**,** 85-92.
MÉNÉTRIER-CAUX, C., FAGET, J., BIOTA, C., GOBERT, M., BLAY, J. Y. & CAUX, C. 2012. Innate immune recognition of breast tumor cells mediates CCL22 secretion favoring Treg recruitment within tumor environment. *Oncoimmunology,* 1**,** 759-761.
METELLI, A., SALEM, M., WALLACE, C. H., WU, B. X., LI, A., LI, X. & LI, Z. 2018. Immunoregulatory functions and the therapeutic implications of GARP-TGF-β in inflammation and cancer. *J Hematol Oncol,* 11**,** 24.
MEZZAPELLE, R., LEO, M., CAPRIOGLIO, F., COLLEY, L. S., LAMARCA, A., SABATINO, L., COLANTUONI, V., CRIPPA, M. P. & BIANCHI, M. E. 2022. CXCR4/CXCL12 Activities in the Tumor Microenvironment and Implications for Tumor Immunotherapy. *Cancers (Basel),* 14.
MI, H. & THOMAS, P. 2009. PANTHER pathway: an ontology-based pathway database coupled with data analysis tools. *Methods Mol Biol,* 563**,** 123-40.
MICHAELI, T., MICHAELI, J. & MICHAELI, D. 2021. Testicular cancer follow-up costs in Germany from 2000 to 2015. *Journal of Cancer Research and Clinical Oncology,* 147**,** 2249-2258.
MIKHAK, Z., FUKUI, M., FARSIDJANI, A., MEDOFF, B. D., TAGER, A. M. & LUSTER, A. D. 2009. Contribution of CCR4 and CCR8 to antigen-specific T(H)2 cell trafficking in allergic pulmonary inflammation. *J Allergy Clin Immunol,* 123**,** 67-73.e3.
MITTRÜCKER, H. W., VISEKRUNA, A. & HUBER, M. 2014. Heterogeneity in the differentiation and function of $CD8^+$ T cells. *Arch Immunol Ther Exp (Warsz),* 62**,** 449-58.
MIZUKAMI, Y., KONO, K., KAWAGUCHI, Y., AKAIKE, H., KAMIMURA, K., SUGAI, H. & FUJII, H. 2008. CCL17 and CCL22 chemokines within tumor microenvironment are related to accumulation of Foxp3+ regulatory T cells in gastric cancer. *Int J Cancer,* 122**,** 2286-93.
MOCH, H., AMIN, M. B., BERNEY, D. M., COMPÉRAT, E. M., GILL, A. J., HARTMANN, A., MENON, S., RASPOLLINI, M. R., RUBIN, M. A. & SRIGLEY, J. R. 2022. The 2022 World Health Organization classification of tumours of the urinary system and male genital organs—part A: renal, penile, and testicular tumours. *European urology*.
MØLLER, H. & SKAKKEBAEK, N. E. 1999. Risk of testicular cancer in subfertile men: case-control study. *Bmj,* 318**,** 559-62.

MORIKAWA, H. & SAKAGUCHI, S. 2014. Genetic and epigenetic basis of Treg cell development and function: from a FoxP3-centered view to an epigenome-defined view of natural Treg cells. *Immunol Rev,* 259**,** 192-205.
MOSSADEGH-KELLER, N., GENTEK, R., GIMENEZ, G., BIGOT, S., MAILFERT, S. & SIEWEKE, M. H. 2017. Developmental origin and maintenance of distinct testicular macrophage populations. *Journal of Experimental Medicine,* 214**,** 2829-2841.
MOSSADEGH-KELLER, N. & SIEWEKE, M. H. 2018. Testicular macrophages: Guardians of fertility. *Cellular immunology,* 330**,** 120-125.
MUCCI, L. A., HJELMBORG, J. B., HARRIS, J. R., CZENE, K., HAVELICK, D. J., SCHEIKE, T., GRAFF, R. E., HOLST, K., MÖLLER, S., UNGER, R. H., MCINTOSH, C., NUTTALL, E., BRANDT, I., PENNEY, K. L., HARTMAN, M., KRAFT, P., PARMIGIANI, G., CHRISTENSEN, K., KOSKENVUO, M., HOLM, N. V., HEIKKILÄ, K., PUKKALA, E., SKYTTHE, A., ADAMI, H. O. & KAPRIO, J. 2016. Familial Risk and Heritability of Cancer Among Twins in Nordic Countries. *Jama,* 315**,** 68-76.
MURAKAMI, J., WU, L., KOHNO, M., CHAN, M.-L., ZHAO, Y., YUN, Z., CHO, B. J. & DE PERROT, M. 2021. Triple-modality therapy maximizes antitumor immune responses in a mouse model of mesothelioma. *Science Translational Medicine,* 13**,** eabd9882.
NAKA, T., NISHIMOTO, N. & KISHIMOTO, T. 2002. The paradigm of IL-6: from basic science to medicine. *Arthritis Research & Therapy,* 4**,** 1-10.
NAKANISHI, K. 2018. Unique action of interleukin-18 on T cells and other immune cells. *Frontiers in immunology,* 9**,** 763.
NAKANOMA, T., NAKAMURA, K., DEGUCHI, N., FUJIMOTO, J., TAZAKI, H. & HATA, J. 1992. Immunohistological analysis of tumour infiltrating lymphocytes in seminoma using monoclonal antibodies. *Virchows Arch A Pathol Anat Histopathol,* 421**,** 409-13.
NANDI, B., PAI, C., HUANG, Q., PRABHALA, R. H., MUNSHI, N. C. & GOLD, J. S. 2014. CCR6, the sole receptor for the chemokine CCL20, promotes spontaneous intestinal tumorigenesis. *PLoS One,* 9**,** e97566.
NESTLER, T., DALVI, P., HAIDL, F., WITTERSHEIM, M., VON BRANDENSTEIN, M., PAFFENHOLZ, P., WAGENER-RYCZEK, S., PFISTER, D., KOITZSCH, U., HELLMICH, M., BUETTNER, R., ODENTHAL, M. & HEIDENREICH, A. 2022. Transcriptome analysis reveals upregulation of immune response pathways at the invasive tumour front of metastatic seminoma germ cell tumours. *British Journal of Cancer,* 126**,** 937-947.
NICU, A.-T., MEDAR, C., CHIFIRIUC, M. C., PIRCALABIORU, G. G. & BURLIBASA, L. 2022. Epigenetics and testicular cancer: bridging the gap between fundamental biology and patient care. *Frontiers in Cell and Developmental Biology,* 10.
NIE, H., ZHENG, Y., LI, R., GUO, T. B., HE, D., FANG, L., LIU, X., XIAO, L., CHEN, X. & WAN, B. 2013. Phosphorylation of FOXP3 controls regulatory T cell function and is inhibited by TNF-α in rheumatoid arthritis. *Nature medicine,* 19**,** 322-328.
NIE, H., ZHENG, Y., LI, R. & ZHANG, J. 2016. Reply to suppressive activity of human regulatory T cells is maintained in the presence of TNF. *Nature medicine,* 22**,** 18-19.
NIEMI, M., SHARPE, R. & BROWN, W. 1986. Macrophages in the interstitial tissue of the rat testis. *Cell and tissue research,* 243**,** 337-344.
NISHIKAWA, H., KATO, T., TAWARA, I., SAITO, K., IKEDA, H., KURIBAYASHI, K., ALLEN, P. M., SCHREIBER, R. D., SAKAGUCHI, S., OLD, L. J. & SHIKU, H. 2005. Definition of target antigens for naturally occurring CD4(+) CD25(+) regulatory T cells. *J Exp Med,* 201**,** 681-6.
NOURI, A. M., HUSSAIN, R. F., OLIVER, R. T., HANDY, A. M., BARTKOVA, I. & BODMER, J. G. 1993. Immunological paradox in testicular tumours: the presence of a large number of activated T-cells despite the complete absence of MHC antigens. *Eur J Cancer,* 29a**,** 1895-9.
NURIEVA, R. I., CHUNG, Y., HWANG, D., YANG, X. O., KANG, H. S., MA, L., WANG, Y.-H., WATOWICH, S. S., JETTEN, A. M. & TIAN, Q. 2008. Generation of T follicular helper cells is mediated by interleukin-21 but independent of T helper 1, 2, or 17 cell lineages. *Immunity,* 29**,** 138-149.

NURIEVA, R. I., CHUNG, Y., MARTINEZ, G. J., YANG, X. O., TANAKA, S., MATSKEVITCH, T. D., WANG, Y. H. & DONG, C. 2009. Bcl6 mediates the development of T follicular helper cells. *Science,* 325**,** 1001-5.

NURIEVA, R. I., PODD, A., CHEN, Y., ALEKSEEV, A. M., YU, M., QI, X., HUANG, H., WEN, R., WANG, J., LI, H. S., WATOWICH, S. S., QI, H., DONG, C. & WANG, D. 2012. STAT5 protein negatively regulates T follicular helper (Tfh) cell generation and function. *J Biol Chem,* 287**,** 11234-9.

O'DONNELL, L., REBOURCET, D., DAGLEY, L. F., SGAIER, R., INFUSINI, G., O'SHAUGHNESSY, P. J., CHALMEL, F., FIETZ, D., WEIDNER, W. & LEGRAND, J. M. 2021. Sperm proteins and cancer-testis antigens are released by the seminiferous tubules in mice and men. *The FASEB Journal,* 35**,** e21397.

OESTREICH, K. J., MOHN, S. E. & WEINMANN, A. S. 2012. Molecular mechanisms that control the expression and activity of Bcl-6 in TH1 cells to regulate flexibility with a TFH-like gene profile. *Nat Immunol,* 13**,** 405-11.

OGBE, A., MIAO, T., SYMONDS, A. L., OMODHO, B., SINGH, R., BHULLAR, P., LI, S. & WANG, P. 2015. Early Growth Response Genes 2 and 3 Regulate the Expression of Bcl6 and Differentiation of T Follicular Helper Cells. *J Biol Chem,* 290**,** 20455-65.

OH, D. Y. & FONG, L. 2021. Cytotoxic CD4+ T cells in cancer: Expanding the immune effector toolbox. *Immunity,* 54**,** 2701-2711.

OHUE, Y. & NISHIKAWA, H. 2019. Regulatory T (Treg) cells in cancer: Can Treg cells be a new therapeutic target? *Cancer Sci,* 110**,** 2080-2089.

OLKHANUD, P. B., DAMDINSUREN, B., BODOGAI, M., GRESS, R. E., SEN, R., WEJKSZA, K., MALCHINKHUU, E., WERSTO, R. P. & BIRAGYN, A. 2011. Tumor-Evoked Regulatory B Cells Promote Breast Cancer Metastasis by Converting Resting CD4+ T Cells to T-Regulatory CellsCancer-Promoting Role of B CellsCancer-Promoting Role of B Cells. *Cancer research,* 71**,** 3505-3515.

ONISHI, Y., FEHERVARI, Z., YAMAGUCHI, T. & SAKAGUCHI, S. 2008. Foxp3+ natural regulatory T cells preferentially form aggregates on dendritic cells in vitro and actively inhibit their maturation. *Proc Natl Acad Sci U S A,* 105**,** 10113-8.

ONIZUKA, S., TAWARA, I., SHIMIZU, J., SAKAGUCHI, S., FUJITA, T. & NAKAYAMA, E. 1999. Tumor rejection by in vivo administration of anti-CD25 (interleukin-2 receptor alpha) monoclonal antibody. *Cancer Res,* 59**,** 3128-33.

OVERACRE-DELGOFFE, A. E., CHIKINA, M., DADEY, R. E., YANO, H., BRUNAZZI, E. A., SHAYAN, G., HORNE, W., MOSKOVITZ, J. M., KOLLS, J. K., SANDER, C., SHUAI, Y., NORMOLLE, D. P., KIRKWOOD, J. M., FERRIS, R. L., DELGOFFE, G. M., BRUNO, T. C., WORKMAN, C. J. & VIGNALI, D. A. A. 2017. Interferon-γ Drives T(reg) Fragility to Promote Anti-tumor Immunity. *Cell,* 169**,** 1130-1141.e11.

PAI, S. Y., TRUITT, M. L. & HO, I. C. 2004. GATA-3 deficiency abrogates the development and maintenance of T helper type 2 cells. *Proc Natl Acad Sci U S A,* 101**,** 1993-8.

PAIJENS, S. T., VLEDDER, A., DE BRUYN, M. & NIJMAN, H. W. 2021. Tumor-infiltrating lymphocytes in the immunotherapy era. *Cell Mol Immunol,* 18**,** 842-859.

PAPA, I., SALIBA, D., PONZONI, M., BUSTAMANTE, S., CANETE, P. F., GONZALEZ-FIGUEROA, P., MCNAMARA, H. A., VALVO, S., GRIMBALDESTON, M., SWEET, R. A., VOHRA, H., COCKBURN, I. A., MEYER-HERMANN, M., DUSTIN, M. L., DOGLIONI, C. & VINUESA, C. G. 2017. T(FH)-derived dopamine accelerates productive synapses in germinal centres. *Nature,* 547**,** 318-323.

PARK, J. S., KIM, J., ELGHIATY, A. & HAM, W. S. 2018. Recent global trends in testicular cancer incidence and mortality. *Medicine,* 97.

PATHAN, M., KEERTHIKUMAR, S., ANG, C.-S., GANGODA, L., QUEK, C. Y. J., WILLIAMSON, N. A., MOURADOV, D., SIEBER, O. M., SIMPSON, R. J., SALIM, A., BACIC, A., HILL, A. F., STROUD, D. A., RYAN, M. T., AGBINYA, J. I., MARIADASON, J. M., BURGESS, A. W. & MATHIVANAN, S. 2015. FunRich: An open access standalone functional enrichment and interaction network analysis tool. *Proteomics,* 15**,** 2597-2601.

PATIL, R. S., SHAH, S. U., SHRIKHANDE, S. V., GOEL, M., DIKSHIT, R. P. & CHIPLUNKAR, S. V. 2016. IL17 producing γδT cells induce angiogenesis and are associated with poor survival in gallbladder cancer patients. *Int J Cancer,* 139**,** 869-81.

PAUL, M. S. & OHASHI, P. S. 2020. The roles of CD8+ T cell subsets in antitumor immunity. *Trends in Cell Biology,* 30**,** 695-704.

PEARCE, E. L., MULLEN, A. C., MARTINS, G. A., KRAWCZYK, C. M., HUTCHINS, A. S., ZEDIAK, V. P., BANICA, M., DICIOCCIO, C. B., GROSS, D. A., MAO, C. A., SHEN, H., CEREB, N., YANG, S. Y., LINDSTEN, T., ROSSANT, J., HUNTER, C. A. & REINER, S. L. 2003. Control of effector CD8+ T cell function by the transcription factor Eomesodermin. *Science,* 302**,** 1041-3.

PEDROS, C., ZHANG, Y., HU, J. K., CHOI, Y. S., CANONIGO-BALANCIO, A. J., YATES, J. R., 3RD, ALTMAN, A., CROTTY, S. & KONG, K. F. 2016. A TRAF-like motif of the inducible costimulator ICOS controls development of germinal center TFH cells via the kinase TBK1. *Nat Immunol,* 17**,** 825-33.

PÉREZ, C. V., THEAS, M. S., JACOBO, P. V., JARAZO-DIETRICH, S., GUAZZONE, V. A. & LUSTIG, L. 2013. Dual role of immune cells in the testis: Protective or pathogenic for germ cells? *Spermatogenesis,* 3**,** e23870.

PICONESE, S., GRI, G., TRIPODO, C., MUSIO, S., GORZANELLI, A., FROSSI, B., PEDOTTI, R., PUCILLO, C. E. & COLOMBO, M. P. 2009. Mast cells counteract regulatory T-cell suppression through interleukin-6 and OX40/OX40L axis toward Th17-cell differentiation. *Blood, The Journal of the American Society of Hematology,* 114**,** 2639-2648.

PISEDDU, I., RÖHRLE, N., KNOTT, M. M. L., MODER, S., EIBER, S., SCHNELL, K., VETTER, V., MEYER, B., LAYRITZ, P., KÜHNEMUTH, B., WIEDEMANN, G. M., GRUEN, J., PERLEBERG, C., RAPP, M., ENDRES, S. & ANZ, D. 2020. Constitutive Expression of CCL22 Is Mediated by T Cell-Derived GM-CSF. *J Immunol,* 205**,** 2056-2065.

PLITAS, G. & RUDENSKY, A. Y. 2016. Regulatory T Cells: Differentiation and Function. *Cancer Immunol Res,* 4**,** 721-5.

PODHORECKA, M., DMOSZYNSKA, A., ROLINSKI, J. & WASIK, E. 2002. T type 1/type 2 subsets balance in B-cell chronic lymphocytic leukemia--the three-color flow cytometry analysis. *Leuk Res,* 26**,** 657-60.

POHOLEK, A. C., HANSEN, K., HERNANDEZ, S. G., ETO, D., CHANDELE, A., WEINSTEIN, J. S., DONG, X., ODEGARD, J. M., KAECH, S. M., DENT, A. L., CROTTY, S. & CRAFT, J. 2010. In vivo regulation of Bcl6 and T follicular helper cell development. *J Immunol,* 185**,** 313-26.

POLIMENO, M., NAPOLITANO, M., COSTANTINI, S., PORTELLA, L., ESPOSITO, A., CAPONE, F., GUERRIERO, E., TROTTA, A., ZANOTTA, S., PUCCI, L., LONGO, N., PERDONÀ, S., PIGNATA, S., CASTELLO, G. & SCALA, S. 2013. Regulatory T cells, interleukin (IL)-6, IL-8, vascular endothelial growth factor (VEGF), CXCL10, CXCL11, epidermal growth factor (EGF) and hepatocyte growth factor (HGF) as surrogate markers of host immunity in patients with renal cell carcinoma. *BJU Int,* 112**,** 686-96.

PÖLLÄNEN, P., SÖDER, O. & UKSILA, J. 1988. Testicular immunosuppressive protein. *Journal of reproductive immunology,* 14**,** 125-138.

PÖLLÄNEN, P., VON EULER, M., SAINIO-PÖLLÄNEN, S., JAHNUKAINEN, K., HAKOVIRTA, H., SÖDER, O. & PARVINEN, M. 1992. Immunosuppressive activity in the rat seminiferous tubules. *Journal of reproductive immunology,* 22**,** 117-126.

POWDERLY, J. D., CHMIELOWSKI, B., BRAHMER, J. R., PIHA-PAUL, S. A., BOWYER, S. E., LORUSSO, P., CATENACCI, D. V. T., WU, C., BARVE, M. A., CHISAMORE, M. J., NASRAH, N., JOHNSON, D. & HO, W. 2020. Phase I/II dose-escalation and expansion study of FLX475 alone and in combination with pembrolizumab in advanced cancer. *Journal of Clinical Oncology,* 38**,** TPS3163-TPS3163.

PURWAR, R., SCHLAPBACH, C., XIAO, S., KANG, H. S., ELYAMAN, W., JIANG, X., JETTEN, A. M., KHOURY, S. J., FUHLBRIGGE, R. C., KUCHROO, V. K., CLARK, R.

A. & KUPPER, T. S. 2012. Robust tumor immunity to melanoma mediated by interleukin-9-producing T cells. *Nat Med,* 18**,** 1248-53.
QIAN, B. Z., LI, J., ZHANG, H., KITAMURA, T., ZHANG, J., CAMPION, L. R., KAISER, E. A., SNYDER, L. A. & POLLARD, J. W. 2011. CCL2 recruits inflammatory monocytes to facilitate breast-tumour metastasis. *Nature,* 475**,** 222-5.
QIN, L., WASEEM, T. C., SAHOO, A., BIEERKEHAZHI, S., ZHOU, H., GALKINA, E. V. & NURIEVA, R. 2018. Insights Into the Molecular Mechanisms of T Follicular Helper-Mediated Immunity and Pathology. *Front Immunol,* 9**,** 1884.
QIN, S., MA, S., HUANG, X., LU, D., ZHOU, Y. & JIANG, H. 2014. Th22 cells are associated with hepatocellular carcinoma development and progression. *Chin J Cancer Res,* 26**,** 135-41.
RAFFIN, C., VO, L. T. & BLUESTONE, J. A. 2020. T(reg) cell-based therapies: challenges and perspectives. *Nat Rev Immunol,* 20**,** 158-172.
RAJPERT-DE MEYTS, E., MCGLYNN, K. A., OKAMOTO, K., JEWETT, M. A. & BOKEMEYER, C. 2016. Testicular germ cell tumours. *Lancet,* 387**,** 1762-74.
RAJPERT-DE MEYTS, E., NIELSEN, J. E., SKAKKEBAEK, N. E. & ALMSTRUP, K. 2015. Diagnostic markers for germ cell neoplasms: from placental-like alkaline phosphatase to micro-RNAs. *Folia Histochemica et Cytobiologica,* 53**,** 177-188.
RAMISCAL, R. R. & VINUESA, C. G. 2013. T-cell subsets in the germinal center. *Immunol Rev,* 252**,** 146-55.
RAPHAEL, I., NALAWADE, S., EAGAR, T. N. & FORSTHUBER, T. G. 2015. T cell subsets and their signature cytokines in autoimmune and inflammatory diseases. *Cytokine,* 74**,** 5-17.
RASHEED, A. U., RAHN, H. P., SALLUSTO, F., LIPP, M. & MÜLLER, G. 2006. Follicular B helper T cell activity is confined to CXCR5(hi)ICOS(hi) CD4 T cells and is independent of CD57 expression. *Eur J Immunol,* 36**,** 1892-903.
REBOURCET, D., O'SHAUGHNESSY, P. J., MONTEIRO, A., MILNE, L., CRUICKSHANKS, L., JEFFREY, N., GUILLOU, F., FREEMAN, T. C., MITCHELL, R. T. & SMITH, L. B. 2014. Sertoli cells maintain Leydig cell number and peritubular myoid cell activity in the adult mouse testis. *PloS one,* 9**,** e105687.
RECH, A. J., MICK, R., MARTIN, S., RECIO, A., AQUI, N. A., POWELL, D. J., JR., COLLIGON, T. A., TROSKO, J. A., LEINBACH, L. I., PLETCHER, C. H., TWEED, C. K., DEMICHELE, A., FOX, K. R., DOMCHEK, S. M., RILEY, J. L. & VONDERHEIDE, R. H. 2012. CD25 blockade depletes and selectively reprograms regulatory T cells in concert with immunotherapy in cancer patients. *Sci Transl Med,* 4**,** 134ra62.
REN, L., YU, Y., WANG, L., ZHU, Z., LU, R. & YAO, Z. 2016. Hypoxia-induced CCL28 promotes recruitment of regulatory T cells and tumor growth in liver cancer. *Oncotarget,* 7**,** 75763-75773.
RES, P. C., PISKIN, G., DE BOER, O. J., VAN DER LOOS, C. M., TEELING, P., BOS, J. D. & TEUNISSEN, M. B. 2010. Overrepresentation of IL-17A and IL-22 producing CD8 T cells in lesional skin suggests their involvement in the pathogenesis of psoriasis. *PLoS One,* 5**,** e14108.
RIBAS, A. 2012. Tumor immunotherapy directed at PD-1. *N Engl J Med,* 366**,** 2517-9.
RIBEIRO, F., PERUCHA, E. & GRACA, L. 2022. T follicular cells: The regulators of germinal center homeostasis. *Immunol Lett,* 244**,** 1-11.
RIGHI, E., KASHIWAGI, S., YUAN, J., SANTOSUOSSO, M., LEBLANC, P., INGRAHAM, R., FORBES, B., EDELBLUTE, B., COLLETTE, B., XING, D., KOWALSKI, M., MINGARI, M. C., VIANELLO, F., BIRRER, M., ORSULIC, S., DRANOFF, G. & POZNANSKY, M. C. 2011. CXCL12/CXCR4 blockade induces multimodal antitumor effects that prolong survival in an immunocompetent mouse model of ovarian cancer. *Cancer Res,* 71**,** 5522-5534.
RIVAL, C., GUAZZONE, V. A., VON WULFFEN, W., HACKSTEIN, H., SCHNEIDER, E., LUSTIG, L., MEINHARDT, A. & FIJAK, M. 2007. Expression of co-stimulatory molecules, chemokine receptors and proinflammatory cytokines in dendritic cells from normal and chronically inflamed rat testis. *Molecular human reproduction,* 13**,** 853-861.

RIVAL, C., LUSTIG, L., IOSUB, R., GUAZZONE, V. A., SCHNEIDER, E., MEINHARDT, A. & FIJAK, M. 2006. Identification of a dendritic cell population in normal testis and in chronically inflamed testis of rats with autoimmune orchitis. *Cell and tissue research,* 324**,** 311-318.

ROAIAH, M., KHATAB, H. & MOSTAFA, T. 2007. Mast cells in testicular biopsies of azoospermic men. *Andrologia,* 39**,** 185-189.

ROBLES, O., JACKSON, J. J., MARSHALL, L., TALAY, O., CHIAN, D., CUTLER, G., DIOKNO, R., HU, D. X., JACOBSON, S., KARBARZ, E., KASSNER, P. D., KETCHAM, J. M., MCKINNELL, J., MELEZA, C., REILLY, M. K., RIEGLER, E., SHUNATONA, H. P., WADSWORTH, A., YOUNAI, A., BROCKSTEDT, D. G., WUSTROW, D. J. & ZIBINSKY, M. 2020. Novel Piperidinyl-Azetidines as Potent and Selective CCR4 Antagonists Elicit Antitumor Response as a Single Agent and in Combination with Checkpoint Inhibitors. *J Med Chem,* 63**,** 8584-8607.

ROMANO, F. J., ROSSETTI, S., CONTEDUCA, V., SCHEPISI, G., CAVALIERE, C., DI FRANCO, R., LA MANTIA, E., CASTALDO, L., NOCERINO, F. & AMETRANO, G. 2016. Role of DNA repair machinery and p53 in the testicular germ cell cancer: a review. *Oncotarget,* 7**,** 85641.

ROMANO, M., FANELLI, G., ALBANY, C. J., GIGANTI, G. & LOMBARDI, G. 2019. Past, Present, and Future of Regulatory T Cell Therapy in Transplantation and Autoimmunity. *Front Immunol,* 10**,** 43.

SAGE, P. T., ALVAREZ, D., GODEC, J., VON ANDRIAN, U. H. & SHARPE, A. H. 2014. Circulating T follicular regulatory and helper cells have memory-like properties. *J Clin Invest,* 124**,** 5191-204.

SAGE, P. T., TAN, C. L., FREEMAN, G. J., HAIGIS, M. & SHARPE, A. H. 2015. Defective TFH cell function and increased TFR cells contribute to defective antibody production in aging. *Cell reports,* 12**,** 163-171.

SAINSON, R. C., THOTAKURA, A. K., KOSMAC, M., BORHIS, G., PARVEEN, N., KIMBER, R., CARVALHO, J., HENDERSON, S. J., PRYKE, K. L. & OKELL, T. 2020. An Antibody Targeting ICOS Increases Intratumoral Cytotoxic to Regulatory T-cell Ratio and Induces Tumor RegressionAntitumor Activity Triggered by an Anti-ICOS Antibody. *Cancer Immunology Research,* 8**,** 1568-1582.

SAITO, H., YAMADA, Y., TAKAYA, S., OSAKI, T. & IKEGUCHI, M. 2015. Clinical relevance of the number of interleukin-17-producing CD 8+ T cells in patients with gastric cancer. *Surg Today,* 45**,** 1429-35.

SAITO, T., NISHIKAWA, H., WADA, H., NAGANO, Y., SUGIYAMA, D., ATARASHI, K., MAEDA, Y., HAMAGUCHI, M., OHKURA, N., SATO, E., NAGASE, H., NISHIMURA, J., YAMAMOTO, H., TAKIGUCHI, S., TANOUE, T., SUDA, W., MORITA, H., HATTORI, M., HONDA, K., MORI, M., DOKI, Y. & SAKAGUCHI, S. 2016. Two FOXP3(+)CD4(+) T cell subpopulations distinctly control the prognosis of colorectal cancers. *Nat Med,* 22**,** 679-84.

SAKAGUCHI, S., MIKAMI, N., WING, J. B., TANAKA, A., ICHIYAMA, K. & OHKURA, N. 2020. Regulatory T Cells and Human Disease. *Annu Rev Immunol,* 38**,** 541-566.

SAKAGUCHI, S., MIYARA, M., COSTANTINO, C. M. & HAFLER, D. A. 2010. FOXP3+ regulatory T cells in the human immune system. *Nat Rev Immunol,* 10**,** 490-500.

SAKAGUCHI, S., SAKAGUCHI, N., ASANO, M., ITOH, M. & TODA, M. 1995. Immunologic self-tolerance maintained by activated T cells expressing IL-2 receptor alpha-chains (CD25). Breakdown of a single mechanism of self-tolerance causes various autoimmune diseases. *J Immunol,* 155**,** 1151-64.

SALAZAR, Y., ZHENG, X., BRUNN, D., RAIFER, H., PICARD, F., ZHANG, Y., WINTER, H., GUENTHER, S., WEIGERT, A., WEIGMANN, B., DUMOUTIER, L., RENAULD, J. C., WAISMAN, A., SCHMALL, A., TUFMAN, A., FINK, L., BRÜNE, B., BOPP, T., GRIMMINGER, F., SEEGER, W., PULLAMSETTI, S. S., HUBER, M. & SAVAI, R. 2020. Microenvironmental Th9 and Th17 lymphocytes induce metastatic spreading in lung cancer. *J Clin Invest,* 130**,** 3560-3575.

SÁNCHEZ-SÁNCHEZ, A. V., GARCÍA-ESPAÑA, A., SÁNCHEZ-GÓMEZ, P., FONT-DE-MORA, J., MERINO, M. & MULLOR, J. L. 2021. The Embryonic Key Pluripotent Factor NANOG Mediates Glioblastoma Cell Migration via the SDF1/CXCR4 Pathway. *Int J Mol Sci,* 22.

SANTAGATA, S., IERANÒ, C., TROTTA, A. M., CAPILUONGO, A., AULETTA, F., GUARDASCIONE, G. & SCALA, S. 2021. CXCR4 and CXCR7 signaling pathways: a focus on the cross-talk between cancer cells and tumor microenvironment. *Frontiers in oncology,* 11**,** 591386.

SASAKI, T., IKEDA, H., SATO, M., OHKURI, T., ABE, H., KUROKI, M., ONODERA, M., MIYAMOTO, M., KONDO, S. & NISHIMURA, T. 2006. Antitumor activity of chimeric immunoreceptor gene-modified Tc1 and Th1 cells against autologous carcinoembryonic antigen-expressing colon cancer cells. *Cancer Sci,* 97**,** 920-7.

SCAPINI, P., LAUDANNA, C., PINARDI, C., ALLAVENA, P., MANTOVANI, A., SOZZANI, S. & CASSATELLA, M. A. 2001. Neutrophils produce biologically active macrophage inflammatory protein-3alpha (MIP-3alpha)/CCL20 and MIP-3beta/CCL19. *Eur J Immunol,* 31**,** 1981-8.

SCHALLER, M. A., LUNDY, S. K., HUFFNAGLE, G. B. & LUKACS, N. W. 2005. CD8+ T cell contributions to allergen induced pulmonary inflammation and airway hyperreactivity. *Eur J Immunol,* 35**,** 2061-70.

SCHMITT, N., LIU, Y., BENTEBIBEL, S. E., MUNAGALA, I., BOURDERY, L., VENUPRASAD, K., BANCHEREAU, J. & UENO, H. 2014. The cytokine TGF-β co-opts signaling via STAT3-STAT4 to promote the differentiation of human TFH cells. *Nat Immunol,* 15**,** 856-65.

SCHMITT, N., MORITA, R., BOURDERY, L., BENTEBIBEL, S. E., ZURAWSKI, S. M., BANCHEREAU, J. & UENO, H. 2009. Human dendritic cells induce the differentiation of interleukin-21-producing T follicular helper-like cells through interleukin-12. *Immunity,* 31**,** 158-69.

SCHUBERT, D., BODE, C., KENEFECK, R., HOU, T. Z., WING, J. B., KENNEDY, A., BULASHEVSKA, A., PETERSEN, B. S., SCHÄFFER, A. A., GRÜNING, B. A., UNGER, S., FREDE, N., BAUMANN, U., WITTE, T., SCHMIDT, R. E., DUECKERS, G., NIEHUES, T., SENEVIRATNE, S., KANARIOU, M., SPECKMANN, C., EHL, S., RENSING-EHL, A., WARNATZ, K., RAKHMANOV, M., THIMME, R., HASSELBLATT, P., EMMERICH, F., CATHOMEN, T., BACKOFEN, R., FISCH, P., SEIDL, M., MAY, A., SCHMITT-GRAEFF, A., IKEMIZU, S., SALZER, U., FRANKE, A., SAKAGUCHI, S., WALKER, L. S. K., SANSOM, D. M. & GRIMBACHER, B. 2014. Autosomal dominant immune dysregulation syndrome in humans with CTLA4 mutations. *Nat Med,* 20**,** 1410-1416.

SCHÜTTE, B., HOLSTEIN, A. & SCHIRREN, C. 1988. Macrophages Lysing Seminoma Cells in Patients with Carcinoma-In-Situ (CIS) of the Testis/Makrophagen, die Seminomzellen lysieren, bei Patienten mit Carcinoma-In-Situ (CIS) des Hodens. *Andrologia,* 20**,** 295-303.

SCHWICKERT, T. A., VICTORA, G. D., FOOKSMAN, D. R., KAMPHORST, A. O., MUGNIER, M. R., GITLIN, A. D., DUSTIN, M. L. & NUSSENZWEIG, M. C. 2011. A dynamic T cell-limited checkpoint regulates affinity-dependent B cell entry into the germinal center. *J Exp Med,* 208**,** 1243-52.

SELAWRY, H. P., KOTB, M., HERROD, H. G. & LU, Z.-N. 1991. Production of a factor, or factors, suppressing IL-2 production and T cell proliferation by Sertoli cell-enriched preparations. A potential role for islet transplantation in an immunologically privileged site. *Transplantation,* 52**,** 846-850.

SELBY, M. J., ENGELHARDT, J. J., QUIGLEY, M., HENNING, K. A., CHEN, T., SRINIVASAN, M. & KORMAN, A. J. 2013. Anti-CTLA-4 antibodies of IgG2a isotype enhance antitumor activity through reduction of intratumoral regulatory T cells. *Cancer Immunol Res,* 1**,** 32-42.

SETCHELL, B. P. 1990. The testis and tissue transplantation: historical aspects. *Journal of reproductive immunology,* 18**,** 1-8.

SHALAPOUR, S., LIN, X. J., BASTIAN, I. N., BRAIN, J., BURT, A. D., AKSENOV, A. A., VRBANAC, A. F., LI, W., PERKINS, A., MATSUTANI, T., ZHONG, Z., DHAR, D., NAVAS-MOLINA, J. A., XU, J., LOOMBA, R., DOWNES, M., YU, R. T., EVANS, R. M., DORRESTEIN, P. C., KNIGHT, R., BENNER, C., ANSTEE, Q. M. & KARIN, M. 2017. Inflammation-induced IgA+ cells dismantle anti-liver cancer immunity. *Nature,* 551**,** 340-345.

SHAMI, A. N., ZHENG, X., MUNYOKI, S. K., MA, Q., MANSKE, G. L., GREEN, C. D., SUKHWANI, M., ORWIG, K. E., LI, J. Z. & HAMMOUD, S. S. 2020. Single-Cell RNA Sequencing of Human, Macaque, and Mouse Testes Uncovers Conserved and Divergent Features of Mammalian Spermatogenesis. *Dev Cell,* 54**,** 529-547.e12.

SHAN, F., SOMASUNDARAM, A., BRUNO, T. C., WORKMAN, C. J. & VIGNALI, D. A. A. 2022. Therapeutic targeting of regulatory T cells in cancer. *Trends Cancer,* 8**,** 944-961.

SHAPOURI-MOGHADDAM, A., MOHAMMADIAN, S., VAZINI, H., TAGHADOSI, M., ESMAEILI, S. A., MARDANI, F., SEIFI, B., MOHAMMADI, A., AFSHARI, J. T. & SAHEBKAR, A. 2018. Macrophage plasticity, polarization, and function in health and disease. *J Cell Physiol,* 233**,** 6425-6440.

SHEU, B. C., LIN, R. H., LIEN, H. C., HO, H. N., HSU, S. M. & HUANG, S. C. 2001. Predominant Th2/Tc2 polarity of tumor-infiltrating lymphocytes in human cervical cancer. *J Immunol,* 167**,** 2972-8.

SHI, J., HOU, S., FANG, Q., LIU, X., LIU, X. & QI, H. 2018. PD-1 Controls Follicular T Helper Cell Positioning and Function. *Immunity,* 49**,** 264-274.e4.

SHIMIZU, J., YAMAZAKI, S. & SAKAGUCHI, S. 1999. Induction of tumor immunity by removing CD25+CD4+ T cells: a common basis between tumor immunity and autoimmunity. *J Immunol,* 163**,** 5211-8.

SHULMAN, Z., GITLIN, A. D., TARG, S., JANKOVIC, M., PASQUAL, G., NUSSENZWEIG, M. C. & VICTORA, G. D. 2013. T follicular helper cell dynamics in germinal centers. *Science,* 341**,** 673-7.

SIEGMUND, S. E., MEHRA, R. & ACOSTA, A. M. 2022. An Update on Diagnostic Tissue-Based Biomarkers in Testicular Tumors. *Human Pathology*.

SIMONETTI, O., GOTERI, G., LUCARINI, G., FILOSA, A., PIERAMICI, T., RUBINI, C., BIAGINI, G. & OFFIDANI, A. 2006. Potential role of CCL27 and CCR10 expression in melanoma progression and immune escape. *Eur J Cancer,* 42**,** 1181-7.

SIMPSON, T. R., LI, F., MONTALVO-ORTIZ, W., SEPULVEDA, M. A., BERGERHOFF, K., ARCE, F., RODDIE, C., HENRY, J. Y., YAGITA, H., WOLCHOK, J. D., PEGGS, K. S., RAVETCH, J. V., ALLISON, J. P. & QUEZADA, S. A. 2013. Fc-dependent depletion of tumor-infiltrating regulatory T cells co-defines the efficacy of anti-CTLA-4 therapy against melanoma. *J Exp Med,* 210**,** 1695-710.

SIPIONE, S., SIMMEN, K. C., LORD, S. J., MOTYKA, B., EWEN, C., SHOSTAK, I., RAYAT, G. R., DUFOUR, J. M., KORBUTT, G. S. & RAJOTTE, R. V. 2006. Identification of a novel human granzyme B inhibitor secreted by cultured sertoli cells. *The Journal of Immunology,* 177**,** 5051-5058.

SISKA, P. J., JOHNPULLE, R. A., ZHOU, A., BORDEAUX, J., KIM, J. Y., DABBAS, B., DAKAPPAGARI, N., RATHMELL, J. C., RATHMELL, W. K. & MORGANS, A. K. 2017a. Deep exploration of the immune infiltrate and outcome prediction in testicular cancer by quantitative multiplexed immunohistochemistry and gene expression profiling. *Oncoimmunology,* 6**,** e1305535.

SISKA, P. J., JOHNPULLE, R. A. N., ZHOU, A., BORDEAUX, J., KIM, J. Y., DABBAS, B., DAKAPPAGARI, N., RATHMELL, J. C., RATHMELL, W. K., MORGANS, A. K., BALKO, J. M. & JOHNSON, D. B. 2017b. Deep exploration of the immune infiltrate and outcome prediction in testicular cancer by quantitative multiplexed immunohistochemistry and gene expression profiling. *Oncoimmunology,* 6**,** e1305535.

SKAKKEBAEK, N. E., RAJPERT-DE MEYTS, E., BUCK LOUIS, G. M., TOPPARI, J., ANDERSSON, A. M., EISENBERG, M. L., JENSEN, T. K., JØRGENSEN, N., SWAN, S. H., SAPRA, K. J., ZIEBE, S., PRISKORN, L. & JUUL, A. 2016. Male Reproductive

Disorders and Fertility Trends: Influences of Environment and Genetic Susceptibility. *Physiol Rev,* 96**,** 55-97.
SLENTER, D. N., KUTMON, M., HANSPERS, K., RIUTTA, A., WINDSOR, J., NUNES, N., MÉLIUS, J., CIRILLO, E., COORT, S. L., DIGLES, D., EHRHART, F., GIESBERTZ, P., KALAFATI, M., MARTENS, M., MILLER, R., NISHIDA, K., RIESWIJK, L., WAAGMEESTER, A., EIJSSEN, L. M. T., EVELO, C. T., PICO, A. R. & WILLIGHAGEN, E. L. 2017. WikiPathways: a multifaceted pathway database bridging metabolomics to other omics research. *Nucleic Acids Research,* 46**,** D661-D667.
SMITH, L., O'SHAUGHNESSY, P. & REBOURCET, D. 2015. Cell-specific ablation in the testis: what have we learned? *Andrology,* 3**,** 1035-1049.
SO, L. & FRUMAN, D. A. 2012. PI3K signalling in B-and T-lymphocytes: new developments and therapeutic advances. *Biochemical Journal,* 442**,** 465-481.
SPILLER, C. M. & BOWLES, J. 2017. Germ cell neoplasia in situ: The precursor cell for invasive germ cell tumors of the testis. *Int J Biochem Cell Biol,* 86**,** 22-25.
SPRANGER, S., SPAAPEN, R. M., ZHA, Y., WILLIAMS, J., MENG, Y., HA, T. T. & GAJEWSKI, T. F. 2013. Up-regulation of PD-L1, IDO, and T(regs) in the melanoma tumor microenvironment is driven by CD8(+) T cells. *Sci Transl Med,* 5**,** 200ra116.
ST PAUL, M., SAIBIL, S. D., LIEN, S. C., HAN, S., SAYAD, A., MULDER, D. T., GARCIA-BATRES, C. R., ELFORD, A. R., ISRANI-WINGER, K., ROBERT-TISSOT, C., ZON, M., KATZ, S. R., SHAW, P. A., CLARKE, B. A., BERNARDINI, M. Q., NGUYEN, L. T., HAIBE-KAINS, B., PUGH, T. J. & OHASHI, P. S. 2020. IL6 Induces an IL22(+) CD8(+) T-cell Subset with Potent Antitumor Function. *Cancer Immunol Res,* 8**,** 321-333.
STEPHENSON, A., EGGENER, S. E., BASS, E. B., CHELNICK, D. M., DANESHMAND, S., FELDMAN, D., GILLIGAN, T., KARAM, J. A., LEIBOVICH, B. & LIAUW, S. L. 2019. Diagnosis and treatment of early stage testicular cancer: AUA guideline. *The Journal of urology,* 202**,** 272-281.
STOCKINGER, B. & OMENETTI, S. 2017. The dichotomous nature of T helper 17 cells. *Nat Rev Immunol,* 17**,** 535-544.
STONE, E. L., PEPPER, M., KATAYAMA, C. D., KERDILES, Y. M., LAI, C. Y., EMSLIE, E., LIN, Y. C., YANG, E., GOLDRATH, A. W., LI, M. O., CANTRELL, D. A. & HEDRICK, S. M. 2015. ICOS coreceptor signaling inactivates the transcription factor FOXO1 to promote Tfh cell differentiation. *Immunity,* 42**,** 239-251.
SUAN, D., NGUYEN, A., MORAN, I., BOURNE, K., HERMES, J. R., ARSHI, M., HAMPTON, H. R., TOMURA, M., MIWA, Y., KELLEHER, A. D., KAPLAN, W., DEENICK, E. K., TANGYE, S. G., BRINK, R., CHTANOVA, T. & PHAN, T. G. 2015. T follicular helper cells have distinct modes of migration and molecular signatures in naive and memory immune responses. *Immunity,* 42**,** 704-18.
SUGIYAMA, D., NISHIKAWA, H., MAEDA, Y., NISHIOKA, M., TANEMURA, A., KATAYAMA, I., EZOE, S., KANAKURA, Y., SATO, E., FUKUMORI, Y., KARBACH, J., JÄGER, E. & SAKAGUCHI, S. 2013. Anti-CCR4 mAb selectively depletes effector-type FoxP3+CD4+ regulatory T cells, evoking antitumor immune responses in humans. *Proc Natl Acad Sci U S A,* 110**,** 17945-50.
SUN, C. M., HALL, J. A., BLANK, R. B., BOULADOUX, N., OUKKA, M., MORA, J. R. & BELKAID, Y. 2007. Small intestine lamina propria dendritic cells promote de novo generation of Foxp3 T reg cells via retinoic acid. *J Exp Med,* 204**,** 1775-85.
SUN, Z., DU, C., XU, P. & MIAO, C. 2019. Surgical trauma-induced CCL18 promotes recruitment of regulatory T cells and colon cancer progression. *J Cell Physiol,* 234**,** 4608-4616.
SZKLARCZYK, D., GABLE, A. L., NASTOU, K. C., LYON, D., KIRSCH, R., PYYSALO, S., DONCHEVA, N. T., LEGEAY, M., FANG, T., BORK, P., JENSEN, L. J. & VON MERING, C. 2021. The STRING database in 2021: customizable protein-protein networks, and functional characterization of user-uploaded gene/measurement sets. *Nucleic Acids Res,* 49**,** D605-d612.
TADA, Y., TOGASHI, Y., KOTANI, D., KUWATA, T., SATO, E., KAWAZOE, A., DOI, T., WADA, H., NISHIKAWA, H. & SHITARA, K. 2018. Targeting VEGFR2 with

Ramucirumab strongly impacts effector/ activated regulatory T cells and CD8(+) T cells in the tumor microenvironment. *J Immunother Cancer,* 6**,** 106.

TAN, M. C., GOEDEGEBUURE, P. S., BELT, B. A., FLAHERTY, B., SANKPAL, N., GILLANDERS, W. E., EBERLEIN, T. J., HSIEH, C. S. & LINEHAN, D. C. 2009. Disruption of CCR5-dependent homing of regulatory T cells inhibits tumor growth in a murine model of pancreatic cancer. *J Immunol,* 182**,** 1746-55.

TANAKA, T., NARAZAKI, M. & KISHIMOTO, T. 2014. IL-6 in inflammation, immunity, and disease. *Cold Spring Harbor perspectives in biology,* 6**,** a016295.

TARBELL, K. V. & RAHMAN, M. J. 2020. Dendritic cells in autoimmune disease. *The autoimmune diseases.* Elsevier.

TEIXEIRA, T. A., PARIZ, J. R., DUTRA, R. T., SALDIVA, P. H., COSTA, E. & HALLAK, J. 2019. Cut-off values of the Johnsen score and Copenhagen index as histopathological prognostic factors for postoperative semen quality in selected infertile patients undergoing microsurgical correction of bilateral subclinical varicocele. *Transl Androl Urol,* 8**,** 346-355.

TOGASHI, Y., KAMADA, T., SASAKI, A., NAKAMURA, Y., FUKUOKA, S., TADA, Y., KAWAZOE, A., SHITARA, K. & NISHIKAWA, H. 2018. Clinicopathological, genomic and immunological features of hyperprogressive disease during PD-1 blockade in gastric cancer patients. American Society of Clinical Oncology.

TOGASHI, Y. & NISHIKAWA, H. 2017. Regulatory T Cells: Molecular and Cellular Basis for Immunoregulation. *Curr Top Microbiol Immunol,* 410**,** 3-27.

TOGASHI, Y., SHITARA, K. & NISHIKAWA, H. 2019. Regulatory T cells in cancer immunosuppression - implications for anticancer therapy. *Nat Rev Clin Oncol,* 16**,** 356-371.

TOSOLINI, M., KIRILOVSKY, A., MLECNIK, B., FREDRIKSEN, T., MAUGER, S., BINDEA, G., BERGER, A., BRUNEVAL, P., FRIDMAN, W. H., PAGÈS, F. & GALON, J. 2011. Clinical impact of different classes of infiltrating T cytotoxic and helper cells (Th1, th2, treg, th17) in patients with colorectal cancer. *Cancer Res,* 71**,** 1263-71.

TRABERT, B., ZUGNA, D., RICHIARDI, L., MCGLYNN, K. A. & AKRE, O. 2013. Congenital malformations and testicular germ cell tumors. *Int J Cancer,* 133**,** 1900-4.

TSUJIKAWA, T., YAGUCHI, T., OHMURA, G., OHTA, S., KOBAYASHI, A., KAWAMURA, N., FUJITA, T., NAKANO, H., SHIMADA, T., TAKAHASHI, T., NAKAO, R., YANAGISAWA, A., HISA, Y. & KAWAKAMI, Y. 2013. Autocrine and paracrine loops between cancer cells and macrophages promote lymph node metastasis via CCR4/CCL22 in head and neck squamous cell carcinoma. *Int J Cancer,* 132**,** 2755-66.

TUNG, K. S., HARAKAL, J., QIAO, H., RIVAL, C., LI, J. C., PAUL, A. G., WHEELER, K., PRAMOONJAGO, P., GRAFER, C. M. & SUN, W. 2017. Egress of sperm autoantigen from seminiferous tubules maintains systemic tolerance. *The Journal of clinical investigation,* 127**,** 1046-1060.

VAHEDI, G., A, C. P., HAND, T. W., LAURENCE, A., KANNO, Y., O'SHEA, J. J. & HIRAHARA, K. 2013. Helper T-cell identity and evolution of differential transcriptomes and epigenomes. *Immunol Rev,* 252**,** 24-40.

VAN DER LEUN, A. M., THOMMEN, D. S. & SCHUMACHER, T. N. 2020. CD8(+) T cell states in human cancer: insights from single-cell analysis. *Nat Rev Cancer,* 20**,** 218-232.

VASANTHAKUMAR, A., MORO, K., XIN, A., LIAO, Y., GLOURY, R., KAWAMOTO, S., FAGARASAN, S., MIELKE, L. A., AFSHAR-STERLE, S., MASTERS, S. L., NAKAE, S., SAITO, H., WENTWORTH, J. M., LI, P., LIAO, W., LEONARD, W. J., SMYTH, G. K., SHI, W., NUTT, S. L., KOYASU, S. & KALLIES, A. 2015. The transcriptional regulators IRF4, BATF and IL-33 orchestrate development and maintenance of adipose tissue-resident regulatory T cells. *Nat Immunol,* 16**,** 276-85.

VELADO-EGUSKIZA, A., GOMEZ-SANTOS, L., BADIOLA, I., SÁEZ, F. J. & ALONSO, E. 2022. Testicular Germ Cell Tumours and Proprotein Convertases. *Cancers,* 14**,** 1633.

VELDHOEN, M., UYTTENHOVE, C., VAN SNICK, J., HELMBY, H., WESTENDORF, A., BUER, J., MARTIN, B., WILHELM, C. & STOCKINGER, B. 2008. Transforming growth

factor-beta 'reprograms' the differentiation of T helper 2 cells and promotes an interleukin 9-producing subset. *Nat Immunol,* 9**,** 1341-6.

VILA-CABALLER, M., GONZÁLEZ-GRANADO, J. M., ZORITA, V., ABU NABAH, Y. N., SILVESTRE-ROIG, C., DEL MONTE-MONGE, A., MOLINA-SÁNCHEZ, P., AIT-OUFELLA, H., ANDRÉS-MANZANO, M. J., SANZ, M. J., WEBER, C., KREMER, L., GUTIÉRREZ, J., MALLAT, Z. & ANDRÉS, V. 2019. Disruption of the CCL1-CCR8 axis inhibits vascular Treg recruitment and function and promotes atherosclerosis in mice. *J Mol Cell Cardiol,* 132**,** 154-163.

VINUESA, C. G., LINTERMAN, M. A., YU, D. & MACLENNAN, I. C. 2016. Follicular Helper T Cells. *Annu Rev Immunol,* 34**,** 335-68.

VISEKRUNA, A., RITTER, J., SCHOLZ, T., CAMPOS, L., GURALNIK, A., PONCETTE, L., RAIFER, H., HAGNER, S., GARN, H., STAUDT, V., BOPP, T., REUTER, S., TAUBE, C., LOSER, K. & HUBER, M. 2013. Tc9 cells, a new subset of CD8(+) T cells, support Th2-mediated airway inflammation. *Eur J Immunol,* 43**,** 606-18.

VOGELZANG, A., MCGUIRE, H. M., YU, D., SPRENT, J., MACKAY, C. R. & KING, C. 2008. A fundamental role for interleukin-21 in the generation of T follicular helper cells. *Immunity,* 29**,** 127-37.

VORON, T., MARCHETEAU, E., PERNOT, S., COLUSSI, O., TARTOUR, E., TAIEB, J. & TERME, M. 2014. Control of the immune response by pro-angiogenic factors. *Front Oncol,* 4**,** 70.

WALI, S., SAHOO, A., PURI, S., ALEKSEEV, A. & NURIEVA, R. 2016. Insights into the development and regulation of T follicular helper cells. *Cytokine,* 87**,** 9-19.

WALKER, J. A. & MCKENZIE, A. N. J. 2018. T(H)2 cell development and function. *Nat Rev Immunol,* 18**,** 121-133.

WALKER, L. S. 2013. Treg and CTLA-4: two intertwining pathways to immune tolerance. *J Autoimmun,* 45**,** 49-57.

WALKER, L. S. & SANSOM, D. M. 2011. The emerging role of CTLA4 as a cell-extrinsic regulator of T cell responses. *Nat Rev Immunol,* 11**,** 852-63.

WALKER, L. S. & SANSOM, D. M. 2015. Confusing signals: recent progress in CTLA-4 biology. *Trends Immunol,* 36**,** 63-70.

WAN, J., WU, Y., JI, X., HUANG, L., CAI, W., SU, Z., WANG, S. & XU, H. 2020. IL-9 and IL-9-producing cells in tumor immunity. *Cell Commun Signal,* 18**,** 50.

WANG, C., HILLSAMER, P. & KIM, C. H. 2011. Phenotype, effector function, and tissue localization of PD-1-expressing human follicular helper T cell subsets. *BMC Immunol,* 12**,** 53.

WANG, D., YANG, L., YU, W., WU, Q., LIAN, J., LI, F., LIU, S., LI, A., HE, Z., LIU, J., SUN, Z., YUAN, W. & ZHANG, Y. 2019a. Colorectal cancer cell-derived CCL20 recruits regulatory T cells to promote chemoresistance via FOXO1/CEBPB/NF-κB signaling. *J Immunother Cancer,* 7**,** 215.

WANG, H., GENG, J., WEN, X., BI, E., KOSSENKOV, A. V., WOLF, A. I., TAS, J., CHOI, Y. S., TAKATA, H., DAY, T. J., CHANG, L. Y., SPROUT, S. L., BECKER, E. K., WILLEN, J., TIAN, L., WANG, X., XIAO, C., JIANG, P., CROTTY, S., VICTORA, G. D., SHOWE, L. C., TUCKER, H. O., ERIKSON, J. & HU, H. 2014. The transcription factor Foxp1 is a critical negative regulator of the differentiation of follicular helper T cells. *Nat Immunol,* 15**,** 667-75.

WANG, M., FIJAK, M., HOSSAIN, H., MARKMANN, M., NÜSING, R. M., LOCHNIT, G., HARTMANN, M. F., WUDY, S. A., ZHANG, L., GU, H., KONRAD, L., CHAKRABORTY, T., MEINHARDT, A. & BHUSHAN, S. 2017a. Characterization of the Micro-Environment of the Testis that Shapes the Phenotype and Function of Testicular Macrophages. *J Immunol,* 198**,** 4327-4340.

WANG, Q., SCHMOECKEL, E., KOST, B. P., KUHN, C., VATTAI, A., VILSMAIER, T., MAHNER, S., MAYR, D., JESCHKE, U. & HEIDEGGER, H. H. 2019b. Higher CCL22+ Cell Infiltration is Associated with Poor Prognosis in Cervical Cancer Patients. *Cancers (Basel),* 11.

WANG, S., LI, Z. & HU, G. 2017b. Prognostic role of intratumoral IL-17A expression by immunohistochemistry in solid tumors: a meta-analysis. *Oncotarget,* 8**,** 66382-66391.
WANG, X., LANG, M., ZHAO, T., FENG, X., ZHENG, C., HUANG, C., HAO, J., DONG, J., LUO, L., LI, X., LAN, C., YU, W., YU, M., YANG, S. & REN, H. 2017c. Cancer-FOXP3 directly activated CCL5 to recruit FOXP3(+)Treg cells in pancreatic ductal adenocarcinoma. *Oncogene,* 36**,** 3048-3058.
WANG, X. F., ZHU, Y. T., WANG, J. J., ZENG, D. X., MU, C. Y., CHEN, Y. B., LEI, W., ZHU, Y. H. & HUANG, J. A. 2017d. The prognostic value of interleukin-17 in lung cancer: A systematic review with meta-analysis based on Chinese patients. *PLoS One,* 12**,** e0185168.
WANG, Z., XIE, H., ZHOU, L., LIU, Z., FU, H., ZHU, Y., XU, L. & XU, J. 2016. CCL2/CCR2 axis is associated with postoperative survival and recurrence of patients with non-metastatic clear-cell renal cell carcinoma. *Oncotarget,* 7**,** 51525-51534.
WARD, S. T., LI, K. K., HEPBURN, E., WESTON, C. J., CURBISHLEY, S. M., REYNOLDS, G. M., HEJMADI, R. K., BICKNELL, R., EKSTEEN, B., ISMAIL, T., ROT, A. & ADAMS, D. H. 2015. The effects of CCR5 inhibition on regulatory T-cell recruitment to colorectal cancer. *Br J Cancer,* 112**,** 319-28.
WASHBURN, R. L., HIBLER, T., KAUR, G. & DUFOUR, J. M. 2022. Sertoli Cell Immune Regulation: A Double-Edged Sword. *Front Immunol,* 13**,** 913502.
WASHBURN, R. L., HIBLER, T., THOMPSON, L. A., KAUR, G. & DUFOUR, J. M. Therapeutic application of Sertoli cells for treatment of various diseases. Seminars in Cell & Developmental Biology, 2021. Elsevier.
WCULEK, S. K., CUETO, F. J., MUJAL, A. M., MELERO, I., KRUMMEL, M. F. & SANCHO, D. 2020. Dendritic cells in cancer immunology and immunotherapy. *Nature Reviews Immunology,* 20**,** 7-24.
WEBER, J. P., FUHRMANN, F., FEIST, R. K., LAHMANN, A., AL BAZ, M. S., GENTZ, L. J., VU VAN, D., MAGES, H. W., HAFTMANN, C., RIEDEL, R., GRÜN, J. R., SCHUH, W., KROCZEK, R. A., RADBRUCH, A., MASHREGHI, M. F. & HUTLOFF, A. 2015. ICOS maintains the T follicular helper cell phenotype by down-regulating Krüppel-like factor 2. *J Exp Med,* 212**,** 217-33.
WEBER, J. P., FUHRMANN, F. & HUTLOFF, A. 2012. T-follicular helper cells survive as long-term memory cells. *Eur J Immunol,* 42**,** 1981-8.
WEI, Y., HUANG, C.-X., XIAO, X., CHEN, D.-P., SHAN, H., HE, H. & KUANG, D.-M. 2021. B cell heterogeneity, plasticity, and functional diversity in cancer microenvironments. *Oncogene,* 40**,** 4737-4745.
WEINSTEIN, J. S., HERMAN, E. I., LAINEZ, B., LICONA-LIMÓN, P., ESPLUGUES, E., FLAVELL, R. & CRAFT, J. 2016. TFH cells progressively differentiate to regulate the germinal center response. *Nat Immunol,* 17**,** 1197-1205.
WEISS, J. M., BILATE, A. M., GOBERT, M., DING, Y., CUROTTO DE LAFAILLE, M. A., PARKHURST, C. N., XIONG, H., DOLPADY, J., FREY, A. B., RUOCCO, M. G., YANG, Y., FLOESS, S., HUEHN, J., OH, S., LI, M. O., NIEC, R. E., RUDENSKY, A. Y., DUSTIN, M. L., LITTMAN, D. R. & LAFAILLE, J. J. 2012. Neuropilin 1 is expressed on thymus-derived natural regulatory T cells, but not mucosa-generated induced Foxp3+ T reg cells. *J Exp Med,* 209**,** 1723-42, s1.
WEISSLER, K. A. & CATON, A. J. 2014. The role of T-cell receptor recognition of peptide: MHC complexes in the formation and activity of Foxp3+ regulatory T cells. *Immunological reviews,* 259**,** 11-22.
WHEELER, K., TARDIF, S., RIVAL, C., LUU, B., BUI, E., DEL RIO, R., TEUSCHER, C., SPARWASSER, T., HARDY, D. & TUNG, K. S. 2011. Regulatory T cells control tolerogenic versus autoimmune response to sperm in vasectomy. *Proceedings of the National Academy of Sciences,* 108**,** 7511-7516.
WIEDEMANN, G. M., KNOTT, M. M., VETTER, V. K., RAPP, M., HAUBNER, S., FESSELER, J., KÜHNEMUTH, B., LAYRITZ, P., THALER, R., KRUGER, S., ORMANNS, S., MAYR, D., ENDRES, S. & ANZ, D. 2016. Cancer cell-derived IL-1α induces CCL22 and the recruitment of regulatory T cells. *Oncoimmunology,* 5**,** e1175794.

WILLIAMS, J. B., HORTON, B. L., ZHENG, Y., DUAN, Y., POWELL, J. D. & GAJEWSKI, T. F. 2017. The EGR2 targets LAG-3 and 4-1BB describe and regulate dysfunctional antigen-specific CD8+ T cells in the tumor microenvironment. *J Exp Med,* 214**,** 381-400.

WILLIS, S. N., MALLOZZI, S. S., RODIG, S. J., CRONK, K. M., MCARDEL, S. L., CARON, T., PINKUS, G. S., LOVATO, L., SHAMPAIN, K. L. & ANDERSON, D. E. 2009. The microenvironment of germ cell tumors harbors a prominent antigen-driven humoral response. *The Journal of Immunology,* 182**,** 3310-3317.

WILSON, J. M., ROSS, W. G., AGBAI, O. N., FRAZIER, R., FIGLER, R. A., RIEGER, J., LINDEN, J. & ERNST, P. B. 2009. The A2B adenosine receptor impairs the maturation and immunogenicity of dendritic cells. *J Immunol,* 182**,** 4616-23.

WING, K., ONISHI, Y., PRIETO-MARTIN, P., YAMAGUCHI, T., MIYARA, M., FEHERVARI, Z., NOMURA, T. & SAKAGUCHI, S. 2008. CTLA-4 control over Foxp3+ regulatory T cell function. *Science,* 322**,** 271-5.

WING, K. & SAKAGUCHI, S. 2010. Regulatory T cells exert checks and balances on self tolerance and autoimmunity. *Nat Immunol,* 11**,** 7-13.

WINNALL, W. R., MUIR, J. A. & HEDGER, M. P. 2011. Rat resident testicular macrophages have an alternatively activated phenotype and constitutively produce interleukin-10 in vitro. *J Leukoc Biol,* 90**,** 133-43.

WU, X., GU, Z., CHEN, Y., CHEN, B., CHEN, W., WENG, L. & LIU, X. 2019. Application of PD-1 blockade in cancer immunotherapy. *Computational and structural biotechnology journal,* 17**,** 661-674.

XIA, M., HU, S., FU, Y., JIN, W., YI, Q., MATSUI, Y., YANG, J., MCDOWELL, M. A., SARKAR, S., KALIA, V. & XIONG, N. 2014. CCR10 regulates balanced maintenance and function of resident regulatory and effector T cells to promote immune homeostasis in the skin. *J Allergy Clin Immunol,* 134**,** 634-644.e10.

XIE, Z., BAILEY, A., KULESHOV, M. V., CLARKE, D. J. B., EVANGELISTA, J. E., JENKINS, S. L., LACHMANN, A., WOJCIECHOWICZ, M. L., KROPIWNICKI, E., JAGODNIK, K. M., JEON, M. & MA'AYAN, A. 2021. Gene Set Knowledge Discovery with Enrichr. *Curr Protoc,* 1**,** e90.

XIN, G., ZANDER, R., SCHAUDER, D. M., CHEN, Y., WEINSTEIN, J. S., DROBYSKI, W. R., TARAKANOVA, V., CRAFT, J. & CUI, W. 2018. Single-cell RNA sequencing unveils an IL-10-producing helper subset that sustains humoral immunity during persistent infection. *Nat Commun,* 9**,** 5037.

XU, H., LI, X., LIU, D., LI, J., ZHANG, X., CHEN, X., HOU, S., PENG, L., XU, C., LIU, W., ZHANG, L. & QI, H. 2013. Follicular T-helper cell recruitment governed by bystander B cells and ICOS-driven motility. *Nature,* 496**,** 523-7.

XU, L., CAO, Y., XIE, Z., HUANG, Q., BAI, Q., YANG, X., HE, R., HAO, Y., WANG, H., ZHAO, T., FAN, Z., QIN, A., YE, J., ZHOU, X., YE, L. & WU, Y. 2015. The transcription factor TCF-1 initiates the differentiation of T(FH) cells during acute viral infection. *Nat Immunol,* 16**,** 991-9.

YADAV, M., LOUVET, C., DAVINI, D., GARDNER, J. M., MARTINEZ-LLORDELLA, M., BAILEY-BUCKTROUT, S., ANTHONY, B. A., SVERDRUP, F. M., HEAD, R., KUSTER, D. J., RUMINSKI, P., WEISS, D., VON SCHACK, D. & BLUESTONE, J. A. 2012. Neuropilin-1 distinguishes natural and inducible regulatory T cells among regulatory T cell subsets in vivo. *J Exp Med,* 209**,** 1713-22, s1-19.

YAKIREVICH, E., LEFEL, O., SOVA, Y., STEIN, A., COHEN, O., IZHAK, O. B. & RESNICK, M. B. 2002. Activated status of tumour-infiltrating lymphocytes and apoptosis in testicular seminoma. *J Pathol,* 196**,** 67-75.

YAMANAKA, K., FUJISAWA, M., TANAKA, H., OKADA, H., ARAKAWA, S. & KAMIDONO, S. 2000. Significance of human testicular mast cells and their subtypes in male infertility. *Human Reproduction,* 15**,** 1543-1547.

YAMAZAKI, T., YANG, X. O., CHUNG, Y., FUKUNAGA, A., NURIEVA, R., PAPPU, B., MARTIN-OROZCO, N., KANG, H. S., MA, L., PANOPOULOS, A. D., CRAIG, S.,

WATOWICH, S. S., JETTEN, A. M., TIAN, Q. & DONG, C. 2008. CCR6 regulates the migration of inflammatory and regulatory T cells. *J Immunol,* 181**,** 8391-401.
YAN, L., DE LEUR, K., HENDRIKS, R. W., VAN DER LAAN, L. J. W., SHI, Y., WANG, L. & BAAN, C. C. 2017. T Follicular Helper Cells As a New Target for Immunosuppressive Therapies. *Front Immunol,* 8**,** 1510.
YAN, M., JENE, N., BYRNE, D., MILLAR, E. K., O'TOOLE, S. A., MCNEIL, C. M., BATES, G. J., HARRIS, A. L., BANHAM, A. H., SUTHERLAND, R. L. & FOX, S. B. 2011. Recruitment of regulatory T cells is correlated with hypoxia-induced CXCR4 expression, and is associated with poor prognosis in basal-like breast cancers. *Breast Cancer Res,* 13**,** R47.
YANG, S., CHEN, J., ZHANG, H., JIANG, Y., QIN, T., GAO, S., YUE, Y. & WANG, S. 2020. TNF-a Is a Potent Stimulator of Tc9-Cell Differentiation. *J Immunother,* 43**,** 265-272.
YANG, S., XIE, C., CHEN, Y., WANG, J., CHEN, X., LU, Z., JUNE, R. R. & ZHENG, S. G. 2019. Differential roles of TNFα-TNFR1 and TNFα-TNFR2 in the differentiation and function of CD4+Foxp3+ induced Treg cells in vitro and in vivo periphery in autoimmune diseases. *Cell Death & Disease,* 10**,** 27.
YANG, Y., OCHANDO, J. C., BROMBERG, J. S. & DING, Y. 2007. Identification of a distant T-bet enhancer responsive to IL-12/Stat4 and IFNgamma/Stat1 signals. *Blood,* 110**,** 2494-500.
YAP, T. A., BURRIS, H. A., KUMMAR, S., FALCHOOK, G. S., PACHYNSKI, R. K., LORUSSO, P., TYKODI, S. S., GIBNEY, G. T., GAINOR, J. F. & RAHMA, O. E. 2018. ICONIC: Biologic and clinical activity of first in class ICOS agonist antibody JTX-2011+/-nivolumab (nivo) in patients (pts) with advanced cancers. American Society of Clinical Oncology.
YEH, C. H., NOJIMA, T., KURAOKA, M. & KELSOE, G. 2018. Germinal center entry not selection of B cells is controlled by peptide-MHCII complex density. *Nat Commun,* 9**,** 928.
YEN, H. R., HARRIS, T. J., WADA, S., GROSSO, J. F., GETNET, D., GOLDBERG, M. V., LIANG, K. L., BRUNO, T. C., PYLE, K. J., CHAN, S. L., ANDERS, R. A., TRIMBLE, C. L., ADLER, A. J., LIN, T. Y., PARDOLL, D. M., HUANG, C. T. & DRAKE, C. G. 2009. Tc17 CD8 T cells: functional plasticity and subset diversity. *J Immunol,* 183**,** 7161-8.
YOKOSUKA, T., TAKAMATSU, M., KOBAYASHI-IMANISHI, W., HASHIMOTO-TANE, A., AZUMA, M. & SAITO, T. 2012. Programmed cell death 1 forms negative costimulatory microclusters that directly inhibit T cell receptor signaling by recruiting phosphatase SHP2. *Journal of Experimental Medicine,* 209**,** 1201-1217.
YU, D., RAO, S., TSAI, L. M., LEE, S. K., HE, Y., SUTCLIFFE, E. L., SRIVASTAVA, M., LINTERMAN, M., ZHENG, L., SIMPSON, N., ELLYARD, J. I., PARISH, I. A., MA, C. S., LI, Q. J., PARISH, C. R., MACKAY, C. R. & VINUESA, C. G. 2009. The transcriptional repressor Bcl-6 directs T follicular helper cell lineage commitment. *Immunity,* 31**,** 457-68.
YU, D. & VINUESA, C. G. 2010. The elusive identity of T follicular helper cells. *Trends Immunol,* 31**,** 377-83.
YUEN, G. J., DEMISSIE, E. & PILLAI, S. 2016. B lymphocytes and cancer: a love–hate relationship. *Trends in cancer,* 2**,** 747-757.
YUSUF, I., KAGEYAMA, R., MONTICELLI, L., JOHNSTON, R. J., DITORO, D., HANSEN, K., BARNETT, B. & CROTTY, S. 2010. Germinal center T follicular helper cell IL-4 production is dependent on signaling lymphocytic activation molecule receptor (CD150). *The Journal of Immunology,* 185**,** 190-202.
ZAIDI, M. R. & MERLINO, G. 2011. The two faces of interferon-γ in cancer. *Clin Cancer Res,* 17**,** 6118-24.
ZAPPASODI, R., SERGANOVA, I., COHEN, I. J., MAEDA, M., SHINDO, M., SENBABAOGLU, Y., WATSON, M. J., LEFTIN, A., MANIYAR, R., VERMA, S., LUBIN, M., KO, M., MANE, M. M., ZHONG, H., LIU, C., GHOSH, A., ABU-AKEEL, M., ACKERSTAFF, E., KOUTCHER, J. A., HO, P. C., DELGOFFE, G. M., BLASBERG,

R., WOLCHOK, J. D. & MERGHOUB, T. 2021. CTLA-4 blockade drives loss of T(reg) stability in glycolysis-low tumours. *Nature,* 591**,** 652-658.
ZARAGOZA, B., CHEN, X., OPPENHEIM, J. J., BAEYENS, A., GREGOIRE, S., CHADER, D., GOROCHOV, G., MIYARA, M. & SALOMON, B. L. 2016. Suppressive activity of human regulatory T cells is maintained in the presence of TNF. *Nature medicine,* 22**,** 16-17.
ZHANG, B., CHIKUMA, S., HORI, S., FAGARASAN, S. & HONJO, T. 2016. Nonoverlapping roles of PD-1 and FoxP3 in maintaining immune tolerance in a novel autoimmune pancreatitis mouse model. *Proceedings of the National Academy of Sciences,* 113**,** 8490-8495.
ZHANG, C. Y., QI, Y., LI, X. N., YANG, Y., LIU, D. L., ZHAO, J., ZHU, D. Y., WU, K., ZHOU, X. D. & ZHAO, S. 2015. The role of CCL20/CCR6 axis in recruiting Treg cells to tumor sites of NSCLC patients. *Biomed Pharmacother,* 69**,** 242-8.
ZHANG, R., HUYNH, A., WHITCHER, G., CHANG, J., MALTZMAN, J. S. & TURKA, L. A. 2013a. An obligate cell-intrinsic function for CD28 in Tregs. *The Journal of clinical investigation,* 123.
ZHANG, S., FUJITA, H., MITSUI, H., YANOFSKY, V. R., FUENTES-DUCULAN, J., PETTERSEN, J. S., SUÁREZ-FARIÑAS, M., GONZALEZ, J., WANG, C. Q., KRUEGER, J. G., FELSEN, D. & CARUCCI, J. A. 2013b. Increased Tc22 and Treg/CD8 ratio contribute to aggressive growth of transplant associated squamous cell carcinoma. *PLoS One,* 8**,** e62154.
ZHANG, Y., HOU, F., LIU, X., MA, D., ZHANG, Y., KONG, B. & CUI, B. 2014. Tc17 cells in patients with uterine cervical cancer. *PLoS One,* 9**,** e86812.
ZHANG, Y., TECH, L., GEORGE, L. A., ACS, A., DURRETT, R. E., HESS, H., WALKER, L. S. K., TARLINTON, D. M., FLETCHER, A. L., HAUSER, A. E. & TOELLNER, K. M. 2018. Plasma cell output from germinal centers is regulated by signals from Tfh and stromal cells. *J Exp Med,* 215**,** 1227-1243.
ZHANG, Z. S., GU, Y., LIU, B. G., TANG, H., HUA, Y. & WANG, J. 2020. Oncogenic role of Tc17 cells in cervical cancer development. *World J Clin Cases,* 8**,** 11-19.
ZHAO, C., WANG, D., TANG, L., ZHANG, Z., LI, S., QIAN, M., WU, Z., ZHOU, W., LIU, M., LUO, J., LIU, T., LI, Z. & XIAO, J. 2018. Stromal Cell-Derived CCL20 Promotes Tumor Progression and Osteolysis in Giant Cell Tumor of Bone. *Cell Physiol Biochem,* 51**,** 2472-2483.
ZHOU, M., BRACCI, P. M., MCCOY, L. S., HSUANG, G., WIEMELS, J. L., RICE, T., ZHENG, S., KELSEY, K. T., WRENSCH, M. R. & WIENCKE, J. K. 2015. Serum macrophage-derived chemokine/CCL22 levels are associated with glioma risk, CD4 T cell lymphopenia and survival time. *Int J Cancer,* 137**,** 826-36.
ZHOU, S., SHEN, Z., WANG, Y., MA, H., XU, S., QIN, J., CHEN, L., TAO, H., ZHEN, Z., CHEN, G., ZHANG, Z., LI, R., XIAO, H., ZHONG, C., YANG, Y. & LIANG, C. 2013. CCR7 expression and intratumoral FOXP3+ regulatory T cells are correlated with overall survival and lymph node metastasis in gastric cancer. *PLoS One,* 8**,** e74430.
ZHU, J., YAMANE, H. & PAUL, W. E. 2009. Differentiation of effector CD4 T cell populations. *Annual review of immunology,* 28**,** 445-489.
ZHUANG, Y., PENG, L. S., ZHAO, Y. L., SHI, Y., MAO, X. H., CHEN, W., PANG, K. C., LIU, X. F., LIU, T., ZHANG, J. Y., ZENG, H., LIU, K. Y., GUO, G., TONG, W. D., SHI, Y., TANG, B., LI, N., YU, S., LUO, P., ZHANG, W. J., LU, D. S., YU, P. W. & ZOU, Q. M. 2012. CD8(+) T cells that produce interleukin-17 regulate myeloid-derived suppressor cells and are associated with survival time of patients with gastric cancer. *Gastroenterology,* 143**,** 951-62.e8.
ZNAOR, A., LORTET-TIEULENT, J., JEMAL, A. & BRAY, F. 2014. International variations and trends in testicular cancer incidence and mortality. *European urology,* 65**,** 1095-1106.

Supplementary Figures

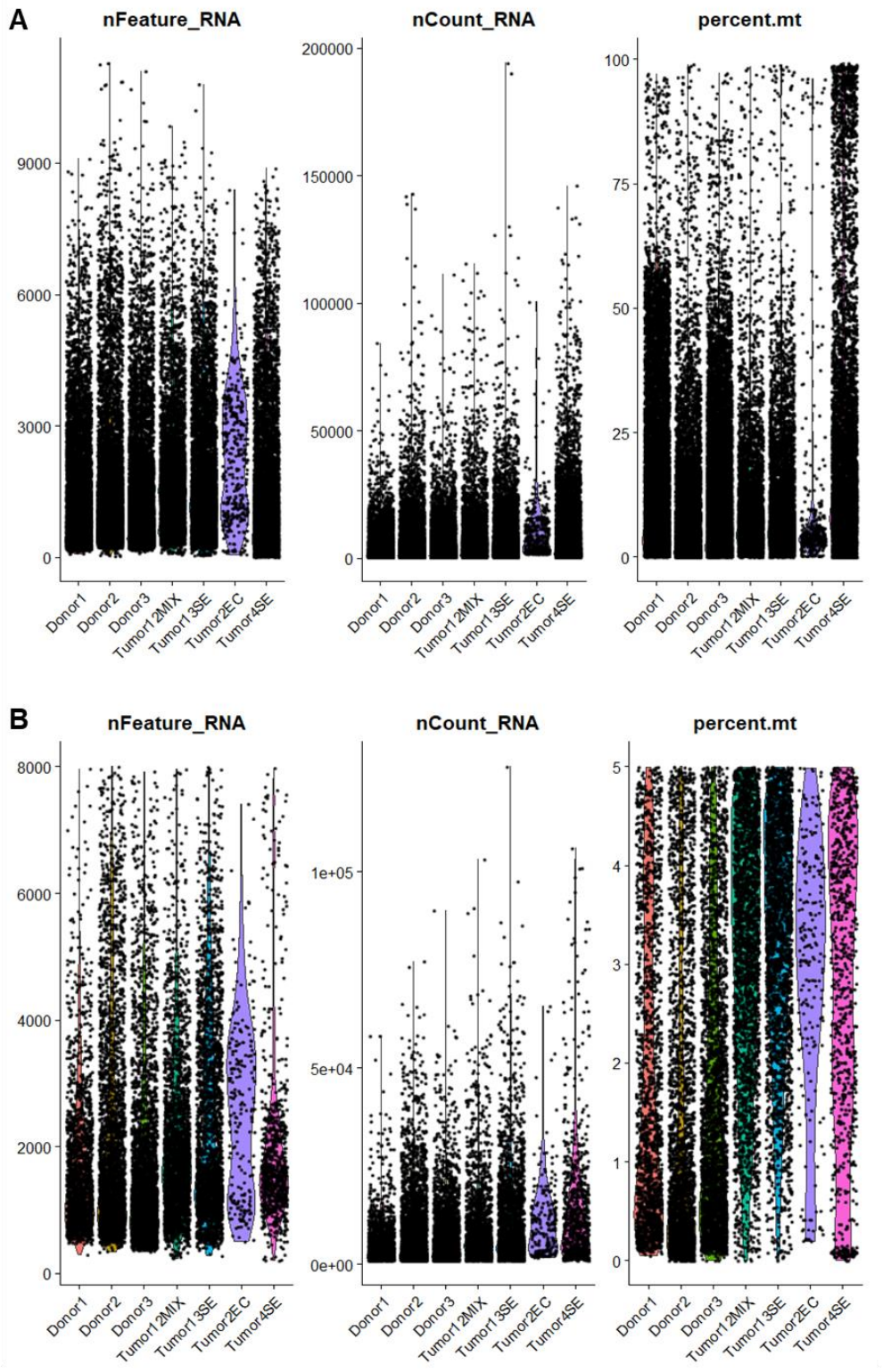

Supplementary Figure 1: Analytical filtration of scRNA-seq data. Violin plots show the quality control metrics before (A) and after analytical filtration (B) of nCount_RNA (the total number of molecules detected within a cell) > 1000, nFeature_RNA (the number of genes detected in each cell) > 200-< 8000 and percent.mt (mitochondrial genes) < 5.

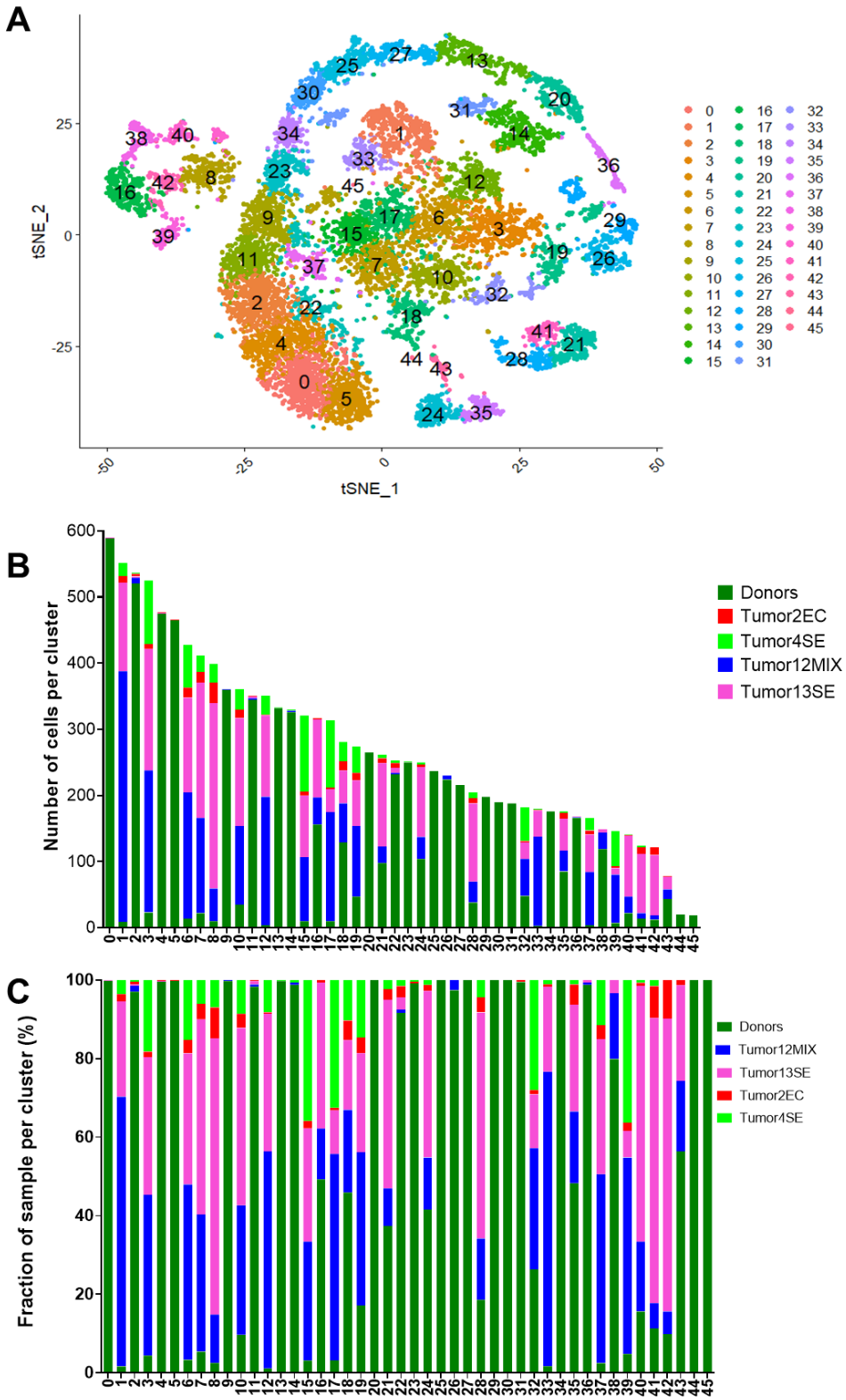

Supplementary Figure 2 The clustering information of cells in the scRNA-seq data sets. A. tSNE presentation of primary clusters (before identification) of different cell landscape in donors (n=3; pooled data) and TGCT samples (Tumor12MIX: mixed TGCT, Tumor13SE: seminoma, Tumor4SE: seminoma, Tumor2EC: embryonal carcinoma). B. Bar plot shows the number of cells per cluster from donors and TGCT samples. C. Bar plot shows the relative contribution of each cluster by studied samples.

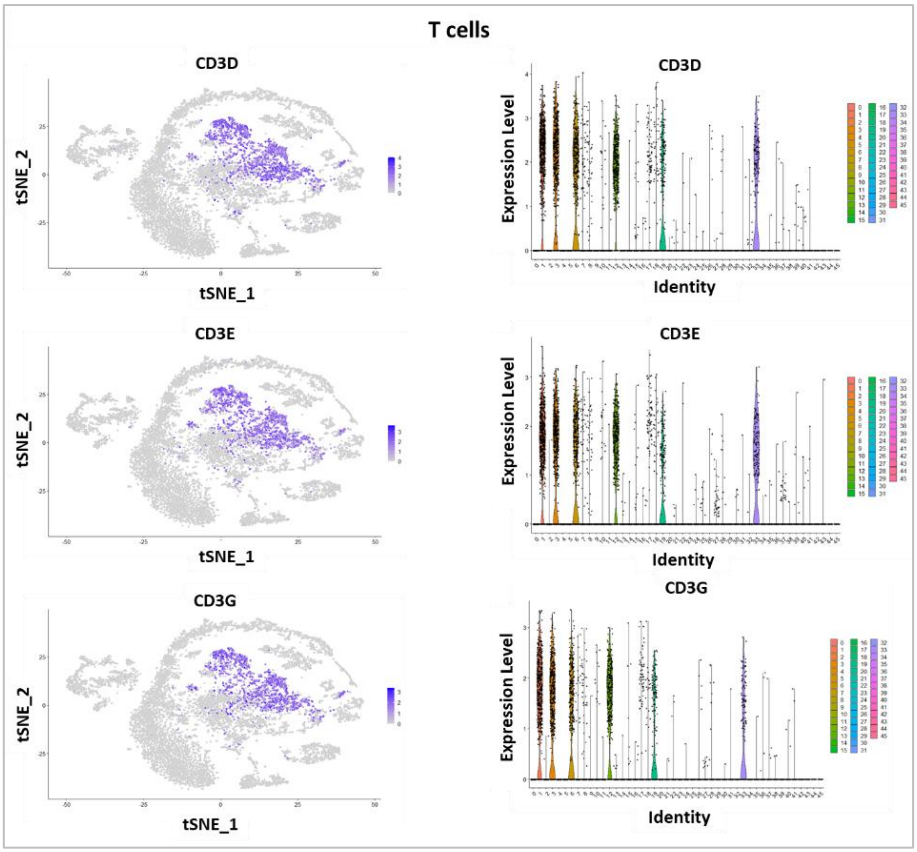

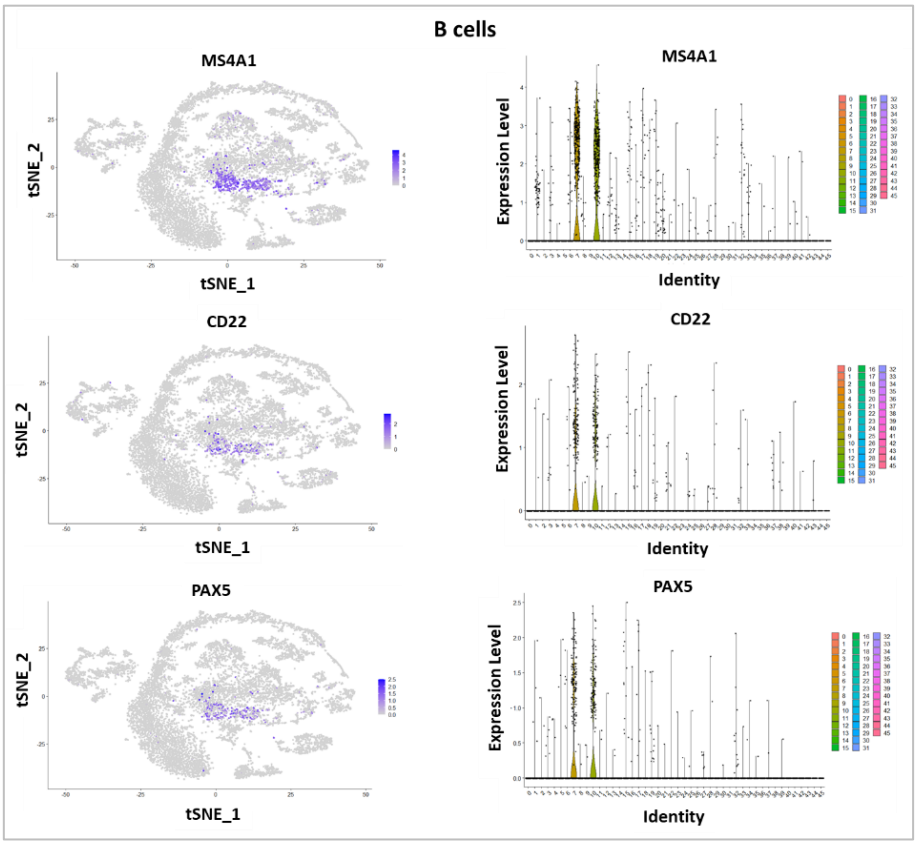

Supplementary Figure 3 Cont.

Supplementary Figure 3 Cont.

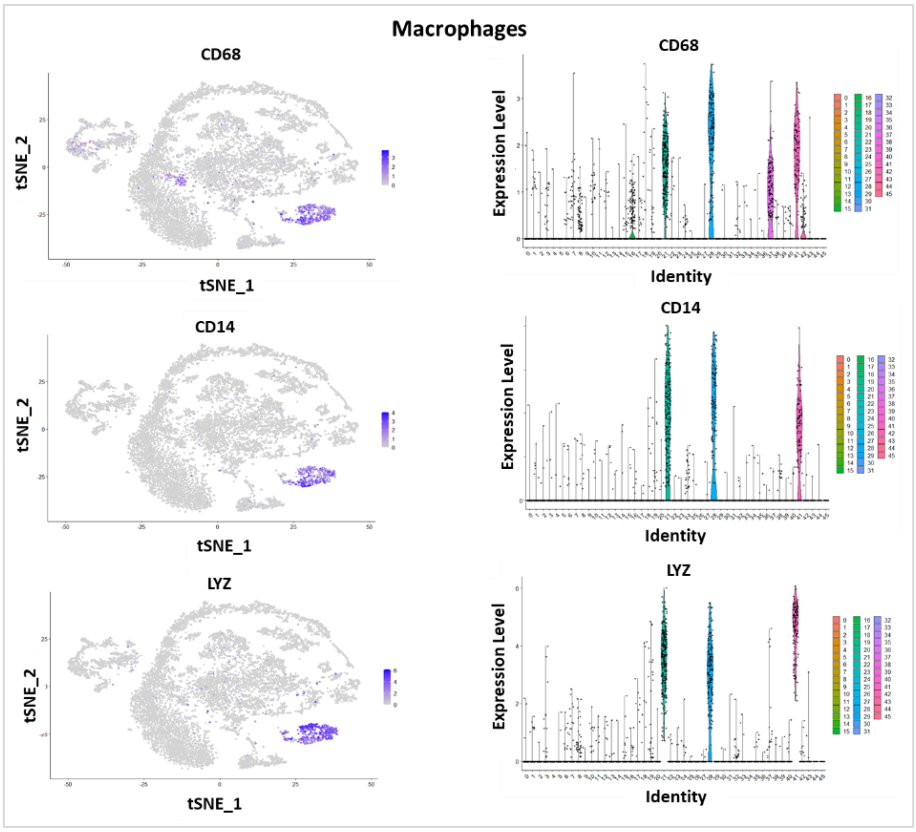

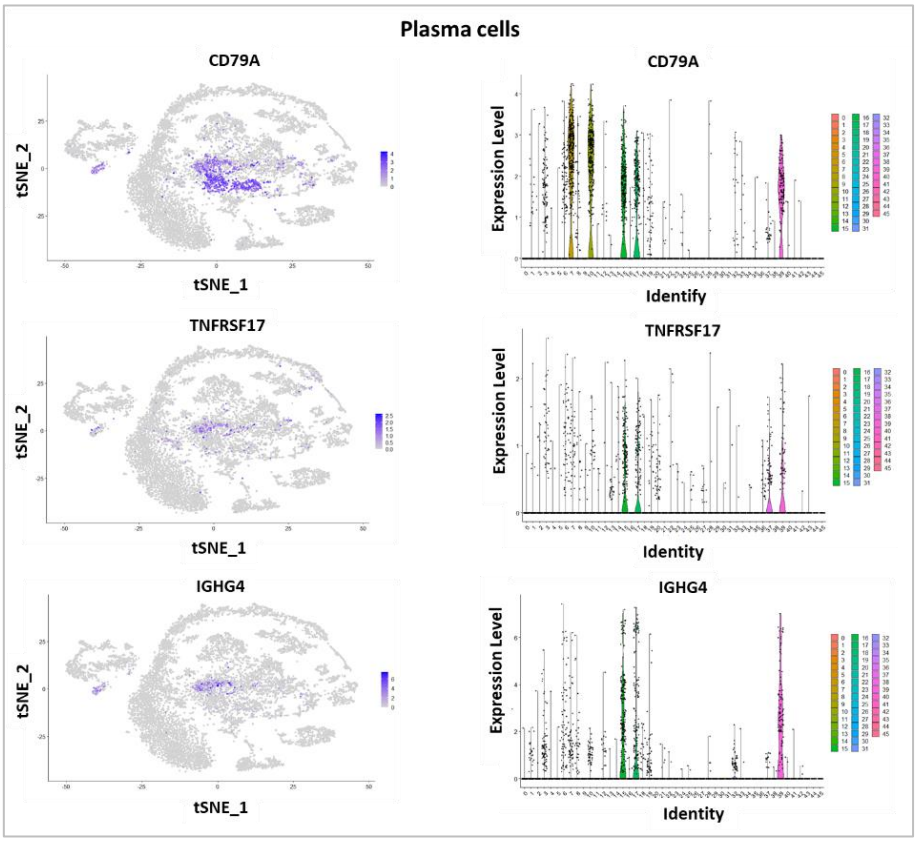

Supplementary Figure 3 Cont.

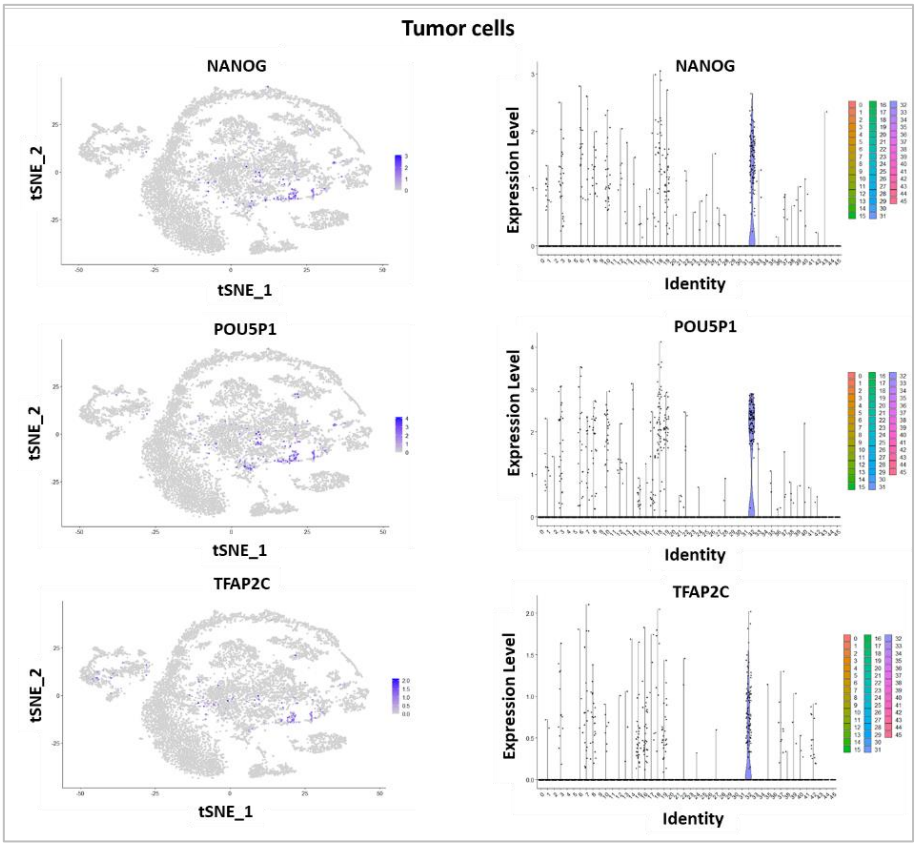

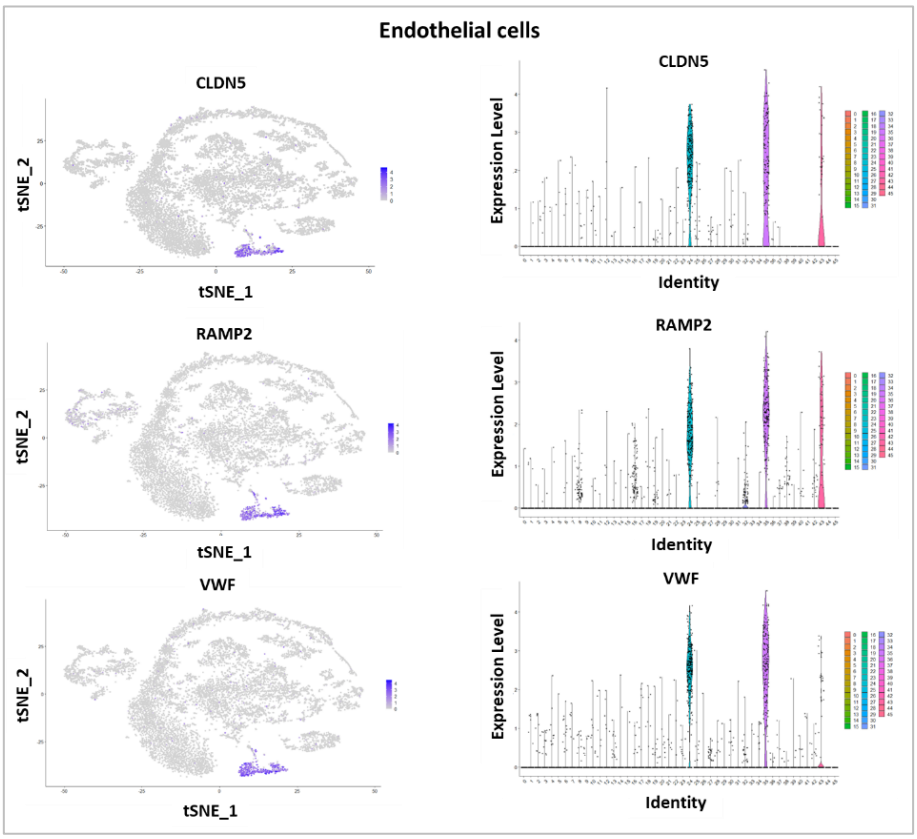

Supplementary Figure 3 Cont.

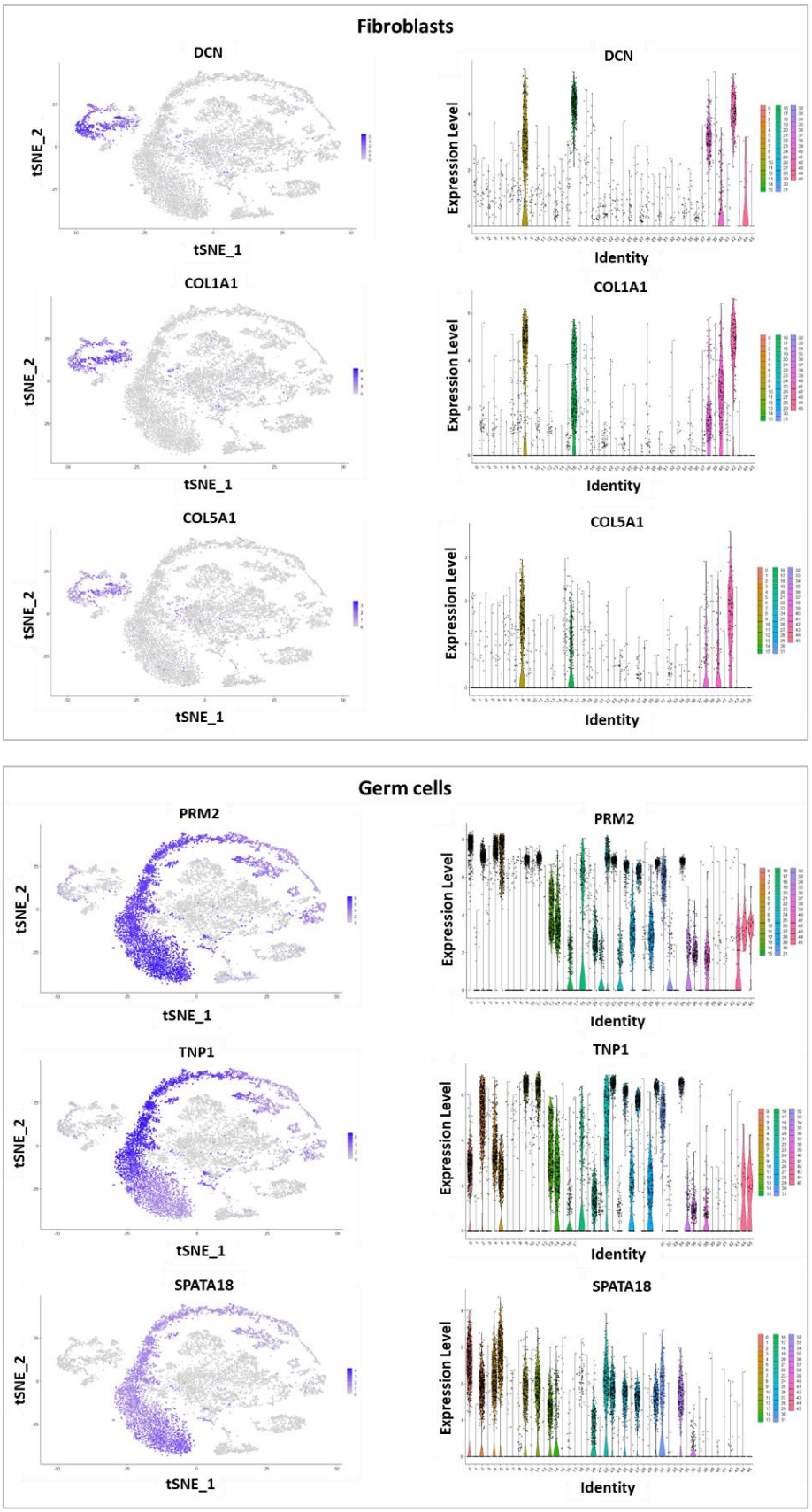

Supplementary Figure 3 Identification of primary clusters. tSNE plots and Violin plots show the expression of selected markers for each cell type throughout 46 clusters.

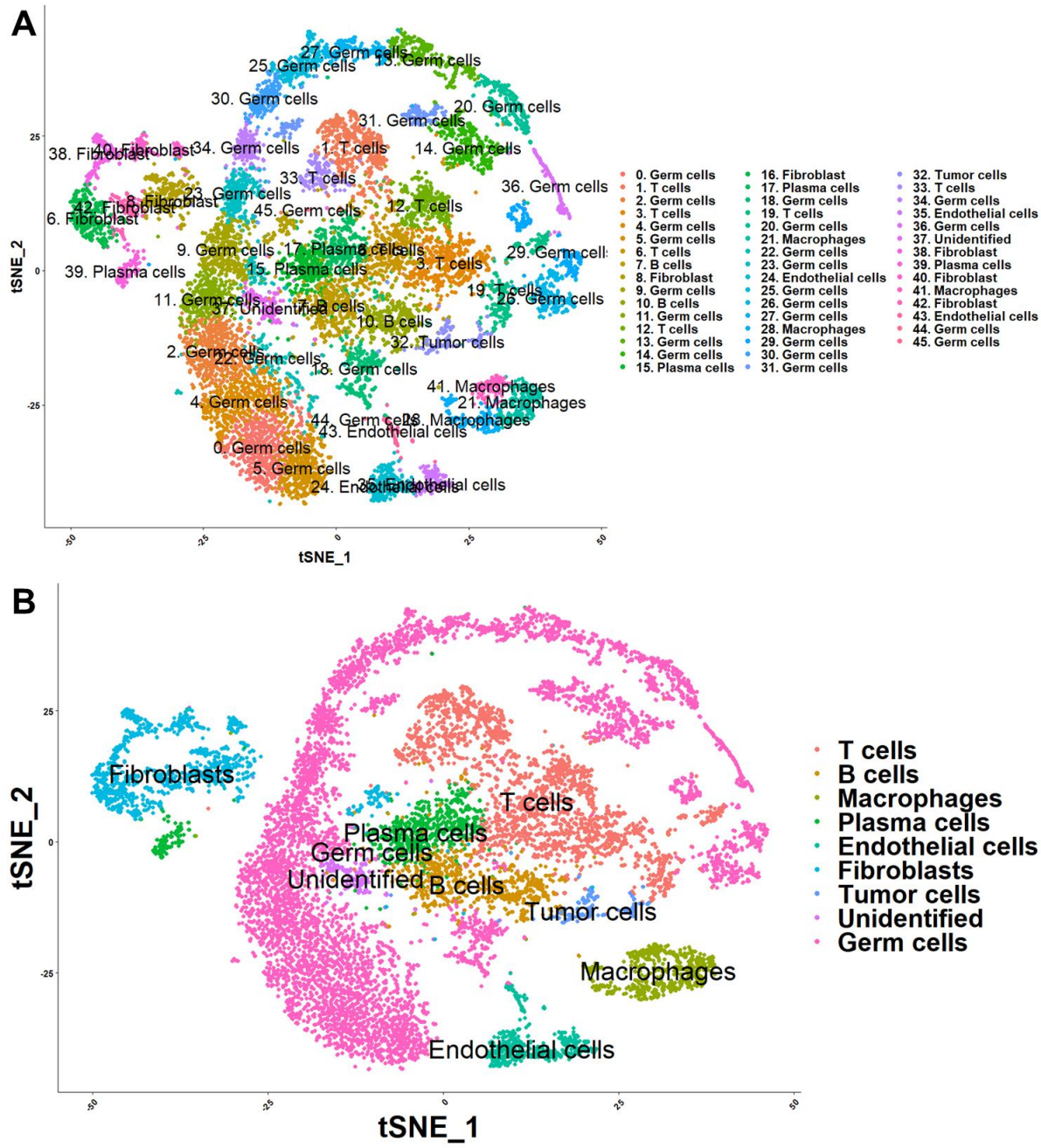

Supplementary Figure 4 Visualization of identified cell types in two dimensions with tSNE. A. Putative cell cluster labels are based on the differential gene expression of known markers for each cell type in 46 clusters. B. Simplified representation of different cell types found in the analyzed subjects.

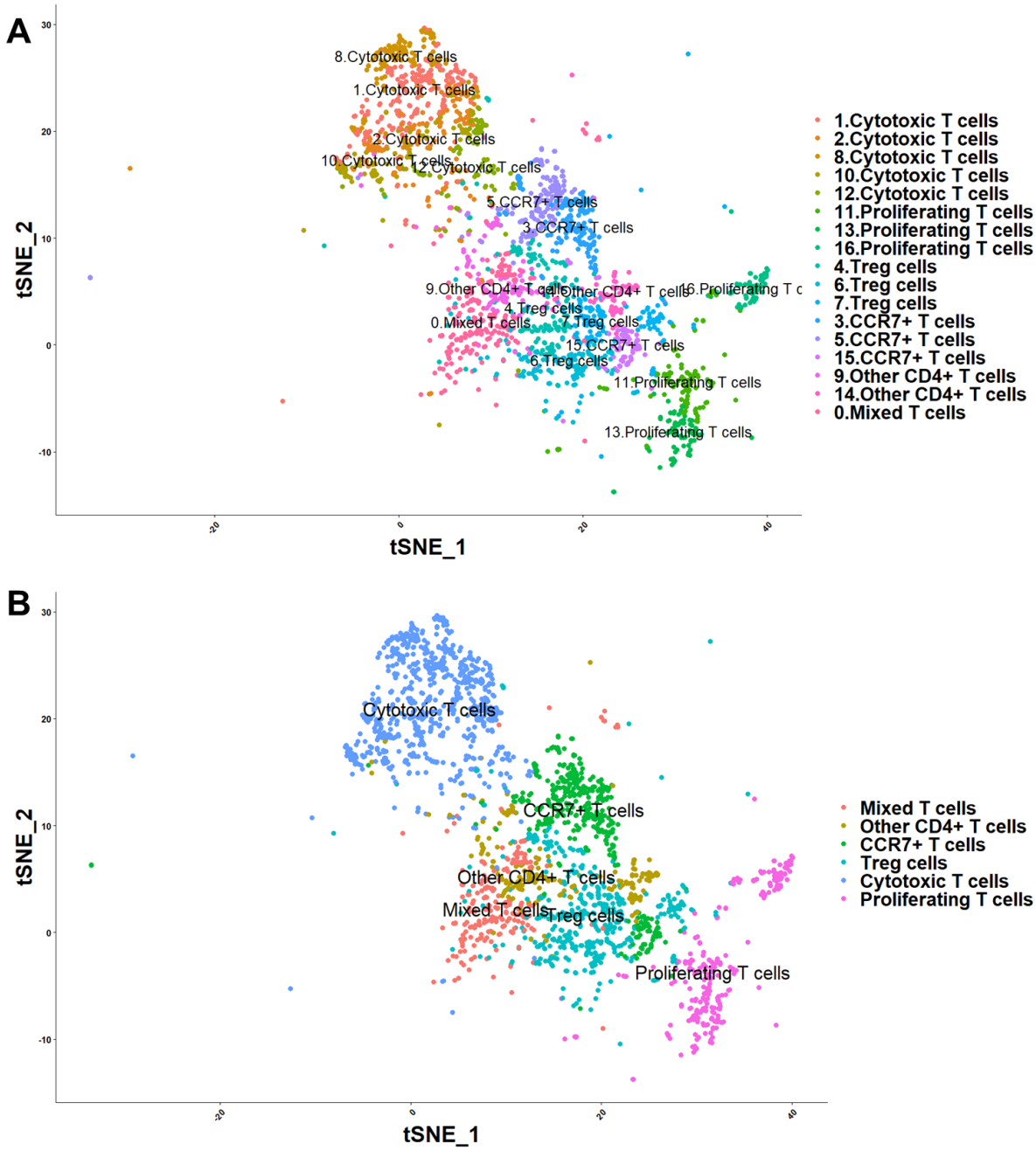

Supplementary Figure 5: Visualization of identified cell types in two dimensions with tSNE. A. Putative cell cluster labels are based on the differential gene expression of known markers for each T cell subtypes in 17 clusters. B. Simplified representation of different T cell subtypes found in the analyzed subjects.

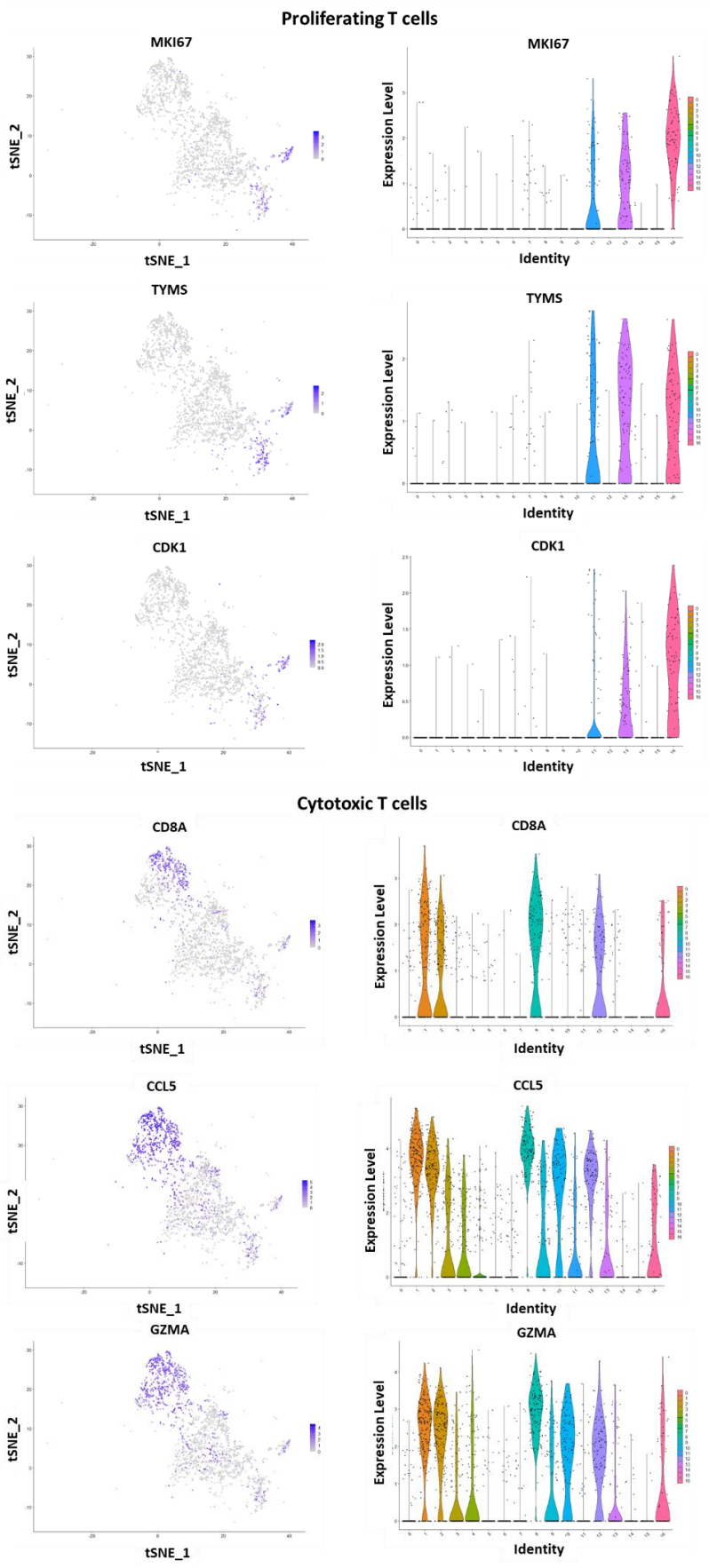

Supplementary Figure 6 Cont.

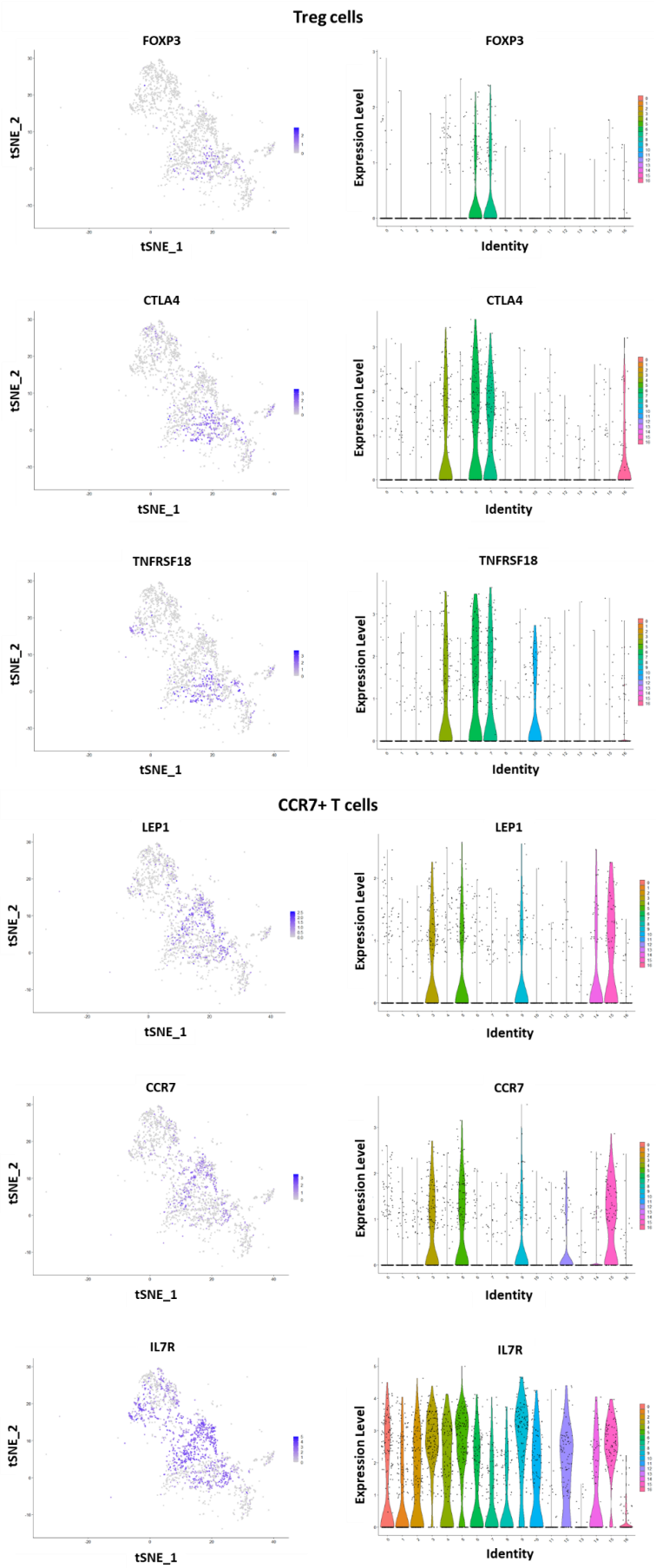

Supplementary Figure 6 Cont.

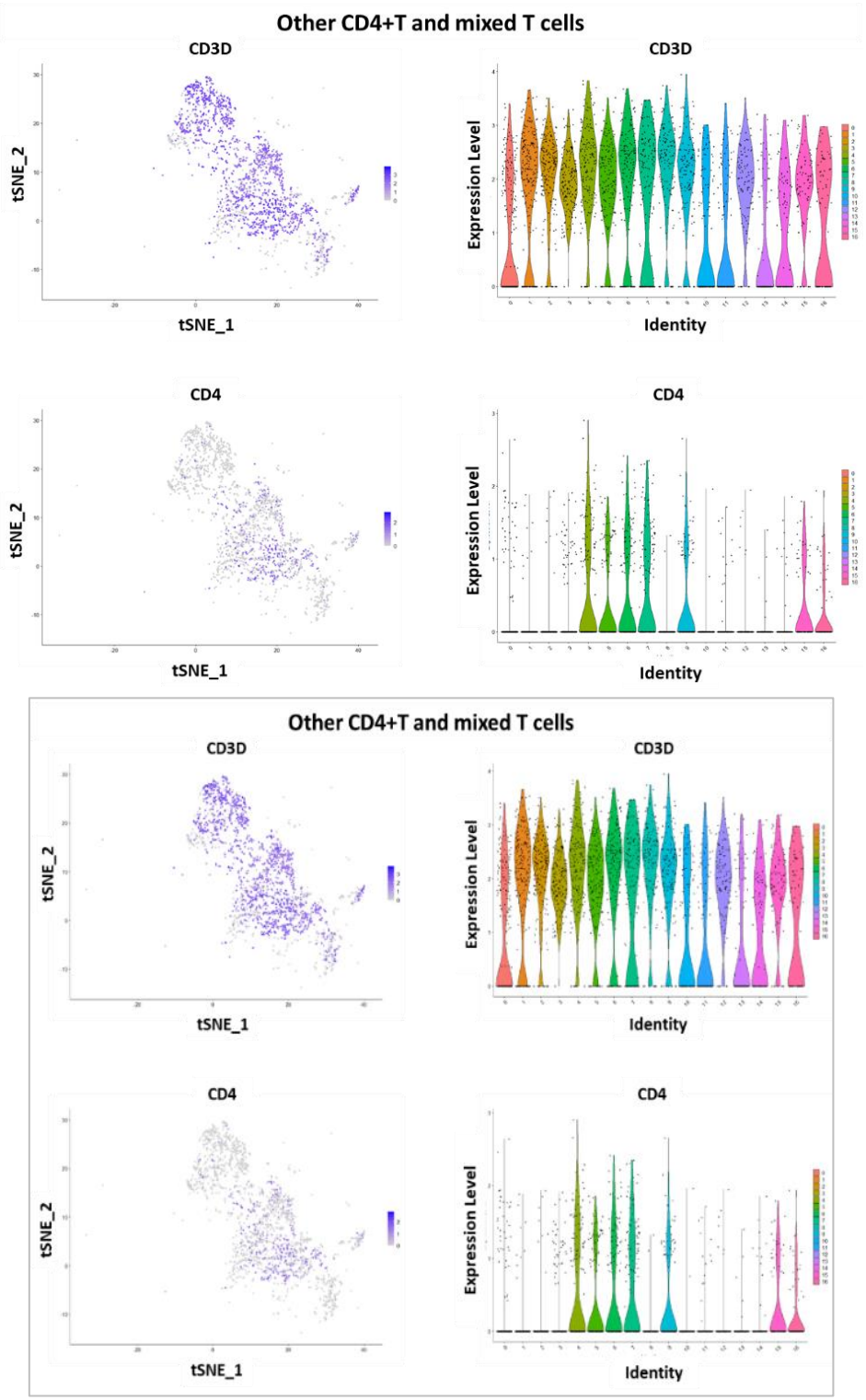

Supplementary Figure 6 Identification of secondary clusters of T cells. tSNE plots and Violin plots show the expression of selected markers for each T cell subtypes throughout 17 clusters.

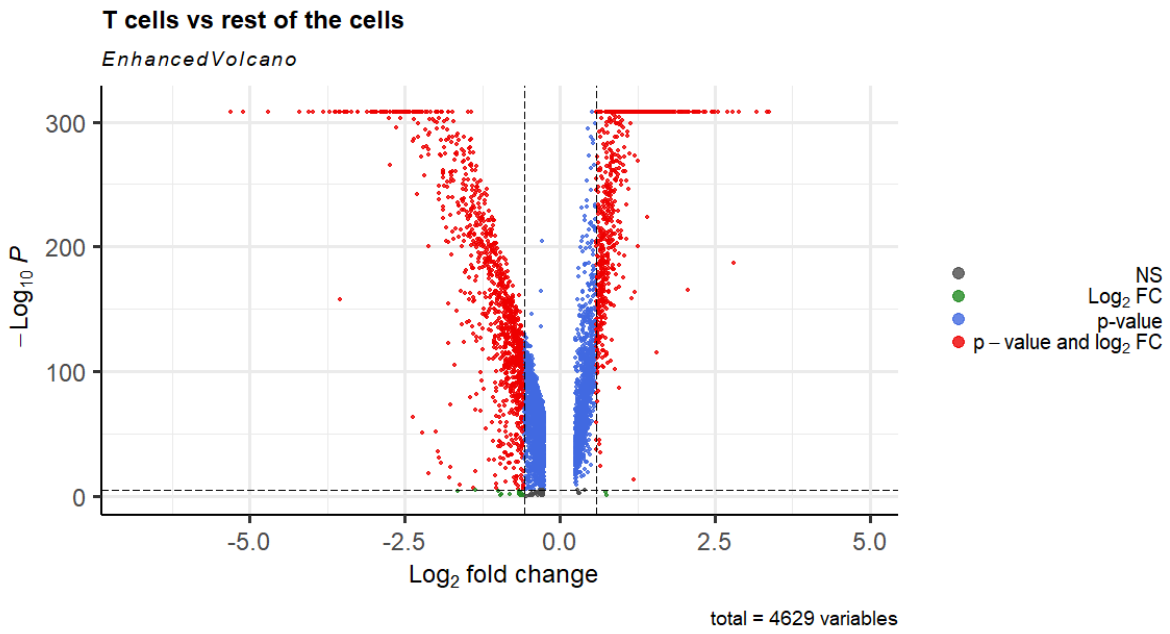

Supplementary Figure 7 Differential gene expression analysis of T cells vs rest of the cells in human testis.

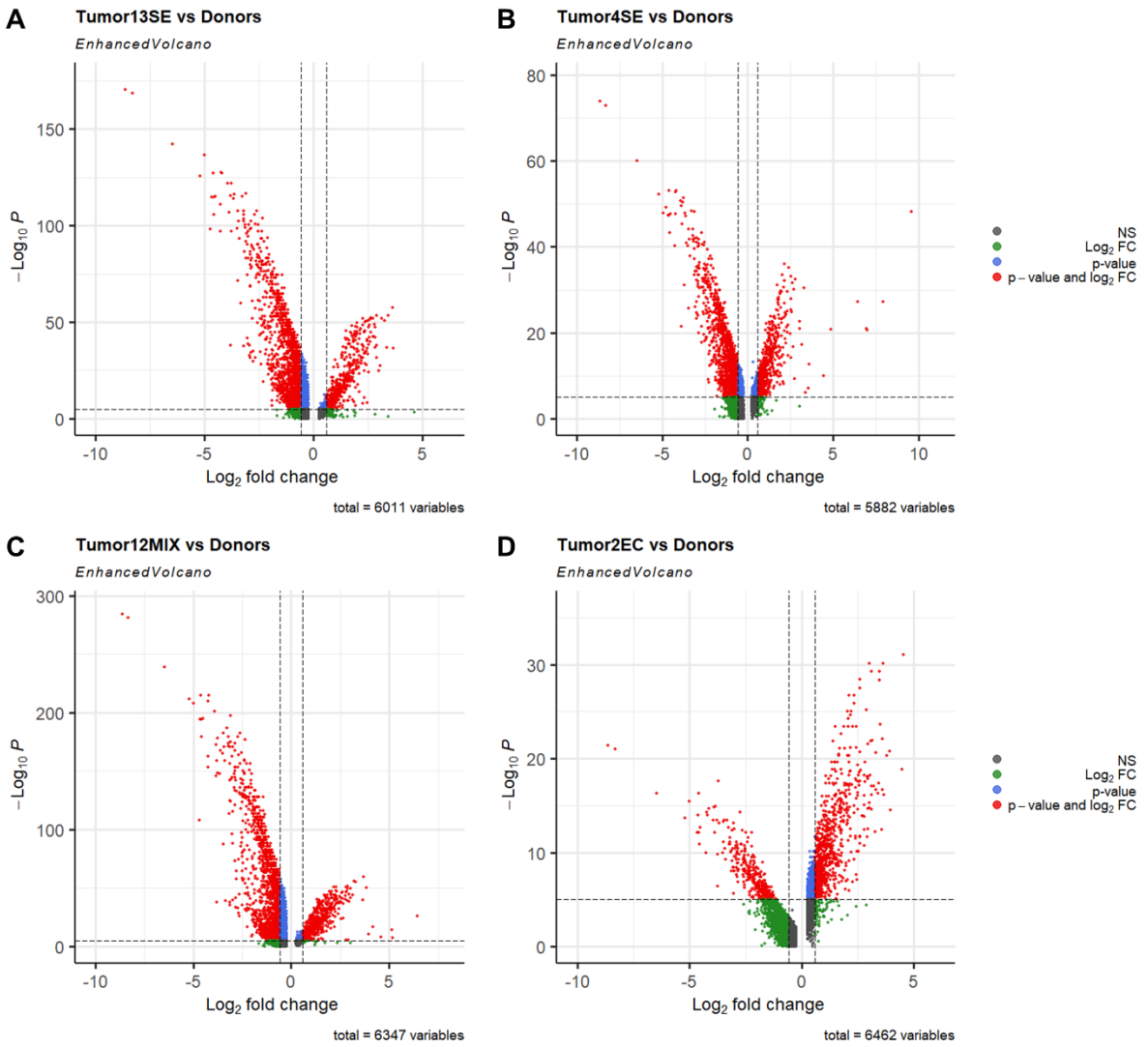

Supplementary Figure 8 Differential gene expression analysis of T cells from different TGCT vs Donors. Volcano plot shows the differential gene expressions of T cells from Tumor 13SE vs Donors (A), Tumor 4SE vs Donors (B), Tumor 12MIX vs Donors (C) and Tumor 2EC vs Donors (D).

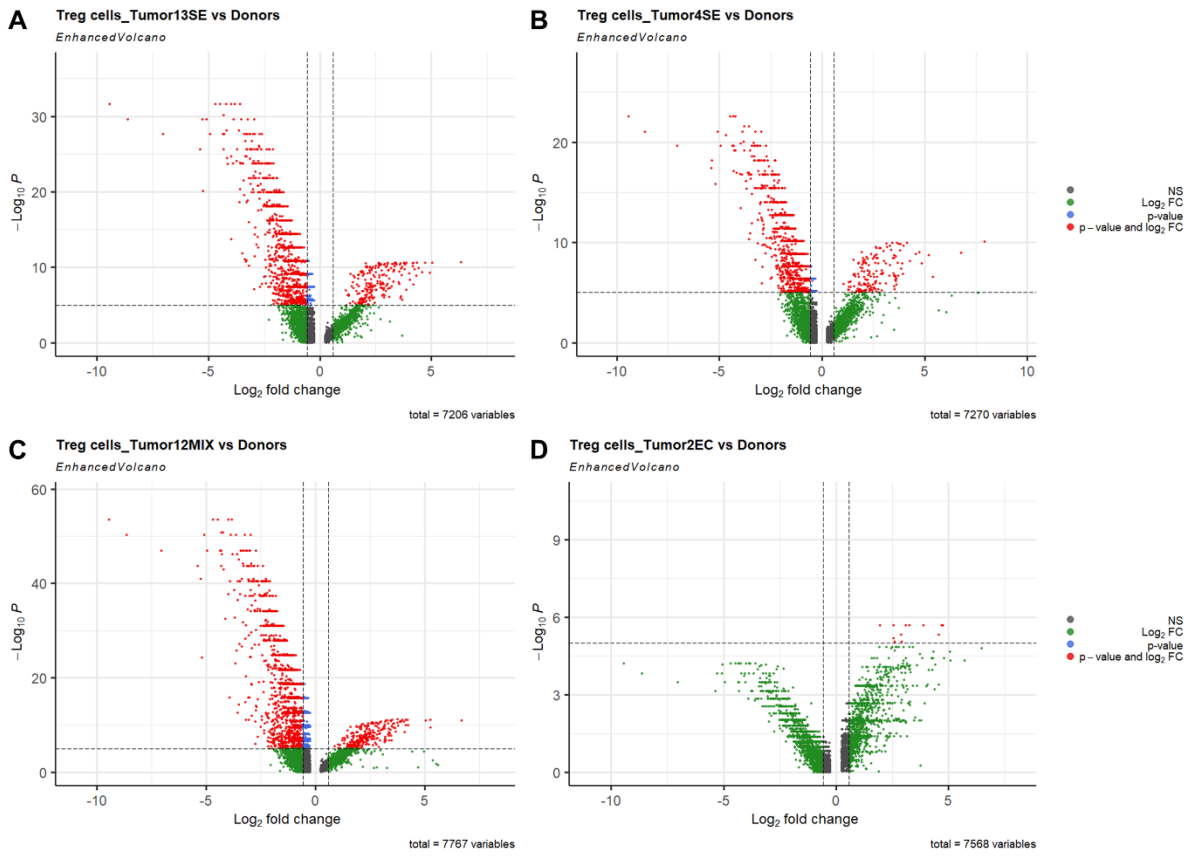

Supplementary Figure 9: Differential gene expression analysis of Treg cells from different TGCT vs Donors. Volcano plot shows the differential gene expressions of T cells from Tumor 13SE vs Donors (A), Tumor 4SE vs Donors (B), Tumor 12MIX vs Donors (C) and Tumor 2EC vs Donors (D).

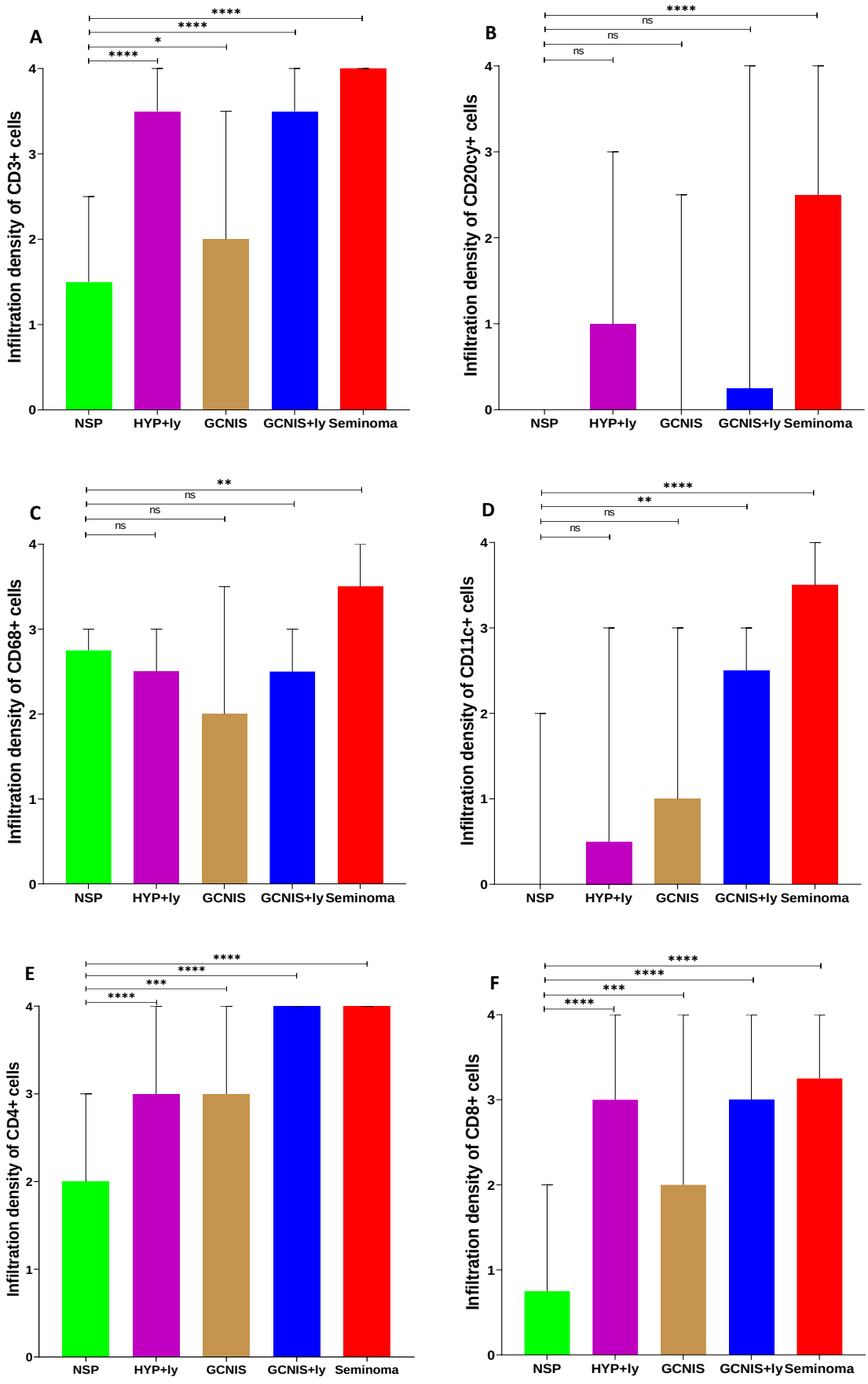

Supplementary Figure 10 See next page for caption

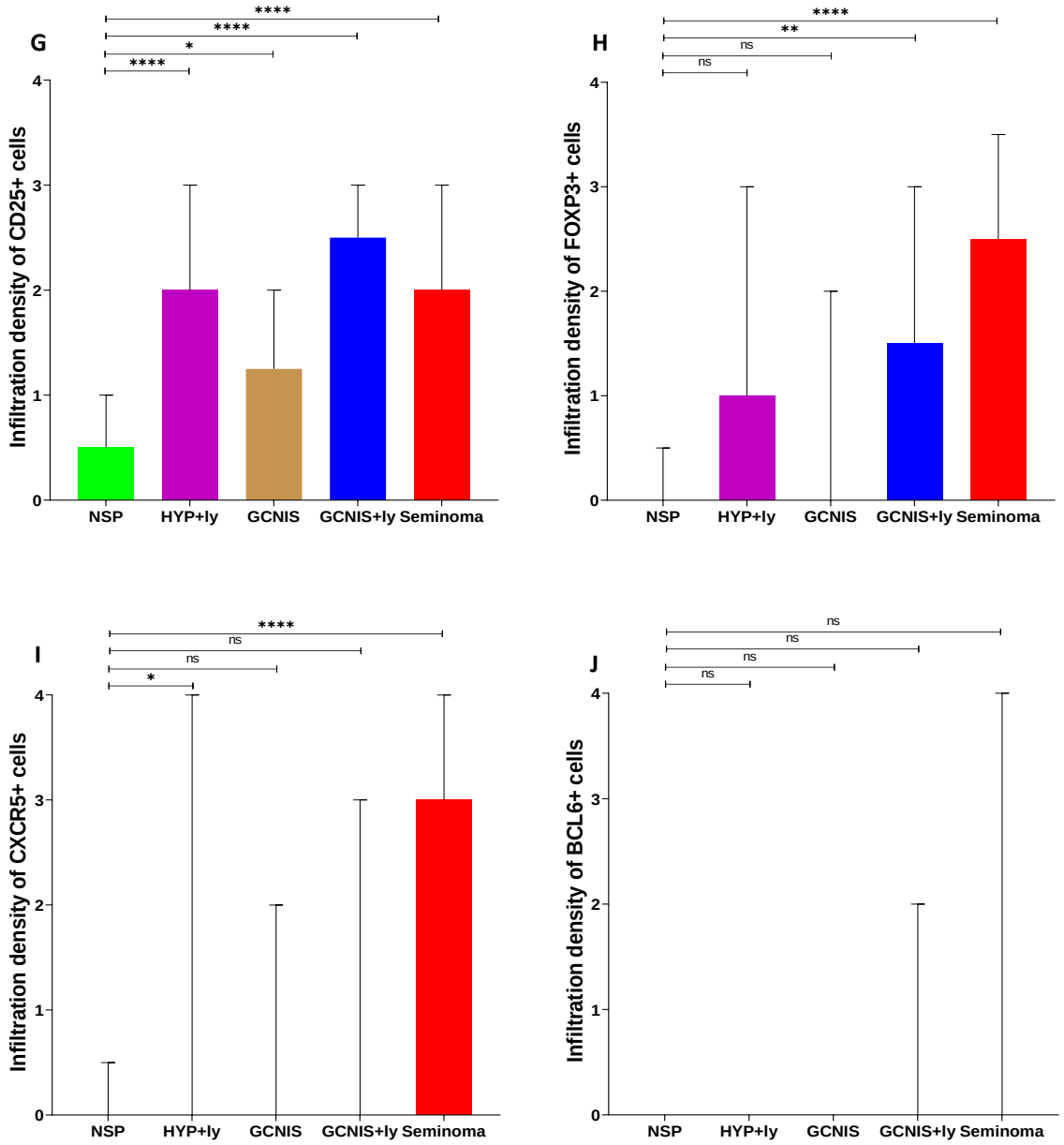

Supplementary Figure 10 Cumulative representation of the infiltration density of different immune cells in different samples. Infiltration density 0=absent, 1=single cells, 2=scatter, 3=sparse, 4=dense. Significance tested by ordinary one-way ANOVA including Tukey's Honest Significant Difference Test [(Not significant (ns)= p-value ≥ 0.05), (Significant, *= p-value 0.01 to 0.05, **= p-value = 0.001 to 0.01, ***= p-value 0.0001 to 0.001, ****= p-value <0.0001)].

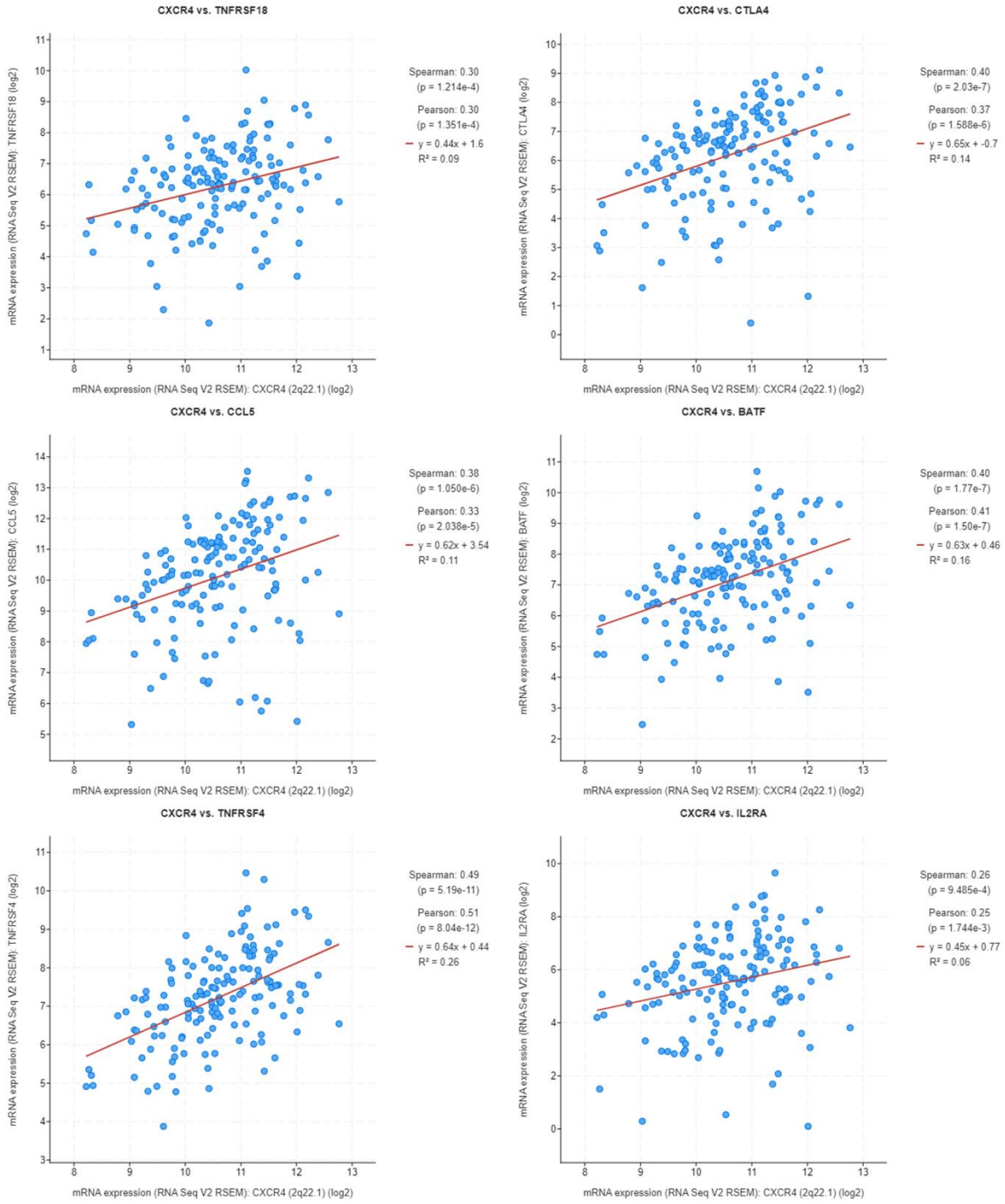

Supplementary Figure 11 Cont.

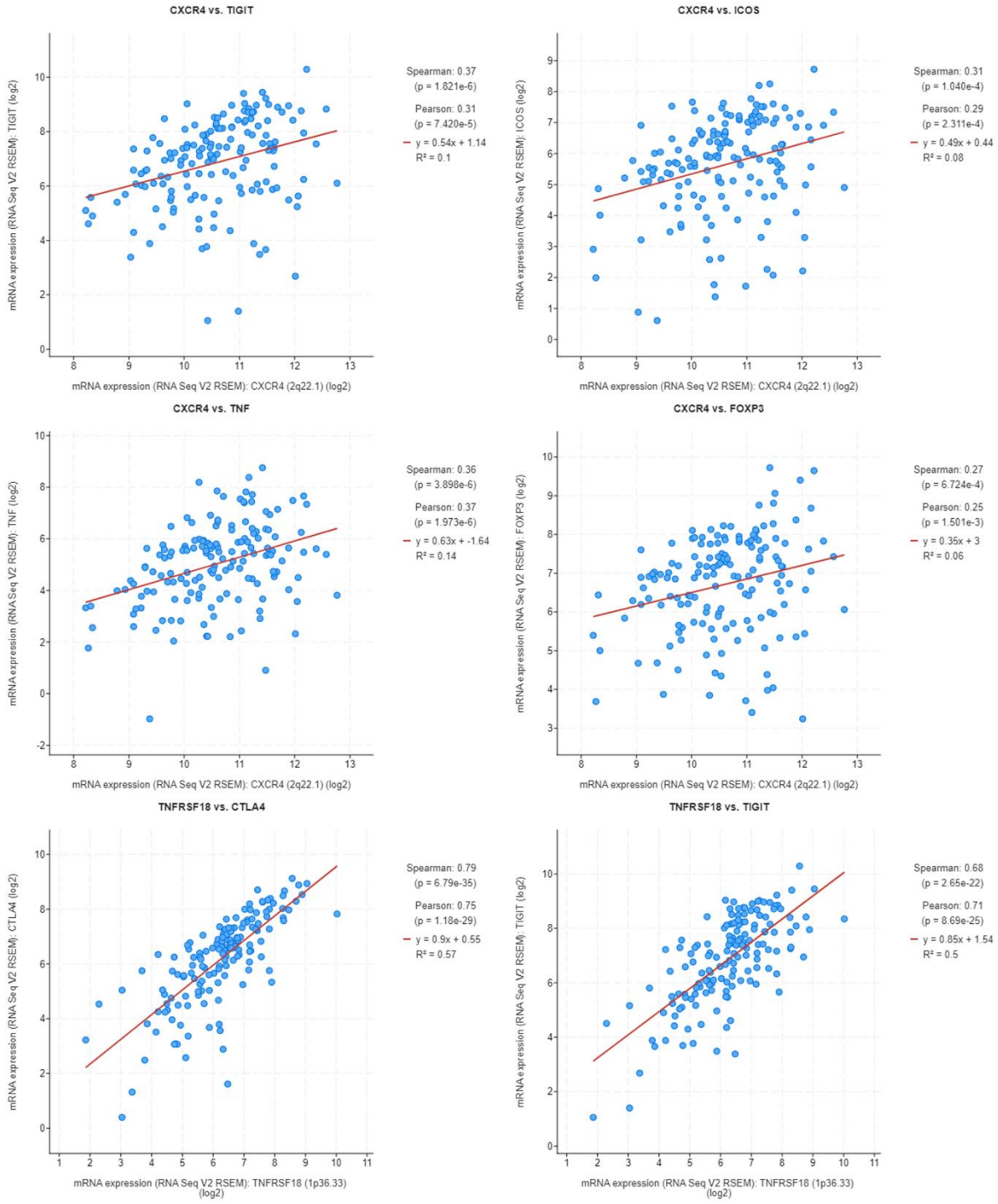

Supplementary Figure 11 Cont.

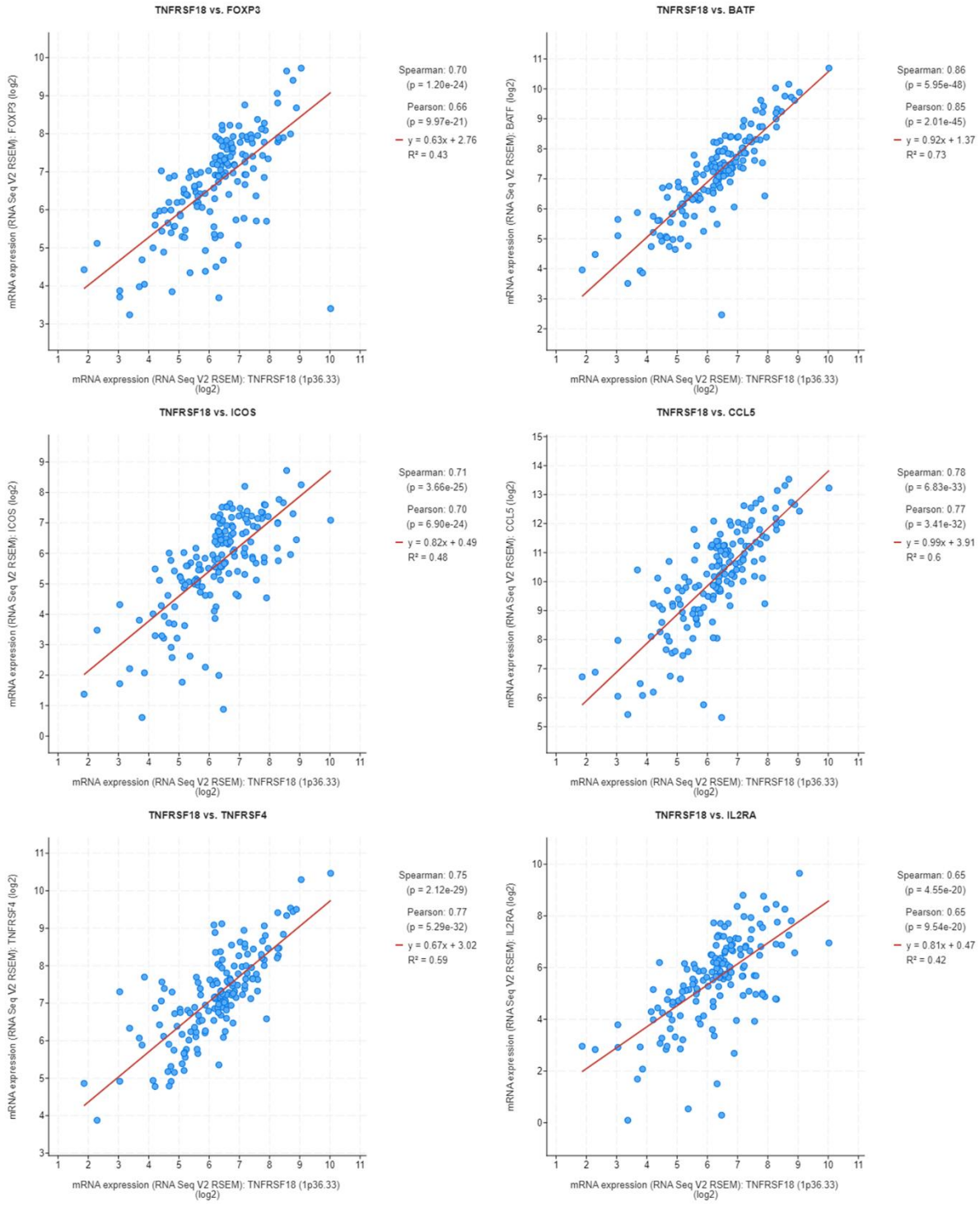

Supplementary Figure 11 Cont.

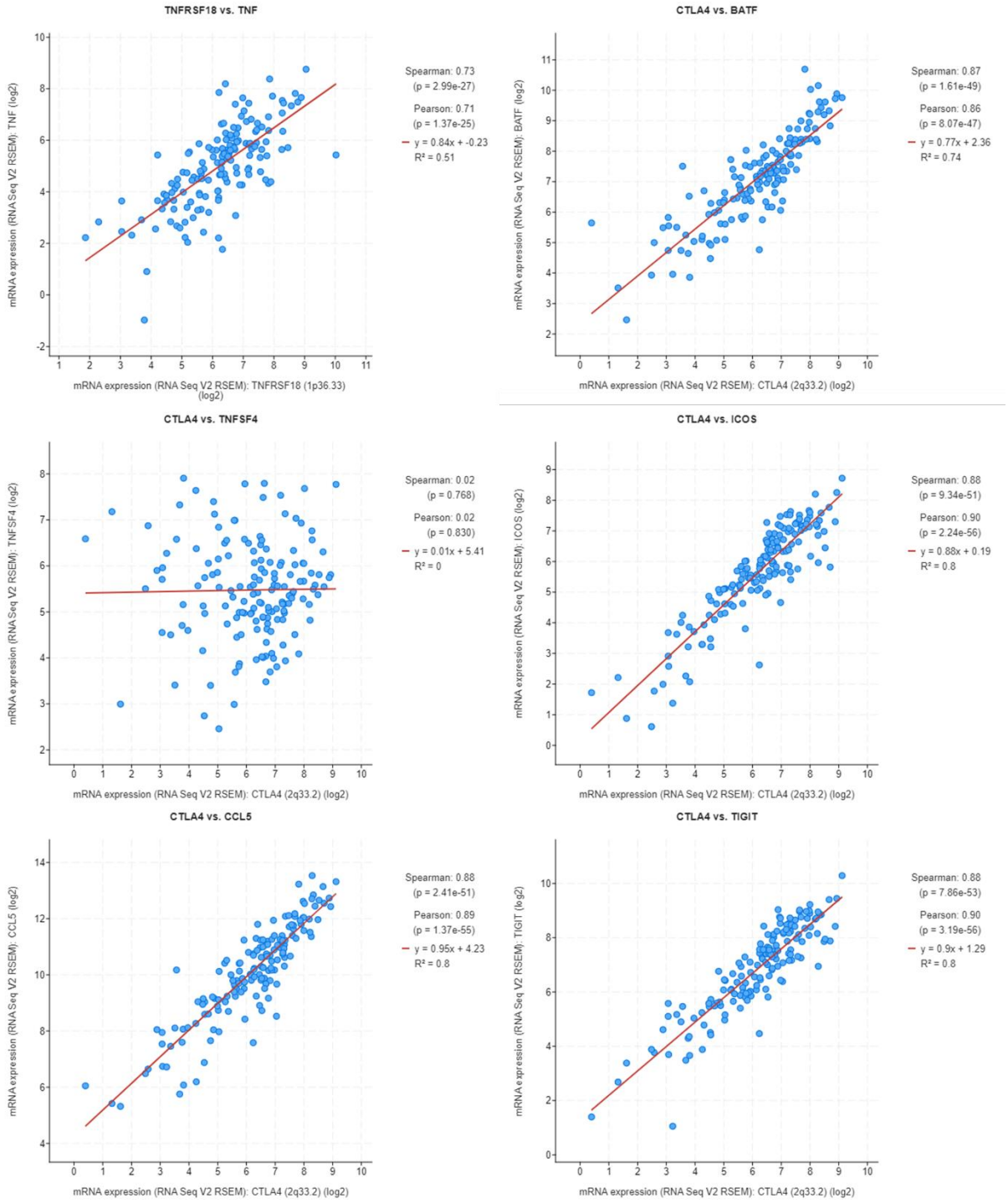

Supplementary Figure 11 Cont.

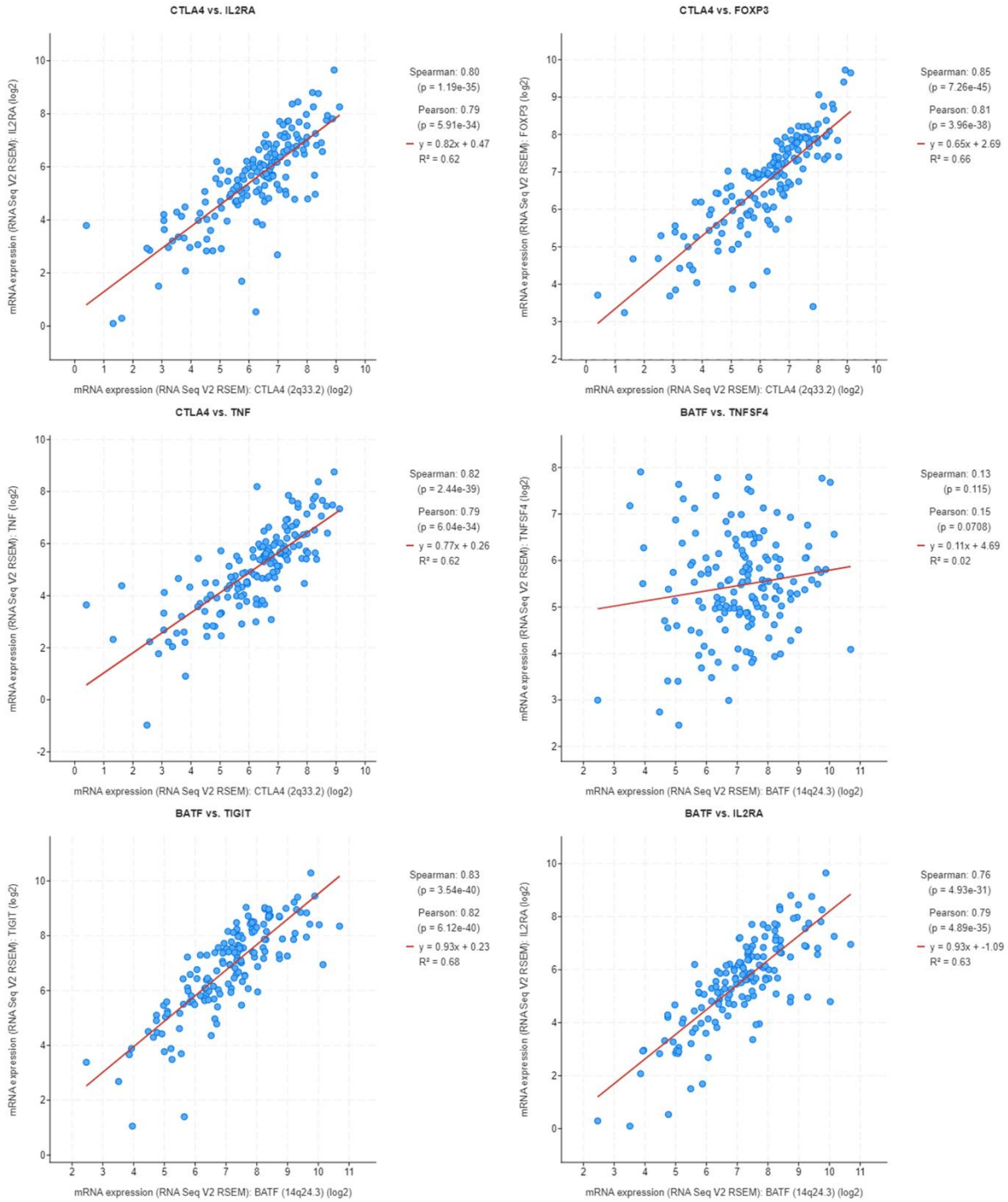

Supplementary Figure 11 Cont.

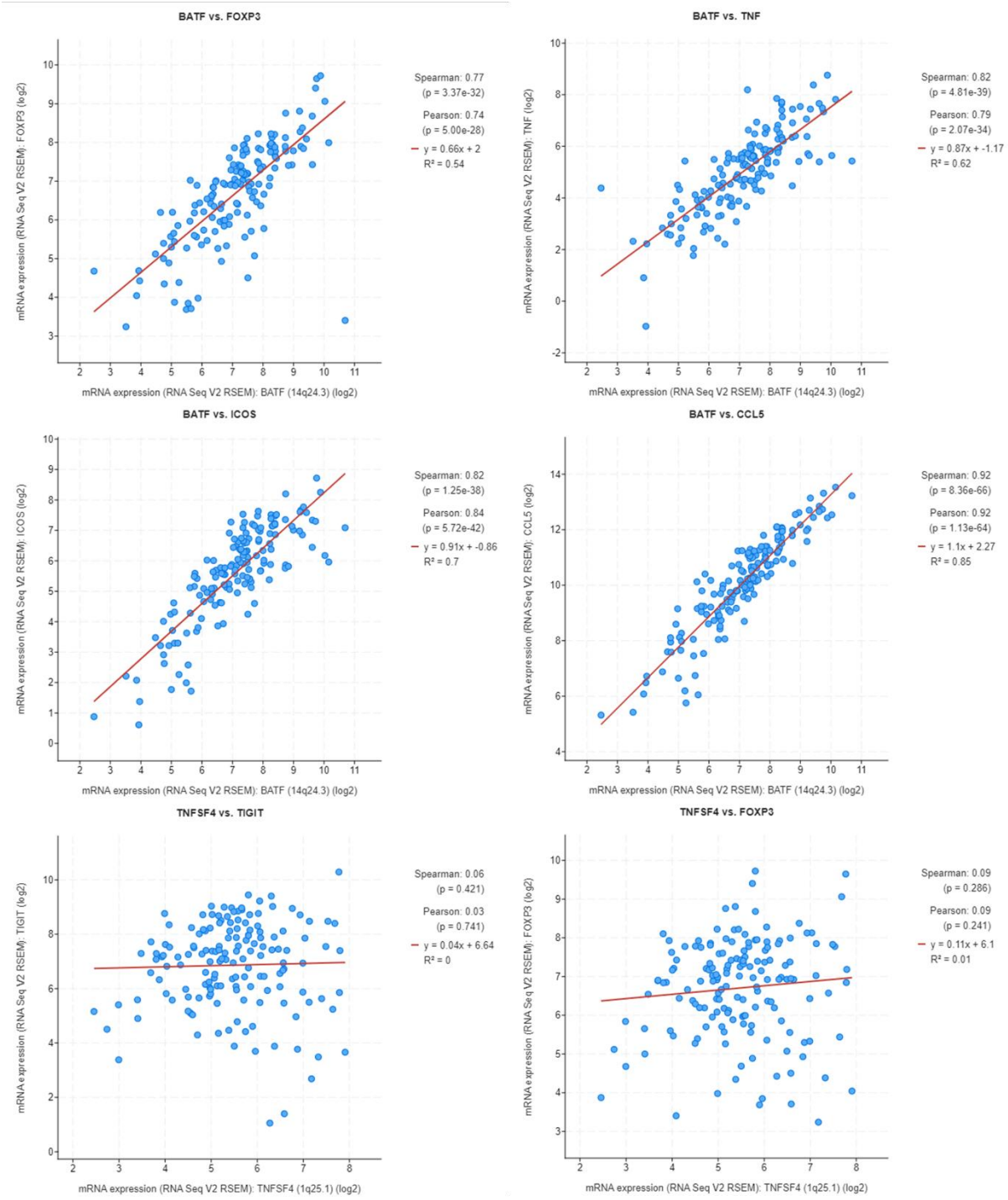

Supplementary Figure 11 Cont.

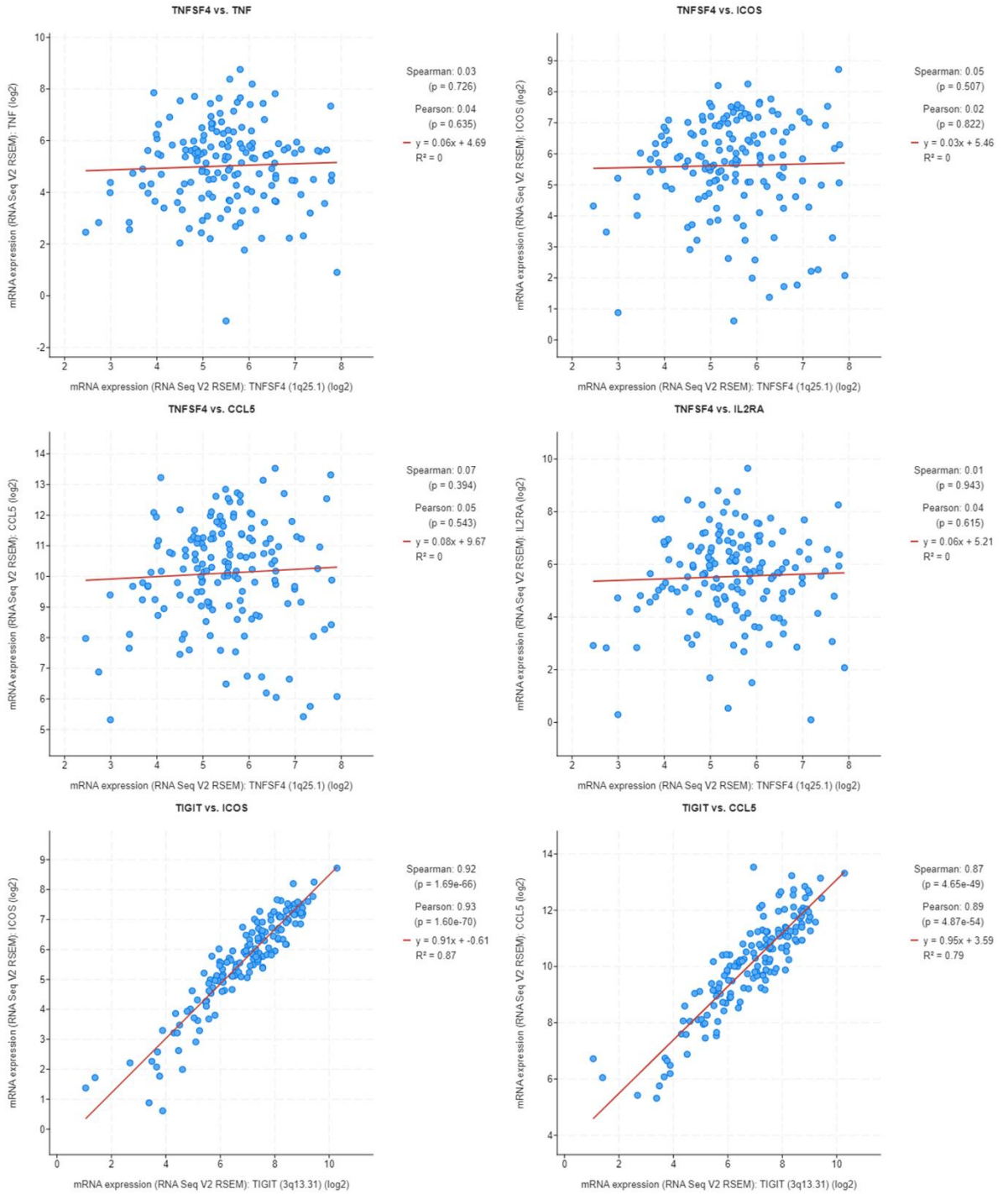

Supplementary Figure 11 Cont.

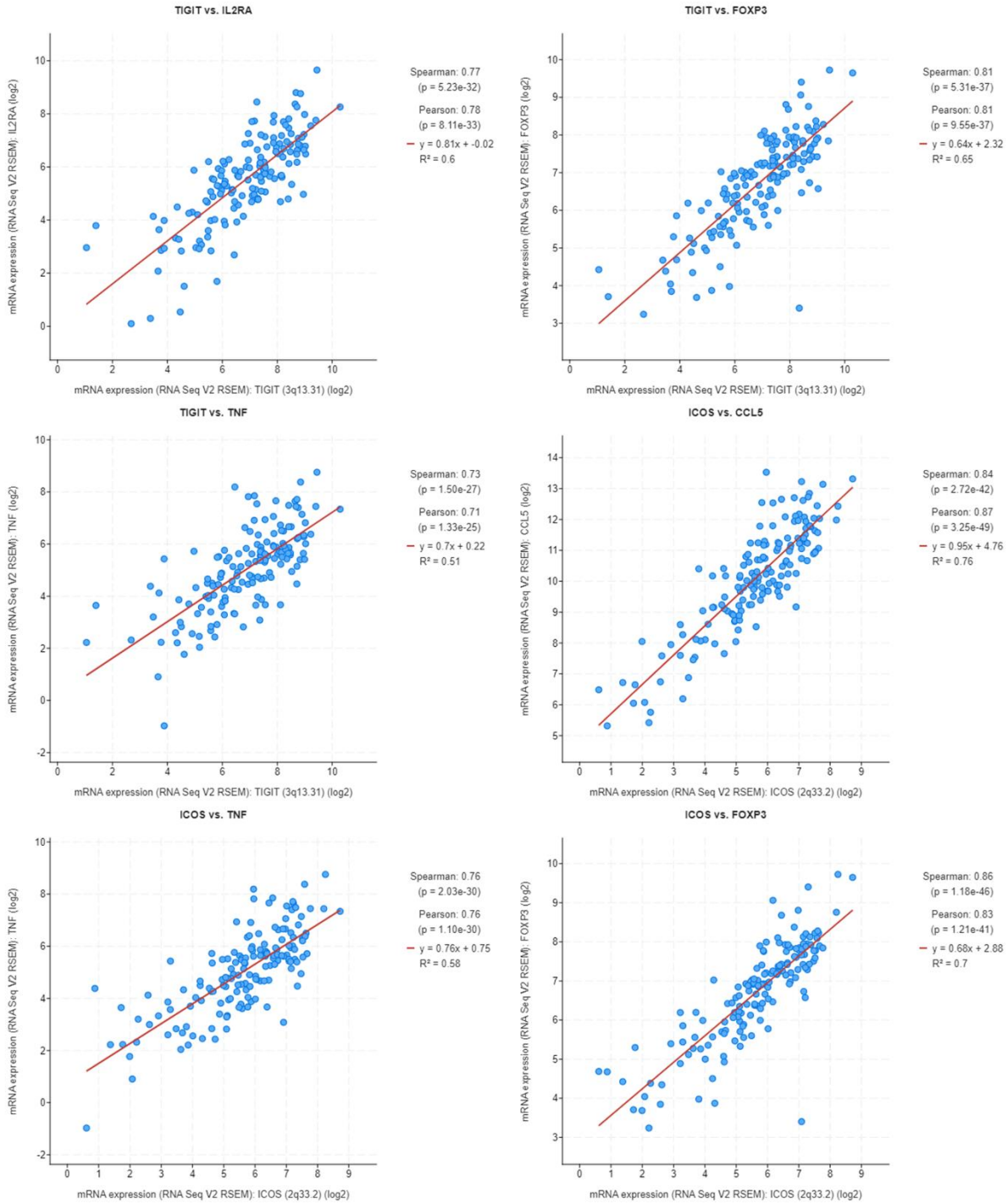

Supplementary Figure 11 Cont.

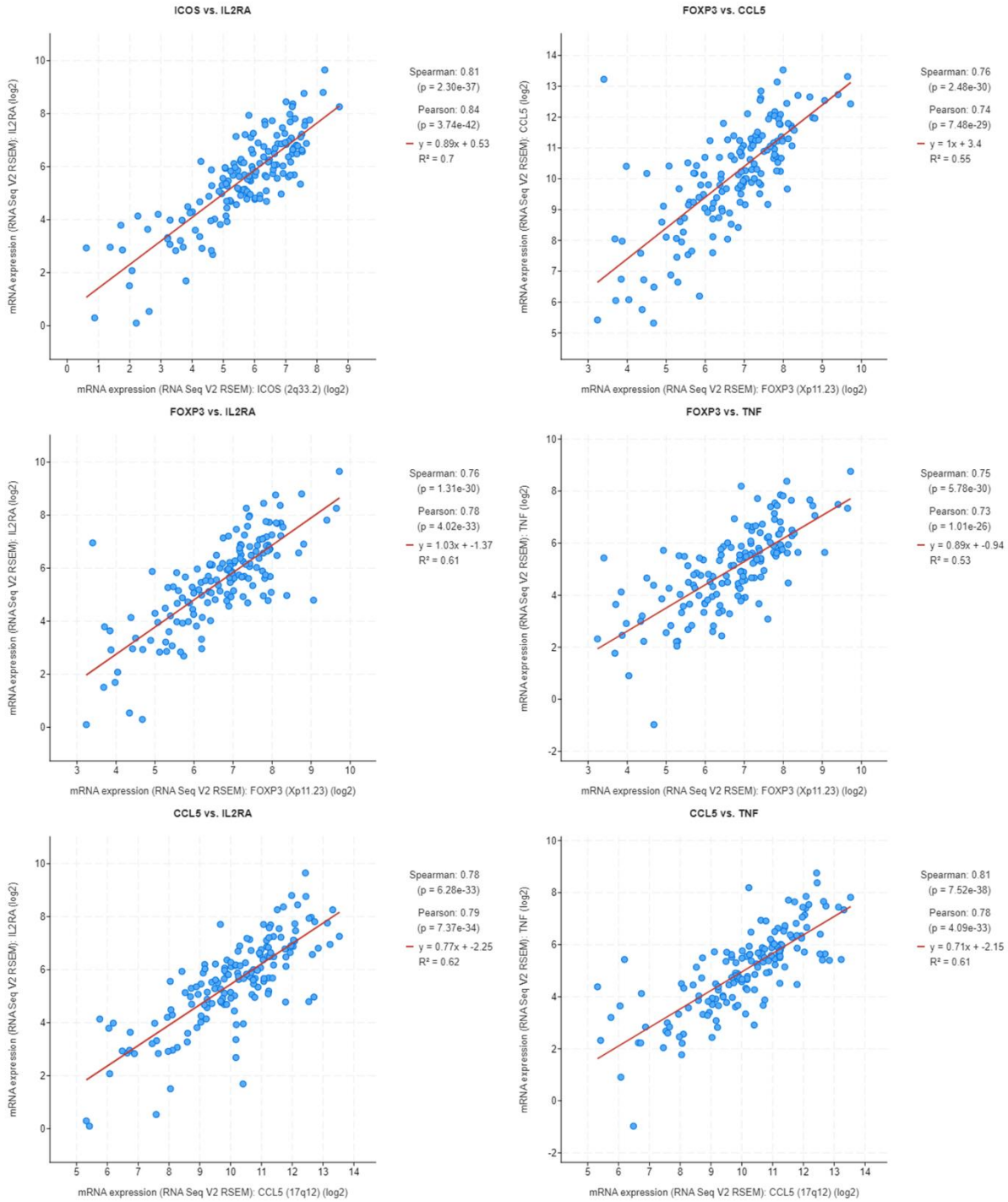

Supplementary Figure 11 Co-expression analysis of Treg-associated signature genes in TGCT samples (150 patients / 156 samples) from an open-access resource, named cBioPortal for interactive exploration of TGCT genomics data sets.

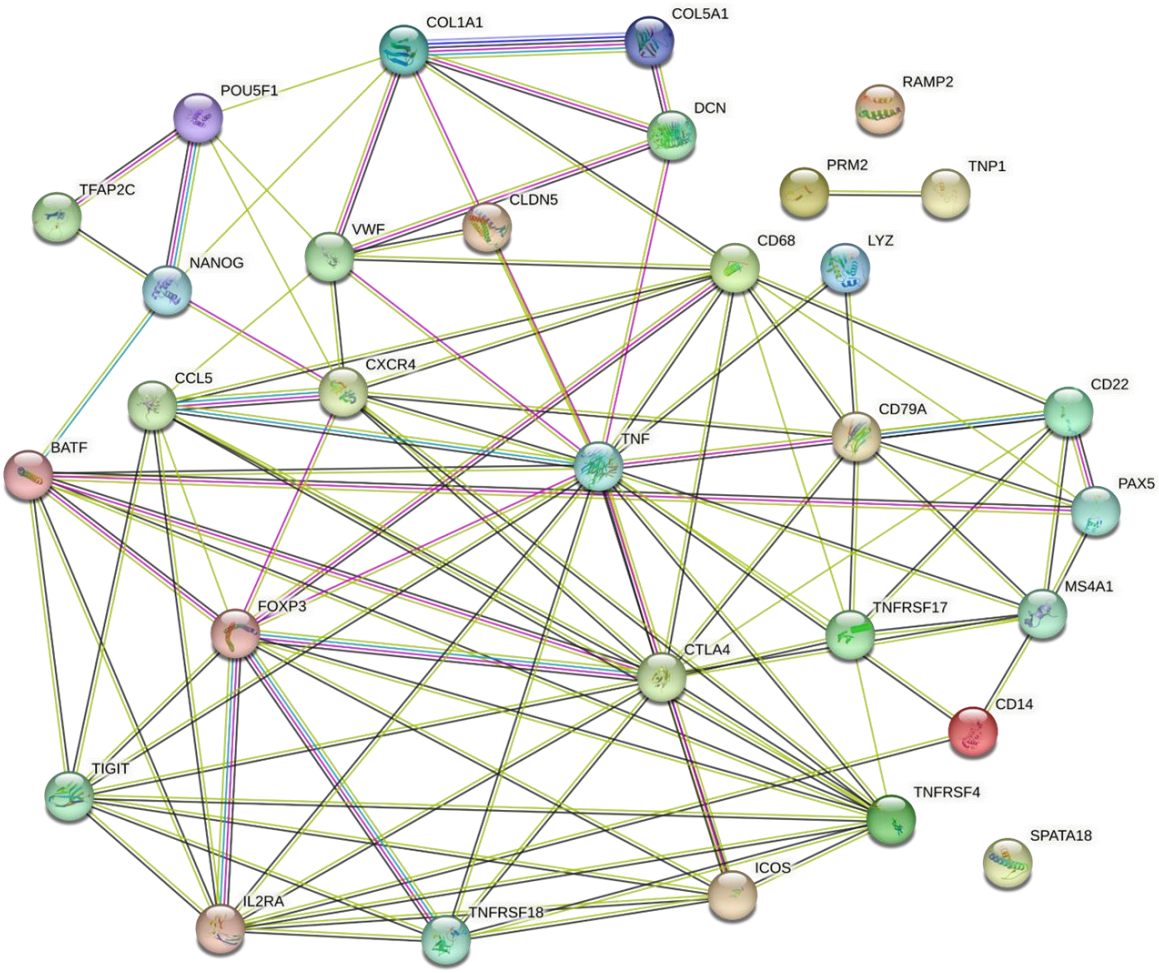

Supplementary Figure 12 The protein-protein interaction network (PPI) of selected Treg proteins with other markers used to detect different cells in the testicular microenvironment was generated by STRING. Colored nodes indicate query proteins and first shell of interaction, filled nodes represent known or predicted 3D structure. Pastel color edges represent the known interactions from curated databases, pink color edges represent known interactions determined experimentally, green color edges represent predicted interactions between neighboring genes, red color edges represent the predicted gene fusion interaction, blue color edges represent the predicted co-occurrence of gene interaction. Other color edges, for example olive color represents text-mining, black color represents co-expression and purple color represents protein homology.

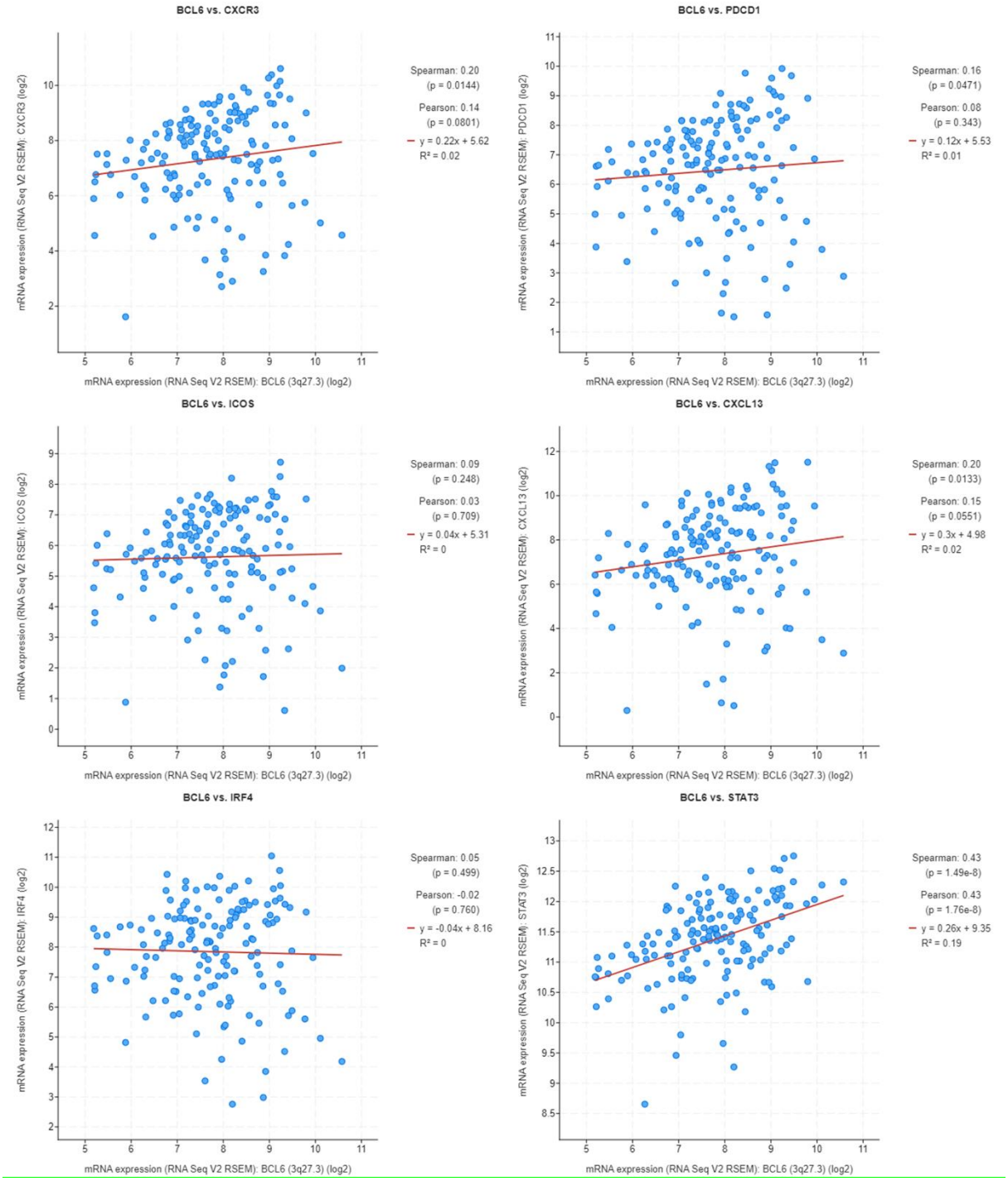

Supplementary Figure 13 Cont.

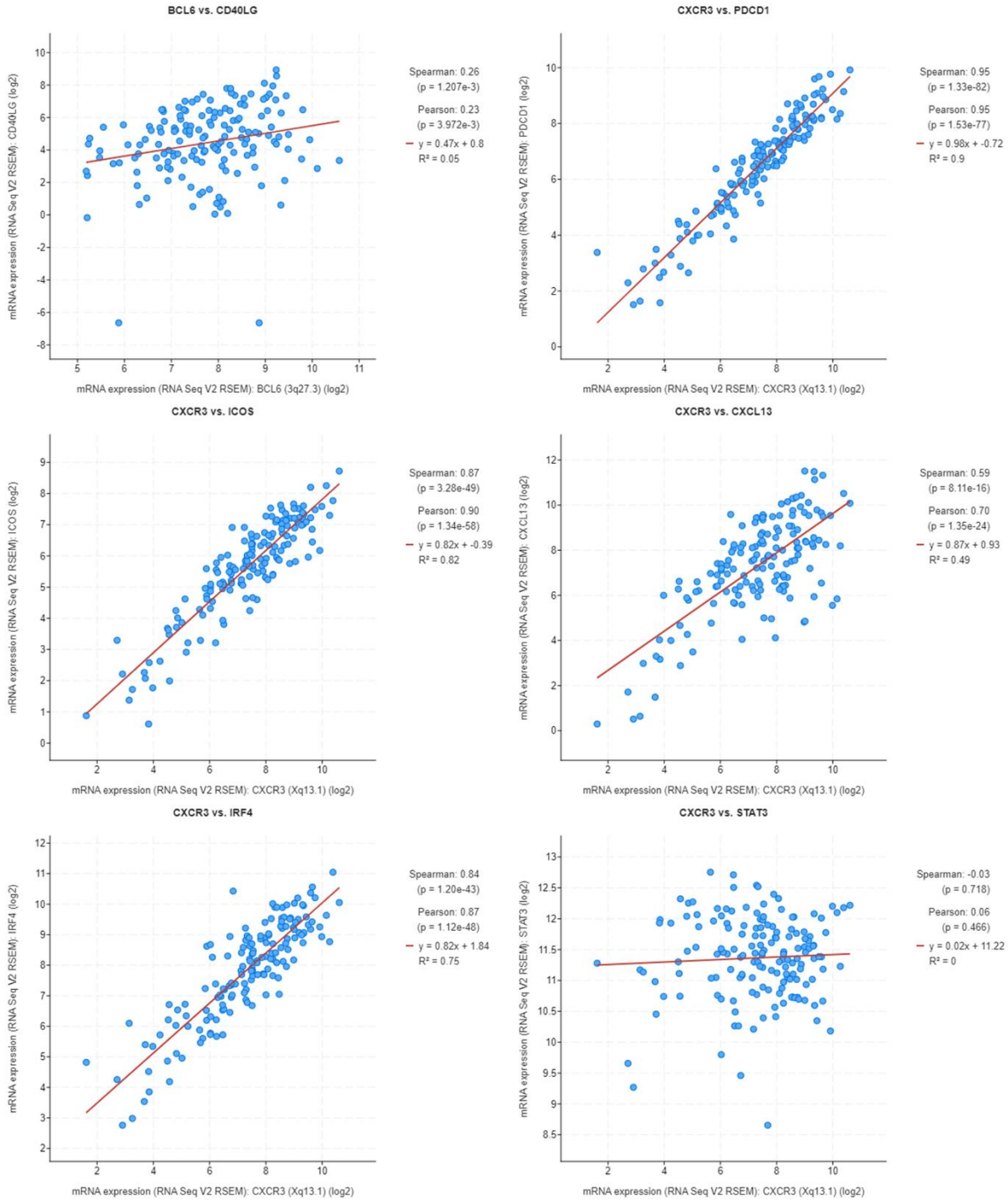

Supplementary Figure 13 Cont.

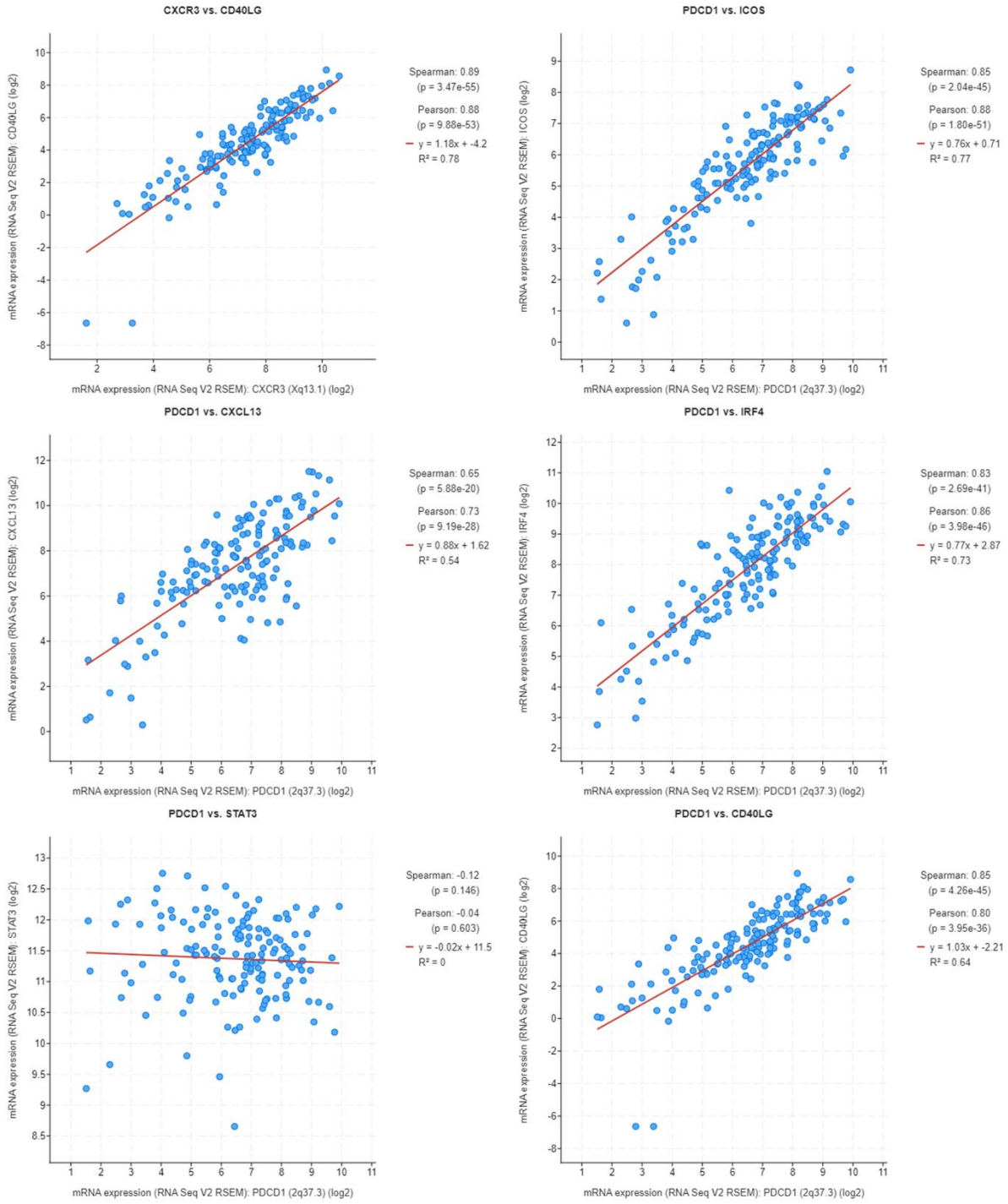

Supplementary Figure 13 Cont.

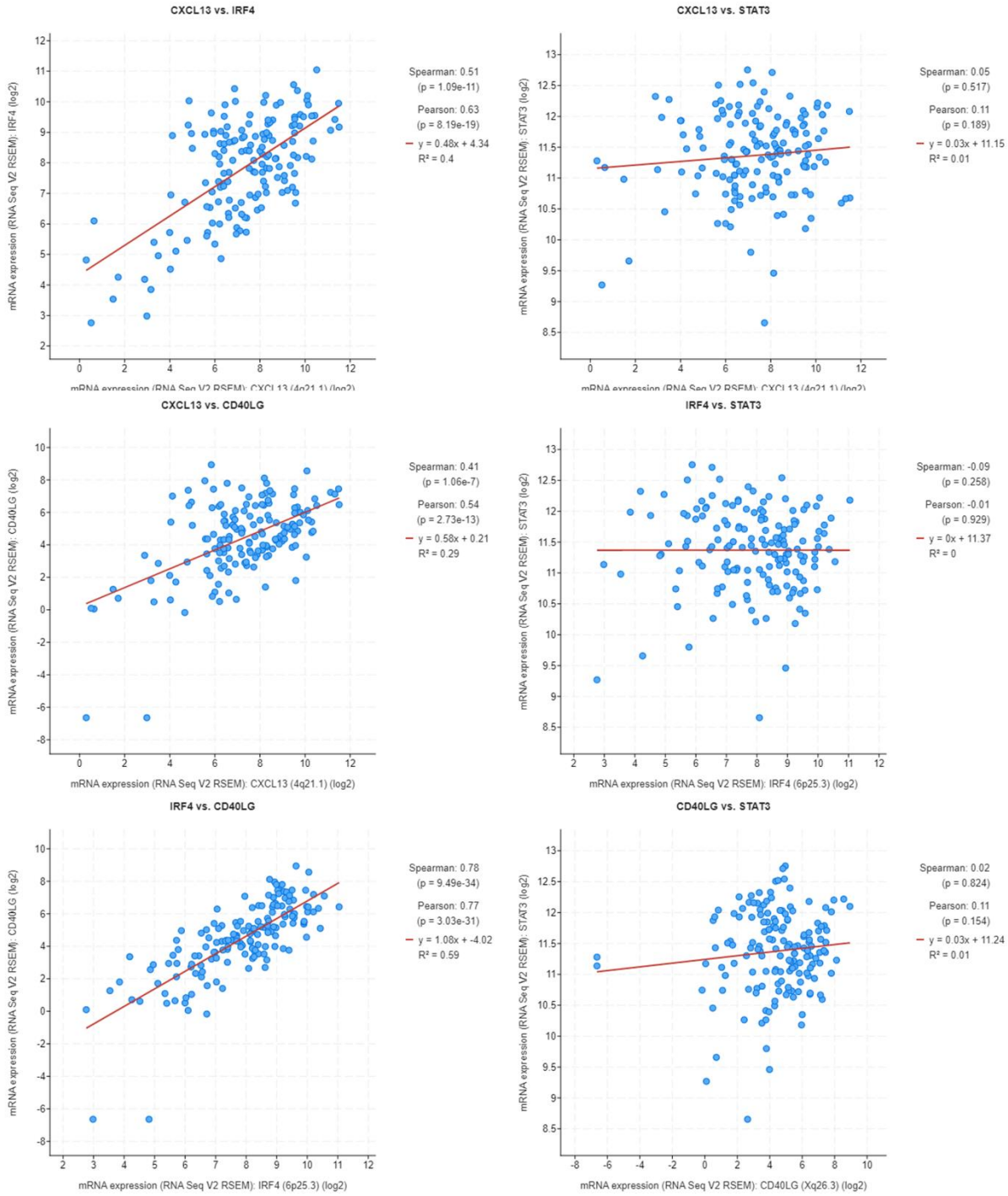

Supplementary Figure 13 Co-expression analysis of Tfh-associated signature genes in TGCT samples (150 patients / 156 samples) from an open-access resource, named cBioPortal for interactive exploration of TGCT genomics data sets.

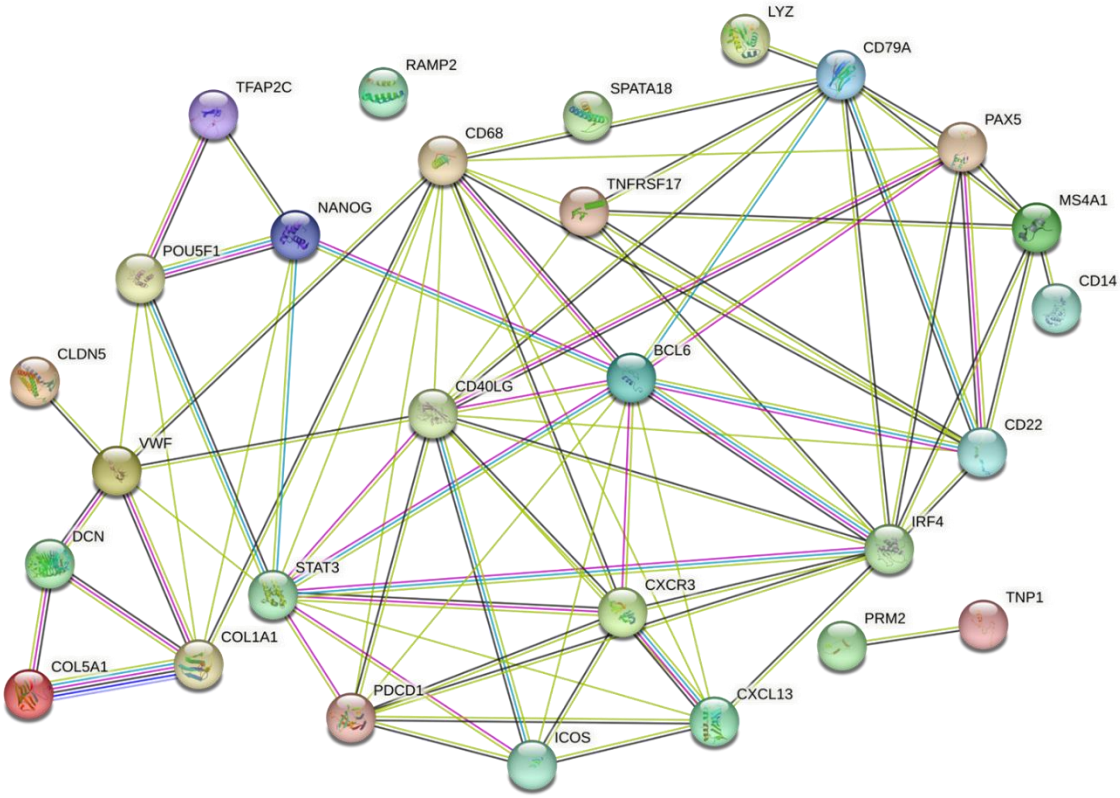

Supplementary Figure 14 The protein-protein interaction network (PPI) of selected Tfh proteins with other markers used to detect different cells in the testicular microenvironment was generated by STRING. Colored nodes indicate query proteins and first shell of interaction, filled nodes represent known or predicted 3D structure. Pastel color edges represent the known interactions from curated databases, pink color edges represent known interactions determined experimentally, green color edges represent predicted interactions between neighboring genes, red color edges represent the predicted gene fusion interaction, blue color edges represent the predicted co-occurrence of gene interaction. Other color edges, for example olive color represents textmining, black color represents co-expression and purple color represents protein homology.

	T cells	B cells	Macrophages	Endothelial cells	Fibroblasts	Germ cells	Unidentified	Tumor cells	Plasma cells
T cells									
B cells	833 (56,8%)								
Macrophages	982 (60,1%)	963 (60,3%)							
Endothelial cells	969 (58,8%)	957 (59,6%)	1175 (69,0%)						
Fibroblasts	915 (56,8%)	887 (56,0%)	1090 (64,2%)	1075 (62,8%)					
Germ cells	1012 (61,4%)	1013 (63,6%)	1218 (71,5%)	1220 (71,6%)	1132 (66,6%)				
Unidentified	720 (49,0%)	671 (45,9%)	815 (49,9%)	811 (49,5%)	758 (47,4%)	844 (51,2%)			
Tumor cells	694 (44,8%)	670 (44,2%)	832 (49,8%)	826 (49,2%)	769 (46,8%)	849 (50,0%)	601 (40,8%)		
Plasma cells	769 (52,1%)	738 (50,9%)	920 (58,0%)	884 (54,5%)	842 (53,6%)	924 (56,9%)	622 (42,8%)	677 (46,6%)	

Supplementary Figure 15 Overview of differentially expressed genes in the different cells present in the human testicular tissue microenvironment.

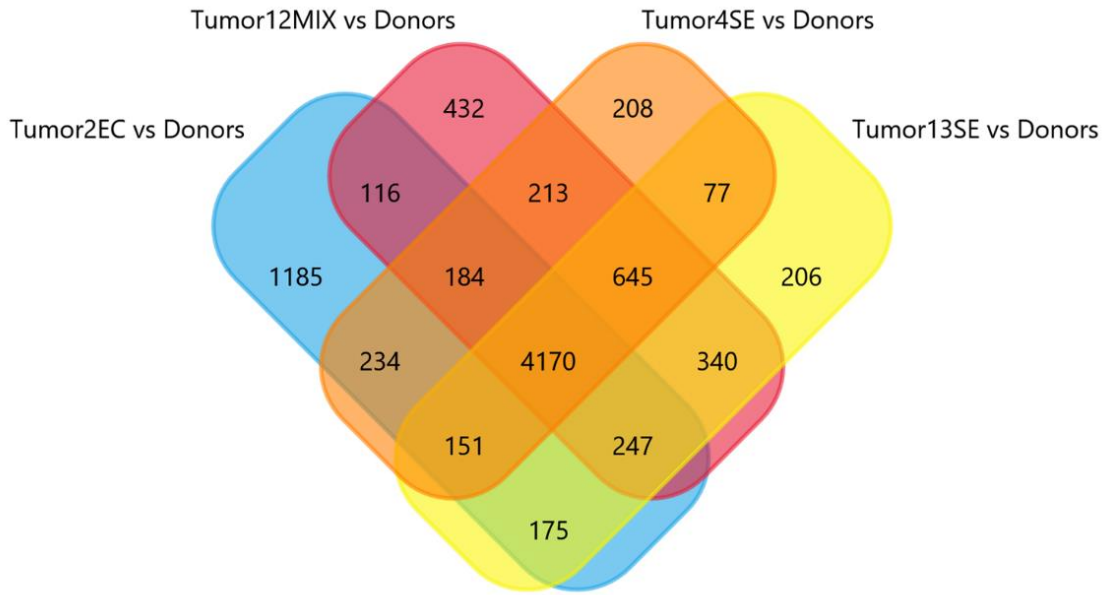

Supplementary Figure 16 Identical and non-identical numbers of differentially expressed genes (unfiltered) across the different tumor T cells compared to donor T cells.

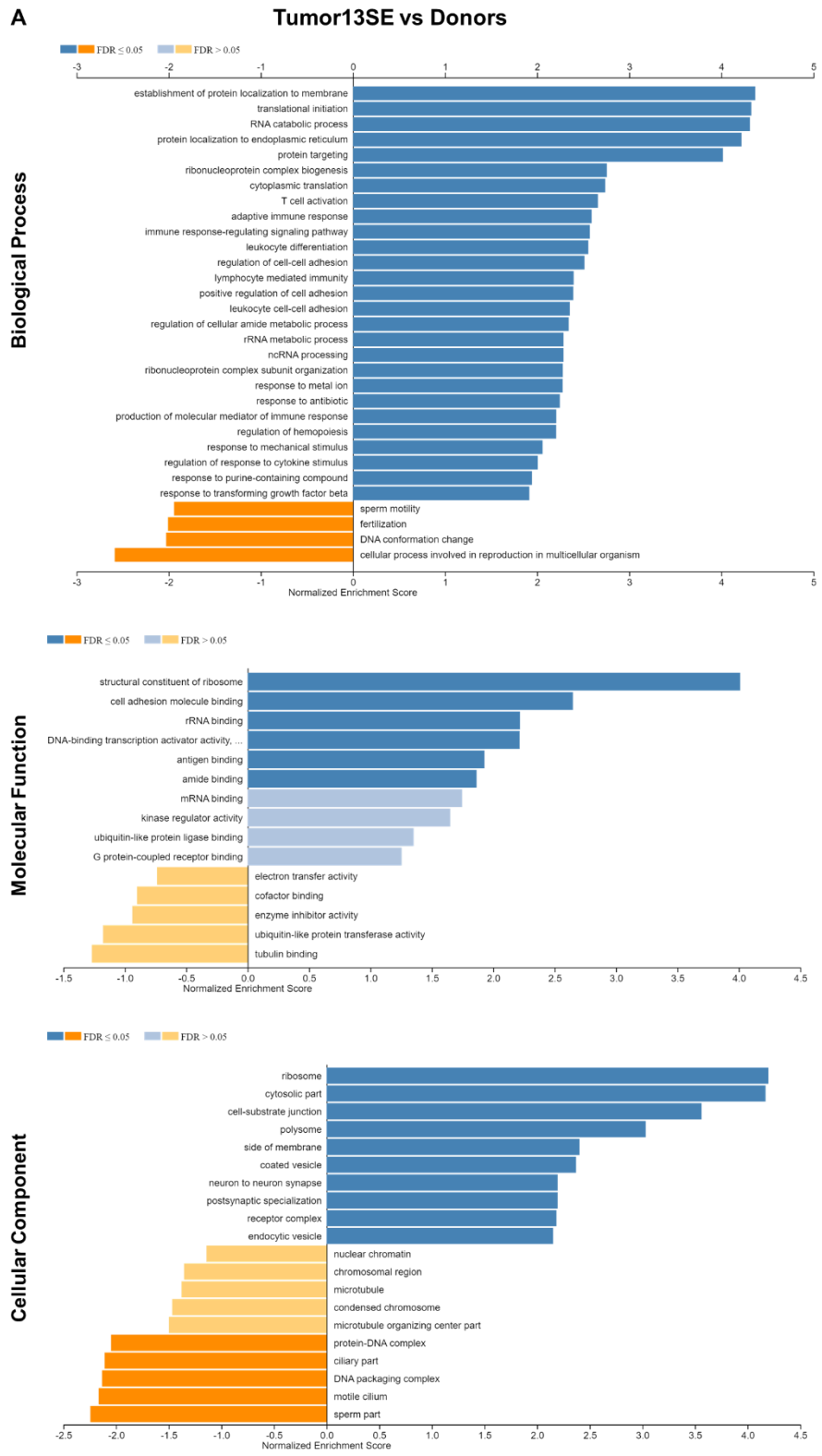

Supplementary Figure 17 Cont.

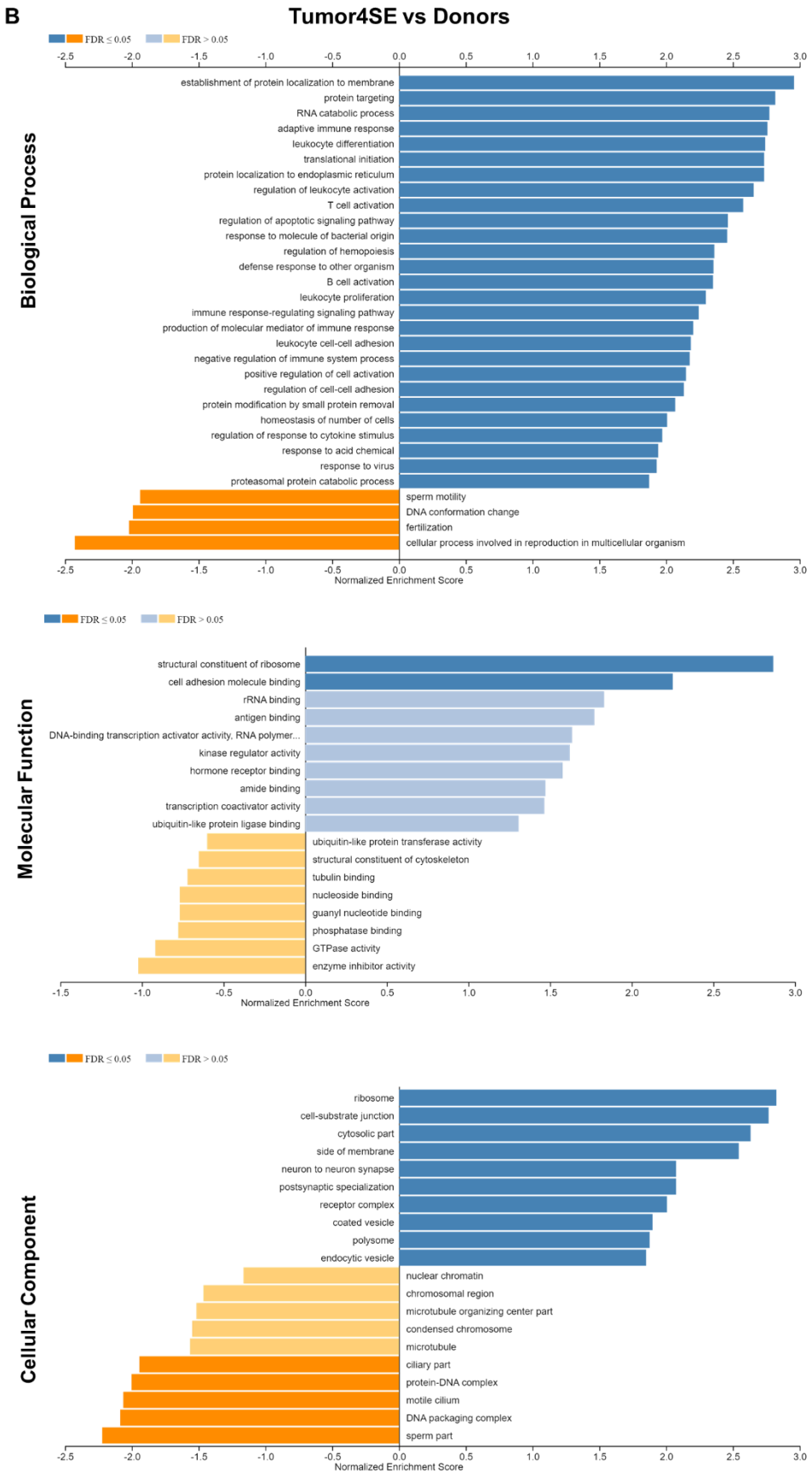

Supplementary Figure 17 Cont.

C

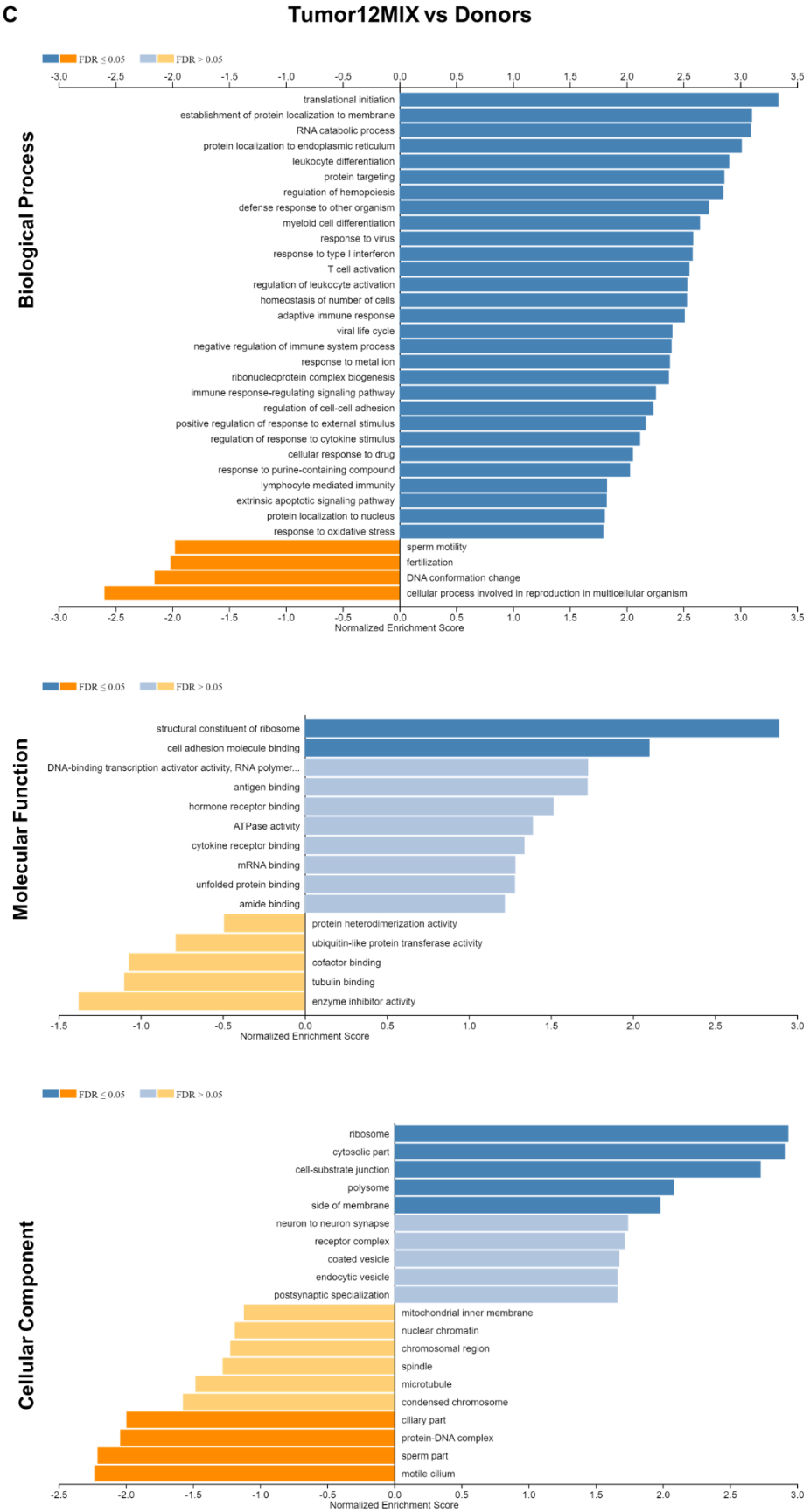

Supplementary Figure 17 Cont.

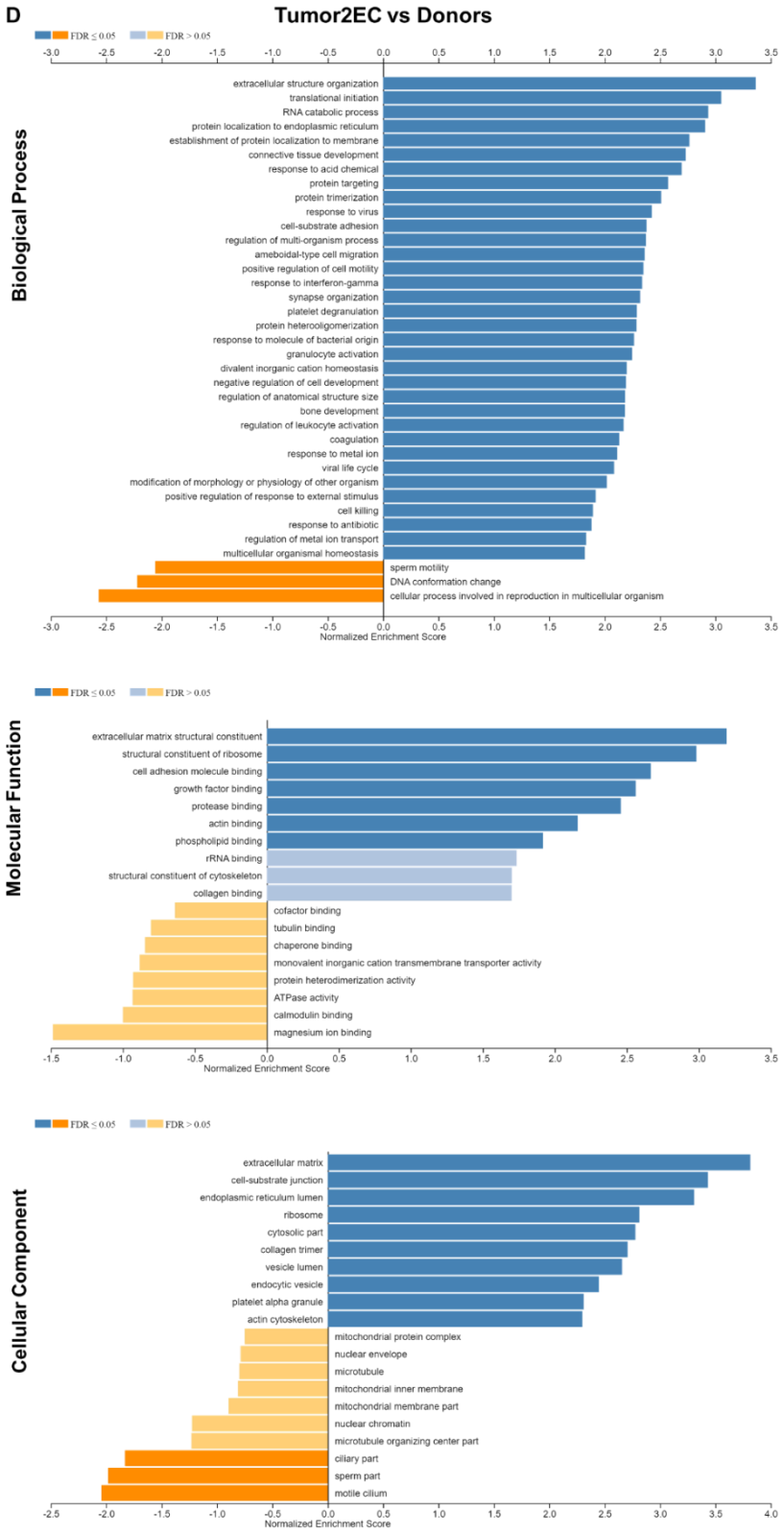

Supplementary Figure 17 Gene set enrichment analysis-GO analysis of top 300 (150 up expressed and 150 down expressed) gene in T cells from different TGCTs vs Donors by WebGestalt. Bar chart showed the top GO terms for biological process, molecular function and cellular component of Tumor13SE vs Donors (A), Tumor4SE vs Donors (B), Tumor12MIX vs Donors (C) and Tumor2EC vs Donors (D) respectively. Bar charts length and color represent the significance of respective term.

Supplementary Figure 18 Cont.

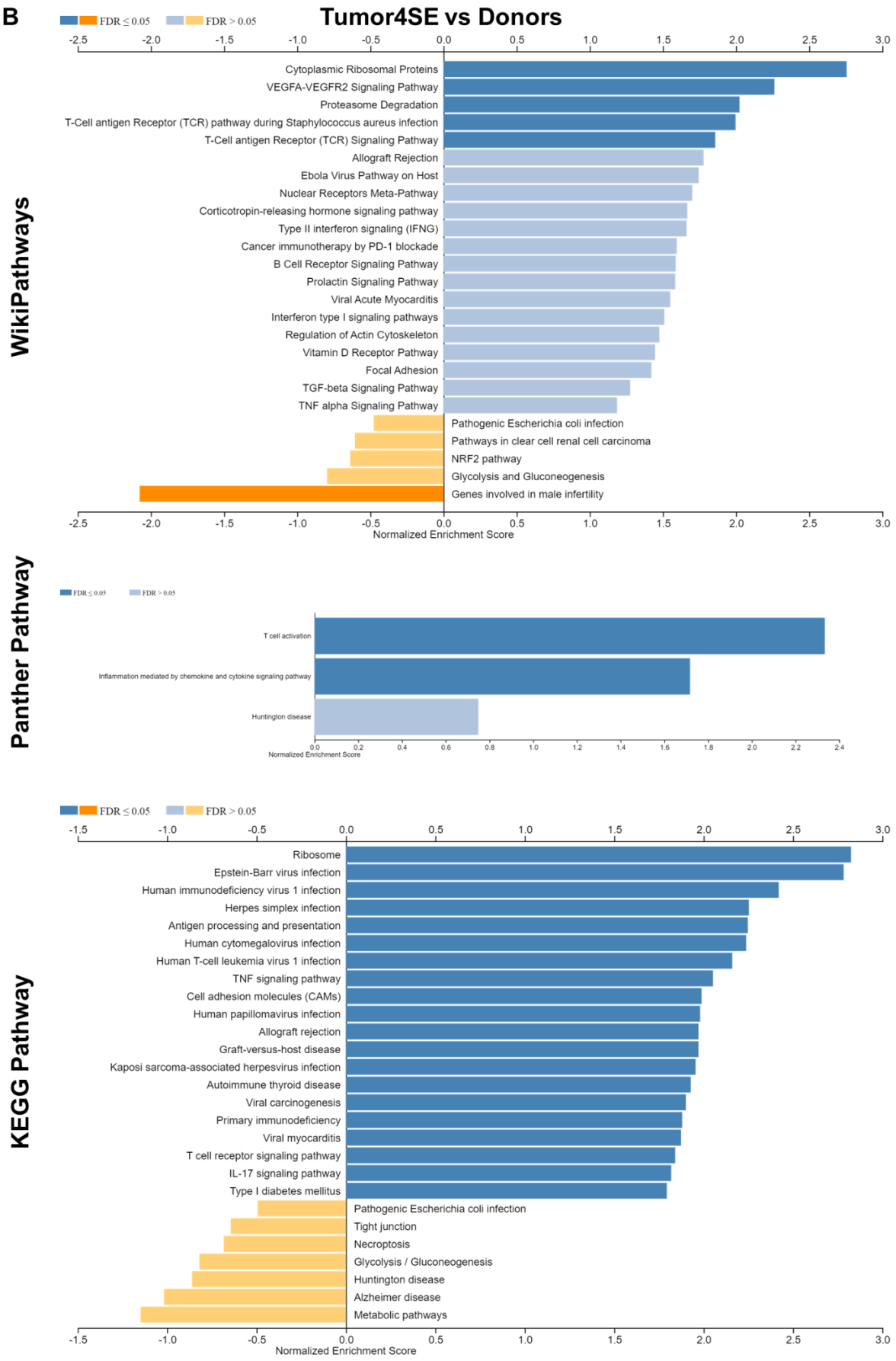

Supplementary Figure 18 Cont.

C

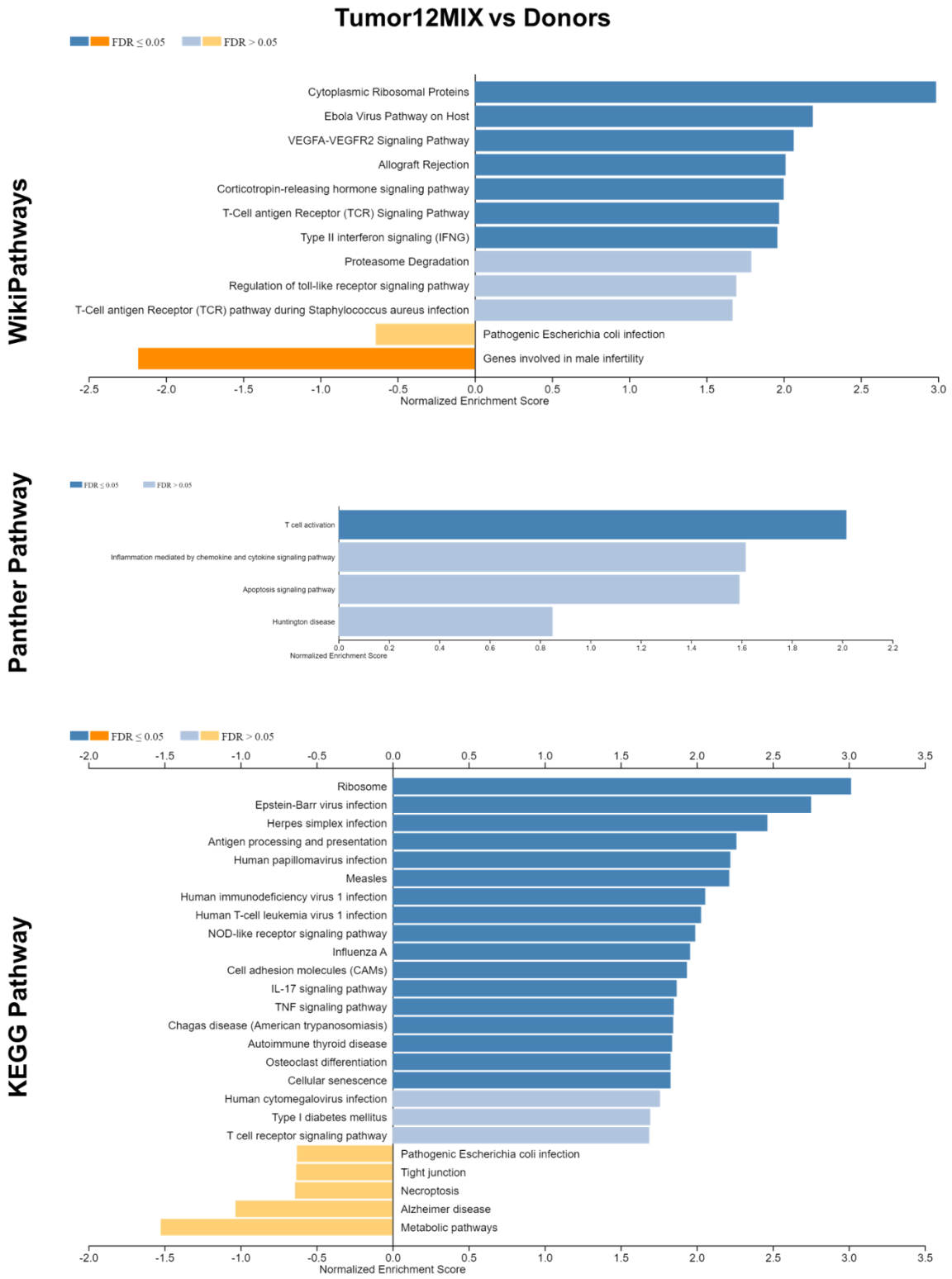

Supplementary Figure 18 Cont.

Supplementary Figure 18 Gene set enrichment analysis- Pathway analysis analysis of top 300 (150 up expressed and 150 down expressed) gene in T cells from different TGCTs vs Donors by WebGestalt. Bar chart showed the top GO terms for biological process, molecular function and cellular component of Tumor13SE vs Donors (A), Tumor4SE vs Donors (B), Tumor12MIX vs Donors and Tumor2EC vs Donors (D) respectively. Bar charts length and color represent the significance of respective term.

Supplementary Tables

Supplementary Table 1 Sample heterogeneity in terms of weight and cells number (analyzed events) in flow cytometry

Sample localization	Sample weight range			Total live cells range		
	Seminoma	Embryonal carcinoma (≥80%)	Mixed Tumors	Seminoma	Embryonal carcinoma (≥80%)	Mixed Tumors
Tumor	3.4 -1827 mg	76 - 835 mg	26.4 -577 mg	538-923897	6493-252399	1031-48751
Tumor-Adj	6.3-101.4 mg	42.6 -156 mg	15.6-80.5 mg	294-110997	2210-273187	1093-94652
Tumor-Dis	6.3-122.9 mg	34-71.1 mg	16.5-46.9 mg	1592-21096	3761-117875	1349-28063
Contralateral 1	3.3- 20.8 mg	3-13 mg	3.6- 12.3 mg	3008-19074	2362-5241	2527-23000
Contralateral 2	5.59-40.12 mg	2.9-6.5 mg	1.5-49.2 mg	2364-46410	1780-13006	1157-81665

Supplementary Table 2 Number of cells in the scRNA-seq data sets analyzed in the current study.

<table>
<tr><td></td><td></td><td colspan="6">Cell number</td></tr>
<tr><td></td><td></td><td>Estimated cell number (cell ranger 10x)</td><td>Primary aggregation (only Donors)</td><td>Secondary aggregation (all samples)</td><td colspan="3">Cell after filtration and normalization</td></tr>
<tr><td rowspan="2">Donor1</td><td>Technical replicate 1</td><td>4276</td><td rowspan="2">7628</td><td rowspan="10">44012</td><td>1592</td><td rowspan="8">4440</td><td rowspan="10">10153</td></tr>
<tr><td>Technical replicate 2</td><td>3352</td><td rowspan="2">2748</td></tr>
<tr><td rowspan="2">Donor2</td><td>Technical replicate 1</td><td>3744</td><td rowspan="2">7627</td></tr>
<tr><td>Technical replicate 2</td><td>3883</td></tr>
<tr><td rowspan="2">Donor3</td><td>Technical replicate 1</td><td>4402</td><td rowspan="2">10033</td><td>2773</td></tr>
<tr><td>Technical replicate 2</td><td>5631</td></tr>
<tr><td>Tumor12MIX</td><td>-</td><td>5878</td><td>-</td><td>2327</td><td rowspan="4">5713</td></tr>
<tr><td>Tumor13SE</td><td>-</td><td>6397</td><td>-</td><td>2440</td></tr>
<tr><td>Tumor2EC</td><td>-</td><td>347</td><td>-</td><td>208</td></tr>
<tr><td>Tumor4SE</td><td>-</td><td>6102</td><td>-</td><td>738</td></tr>
</table>

Supplementary Table 3 Infiltration density and distribution of Individual NSP samples.

CD3 (n=10)			
Density	**Distribution**	**Percentages of distribution**	**Median infiltration density score**
1.5	Disseminated	80%	1.5
1	Disseminated		
1.5	Disseminated		
1.5	Disseminated		
1.5	Disseminated		
1	Disseminated		
1.5	Disseminated		
1.5	Disseminated		
2.5	Focal	10%	2.5
0	Absent	10%	0
CD20cy (n=10)			
0	Absent	100%	0
0	Absent		
0	Absent		
0	Absent		
0	Absent		
0	Absent		
0	Absent		
0	Absent		
0	Absent		
0	Absent		
CD68 (n=10)			
2.5	Disseminated	100%	2.75
3	Disseminated		
2	Disseminated		
3	Disseminated		
1.5	Disseminated		
2	Disseminated		
3	Disseminated		
2	Disseminated		
3	Disseminated		
3	Disseminated		
CD11c (n=10)			
0.5	Disseminated	10%	0.5
2	Focal	30%	1
1	Focal		
0.5	Focal		
0	Absent	60%	0
0	Absent		
0	Absent		
0	Absent		
0	Absent		
0	Absent		
CD4 (n=10)			
2	Disseminated	90%	2
1	Disseminated		
2	Disseminated		
0.5	Disseminated		
2.5	Disseminated		
3	Disseminated		
2.5	Disseminated		
2	Disseminated		
3	Disseminated		
0	Absent	10%	0

CD8a (n=10)			
Density	**Distribution**	**Percentages of distribution**	**Median infiltration density score**
0.5	Disseminated	70%	1
0.5	Disseminated		
1	Disseminated		
2	Disseminated		
1	Disseminated		
0.5	Disseminated		
1	Disseminated		
2	Focal	30%	0.5
0.5	Focal		
0.5	Focal		
CD25 (n=10)			
1	Disseminated	10%	1
0.5	Focal	60%	0.5
0.5	Focal		
0.5	Focal		
0.5	Focal		
0.5	Focal		
1	Focal		
0	Absent	30%	0
0	Absent		
0	Absent		
FOXP3 (n=10)			
0.5	Focal	30%	0.5
0.5	Focal		
0.5	Focal		
0	Absent	70%	0
0	Absent		
0	Absent		
0	Absent		
0	Absent		
0	Absent		
0	Absent		
0	Absent		
CXCR5 (n=10)			
0.5	Disseminated	10%	0.5
0	Absent	90%	0
0	Absent		
0	Absent		
0	Absent		
0	Absent		
0	Absent		
0	Absent		
0	Absent		
0	Absent		
BCL6 (n=10)			
0	Absent	100%	0
0	Absent		
0	Absent		
0	Absent		
0	Absent		
0	Absent		
0	Absent		
0	Absent		
0	Absent		
0	Absent		

Supplementary Table 4 Infiltration density and distribution of Individual HYP+ly samples.

CD3 (n=15)			
Density	**Distribution**	**Percentages of distribution**	**Median infiltration density score**
1.5	Disseminated	33.33%	1.5
1	Disseminated		
3.5	Disseminated		
1.5	Disseminated		
3.5	Disseminated		
3.5	Multifocal	53.33%	3.75
2	Multifocal		
4	Multifocal		
4	Multifocal		
3	Multifocal		
4	Multifocal		
4	Multifocal		
3	Multifocal		
4	Focal	13.33%	3.5
3	Focal		
CD20cy (n=14)			
3	Multifocal	7.14%	3
2	Focal	50%	2
0.5	Focal		
2.5	Focal		
2	Focal		
3	Focal		
2	Focal		
1.5	Focal		
0	Absent	42.86%	0
0	Absent		
0	Absent		
0	Absent		
0	Absent		
0	Absent		
CD68 (n=14)			
2.5	Disseminated	64.29%	2.5
3	Disseminated		
2	Disseminated		
2.5	Disseminated		
1.5	Disseminated		
3	Disseminated		
3	Disseminated		
2	Disseminated		
2	Disseminated		
3	Multifocal	14.29%	2.5
2	Multifocal		
3	Focal	21.43%	2.5
2	Focal		
2.5	Focal		
CD11c (n=12)			
3	Multifocal	33.33%	2.75
2.5	Multifocal		
3	Multifocal		
1.5	Multifocal		
1	Focal	16.67%	2
3	Focal		
0	Absent	50%	0
0	Absent		
0	Absent		
0	Absent		
0	Absent		
0	Absent		

CD4 (n=12)			
Density	**Distribution**	**Percentages of distribution**	**Median infiltration density score**
3	Disseminated	33.33%	3
3	Disseminated		
2.5	Disseminated		
3	Disseminated		
4	Multifocal	41.67%	4
4	Multifocal		
3	Multifocal		
4	Multifocal		
4	Multifocal		
3	Focal	25%	3
4	Focal		
3	Focal		
CD8a (n=11)			
2	Disseminated	9.09%	2
3	Multifocal	63.64%	3
2	Multifocal		
3	Multifocal		
3.5	Multifocal		
2	Multifocal		
3	Multifocal		
3	Multifocal		
4	Focal	27.27%	2
0.5	Focal		
2	Focal		
CD25 (n=11)			
1	Disseminated	27.27%	1
1	Disseminated		
1	Disseminated		
2.5	Multifocal	36.36%	2.25
2	Multifocal		
2	Multifocal		
3	Multifocal		
2.5	Focal	36.36%	2.25
1.5	Focal		
3	Focal		
2	Focal		
FOXP3 (n=12)			
2	Disseminated	8.33%	2
2	Multifocal	16.67%	2
2	Multifocal		
1	Focal	33.33%	1.5
3	Focal		
1	Focal		
2	Focal		
0	Absent	41.67%	0
0	Absent		
0	Absent		
0	Absent		
0	Absent		

Supplementary Table 4: cont.

Supplementary Table 4: cont.

CXCR5 (n=11)			
Density	**Distribution**	**Percentages of distribution**	**Median infiltration density score**
2.5	Multifocal	9.09%	2.5
4	Focal	36.36%	3.75
2	Focal		
4	Focal		
3.5	Focal		
0	Absent	54.56%	0
0	Absent		
0	Absent		
0	Absent		
0	Absent		
0	Absent		

BCL6 (n=12)			
Density	**Distribution**	**Percentages of distribution**	**Median infiltration density score**
0	Absent	100%	0
0	Absent		
0	Absent		
0	Absent		
0	Absent		
0	Absent		
0	Absent		
0	Absent		
0	Absent		
0	Absent		
0	Absent		
0	Absent		

Supplementary Table 5 Infiltration density and distribution of Individual GCNIS samples.

CD3 (n=15)			
Density	**Distribution**	**Percentages of distribution**	**Median infiltration density score**
2	Disseminated	66.67%	2
1.5	Disseminated		
1.5	Disseminated		
1.5	Disseminated		
1.5	Disseminated		
2	Disseminated		
3	Disseminated		
2	Disseminated		
2	Disseminated		
3	Disseminated		
3.5	Multifocal	26.67%	2.75
2.5	Multifocal		
2	Multifocal		
3	Multifocal		
3	Focal	6.67%	3
CD20cy (n=14)			
1	Disseminated	7.14%	1
0.5	Focal	14.29%	1.5
2.5	Focal		
0	Absent	78.57%	0
0	Absent		
0	Absent		
0	Absent		
0	Absent		
0	Absent		
0	Absent		
0	Absent		
0	Absent		
0	Absent		
0	Absent		
CD68 (n=15)			
2.5	Disseminated	93.33%	2.25
2	Disseminated		
2.5	Disseminated		
3.5	Disseminated		
1.5	Disseminated		
2	Disseminated		
1.5	Disseminated		
2	Disseminated		
2	Disseminated		
2.5	Disseminated		
2.5	Disseminated		
2	Disseminated		
2.5	Disseminated		
3	Disseminated		
0	Absent	6.67	0

CD11c (n=15)			
Density	**Distribution**	**Percentages of distribution**	**Median infiltration density score**
3	Disseminated	53.33%	1
0.5	Disseminated		
2	Disseminated		
2	Disseminated		
1	Disseminated		
1	Disseminated		
1	Disseminated		
1	Disseminated		
0.5	Multifocal	6.67%	3
3	Focal	13.33%	2.5
2	Focal		
0	Absent	26.67%	0
0	Absent		
0	Absent		
0	Absent		
CD4 (n=14)			
2.5	Disseminated	78.57%	3
3	Disseminated		
3	Disseminated		
3	Disseminated		
2.5	Disseminated		
3	Disseminated		
3	Disseminated		
3	Disseminated		
3	Disseminated		
3	Disseminated		
2.5	Disseminated		
4	Multifocal	21.43%	3
3	Multifocal		
3	Multifocal		
CD8a (n=14)			
2	Disseminated	71.43%	2
2	Disseminated		
2	Disseminated		
1.5	Disseminated		
1.5	Disseminated		
2	Disseminated		
2.5	Disseminated		
3	Disseminated		
1.5	Disseminated		
2	Disseminated		
3.5	Multifocal	28.57%	3.25
2	Multifocal		
4	Multifocal		
3	Multifocal		

Supplementary Table 5 cont.

Supplementary Table 5 cont.

CD25 (n=14)			
Density	**Distribution**	**Percentages of distribution**	**Median infiltration density score**
1.5	Disseminated	64.29%	1
1	Disseminated		
0.5	Disseminated		
1	Disseminated		
1	Disseminated		
1	Disseminated		
1.5	Disseminated		
2	Disseminated		
1.5	Disseminated		
2	Multifocal	21.43%	2
2	Multifocal		
2	Multifocal		
0	Absent	14.29%	0
0	Absent		
FOXP3 (n=14)			
0.5	Disseminated	35.71%	0.5
1.5	Disseminated		
2	Disseminated		
0.5	Disseminated		
0.5	Disseminated		
0.5	Focal	7.14%	0.5
0	Absent	57.14%	0
0	Absent		
0	Absent		
0	Absent		
0	Absent		
0	Absent		
0	Absent		
0	Absent		
0	Absent		

CXCR5 (n=14)			
Density	**Distribution**	**Percentages of distribution**	**Median infiltration density score**
1.5	Disseminated	14.29%	1.25
1	Disseminated		
2	Multifocal	7.14%	2
0.5	Focal	7.14%	0.5
0	Absent	71.43%	0
0	Absent		
0	Absent		
0	Absent		
0	Absent		
0	Absent		
0	Absent		
0	Absent		
0	Absent		
0	Absent		
BCL6 (n=14)			
0	Absent	100%	0
0	Absent		
0	Absent		
0	Absent		
0	Absent		
0	Absent		
0	Absent		
0	Absent		
0	Absent		
0	Absent		
0	Absent		
0	Absent		
0	Absent		

Supplementary Table 6 Infiltration density and distribution of Individual GCNIS+ly samples

CD3 (n=16)			
Density	**Distribution**	**Percentages of distribution**	**Median infiltration density score**
2	Disseminated	18.75%	2
2	Disseminated		
2	Disseminated		
3.5	Multifocal	75%	3.5
3.5	Multifocal		
3.5	Multifocal		
3.5	Multifocal		
4	Multifocal		
3.5	Multifocal		
2.5	Multifocal		
4	Multifocal		
3	Multifocal		
4	Multifocal		
3.5	Multifocal		
2.5	Multifocal		
4	Focal	6.25%	4
CD20cy (n=16)			
2	Multifocal	18.75%	2
2	Multifocal		
4	Multifocal		
1.5	Focal	31.25%	1.5
4	Focal		
1.5	Focal		
1	Focal		
0.5	Focal		
0	Absent	50%	0
0	Absent		
0	Absent		
0	Absent		
0	Absent		
0	Absent		
0	Absent		
0	Absent		
CD68 (n=15)			
3	Disseminated	86.67%	2.5
2	Disseminated		
3	Disseminated		
3	Disseminated		
2.5	Disseminated		
2	Disseminated		
3	Disseminated		
2.5	Disseminated		
2	Disseminated		
2.5	Disseminated		
1.5	Disseminated		
2	Disseminated		
2	Disseminated		
2	Multifocal	13.33%	2.25
2.5	Multifocal		

CD11c (n=15)			
Density	**Distribution**	**Percentages of distribution**	**Median infiltration density score**
1.5	Disseminated	13.33%	1.75
2	Disseminated		
3	Multifocal	33.33%	3
3	Multifocal		
2.5	Multifocal		
3	Multifocal		
2.5	Multifocal		
2.5	Focal	26.67%	2.5
1.5	Focal		
2.5	Focal		
3	Focal		
0	Absent	26.67%	0
0	Absent		
0	Absent		
0	Absent		
CD4 (n=15)			
2	Disseminated	40%	3
3	Disseminated		
3	Disseminated		
3	Disseminated		
3	Disseminated		
3	Disseminated		
4	Multifocal	60%	4
4	Multifocal		
4	Multifocal		
3.5	Multifocal		
4	Multifocal		
4	Multifocal		
4	Multifocal		
4	Multifocal		
4	Multifocal		
CD8a (n=15)			
2	Disseminated	13.33%	2
2	Disseminated		
3	Multifocal	80%	3
3	Multifocal		
3	Multifocal		
4	Multifocal		
3	Multifocal		
2.5	Multifocal		
4	Multifocal		
3.5	Multifocal		
3	Multifocal		
3	Multifocal		
2	Multifocal		
4	Multifocal		
3	Focal	6.67%	3

Supplementary Table 6 cont.

CD25 (n=12)			
Density	**Distribution**	**Percentages of distribution**	**Median infiltration density score**
2.5	Disseminated	41.67%	2
2	Disseminated		
1.5	Disseminated		
2	Disseminated		
0.5	Disseminated		
2.5	Multifocal	41.67%	2.5
2.5	Multifocal		
2.5	Multifocal		
2.5	Multifocal		
3	Multifocal		
3	Focal	16.67%	3
3	Focal		
FOXP3 (n=15)			
1.5	Disseminated	33.33%	1
0.5	Disseminated		
1	Disseminated		
3	Disseminated		
1	Disseminated		
2	Multifocal	33.33%	2
2	Multifocal		
2	Multifocal		
2	Multifocal		
2	Multifocal		
0.5	Focal	13.33%	1.25
2	Focal		
0	Absent	20%	0
0	Absent		
0	Absent		

CXCR5 (n=16)			
Density	**Distribution**	**Percentages**	**Median infiltration density score**
1.5	Multifocal	18.75%	2
3	Multifocal		
2	Multifocal		
0.5	Focal	25%	1
3	Focal		
1.5	Focal		
0.5	Focal		
0	Absent	56.25%	0
0	Absent		
0	Absent		
0	Absent		
0	Absent		
0	Absent		
0	Absent		
0	Absent		
0	Absent		
BCL6 (n=16)			
2	Multifocal	6.25%	2
0	Absent	93.75%	0
0	Absent		
0	Absent		
0	Absent		
0	Absent		
0	Absent		
0	Absent		
0	Absent		
0	Absent		
0	Absent		
0	Absent		
0	Absent		
0	Absent		
0	Absent		

Supplementary Table 7 Infiltration density and distribution of Individual seminoma samples

CD3 (n=28)			
Density	Distribution	Percentages of distribution	Median infiltration density score
4	Disseminated	89.29%	4
4	Disseminated		
4	Disseminated		
4	Disseminated		
4	Disseminated		
4	Disseminated		
4	Disseminated		
4	Disseminated		
4	Disseminated		
4	Disseminated		
3	Disseminated		
4	Disseminated		
3	Disseminated		
3	Disseminated		
3	Disseminated		
2	Disseminated		
4	Disseminated		
4	Disseminated		
4	Disseminated		
3	Disseminated		
2.5	Disseminated		
4	Disseminated		
2.5	Disseminated		
4	Disseminated		
4	Disseminated		
4	Multifocal	10.71%	4
3.5	Multifocal		
4	Multifocal		
CD20cy (n=28)			
2	Disseminated	35.71%	2
3	Disseminated		
2	Disseminated		
1.5	Disseminated		
2.5	Disseminated		
2.5	Disseminated		
2	Disseminated		
1	Disseminated		
2	Disseminated		
1	Disseminated		
2.5	Multifocal	57.14%	2.75
3.5	Multifocal		
4	Multifocal		
3	Multifocal		
4	Multifocal		
4	Multifocal		
4	Multifocal		
4	Multifocal		
2	Multifocal		
2.5	Multifocal		
2	Multifocal		
4	Multifocal		
2.5	Multifocal		
2.5	Multifocal		
2.5	Multifocal		
2.5	Multifocal		
2.5	Focal	3.57%	2.5
0	Absent	3.57%	0

CD68 (n=27)			
Density	**Distribution**	**Percentages**	Median infiltration density score
4	Disseminated	92.59%	3.5
3.5	Disseminated		
4	Disseminated		
4	Disseminated		
4	Disseminated		
3.5	Disseminated		
4	Disseminated		
4	Disseminated		
3	Disseminated		
3.5	Disseminated		
3.5	Disseminated		
2	Disseminated		
2.5	Disseminated		
2.5	Disseminated		
3.5	Disseminated		
2.5	Disseminated		
3	Disseminated		
3	Disseminated		
2.5	Disseminated		
3.5	Disseminated		
3.5	Disseminated		
4	Disseminated		
2.5	Disseminated		
4	Disseminated		
3	Disseminated		
3.5	Multifocal	7.40%	3.75
4	Multifocal		
CD11c (n=28)			
4	Disseminated	75%	3.5
4	Disseminated		
4	Disseminated		
4	Disseminated		
4	Disseminated		
3.5	Disseminated		
4	Disseminated		
4	Disseminated		
3.5	Disseminated		
3.5	Disseminated		
2.5	Disseminated		
2.5	Disseminated		
3.5	Disseminated		
4	Disseminated		
3.5	Disseminated		
3.5	Disseminated		
4	Disseminated		
2.5	Disseminated		
3	Disseminated		
4	Disseminated		
3	Disseminated		
3.5	Multifocal	25%	3.5
4	Multifocal		
3.5	Multifocal		
3.5	Multifocal		
4	Multifocal		
3.5	Multifocal		
3.5	Multifocal		

Supplementary Table 7 cont.

CD4 (n=26)			
Density	**Distribution**	**Percentages**	Median infiltration density score
4	Disseminated	88.46%	4
4	Disseminated		
4	Disseminated		
4	Disseminated		
4	Disseminated		
4	Disseminated		
4	Disseminated		
3.5	Disseminated		
4	Disseminated		
4	Disseminated		
4	Disseminated		
3	Disseminated		
3	Disseminated		
3	Disseminated		
3	Disseminated		
4	Disseminated		
3	Disseminated		
3.5	Disseminated		
4	Disseminated		
4	Disseminated		
3	Disseminated		
4	Disseminated		
4	Disseminated		
4	Multifocal	7.69%	3.5
3	Multifocal		
4	Focal	3.84%	4

CD8 (n=26)			
Density	**Distribution**	**Percentages**	**Median infiltration density score**
4	Disseminated	100%	3.25
4	Disseminated		
3	Disseminated		
4	Disseminated		
3	Disseminated		
3	Disseminated		
4	Disseminated		
4	Disseminated		
4	Disseminated		
3	Disseminated		
4	Disseminated		
3.5	Disseminated		
3	Disseminated		
3	Disseminated		
3	Disseminated		
2	Disseminated		
3	Disseminated		
3.5	Disseminated		
4	Disseminated		
3	Disseminated		
3	Disseminated		
3	Disseminated		
2	Disseminated		
4	Disseminated		
4	Disseminated		
4	Disseminated		

CD25 (n=24)			
Density	**Distribution**	**Percentages**	**Median infiltration density score**
2.5	Disseminated	91.67%	2
3	Disseminated		
2	Disseminated		
2	Disseminated		
2	Disseminated		
2	Disseminated		
2	Disseminated		
3	Disseminated		
2	Disseminated		
1.5	Disseminated		
1	Disseminated		
2	Disseminated		
2.5	Disseminated		
2	Disseminated		
2.5	Disseminated		
2.5	Disseminated		
2	Disseminated		
2	Disseminated		
3	Disseminated		
1	Disseminated		
2	Disseminated		
2	Disseminated		
3	Multifocal	8.33%	2.25
1.5	Multifocal		

FOXP3 (n=26)			
Density	**Distribution**	**Percentages**	**Median infiltration density score**
2.5	Disseminated	92.30%	2.5
3	Disseminated		
2.5	Disseminated		
2	Disseminated		
2	Disseminated		
3	Disseminated		
2	Disseminated		
3	Disseminated		
2.5	Disseminated		
3.5	Disseminated		
2.5	Disseminated		
2.5	Disseminated		
2.5	Disseminated		
2	Disseminated		
2	Disseminated		
2	Disseminated		
1.5	Disseminated		
3	Disseminated		
3	Disseminated		
2	Disseminated		
2.5	Disseminated		
1	Disseminated		
3	Disseminated		
3	Disseminated		
0	Absent	7.69%	0
0	Absent		

Supplementary Table 7 cont.

BCL6 (n=27)			
Density	**Distribution**	**Percentages**	**Average infiltration density score**
1	Disseminated	11.11%	1
1	Disseminated		
2	Disseminated		
3	Multifocal	14.81%	3.5
4	Multifocal		
4	Multifocal		
2.5	Multifocal		
4	Focal	11.11%	2
2	Focal		
0.5	Focal		
0	Absent	45.90%	0
0	Absent		
0	Absent		
0	Absent		
0	Absent		
0	Absent		
0	Absent		
0	Absent		
0	Absent		
0	Absent		
0	Absent		
0	Absent		
0	Absent		
0	Absent		
0	Absent		
0	Absent		
0	Absent		

CXCR5 (n=24)			
Density	**Distribution**	**Percentages**	**Median infiltration density score**
2.5	Disseminated	41.67%	2
2	Disseminated		
2	Disseminated		
4	Disseminated		
2	Disseminated		
2	Disseminated		
2.5	Disseminated		
1	Disseminated		
1	Disseminated		
2.5	Disseminated		
4	Multifocal	58.33%	4
4	Multifocal		
4	Multifocal		
4	Multifocal		
4	Multifocal		
2	Multifocal		
4	Multifocal		
4	Multifocal		
2.5	Multifocal		
4	Multifocal		
3	Multifocal		
3.5	Multifocal		
3	Multifocal		
4	Multifocal		

Supplementary Table 8 Statistical analysis of the multiple comparisons across the samples. The mean of each column was compared with the mean of every other column. Significance tested by ordinary one-way ANOVA including Tukey's Honest Significant Difference Test [(Not significant (ns)= p-value ≥ 0.05), (Significant, *= p-value 0.01 to 0.05, **= p-value = 0.001 to 0.01, ***= p-value 0.0001 to 0.001, ****= p-value <0.0001)].

Ordinary one-way ANOVA of CD3+ cells		
Tukey's multiple comparisons test	**Adjusted P Value**	**Summary**
NSP vs. HYP+ly	<0.0001	****
NSP vs. GCNIS	0.0268	*
NSP vs. GCNIS+ly	<0.0001	****
NSP vs. Seminoma	<0.0001	****
HYP+ly vs. GCNIS	0.0452	*
HYP+ly vs. GCNIS+ly	0.9779	ns
HYP+ly vs. Seminoma	0.1024	ns
GCNIS vs. GCNIS+ly	0.0077	**
GCNIS vs. Seminoma	<0.0001	****
GCNIS+ly vs. Seminoma	0.3352	ns
Ordinary one-way ANOVA of CD20cy+ cells		
Tukey's multiple comparisons test	**Adjusted P Value**	**Summary**
NSP vs. HYP+ly	0.0559	ns
NSP vs. GCNIS	0.9630	ns
NSP vs. GCNIS+ly	0.1082	ns
NSP vs. Seminoma	<0.0001	****
HYP+ly vs. GCNIS	0.1622	ns
HYP+ly vs. GCNIS+ly	0.9951	ns
HYP+ly vs. Seminoma	0.0011	**
GCNIS vs. GCNIS+ly	0.2917	ns
GCNIS vs. Seminoma	<0.0001	****
GCNIS+ly vs. Seminoma	0.0001	***
Ordinary one-way ANOVA of CD68+ cells		
Tukey's multiple comparisons test	**Adjusted P Value**	**Summary**
NSP vs. HYP+ly	0.9986	ns
NSP vs. GCNIS	0.5838	ns
NSP vs. GCNIS+ly	0.9834	ns
NSP vs. Seminoma	0.0029	**
HYP+ly vs. GCNIS	0.6908	ns
HYP+ly vs. GCNIS+ly	0.9988	ns
HYP+ly vs. Seminoma	0.0002	***
GCNIS vs. GCNIS+ly	0.8325	ns
GCNIS vs. Seminoma	<0.0001	****
GCNIS+ly vs. Seminoma	<0.0001	****
Ordinary one-way ANOVA of CD11c+ cells		
Tukey's multiple comparisons test	**Adjusted P Value**	**Summary**
NSP vs. HYP+ly	0.3260	ns
NSP vs. GCNIS	0.3228	ns
NSP vs. GCNIS+ly	0.0044	**
NSP vs. Seminoma	<0.0001	****
HYP+ly vs. GCNIS	>0.9999	ns

Supplementary Table 8 continue		
Tukey's multiple comparisons test	**Adjusted P Value**	**Summary**
HYP+ly vs. GCNIS+ly	0.4187	ns
HYP+ly vs. Seminoma	<0.0001	****
GCNIS vs. GCNIS+ly	0.3066	ns
GCNIS vs. Seminoma	<0.0001	****
GCNIS+ly vs. Seminoma	<0.0001	****
Ordinary one-way ANOVA of CD4+ cells		
Tukey's multiple comparisons test	**Adjusted P Value**	**Summary**
NSP vs. HYP+ly	<0.0001	****
NSP vs. GCNIS	0.0002	***
NSP vs. GCNIS+ly	<0.0001	****
NSP vs. Seminoma	<0.0001	****
HYP+ly vs. GCNIS	0.4052	ns
HYP+ly vs. GCNIS+ly	0.9824	ns
HYP+ly vs. Seminoma	0.5454	ns
GCNIS vs. GCNIS+ly	0.1193	ns
GCNIS vs. Seminoma	0.0037	**
GCNIS+ly vs. Seminoma	0.8548	ns
Ordinary one-way ANOVA of CD8+ cells		
Tukey's multiple comparisons test	**Adjusted P Value**	**Summary**
NSP vs. HYP+ly	<0.0001	****
NSP vs. GCNIS	0.0002	***
NSP vs. GCNIS+ly	<0.0001	****
NSP vs. Seminoma	<0.0001	****
HYP+ly vs. GCNIS	0.9366	ns
HYP+ly vs. GCNIS+ly	0.5030	ns
HYP+ly vs. Seminoma	0.0144	*
GCNIS vs. GCNIS+ly	0.0912	ns
GCNIS vs. Seminoma	0.0003	***
GCNIS+ly vs. Seminoma	0.4671	ns
Ordinary one-way ANOVA of CD25+ cells		
Tukey's multiple comparisons test	**Adjusted P Value**	**Summary**
NSP vs. HYP+ly	<0.0001	****
NSP vs. GCNIS	0.0361	*
NSP vs. GCNIS+ly	<0.0001	****
NSP vs. Seminoma	<0.0001	****
HYP+ly vs. GCNIS	0.0374	*
HYP+ly vs. GCNIS+ly	0.7026	ns
HYP+ly vs. Seminoma	0.9454	ns
GCNIS vs. GCNIS+ly	0.0005	***
GCNIS vs. Seminoma	0.0005	***
GCNIS+ly vs. Seminoma	0.9440	ns
Ordinary one-way ANOVA of FOXP3+ cells		
Tukey's multiple comparisons test	**Adjusted P Value**	**Summary**
NSP vs. HYP+ly	0.0759	ns
NSP vs. GCNIS	0.9543	ns
NSP vs. GCNIS+ly	0.0096	**
NSP vs. Seminoma	<0.0001	****

Supplementary Table 8 continue		
Tukey's multiple comparisons test	**Adjusted P Value**	**Summary**
HYP+ly vs. GCNIS	0.2248	ns
HYP+ly vs. GCNIS+ly	0.9613	ns
HYP+ly vs. Seminoma	0.0013	**
GCNIS vs. GCNIS+ly	0.0344	*
GCNIS vs. Seminoma	<0.0001	****
GCNIS+ly vs. Seminoma	0.0063	**
Ordinary one-way ANOVA of CXCR5+ cells		
Tukey's multiple comparisons test	**Adjusted P Value**	**Summary**
NSP vs. HYP+ly	0.0283	*
NSP vs. GCNIS	0.9566	ns
NSP vs. GCNIS+ly	0.4834	ns
NSP vs. Seminoma	<0.0001	****
HYP+ly vs. GCNIS	0.0898	ns
HYP+ly vs. GCNIS+ly	0.4474	ns
HYP+ly vs. Seminoma	0.0018	**
GCNIS vs. GCNIS+ly	0.8509	ns
GCNIS vs. Seminoma	<0.0001	****
GCNIS+ly vs. Seminoma	<0.0001	****
Ordinary one-way ANOVA of BCL6+ cells		
Tukey's multiple comparisons test	**Adjusted P Value**	**Summary**
NSP vs. HYP+ly	>0.9999	ns
NSP vs. GCNIS	>0.9999	ns
NSP vs. GCNIS+ly	0.9965	ns
NSP vs. Seminoma	0.0544	ns
HYP+ly vs. GCNIS	>0.9999	ns
HYP+ly vs. GCNIS+ly	0.9956	ns
HYP+ly vs. Seminoma	0.0338	*
GCNIS vs. GCNIS+ly	0.9949	ns
GCNIS vs. Seminoma	0.0220	*
GCNIS+ly vs. Seminoma	0.0514	ns

Supplementary Table 9 CD3+T cells- statistical analysis of the multiple comparisons across the different localisation of TGCT samples. The mean of each column was compared with the mean of every other column. Significance tested by ordinary one-way ANOVA including Tukey's Honest Significant Difference Test [(Not significant (ns)= p-value ≥ 0.05), (Significant, *= p-value 0.01 to 0.05, **= p-value = 0.001 to 0.01, ***= p-value 0.0001 to 0.001, ****= p-value <0.0001)]. Most important comparison are in bold.

Ordinary one-way ANOVA of CD3+ T cells		
Tukey's multiple comparisons test	**Adjusted P Value**	**Summary**
Seminoma-Tumor vs. Seminoma-Tumor-Adj	0.0012	**
Seminoma-Tumor vs. Seminoma-Tumor-Dis	<0.0001	****
Seminoma-Tumor vs. Seminoma-Contralateral 1	**<0.0001**	****
Seminoma-Tumor vs. Seminoma-Contralateral 2	**<0.0001**	****
Seminoma-Tumor-Adj vs. Seminoma-Tumor-Dis	0.9985	ns
Seminoma-Tumor-Adj vs. Seminoma-Contralateral 1	**0.9645**	**ns**
Seminoma-Tumor-Adj vs. Seminoma-Contralateral 2	**0.7251**	**ns**
Seminoma-Tumor-Dis vs. Seminoma-Contralateral 1	**>0.9999**	**ns**
Seminoma-Tumor-Dis vs. Seminoma-Contralateral 2	**0.9986**	**ns**
Seminoma-Contralateral 1 vs. Seminoma-Contralateral 2	>0.9999	ns
Embryonal carcinoma (≥80%) -Tumor vs. Embryonal carcinoma (≥80%)-Tumor-Adj	0.0180	*
Embryonal carcinoma (≥80%) -Tumor vs. Embryonal carcinoma (≥80%)-Tumor-Dis	0.0281	*
Embryonal carcinoma (≥80%) -Tumor vs. Embryonal carcinoma (≥80%)-Contralateral 1	**0.0104**	****
Embryonal carcinoma (≥80%) -Tumor vs. Embryonal carcinoma (≥80%)-Contralateral 2	**0.0126**	****
Embryonal carcinoma (≥80%)-Tumor-Adj vs. Embryonal carcinoma (≥80%)-Tumor-Dis	>0.9999	ns
Embryonal carcinoma (≥80%)-Tumor-Adj vs. Embryonal carcinoma (≥80%)-Contralateral 1	**>0.9999**	**ns**
Embryonal carcinoma (≥80%)-Tumor-Adj vs. Embryonal carcinoma (≥80%)-Contralateral 2	**>0.9999**	**ns**
Embryonal carcinoma (≥80%)-Tumor-Dis vs. Embryonal carcinoma (≥80%)-Contralateral 1	**>0.9999**	**ns**
Embryonal carcinoma (≥80%)-Tumor-Dis vs. Embryonal carcinoma (≥80%)-Contralateral 2	**>0.9999**	**ns**
Embryonal carcinoma (≥80%)-Contralateral 1 vs. Embryonal carcinoma (≥80%)-Contralateral 2	>0.9999	ns
Mixed Tumors-Tumor vs. Mixed Tumors-Tumor-Adj	0.8917	ns
Mixed Tumors-Tumor vs. Mixed Tumors-Tumor-Dis	0.4644	ns
Mixed Tumors-Tumor vs. Mixed Tumors-Contralateral 1	**0.2494**	**ns**
Mixed Tumors-Tumor vs. Mixed Tumors-Contralateral 2	**0.2989**	**ns**
Mixed Tumors-Tumor-Adj vs. Mixed Tumors-Tumor-Dis	>0.9999	ns
Mixed Tumors-Tumor-Adj vs. Mixed Tumors-Contralateral 1	**0.9955**	**ns**
Mixed Tumors-Tumor-Adj vs. Mixed Tumors-Contralateral 2	**0.9980**	**ns**
Mixed Tumors-Tumor-Dis vs. Mixed Tumors-Contralateral 1	**>0.9999**	**ns**
Mixed Tumors-Tumor-Dis vs. Mixed Tumors-Contralateral 2	**>0.9999**	**ns**
Mixed Tumors-Contralateral 1 vs. Mixed Tumors-Contralateral 2	>0.9999	ns

Supplementary Table 10 CD4+Th cells: statistical analysis of the multiple comparisons across the different localisation of TGCT samples. The mean of each column was compared with the mean of every other column. Significance tested by ordinary one-way ANOVA including Tukey's Honest Significant Difference Test [(Not significant (ns)= p-value ≥ 0.05), (Significant, *= p-value 0.01 to 0.05, **= p-value = 0.001 to 0.01, ***= p-value 0.0001 to 0.001, ****= p-value <0.0001)]. Most important comparison are in bold.

Ordinary one-way ANOVA of CD4+ Th cells		
Tukey's multiple comparisons test	**Adjusted P Value**	**Summary**
Seminoma-Tumor vs. Seminoma-Tumor-Adj	0.0003	***
Seminoma-Tumor vs. Seminoma-Tumor-Dis	<0.0001	****
Seminoma-Tumor vs. Seminoma-Contralateral 1	<0.0001	****
Seminoma-Tumor vs. Seminoma-Contralateral 2	<0.0001	****
Seminoma-Tumor-Adj vs. Seminoma-Tumor-Dis	0.8453	ns
Seminoma-Tumor-Adj vs. Seminoma-Contralateral 1	0.9780	ns
Seminoma-Tumor-Adj vs. Seminoma-Contralateral 2	0.9256	ns
Seminoma-Tumor-Dis vs. Seminoma-Contralateral 1	>0.9999	ns
Seminoma-Tumor-Dis vs. Seminoma-Contralateral 2	>0.9999	ns
Seminoma-Contralateral 1 vs. Seminoma-Contralateral 2	>0.9999	ns
Embryonal carcinoma (≥80%) -Tumor vs. Embryonal carcinoma (≥80%)-Tumor-Adj	0.0052	**
Embryonal carcinoma (≥80%) -Tumor vs. Embryonal carcinoma (≥80%)-Tumor-Dis	0.0018	**
Embryonal carcinoma (≥80%) -Tumor vs. Embryonal carcinoma (≥80%)-Contralateral 1	0.0017	**
Embryonal carcinoma (≥80%) -Tumor vs. Embryonal carcinoma (≥80%)-Contralateral 2	0.0216	*
Embryonal carcinoma (≥80%)-Tumor-Adj vs. Embryonal carcinoma (≥80%)-Tumor-Dis	>0.9999	ns
Embryonal carcinoma (≥80%)-Tumor-Adj vs. Embryonal carcinoma (≥80%)-Contralateral 1	>0.9999	ns
Embryonal carcinoma (≥80%)-Tumor-Adj vs. Embryonal carcinoma (≥80%)-Contralateral 2	>0.9999	ns
Embryonal carcinoma (≥80%)-Tumor-Dis vs. Embryonal carcinoma (≥80%)-Contralateral 1	>0.9999	ns
Embryonal carcinoma (≥80%)-Tumor-Dis vs. Embryonal carcinoma (≥80%)-Contralateral 2	>0.9999	ns
Embryonal carcinoma (≥80%)-Contralateral 1 vs. Embryonal carcinoma (≥80%)-Contralateral 2	>0.9999	ns
Mixed Tumors-Tumor vs. Mixed Tumors-Tumor-Adj	0.4101	ns
Mixed Tumors-Tumor vs. Mixed Tumors-Tumor-Dis	0.0296	*
Mixed Tumors-Tumor vs. Mixed Tumors-Contralateral 1	0.0262	*
Mixed Tumors-Tumor vs. Mixed Tumors-Contralateral 2	0.1501	ns
Mixed Tumors-Tumor-Adj vs. Mixed Tumors-Tumor-Dis	0.9982	ns
Mixed Tumors-Tumor-Adj vs. Mixed Tumors-Contralateral 1	0.9810	ns
Mixed Tumors-Tumor-Adj vs. Mixed Tumors-Contralateral 2	>0.9999	ns
Mixed Tumors-Tumor-Dis vs. Mixed Tumors-Contralateral 1	>0.9999	ns
Mixed Tumors-Tumor-Dis vs. Mixed Tumors-Contralateral 2	>0.9999	ns
Mixed Tumors-Contralateral 1 vs. Mixed Tumors-Contralateral 2	>0.9999	ns

Supplementary Table 11 CD8+Tc cells: statistical analysis of the multiple comparisons across the different localisation of TGCT samples. The mean of each column was compared with the mean of every other column. Significance tested by ordinary one-way ANOVA including Tukey's Honest Significant Difference Test [(Not significant (ns)= p-value ≥ 0.05), (Significant, *= p-value 0.01 to 0.05, **= p-value = 0.001 to 0.01, ***= p-value 0.0001 to 0.001, ****= p-value <0.0001)]. Most important comparison are in bold.

Ordinary one-way ANOVA of CD8+ Tc cells		
Tukey's multiple comparisons test	**Adjusted P Value**	**Summary**
Seminoma-Tumor vs. Seminoma-Tumor-Adj	0.3704	ns
Seminoma-Tumor vs. Seminoma-Tumor-Dis	0.0512	ns
Seminoma-Tumor vs. Seminoma-Contralateral 1	0.0525	ns
Seminoma-Tumor vs. Seminoma-Contralateral 2	0.0173	*
Seminoma-Tumor-Adj vs. Seminoma-Tumor-Dis	0.9998	ns
Seminoma-Tumor-Adj vs. Seminoma-Contralateral 1	0.9901	ns
Seminoma-Tumor-Adj vs. Seminoma-Contralateral 2	0.9609	ns
Seminoma-Tumor-Dis vs. Seminoma-Contralateral 1	>0.9999	ns
Seminoma-Tumor-Dis vs. Seminoma-Contralateral 2	>0.9999	ns
Seminoma-Contralateral 1 vs. Seminoma-Contralateral 2	>0.9999	ns
Embryonal carcinoma (≥80%) -Tumor vs. Embryonal carcinoma (≥80%)-Tumor-Adj	0.2172	ns
Embryonal carcinoma (≥80%) -Tumor vs. Embryonal carcinoma (≥80%)-Tumor-Dis	0.7592	ns
Embryonal carcinoma (≥80%) -Tumor vs. Embryonal carcinoma (≥80%)-Contralateral 1	0.0713	ns
Embryonal carcinoma (≥80%) -Tumor vs. Embryonal carcinoma (≥80%)-Contralateral 2	0.9910	ns
Embryonal carcinoma (≥80%)-Tumor-Adj vs. Embryonal carcinoma (≥80%)-Tumor-Dis	>0.9999	ns
Embryonal carcinoma (≥80%)-Tumor-Adj vs. Embryonal carcinoma (≥80%)-Contralateral 1	>0.9999	ns
Embryonal carcinoma (≥80%)-Tumor-Adj vs. Embryonal carcinoma (≥80%)-Contralateral 2	0.9892	ns
Embryonal carcinoma (≥80%)-Tumor-Dis vs. Embryonal carcinoma (≥80%)-Contralateral 1	0.9964	ns
Embryonal carcinoma (≥80%)-Tumor-Dis vs. Embryonal carcinoma (≥80%)-Contralateral 2	>0.9999	ns
Embryonal carcinoma (≥80%)-Contralateral 1 vs. Embryonal carcinoma (≥80%)-Contralateral 2	0.8593	ns
Mixed Tumors-Tumor vs. Mixed Tumors-Tumor-Adj	0.9927	ns
Mixed Tumors-Tumor vs. Mixed Tumors-Tumor-Dis	0.9780	ns
Mixed Tumors-Tumor vs. Mixed Tumors-Contralateral 1	0.8948	ns
Mixed Tumors-Tumor vs. Mixed Tumors-Contralateral 2	0.8933	ns
Mixed Tumors-Tumor-Adj vs. Mixed Tumors-Tumor-Dis	>0.9999	ns
Mixed Tumors-Tumor-Adj vs. Mixed Tumors-Contralateral 1	>0.9999	ns
Mixed Tumors-Tumor-Adj vs. Mixed Tumors-Contralateral 2	>0.9999	ns
Mixed Tumors-Tumor-Dis vs. Mixed Tumors-Contralateral 1	>0.9999	ns
Mixed Tumors-Tumor-Dis vs. Mixed Tumors-Contralateral 2	>0.9999	ns
Mixed Tumors-Contralateral 1 vs. Mixed Tumors-Contralateral 2	>0.9999	ns

Supplementary Table 12 CD68+Macrophages cells: statistical analysis of the multiple comparisons across the different localisation of TGCT samples. The mean of each column was compared with the mean of every other column. Significance teted by Ordinary One-way ANOVA including Tukey's Honest Significant Difference test [{Not significant (ns): p value ≥ 0.05}, {Significant (*): p value = 0.01 to 0.05}, {Very significant (**): p value = 0.001 to 0.01}, {Extremely significant (***): p value = 0.0001 to 0.001}, {Extremely significant (****): p value <0.0001}]. Most important comparison are in bold.

Ordinary one-way ANOVA of CD68+ Macrophages cells		
Tukey's multiple comparisons test	**Adjusted P Value**	**Summary**
Seminoma-Tumor vs. Seminoma-Tumor-Adj	>0.9999	ns
Seminoma-Tumor vs. Seminoma-Tumor-Dis	0.9972	ns
Seminoma-Tumor vs. Seminoma-Contralateral 1	>0.9999	ns
Seminoma-Tumor vs. Seminoma-Contralateral 2	>0.9999	ns
Seminoma-Tumor-Adj vs. Seminoma-Tumor-Dis	0.9929	ns
Seminoma-Tumor-Adj vs. Seminoma-Contralateral 1	>0.9999	ns
Seminoma-Tumor-Adj vs. Seminoma-Contralateral 2	>0.9999	ns
Seminoma-Tumor-Dis vs. Seminoma-Contralateral 1	>0.9999	ns
Seminoma-Tumor-Dis vs. Seminoma-Contralateral 2	0.9993	ns
Seminoma-Contralateral 1 vs. Seminoma-Contralateral 2	>0.9999	ns
Embryonal carcinoma (≥80%) -Tumor vs. Embryonal carcinoma (≥80%)-Tumor-Adj	0.4670	ns
Embryonal carcinoma (≥80%) -Tumor vs. Embryonal carcinoma (≥80%)-Tumor-Dis	0.5318	ns
Embryonal carcinoma (≥80%) -Tumor vs. Embryonal carcinoma (≥80%)-Contralateral 1	>0.9999	ns
Embryonal carcinoma (≥80%) -Tumor vs. Embryonal carcinoma (≥80%)-Contralateral 2	0.7846	ns
Embryonal carcinoma (≥80%)-Tumor-Adj vs. Embryonal carcinoma (≥80%)-Tumor-Dis	>0.9999	ns
Embryonal carcinoma (≥80%)-Tumor-Adj vs. Embryonal carcinoma (≥80%)-Contralateral 1	0.9657	ns
Embryonal carcinoma (≥80%)-Tumor-Adj vs. Embryonal carcinoma (≥80%)-Contralateral 2	>0.9999	ns
Embryonal carcinoma (≥80%)-Tumor-Dis vs. Embryonal carcinoma (≥80%)-Contralateral 1	0.9697	ns
Embryonal carcinoma (≥80%)-Tumor-Dis vs. Embryonal carcinoma (≥80%)-Contralateral 2	>0.9999	ns
Embryonal carcinoma (≥80%)-Contralateral 1 vs. Embryonal carcinoma (≥80%)-Contralateral 2	0.9972	ns
Mixed Tumors-Tumor vs. Mixed Tumors-Tumor-Adj	0.9927	ns
Mixed Tumors-Tumor vs. Mixed Tumors-Tumor-Dis	0.9780	ns
Mixed Tumors-Tumor vs. Mixed Tumors-Contralateral 1	0.8948	ns
Mixed Tumors-Tumor vs. Mixed Tumors-Contralateral 2	0.8933	ns
Mixed Tumors-Tumor-Adj vs. Mixed Tumors-Tumor-Dis	>0.9999	ns
Mixed Tumors-Tumor-Adj vs. Mixed Tumors-Contralateral 1	>0.9999	ns
Mixed Tumors-Tumor-Adj vs. Mixed Tumors-Contralateral 2	>0.9999	ns
Mixed Tumors-Tumor-Dis vs. Mixed Tumors-Contralateral 1	>0.9999	ns
Mixed Tumors-Tumor-Dis vs. Mixed Tumors-Contralateral 2	>0.9999	ns
Mixed Tumors-Contralateral 1 vs. Mixed Tumors-Contralateral 2	>0.9999	ns

Supplementary Table 13 CD20cy+ B cells: statistical analysis of the multiple comparisons across the different localisation of TGCT samples. The mean of each column was compared with the mean of every other column. Significance tested by ordinary one-way ANOVA including Tukey's Honest Significant Difference Test [(Not significant (ns)= p-value ≥ 0.05), (Significant, *= p-value 0.01 to 0.05, **= p-value = 0.001 to 0.01, ***= p-value 0.0001 to 0.001, ****= p-value <0.0001)]. Most important comparison are in bold.

Ordinary one-way ANOVA of CD20cy B cells		
Tukey's multiple comparisons test	**Adjusted P Value**	**Summary**
Seminoma-Tumor vs. Seminoma-Tumor-Adj	0.9974	ns
Seminoma-Tumor vs. Seminoma-Tumor-Dis	>0.9999	ns
Seminoma-Tumor vs. Seminoma-Contralateral 1	0.9859	ns
Seminoma-Tumor vs. Seminoma-Contralateral 2	0.9227	ns
Seminoma-Tumor-Adj vs. Seminoma-Tumor-Dis	>0.9999	ns
Seminoma-Tumor-Adj vs. Seminoma-Contralateral 1	>0.9999	ns
Seminoma-Tumor-Adj vs. Seminoma-Contralateral 2	>0.9999	ns
Seminoma-Tumor-Dis vs. Seminoma-Contralateral 1	>0.9999	ns
Seminoma-Tumor-Dis vs. Seminoma-Contralateral 2	0.9996	ns
Seminoma-Contralateral 1 vs. Seminoma-Contralateral 2	>0.9999	ns
Embryonal carcinoma (≥80%) -Tumor vs. Embryonal carcinoma (≥80%)-Tumor-Adj	>0.9999	ns
Embryonal carcinoma (≥80%) -Tumor vs. Embryonal carcinoma (≥80%)-Tumor-Dis	>0.9999	ns
Embryonal carcinoma (≥80%) -Tumor vs. Embryonal carcinoma (≥80%)-Contralateral 1	>0.9999	ns
Embryonal carcinoma (≥80%) -Tumor vs. Embryonal carcinoma (≥80%)-Contralateral 2	>0.9999	ns
Embryonal carcinoma (≥80%)-Tumor-Adj vs. Embryonal carcinoma (≥80%)-Tumor-Dis	>0.9999	ns
Embryonal carcinoma (≥80%)-Tumor-Adj vs. Embryonal carcinoma (≥80%)-Contralateral 1	>0.9999	ns
Embryonal carcinoma (≥80%)-Tumor-Adj vs. Embryonal carcinoma (≥80%)-Contralateral 2	>0.9999	ns
Embryonal carcinoma (≥80%)-Tumor-Dis vs. Embryonal carcinoma (≥80%)-Contralateral 1	>0.9999	ns
Embryonal carcinoma (≥80%)-Tumor-Dis vs. Embryonal carcinoma (≥80%)-Contralateral 2	>0.9999	ns
Embryonal carcinoma (≥80%)-Contralateral 1 vs. Embryonal carcinoma (≥80%)-Contralateral 2	>0.9999	ns
Mixed Tumors-Tumor vs. Mixed Tumors-Tumor-Adj	0.3646	ns
Mixed Tumors-Tumor vs. Mixed Tumors-Tumor-Dis	0.3468	ns
Mixed Tumors-Tumor vs. Mixed Tumors-Contralateral 1	0.3842	ns
Mixed Tumors-Tumor vs. Mixed Tumors-Contralateral 2	0.6255	ns
Mixed Tumors-Tumor-Adj vs. Mixed Tumors-Tumor-Dis	>0.9999	ns
Mixed Tumors-Tumor-Adj vs. Mixed Tumors-Contralateral 1	>0.9999	ns
Mixed Tumors-Tumor-Adj vs. Mixed Tumors-Contralateral 2	>0.9999	ns
Mixed Tumors-Tumor-Dis vs. Mixed Tumors-Contralateral 1	>0.9999	ns
Mixed Tumors-Tumor-Dis vs. Mixed Tumors-Contralateral 2	>0.9999	ns
Mixed Tumors-Contralateral 1 vs. Mixed Tumors-Contralateral 2	>0.9999	ns

Supplementary Table 14 CD25+FOXP3+ Treg cells: statistical analysis of the multiple comparisons across the different localisation of TGCT samples. The mean of each column was compared with the mean of every other column. Significance tested by ordinary one-way ANOVA including Tukey's Honest Significant Difference Test [(Not significant (ns)= p-value ≥ 0.05), (Significant, *= p-value 0.01 to 0.05, **= p-value = 0.001 to 0.01, ***= p-value 0.0001 to 0.001, ****= p-value <0.0001)]. Most important comparison are in bold.

Ordinary one-way ANOVA of CD25+FOXP3+ Treg		
Tukey's multiple comparisons test	**Adjusted P Value**	**Summary**
Seminoma-Tumor vs. Seminoma-Tumor-Adj	0.0374	*
Seminoma-Tumor vs. Seminoma-Tumor-Dis	0.4000	ns
Seminoma-Tumor vs. Seminoma-Contralateral 1	0.0380	*
Seminoma-Tumor vs. Seminoma-Contralateral 2	0.0022	**
Seminoma-Tumor-Adj vs. Seminoma-Tumor-Dis	>0.9999	ns
Seminoma-Tumor-Adj vs. Seminoma-Contralateral 1	>0.9999	ns
Seminoma-Tumor-Adj vs. Seminoma-Contralateral 2	0.9992	ns
Seminoma-Tumor-Dis vs. Seminoma-Contralateral 1	0.9997	ns
Seminoma-Tumor-Dis vs. Seminoma-Contralateral 2	0.9431	ns
Seminoma-Contralateral 1 vs. Seminoma-Contralateral 2	>0.9999	ns
Embryonal carcinoma (≥80%) -Tumor vs. Embryonal carcinoma (≥80%)-Tumor-Adj	0.9813	ns
Embryonal carcinoma (≥80%) -Tumor vs. Embryonal carcinoma (≥80%)-Tumor-Dis	0.9958	ns
Embryonal carcinoma (≥80%) -Tumor vs. Embryonal carcinoma (≥80%)-Contralateral 1	0.9974	ns
Embryonal carcinoma (≥80%) -Tumor vs. Embryonal carcinoma (≥80%)-Contralateral 2	0.9985	ns
Embryonal carcinoma (≥80%)-Tumor-Adj vs. Embryonal carcinoma (≥80%)-Tumor-Dis	>0.9999	ns
Embryonal carcinoma (≥80%)-Tumor-Adj vs. Embryonal carcinoma (≥80%)-Contralateral 1	>0.9999	ns
Embryonal carcinoma (≥80%)-Tumor-Adj vs. Embryonal carcinoma (≥80%)-Contralateral 2	>0.9999	ns
Embryonal carcinoma (≥80%)-Tumor-Dis vs. Embryonal carcinoma (≥80%)-Contralateral 1	>0.9999	ns
Embryonal carcinoma (≥80%)-Tumor-Dis vs. Embryonal carcinoma (≥80%)-Contralateral 2	>0.9999	ns
Embryonal carcinoma (≥80%)-Contralateral 1 vs. Embryonal carcinoma (≥80%)-Contralateral 2	>0.9999	ns
Mixed Tumors-Tumor vs. Mixed Tumors-Tumor-Adj	>0.9999	ns
Mixed Tumors-Tumor vs. Mixed Tumors-Tumor-Dis	>0.9999	ns
Mixed Tumors-Tumor vs. Mixed Tumors-Contralateral 1	>0.9999	ns
Mixed Tumors-Tumor vs. Mixed Tumors-Contralateral 2	0.9973	ns
Mixed Tumors-Tumor-Adj vs. Mixed Tumors-Tumor-Dis	>0.9999	ns
Mixed Tumors-Tumor-Adj vs. Mixed Tumors-Contralateral 1	>0.9999	ns
Mixed Tumors-Tumor-Adj vs. Mixed Tumors-Contralateral 2	0.9646	ns
Mixed Tumors-Tumor-Dis vs. Mixed Tumors-Contralateral 1	>0.9999	ns
Mixed Tumors-Tumor-Dis vs. Mixed Tumors-Contralateral 2	0.9718	ns
Mixed Tumors-Contralateral 1 vs. Mixed Tumors-Contralateral 2	0.9995	ns

Supplementary Table 15 CXCR5+BCL6+ Tfh cells: statistical analysis of the multiple comparisons across the different localisation of TGCT samples. The mean of each column was compared with the mean of every other column. Significance tested by ordinary one-way ANOVA including Tukey's Honest Significant Difference Test [(Not significant (ns)= p-value ≥ 0.05), (Significant, *= p-value 0.01 to 0.05, **= p-value = 0.001 to 0.01, ***= p-value 0.0001 to 0.001, ****= p-value <0.0001)]. Most important comparison are in bold.

Ordinary one-way ANOVA of CXCR5+BCL6+ Tfh		
Tukey's multiple comparisons test	**Adjusted P Value**	**Summary**
Seminoma-Tumor vs. Seminoma-Tumor-Adj	0.2294	ns
Seminoma-Tumor vs. Seminoma-Tumor-Dis	0.9782	ns
Seminoma-Tumor vs. Seminoma-Contralateral 1	0.8401	ns
Seminoma-Tumor vs. Seminoma-Contralateral 2	0.2904	ns
Seminoma-Tumor-Adj vs. Seminoma-Tumor-Dis	0.9978	ns
Seminoma-Tumor-Adj vs. Seminoma-Contralateral 1	>0.9999	ns
Seminoma-Tumor-Adj vs. Seminoma-Contralateral 2	>0.9999	ns
Seminoma-Tumor-Dis vs. Seminoma-Contralateral 1	>0.9999	ns
Seminoma-Tumor-Dis vs. Seminoma-Contralateral 2	0.9985	ns
Seminoma-Contralateral 1 vs. Seminoma-Contralateral 2	>0.9999	ns
Embryonal carcinoma (≥80%) -Tumor vs. Embryonal carcinoma (≥80%)-Tumor-Adj	>0.9999	ns
Embryonal carcinoma (≥80%) -Tumor vs. Embryonal carcinoma (≥80%)-Tumor-Dis	>0.9999	ns
Embryonal carcinoma (≥80%) -Tumor vs. Embryonal carcinoma (≥80%)-Contralateral 1	>0.9999	ns
Embryonal carcinoma (≥80%) -Tumor vs. Embryonal carcinoma (≥80%)-Contralateral 2	>0.9999	ns
Embryonal carcinoma (≥80%)-Tumor-Adj vs. Embryonal carcinoma (≥80%)-Tumor-Dis	>0.9999	ns
Embryonal carcinoma (≥80%)-Tumor-Adj vs. Embryonal carcinoma (≥80%)-Contralateral 1	>0.9999	ns
Embryonal carcinoma (≥80%)-Tumor-Adj vs. Embryonal carcinoma (≥80%)-Contralateral 2	>0.9999	ns
Embryonal carcinoma (≥80%)-Tumor-Dis vs. Embryonal carcinoma (≥80%)-Contralateral 1	>0.9999	ns
Embryonal carcinoma (≥80%)-Tumor-Dis vs. Embryonal carcinoma (≥80%)-Contralateral 2	>0.9999	ns
Embryonal carcinoma (≥80%)-Contralateral 1 vs. Embryonal carcinoma (≥80%)-Contralateral 2	>0.9999	ns
Mixed Tumors-Tumor vs. Mixed Tumors-Tumor-Adj	0.9991	ns
Mixed Tumors-Tumor vs. Mixed Tumors-Tumor-Dis	>0.9999	ns
Mixed Tumors-Tumor vs. Mixed Tumors-Contralateral 1	0.9904	ns
Mixed Tumors-Tumor vs. Mixed Tumors-Contralateral 2	0.9975	ns
Mixed Tumors-Tumor-Adj vs. Mixed Tumors-Tumor-Dis	>0.9999	ns
Mixed Tumors-Tumor-Adj vs. Mixed Tumors-Contralateral 1	>0.9999	ns
Mixed Tumors-Tumor-Adj vs. Mixed Tumors-Contralateral 2	>0.9999	ns
Mixed Tumors-Tumor-Dis vs. Mixed Tumors-Contralateral 1	>0.9999	ns
Mixed Tumors-Tumor-Dis vs. Mixed Tumors-Contralateral 2	>0.9999	ns
Mixed Tumors-Contralateral 1 vs. Mixed Tumors-Contralateral 2	>0.9999	ns